**Title**
California Salt Marsh Accretion, Ecosystem Services, and Disturbance Responses In the Face of Climate Change



**Author**
Brown, Lauren

**Publication Date**
2019

UNIVERSITY OF CALIFORNIA

Los Angeles

# California Salt Marsh Accretion, Ecosystem Services, and Disturbance Responses In the Face of Climate Change

A dissertation submitted in partial satisfaction of the requirements for the degree of Doctor of Philosophy in Geography

by

Lauren Nicole Brown

2019

ABSTRACT OF THE DISSERTATION

California Salt Marsh Accretion,
Ecosystem Services, and Disturbance Responses
In the Face of Climate Change

by

Lauren Nicole Brown
Doctor of Philosophy in Geography
University of California, Los Angeles, 2019
Professor Glen Michael MacDonald, Chair

Coastal salt marsh ecosystems in California are at risk from projected rates of sea-level rise (SLR) of up to an order of magnitude higher than rates seen over the past 6,000 years of stable sea levels (Griggs, Cayan, Tebaldi, Fricker, & Árvai, 2017). With rates of this magnitude, salt marsh area, already limited by land use changes in the 19$^{th}$ and 20$^{th}$ centuries, could be completely lost by 2100 (Thorne et al., 2018). To better understand how California salt marshes are adapting to modern acceleration of SLR, over 100 sediment cores were collected from 13 salt marsh sites, ranging from Humboldt Bay to Tijuana River Estuary. Sediment accretion rates over the past several hundred years were measured using radiocesium, radiolead, and radiocarbon dating on 32 cores. Valuation of the carbon storage, an ecosystem service known as blue carbon provided by salt marshes, presents an opportunity to help preserve and restore sites threatened by SLR through carbon credits (Bear, 2017; Callaway, Borgnis, Turner, & Milan, 2012; Mcleod et al., 2011), but there are many questions which much be addressed before this can become a reality for the state of California (Macreadie et al., 2019). A standardized protocol for estimation of carbon content from loss-on-ignition (LOI) was developed with an emphasis on quantifying

error and uncertainty in carbon measurements for blue carbon purposes. Using a conversion between soil organic matter and soil organic carbon shown to be effective for California salt marshes, carbon content was estimated through LOI analysis of 61 sediment cores. The impact of climate change in these ecosystems was further explored in the first documented record of a fire in a Pacific coast salt marsh at Mugu Lagoon.

California salt marsh sediment accretion averages at 2.93 ± 1.9 mm $yr^{-1}$, which is lower than average rates from regions such as the US Gulf and East coasts. Rates of accretion and relative SLR (RSLR) show a non-linear relationship with highest accretion occurring at rates of RSLR from 2 – 6 mm $yr^{-1}$. Linear relationships between SLR and accretion are comparatively weak, but are stronger in the low elevations of salt marsh habitat. Salt marshes in the state annually sequester about 0.08% of state-wide annual greenhouse gas emissions and store about 23% of one year's emissions in their soils (as compared to 2016 emissions). Because of limited area, these habitats will not serve as an effective mitigation strategy at the state level, but loss of this habitat may release up to 27 ± 0.3 Tg stored carbon, potentially valued at about $1.4 billion (using an estimate of $15/tonne $CO_2$ equivalent). Preservation of current habitat through facilitation of sediment accretion will have the largest positive impact on carbon storage and sequestration, as well as protect salt marsh habitat from being lost to SLR. Analysis of the persistent effects of a recent marsh fire at Mugu Lagoon demonstrates that drought-stress may slow California salt marsh response to disturbance by one or more growing seasons and highlights the uncertain impacts of climate change on system function. This dissertation provides important baseline data for salt marsh sediment accretion, salt marsh carbon stocks and sequestrations rates, recommends best practices for use of LOI as a measure of soil organic carbon, and examines ecosystem recovery under multiple stressors. This work can be used in

vulnerability assessments, ecosystem models, and valuation of ecosystem services for California salt marshes.

The dissertation of Lauren Nicole Brown is approved.

Thomas Welch Gillespie

Kyle C Cavanaugh

Richard F Ambrose

Glen Michael MacDonald, Committee Chair

University of California, Los Angeles

2019

For Dad, with all my love

---

I think you'd have loved the smell of the salt marsh in the morning. The infinite possibility of thousand-year-old sediments and the stories they tell. I might have walked with you through places you'd known before me and we would have traded their stories. Like the stories you told me of the places we'd learned together as I grew up.

You may not have walked with me this time, but you taught me all the same.

## Table of Contents

## List of Figures



## List of Tables

## List of Appendix Figures



## List of Appendix Tables

## List of Abbreviations

| | |
|---|---|
| $^{137}Cs$ | Radiocesium |
| $^{14}C$ | Radiocarbon |
| $^{210}Pb$ | Radiolead |
| $^{210}Pb_{ex}$ | Excess radiolead |
| $^{210}Pb_{supp}$ | Supported radiolead |
| ANOVA | Analysis of variance |
| BD | Bulk density |
| BOL | Bolinas Lagoon |
| BP | Before present |
| $CaCO_3$ | Calcium carbonate |
| $CO_2$ | Carbon dioxide |
| $CO_2e$ | Carbon dioxide equivalent |
| CSI | Core Scientific International |
| CVH | Coastal vegetated habitat |
| DEM | Digital elevation model |
| HCl | Hydrochloric acid |
| HKS | Hookton Slough |
| IC | Inorganic Carbon |
| LOI | Loss-on-ignition |
| MAP | Mean annual precipitation |
| MAT | Mean annual temperature |
| MB | Mission Bay |
| MGL | Mugu Lagoon |
| MOB | Morro Bay |
| MRH | Mad River High |
| MRL | Mad River Low |
| NAVD88 | North American Vertical Datum 1988 |
| NDVI | Normalized vegetation difference index |
| NMDS | Non-metric multidimensional scaling |
| NOAA | National Oceanic and Atmospheric Administration |
| NWI | National Wetlands Inventory |
| PCA | Principal components analysis |
| PDSI | Palmer drought severity index |
| PTL | Petaluma Marsh |
| QMU | Queen Mary University |
| RSLR | Relative sea-level rise |
| SB | Seal Beach |
| SLR | Sea-level rise |
| SOC | Soil organic carbon |
| SOM | Soil organic matter |
| SWL | Structural water loss |
| TGA | Thermogravimetric analysis |
| TJE | Tijuana River Estuary |
| TRM | Triangle Marsh |
| UCLA | University of California, Los Angeles |

| | |
|---|---|
| UNB | Upper Newport Bay |
| USC | University of Southern California |
| USGS | United States Geologic Survey |
| VLS | Vertical land subsidence |
| WB | Walkley-Black |
| WTS | White Slough |

**Acknowledgements**

There are so many people that deserve credit for helping bring this project to life. First, I would like to thank my advisor, Glen MacDonald, for giving me the opportunities I needed to succeed. Over the past seven years, I have been incredibly grateful for the guidance he gave by pushing me in a likely direction, the independence I have had in developing this project as my own, and the support I knew Glen would provide when I inevitably stumbled. I would also like to thank my committee members. Rich Ambrose has been key to helping someone who grew up in the Colorado Rockies finish a dissertation on the coast of California. His comments on drafts and guidance through ecological methods have made me into a much better scientist. Tom Gillespie has helped with everything plants, remote sensing, and his unbounded enthusiasm was definitely needed to get past some of the hurdles of graduate student life. Kyle Cavanaugh has helped to remind me that not everything on the coast is about salt marshes and to take a larger-scale view.

Next, I have to thank my labmates. I have learned so much about graduate school, research, and life from this amazing group of people. First, to Jim Holmquist who helped me as a graduate student, as a post-doc at UCLA, and, now, as a researcher at the Smithsonian. I was so lucky to have someone like Jim to show me the ropes in my early days at UCLA and am so grateful for all the opportunities that he has provided me since. To Katie Glover, Kate Willis, Marcus Thompson, Scott Lydon, Remi Bardou, and honorary lab-member Jordan Rosencranz, who were like siblings as I got my feet under me for the first few years: I owe you all so much for helping out with field work and lab work and remote sensing. Hopefully we'll end up at Neptune's Net again sometime soon. To Elly Fard, Jessie George, and honorary lab-member Monica Dimson, thank you all for embracing me almost as part of your cohort and as a great friend. I miss you all. Elly, I could not imagine anyone better to be taking on the mantle of the MacDonald lab salt marsh core collection. A huge thank you goes to Lisa Martinez and Elly for their help on Chapters 2 & 3, as well as their help with all other things related to marshes. I also would like to thank post-docs Julie Loisel, Sophie Webber, Simona Avnaim-Katav, Shuheng Li, and Chunyu Dong for all of their guidance and help with my project. It was a pleasure to work with all of you. Finally, to the most recent members of the lab, Jiwoo Han and Ben Nauman, thank you so much for all your help with field work, lab work, and core organization. I wish you the best in the years to come!

As field work and lab work made up a huge part of this dissertation, I have so many people to thank for volunteering their time and expertise. I would like to thank Taylor McCleery, Cameron Powell, Megan Brown, and Mike Fischella for all of their support in the field. I would like to give a special thanks to those undergraduate students who worked on my project with me including Keith Schaffer, Maoqiao Mao, Sam Trumbly, Tongwei Wang, Allison Bell and Tian Gao.

I would like to thank the many labs and collaborators whom I have worked with through this project. I would like to thank fellow UCLA graduate students Avishesh Nuepane and

Kebonye Dintwe for helping me with work in the soils lab. To the salt marsh project collaborators at the USGS, especially Karen Thorne and Chase Freeman, I am very grateful to have been a part of such a large project right out of the gate and to have had the opportunity to learn from accomplished scientists working in the field. I owe a big thanks to salt marsh managers including, but definitely not limited to, Kirk Gilligan, Rick Nye, Mason Hill, and Valerie Vartanian for not only helping me gain access to many of these sites but also for the many insights they provided about their ecosystems.

I have had the pleasure of collaborating with many outside labs during this project, so I would like to extend my thanks to John Southon and the UC Irvine AMS lab staff for all of their help over the years. Thanks to Kat Hargan and the Queen Mary University PEARL Lab for help with diatoms and sediment dating. Thank you to Matt Kirby for all his help in particle size analysis. Thank you to Doug Hammond and Nathaniel Kemnitz at USC for sediment dating as well. And thank you to Christine France and Jenelle Whitman from the Smithsonian Museum Conservation Institute and Smithsonian Ecological Research Center.

I would also like to extend my thanks to all the members of the Smithsonian Coastal Carbon Research Coordination Soils Working Group for their help with developing Chapter 3 as well as for the support and opportunities I have had thanks to my participation in the working group.

Chapter 5 of this dissertation is a version of "Multiple Stressors Influence Salt Marsh Recovery after a Spring Fire at Mugu Lagoon, CA" published 2019 in *Wetlands* with co-authors Jordan Rosencranz, Katherine Willis, Richard Ambrose, and Glen MacDonald. I would like to acknowledge Jordan for his help with field work, data analysis, and preparation of the manuscript. I would like to acknowledge Kate for her contribution to the remote sensing analysis and methods section. I would like to thank Glen and Rich for their contributions to experimental design, help with data analysis, and manuscript preparation.

On a more personal note, I would like to thank Ashley Fent for keeping me sane throughout this process. You have been like a sister to me and I would not have been able to last seven years in LA without our weekly happy hours. I also owe a huge debt of gratitude to the many friends and supporters who formed my UCLA Geography family. First, to the best cohort there ever was: Ashley Fent, Sara Hughes, Taylor McCleery, Sarah Halterman, Lincoln Pitcher, Dimitar Anguelov, Dylan Connor, Tyler Harlan, and Heather Agnew. Thanks also to Chelsea Robinson, fellow marsh-enthusiast Cheryl Doughty, Clare Beer, Sam Nowak, Diane Ward, Junzhe Zhang, Huilin Huang, Dian Tri Irawaty, to name only a few.

I would also like to give a special thanks to the UCLA Geography Department staff who have been so helpful throughout this process and made the department function smoothly. Thanks to Kasi McMurray for solving any and every problem I've ever had. Thanks to Vanessa de la Rosa for all her help with the never ending lab supply needs. Thanks to Jenee Misraje, Rebecca Goodine and Nayla Huq for their tireless work. And thanks to Brian Won and Matt Zebrowski for all things mapping and technical.

Finally, I would like to thank my family. I could not have asked for a more supportive family throughout this process and definitely could not have made it to this point without them. To my mother, Jean Brown, thank you for contributing so much to making sure I got the education that you never had the chance to get. To my brother, Tyson Brown, thank you for paving the way through the PhD process and, quite literally, building the desk I wrote my dissertation on. And to my soon-to-be sister-in-law, Lindsay Golem, thank you for welcoming me to Michigan with open arms and supporting me through this process as a sister long before my brother got around to making it official.

# VITA

## EDUCATION

| | | |
|---|---|---|
| 2014 | UCLA | M.A. in Geography |
| 2012 | University of Denver | B.A. in Geography |

## PEER-REVIEWED PUBLICATIONS

Brown, LN, Rosencranz, JA, Willis, KS, Ambrose, RF, & MacDonald, GM. 2019. Multiple Stressors Influence Salt Marsh Recovery after a Spring Fire at Mugu Lagoon, CA. *Wetlands*, 1-13.

Holmquist, JR, Windham-Myers, L, Bliss, N, Crooks, S, Morris, J, Megonigal, PJ, Troxler, T, Weller, D, Callaway, J, Drexler, J, Ferner , MC, Gonneea, ME, Kroeger, KD, Schile-Beers, L, Woo, I, Buffington K, Breithaupt, J, Boyd, BM, Brown, LN, Dix, N, Hice, L, Horton, B, MacDonald, GM, Moyer, RP, Reay, W, Shaw, T, Smith, E, Smoak, JM, Sommerfield, C, Thorne, K, Velinsky, D, Watson, E, Grimes, KW, & Woodrey, M. 2018. Accuracy and Precision of Tidal Wetland Soil Carbon Mapping in the Conterminous United States. *Nature Scientific Reports*. 9478.

Thorne, K, MacDonald, GM, Guntenspergen, G, Ambrose, RF, Buffington, K, Dugger, B, Freeman, C, Janousek, C, Brown, LN, Rosencranz, JA, Holmquist, JR, Smol, J, Hargan, K, Takekawa, J. 2018. U.S. Pacific coastal wetland resilience and vulnerability to sea-level rise. *Science Advances*, 4(2), eaao3270.

Avnaim-Katav, S, Gehrels, R, Brown, LN, Fard, E, MacDonald, GM. Distributions of Salt-Marsh Foraminifera Along the Coast of SW California, USA: 2017. Implications for Sea-Level Reconstructions. *Marine Micropaleontology*, Volume 131, 25-43.

Rosencranz, JA, Brown, LN, Holmquist, JR, Sanchez, Y, MacDonald, GM, Ambrose, RF. 2017. The Role of Sediment Dynamics for Inorganic Accretion Patterns in Southern California's Mediterranean-Climate Salt Marshes. *Estuaries and Coasts,* 40(5), 1371-1384.

Holmquist, JR, Reynolds, L, Brown, LN, Southon, J, Simms, A, & MacDonald, GM. 2015. Marine Radiocarbon Reservoir Values in Southern California Estuaries: Interspecies, Latitudinal and Interannual Variability. *Radiocarbon*, 57(3), 449-458.

## FELLOWSHIPS, AWARDS AND GRANTS

| | |
|---|---|
| 2017 | Barbara Maida Award, UCLA |
| 2018 | Dissertation Year Fellowship, UCLA |
| 2017 | Sustainability, Environmental Achievement in Leadership (SEAL) |
| 2016 | John A. Black Award, Geological Society of America |
| 2014 | Graduate Research Mentorship, UCLA |
| | Graduate Summer Research Mentorship, UCLA |

2013 Graduate Summer Research Mentorship, UCLA
La Kretz Small Grant, UCLA

## PROFESSIONAL AFFILIATIONS

Smithsonian Institute Coastal Carbon Research Coordination Network, Soils Working Group

Member of: Ecological Society of America, Coastal Estuarine Research Federation, American Association of Geographers, American Geophysical Union, Geological Society of America

## SELECTED CONFERENCE PRESENTATIONS

### Oral Presentations

Brown, LN*, Boyd, B, Chapman, S, Janousek, C, Morris J, Noe, G, Sanderman, J, Spivak, A, Holmquist, JR, Megonigal PJ. Improving blue carbon estimates: best practices for quantifying uncertainty in loss-on-ignition. Coastal and Estuarine Research Federation Conference 2019, Mobile, AL.

Brown, LN*, Thorne, K, Ambrose, RF, MacDonald, GM. Quaternary Histories of Salt Marshes in California Provide Environmental Baselines. Geological Society of America Annual Meeting 2017, Seattle, WA.

Brown, LN*, Holmquist, JR, & MacDonald, GM. A Mid-Holocene Record of Sediment Dynamics and High Resolution Accretion Rates in Coastal Salt Marshes From Southern California. Geological Society of America Annual Meeting 2013. Denver, CO.

### Posters

Brown, LN*, Ambrose, RF, MacDonald, GM. Vulnerability, Residence Time, and Trade-offs Matter in Carbon Storage of California Salt Marshes. American Geophysical Union Fall Meeting 2018, Washington D.C.

Brown, LN*, Ambrose, RF, MacDonald, GM. Regional, Spatial, and Temporal Variations in Vertical Accretion Rates of Coastal Salt Marshes in California. American Association of Geographers Annual Meeting, 2016, San Francisco, CA.

Brown, LN*, Willis, K, Ambrose, RF, & MacDonald, GM. Impact and Recovery Pattern of a Spring Fire on a Pacific Coast Marsh – Observations and Implications for Endangered Species. American Geophysical Union Fall Meeting 2015, San Francisco, CA.

Brown, LN*, & MacDonald GM. A Paleoenvironmental Study of California Coastal Wetlands. American Association of Geographers Annual Meeting 2013. Los Angeles, CA.

# 1. Introduction

Coastal salt marshes in California have experienced alarming changes because of human impacts. For as long as humans have lived in North America, there is evidence that they used and modified coastal salt marsh ecosystems for their benefit (Cole & Wahl, 2000). However, in the 19th and 20th centuries, the arrival of European colonizers brought landscape modification, agriculture, industrialization, and population growth to the California coast which resulted in the loss of 75% of coastal salt marsh habitat within approximately one century (Stein et al., 2014). While much of the remaining salt marsh habitat in the state of California is now protected, the next century will test the resiliency of these highly changeable ecosystems with an increase in temperatures of 2 – 5ºC and increases in sea levels anywhere from one to three meters higher than current levels (Stocker et al., 2013). As the majority of salt marsh habitat in the state lies below three meters in elevation, climate change poses an existential threat to this habitat type.

Salt marsh habitat is highly adapted to change, especially in terms of changes to sea level. Plants in the ecosystem, like the common California salt marsh plant *Spartina foliosa*, are ecosystem engineers that can modify their environment and promote elevation growth. For instance after increases in the frequency or depth of inundation due to sea level rise (SLR) plant productivity and sediment trapping have been observed to increase (Mudd, D'Alpaos, & Morris, 2010). Increases the elevation relative to sea level allows the salt marsh to migrate up through the tidal frame along with the tide. This process also works in reverse. As sea levels fall the growth rate and sediment trapping in the salt marsh decreases and salt marsh plants begin to colonize down into the tidal frame. Such a give and take allows for establishment of an equilibrium elevation facilitated by vegetation which, with gradual changes in sea levels, maintains a sediment platform. In this manner salt marshes established their current extent on the

coast of California as sea levels rose following deglaciation 15,000 – 6,000 years ago (Atwater, Hedel, & Helley, 1977). Over the past 6,000 years of stable sea levels, salt marsh area in the state, too, has remained relatively stable until European colonization and 20$^{th}$ century land use changes.

However, the natural, gradual sea-level changes seen since the last glacial period are much different than the projected drastic changes of a meter or more of SLR by the end of the coming century. The ability of salt marshes to keep pace with SLR is highly system-specific, with some marshes able to maintain habitat with over one centimeter of SLR per year, and other marshes with thresholds of a few millimeters per year (Kirwan & Megonigal, 2013). SLR in California under likely scenarios may range from 0 – 17 mm yr$^{-1}$ in some locations by 2100 (Griggs et al., 2017), which could definitely push many salt marshes past their capacity for adaptation. Additionally, these changes are not likely to be linear over the longer timeframe. Increased temperatures and changes to large scale climate patterns, such as ENSO, could result in more damage to salt marsh habitat during individual flood or storm events than the gradual rise of water levels (Barnard et al., 2019). Under these conditions, it is a reality that salt marsh adaptive capacity will be exceeded and habitat will be lost. This is the case for salt marshes along the US Gulf coast, which face higher relative rates of SLR due to land subsidence and see habitat losses on the scale of a football field every day. In California, SLR has not yet reached such a critical stage, but losses of 100% of coastal salt marsh habitat have been projected by 2100 under high SLR scenarios for the state, with significant conversion of current high and mid marsh habitat to low marsh habitat under more moderate SLR scenarios (Thorne et al., 2018). Salt marshes on the west coast are typically much smaller than salt marshes of the US east and gulf coasts (Dahl, 2011), with less room to migrate inland, and may not be able to regain much of the

habitat lost on the seaward margin by habitat gained on the landward margin due to human development (Doody, 2017; Torio & Chmura, 2013). Therefore, the way in which stakeholders and land managers approach preparing their ecosystems to deal with coming climate change will make a huge impact on the amount of salt marsh habitat which remains by 2100.

Monitoring of salt marsh resiliency to SLR can be done in part by assessing how well the salt marsh is maintaining elevation through sediment accretion. Sediment accretion rates are correlated with rates of SLR, but many other factors – such as biomass decay, sediment compaction, subsidence, edge-erosion, potential for migration etc. – can mean that rates of sediment accretion do not completely capture the overall stability of a salt marsh vis-à-vis the rate of SLR. Additionally, because of the adaptive capacity of vegetation productivity and sediment trapping to the rate of SLR, past accretion rates can be very poor predictors of future accretion rates. Past rates of accretion reflect system behavior given past rates of SLR, plant productivity, sediment availability, and hydrologic state. Changes to one of these factors, such as SLR, will in turn change the others. Therefore, while past rates of accretion provide important insight into prior system behavior, they should be used only as the basis of a suite of ecosystem parameters which can be monitored to assess overall system function. But sediment accretion data for salt marshes currently are geographically limited on the US Pacific coast and are needed to fill a data-gap in the understanding of salt marsh accretion for the US. These data can inform stakeholders and managers as to specific vulnerabilities a salt marsh site might have to SLR adaptation and help inform decision-making to preserve salt marsh habitat.

While anticipated rates of SLR present a challenge for natural adaptive capacity, tidal marsh habitat protection and restoration are a management priority for the state. Leveraging ecosystem services, such as water filtration, habitat for endangered species, reduction of storm

surge, nurseries for fisheries, and direct mitigation of climate change through burial of carbon in salt marsh soils presents one potential avenue to incentivize and fund protection and restoration efforts (Barbier et al., 2011). Valuation of carbon storage and sequestration for tidal marshes, in particular, has garnered interest and inspired much research (Callaway et al., 2012; Chmura, 2013; Hopkinson, Cai, & Hu, 2012). Coastal vegetated habitats (CVHs) such as salt marshes, mangroves, and seagrasses have the potential to sequester carbon at rates an order of magnitude higher than terrestrial forests (Mcleod et al., 2011; Nellemann et al., 2009), resulting in these geographically limited ecosystems playing a significant role in global carbon cycling. In order to leverage blue carbon ecosystem services to promote habitat protection and restoration, however, net impacts of carbon removal must be measured and verified. Some protocols exist for measurement and verification of greenhouse gas reductions and removal by wetlands in the state of California through the Verified Carbon Standard (Verified Carbon Standard: A Global Benchmark for Carbon, 2015) and American Carbon Registry (American Carbon Registry, 2017), voluntary carbon markets. But significant logistical, political, administrative, and ethical questions remain to be answered as coastal marsh ecosystems are widely integrated into carbon markets (Vanderklift et al., 2019). Establishment of standard measurement protocol and baseline estimates of carbon stocks and sequestration rates for state salt marshes are steps critically needed to evaluate the potential for using blue carbon valuation to fund salt marsh protection and restoration in the state of California.

Additionally, there are a great many stressors which will arise with climate change outside of accelerated SLR. Human population density in the state of California is clustered around coasts, meaning that the effects of land use change and pollution are also concentrated in this this area. As such, many so-called ‘pristine’ salt marsh sites in the state have suffered from

changes to hydrology, sedimentation, nutrient flow, subsidence from oil and water extraction, and other human-caused stressors which are indirectly related or unrelated to the effects of climate change. The presence of multiple stressors on ecosystems has been shown to reduce overall ecosystem resiliency. As temperatures and sea-levels rise, increasing system resiliency is often a best management practice for stakeholders and land managers. The challenge of anthropogenic climate change is in preparing already-stressed systems to respond to disturbance or perturbations outside of the window of natural variability.

With these factors in mind, the guiding questions behind this dissertation are:

1) What do past accretion rates reveal about the capacity for California salt marshes to keep pace with SLR?
2) What are the potential contributions or losses in the ecosystem service value of carbon storage?
3) How will multiple stressors influence salt marsh response to disturbance?

The dissertation is separated into four chapters. In Chapter 2, **Sediment Accretion in California Salt Marshes**, the results of radiometric dating of sediment cores are presented to provide baseline vertical sediment accretion over the past few hundred years of accelerating SLR. These rates of sediment accretion are compared to marsh elevation, rates of SLR, rates of subsidence, and other environmental factors to determine the most important controls on California salt marsh accretion in the studied timeframe. Chapter 3**, Improving Blue Carbon Estimates: Best Practices for Quantifying Uncertainty in Loss-on-Ignition**, examines the error and uncertainty associated with the most widely-used, cost-effective method of making estimates of soil carbon storage in salt marshes for ecosystem service values. Then, the results of this work are applied in Chapter 4, **California Salt Marsh Blue Carbon**, to estimate salt marsh

storage and sequestration rates across the state and examine what contributes to higher salt marsh carbon storage. Finally, after an unusual disturbance due to a fire in 2013, Chapter 5, **Multiple Stressors Influence Salt Marsh Recovery after a Spring Fire at Mugu Lagoon, CA**, highlights the challenges which salt marshes face not only from accelerated SLR but from long-term and episodic disturbance under multiple climate change stressors and is a re-produced version of an article I published in the journal *Wetlands* in 2019 under the same title.

Quantification of the historic state of salt marsh sediment accretion, contribution to ecosystem services, and early monitoring of climate change impacts to salt marsh ecosystems will better enable stakeholders and managers to make evidence-based, informed decisions in the face of climate change uncertainties. The data collected in this dissertation have been used (Thorne et al., 2018) and will continue to be useful for models of ecosystem vulnerability, ecosystem service value, and as a record of early climate change impacts on the coastal salt marshes of the California coast.

# 2. Sediment Accretion in California Salt Marshes

## 2.1 Abstract

Salt marshes maintain a dynamic equilibrium with changing sea-levels by variability in sediment accretion rates. However, long-term accretion is relatively understudied in California salt marshes. This chapter uses radiocesium ($^{137}Cs$), radiolead ($^{210}Pb$), and radiocarbon dating ($^{14}C$) to estimate vertical accretion rates in 13 salt marsh sites along the California coast and compares these new data to a review of published accretion rates from salt marshes around the globe. Linear and polynomial regression between historic rates of SLR and local rates of SLR plus subsidence (RSLR) is conducted to determine ecosystem state and assess which individual marsh sites are more likely at risk from accelerated SLR. Forward and backward stepwise multiple regression of accretion rates and environmental parameters is used in an attempt to broadly determine the most important controls on accretion rates. California salt marsh sediment accretion averages at $3.28 \pm 0.2$ mm $yr^{-1}$ over the past several decades to centuries. Accretion rates are highest in sites with moderate rates of RLSR (4 – 6 mm $yr^{-1}$) and have the most positive linear response to increases in rates of SLR in the low marsh elevations. Salt marshes which are facing the highest rates of RSLR are those which also exhibit some of the highest rates of sediment accretion, an indication of the adaptive capacity of California salt marshes. But other sites have accreted sediment at much lower rates than rates of SLR and may be at considerable risk from accelerated SLR or local subsidence. Multiple regression shows that elevation, diurnal tidal range, SLR, subsidence, organic matter content, and mean annual temperature are the factors with the most significant effect on accretion rates in this dataset.

## 2.2 Introduction

Coastal salt marsh ecosystems exist because of their unique ability to adapt to changes in sea-level by variability in rates of vertical accretion and horizontal migration (Morris, Sundareshwar, & Nietch, 2002). Their ability for vertical accretion, however, is limited by the availability of mineral material, rate of biomass production, and the rate of sea-level rise (SLR; Kirwan et al., 2010; Kirwan & Megonigal, 2013). Horizontal migration is limited by topography and land use. With accelerated SLR caused by anthropogenic climate change over the next century, limits to landward migration in California salt marsh sites will likely lead to loss of habitat (Craft et al., 2009; Crosby et al., 2016; Schile et al., 2014; Stralberg et al., 2011). For the past 6,000 years global absolute SLR, or eustatic SLR, remained around 1 mm $yr^{-1}$, but that rate is now near 3 mm $yr^{-1}$ due to greenhouse gas warming in the past 200 years (Church & White, 2006). Eustatic sea level changes are expressed differently depending on a number of local factors, such as geomorphology, uplift and subsidence, and offshore ocean circulation, for each coastline. Some areas – like the US Gulf Coast – experience local rates of relative SLR two times greater than the eustatic trend and other areas – like the northwest US coast – can experience local drops in sea-levels even while eustatic sea levels are rising. Over the next 100 years, eustatic sea levels will rise 1 – 3 m or more (Griggs et al., 2017; Stocker et al., 2013). As many salt marshes are already experiencing massive habitat loss under current rates of SLR (Blum & Roberts, 2009; Reed, 1995), increasing rates of eustatic SLR on the magnitude projected indicate that the capacity for sediment accretion in all salt marshes is at risk.

When monitoring the potential vulnerability of any salt marsh system to accelerated SLR, collection of vertical sediment accretion data allows for a baseline assessment of system performance. Most salt marshes show a positive correlation between relative SLR and the rate of

vertical accretion (Craft, 2012). Marshes which may be losing habitat due to rising tides and subsidence can be distinguished from those that have adequate sediment supply and productivity to keep pace with SLR (Craft et al., 2009; Crosby et al., 2016). Vertical accretion data can even be used to distinguish areas of salt marshes which are experiencing lower rates of accretion from areas which are more robust within the same marsh (French, Spencer, Murray, & Arnold, 1995). The collection of local rates of vertical accretion over multiple elevations in a single salt marsh site are therefore critical to understanding how the system is preforming under current and historic conditions. Baseline estimates can then be used, along with other ecosystem data, to make projections about how the ecosystem will perform under accelerated SLR conditions (Schuerch, Vafeidis, Slawig, & Temmerman, 2013; Swanson et al., 2014; Thorne et al., 2018). Baseline data for many of the large salt marshes along the US East and US Gulf coasts have been collected over the past 30 years. Marshes on the west coast, however, are typically much smaller due to the emergent topography (Dahl, 2011; Thorne et al., 2018), have not yet experienced accelerations in SLR on the magnitude of some of the better-studied marshes, and have a much shorter, more limited record of baseline data to draw from (Bear, 2017; Callaway et al., 2012). As accelerated SLR over the next century becomes more of a threat to Pacific coast salt marshes, baseline data on ecosystem function are critical to inform stakeholders and managers how best to make decisions over the coming decades.

California salt marshes, in particular, may respond to changes in SLR quite differently than marshes elsewhere for which much of the baseline data are currently available. The topography of California leaves little area available for marshes to migrate inland as seas rise, the natural response of salt marshes to SLR beyond the capacity of vertical accretion. Urbanization of the California coast – often right up to the very edge of the salt marsh itself – has led some to

predict that salt marsh habitat will be "squeezed" out of existence by SLR on the seaward margin and human development on the landward margin (Thorne et al., 2018; Torio & Chmura, 2013). Their already small areal extent and limited space for inland expansion makes vertical accretion key for US west coast salt marsh survival. Therefore, while west coast SLR may not be of equal magnitude currently, the smaller areal extent and lack of available area for expansion inland indicates that west coast salt marshes are just as endangered as the east coast counterparts but have a much shorter history of data collection.

This chapter presents the results of three measures of vertical accretion rates across 13 salt marsh sites along the California coast. More than 100 sediment cores were collected for this project over a timespan of five years (Figure 2.1). Fifty cores were chosen for high-resolution radiometric analysis based on the location and quality of the core with the aim of creating a database of sediment accretion rates from low, mid, and high elevations at each salt marsh site. A total of 32 cores were dated for radiocesium ($^{137}Cs$), 36 of cores were dated for radiolead ($^{210}Pb$), and 28 cores were dated with radiocarbon ($^{14}C$); 14 cores were successfully dated with all three methods. Sediment accretion rates were calculated for each of these methods and were compared to a review of published accretion rates from over 50 different studies. This chapter aims to answer the questions:

1) How do the newly measured and previously published accretion rates in California compare to published rates in the continental US and around the globe? And what are geographic trends in the state as well as in inter- and intra-site sediment accretion across California?
2) What is the relationship between SLR and sediment accretion for California salt marshes?

3) What controls sediment accretion in California?

This work will contribute to the understanding of how California salt marsh accretion responded to historic SLR relative within the state and relative to other marshes from around the world. Some of this baseline data has already contributed to studies of salt marsh vulnerability to accelerated SLR (Thorne et al., 2018) and it will continue to be useful in future studies, such as those which look at how sediment accretion contributes to ecosystem services like carbon storage (see Chapter 3).

### *2.2.1 Measuring Sediment Accretion*

There are multiple ways of measuring vertical sediment accretion. They range from short-term measures, like sediment traps or marker horizons that monitor accretion over the period several months or years, to long-term estimates using radiocarbon dating ($^{14}C$) to estimate accretion over several centuries. Although all measures generally use the depth of sediment accumulated over the time period in which accumulation took place to calculate an average rate of accumulation, local measures of vertical accretion can vary quite widely based on the time frame over which or how the accretion was observed (Mudd, Howell, & Morris, 2009). Across all ecosystem types, most methods that measure sediment accumulation over shorter time periods report higher rates due to the fact that long-term ecological processes such as organic matter decay and sediment compaction have not yet acted on the soil column. Congruently, the more time that these processes have to act upon the soil column, the smaller the estimated accretion rates will be. The best way to compensate for observation bias is to compare accretion rates to ecological processes across the same timescale. For that reason, I review published data which uses marker horizons on the scale of 1 to 30 years, but I have focused on radiocesium ($^{137}Cs$),

observed over 60 years, radiolead ($^{210}$Pb), observed over 100 – 200 years, and $^{14}$C, observed over hundreds of years or more, as these methods operate on timescales similar to changes in SLR.

The use of $^{137}$Cs as a chronomarker is fairly common in sediment accretion studies (Callaway et al., 2012; Callaway, Nyman, & DeLaune, 1996; Chmura, Helmer, Beecher, & Sunderland, 2001; Frouin et al., 2007; Neubauer, Anderson, Constantine, & Kuehl, 2002; Roberts et al., 2015; Thom, 1992). $^{137}$Cs is not a naturally occurring isotope but was released during testing of atomic weapons starting in 1950 and is first detectable in sediments by 1954 (Ritchie & McHenry, 1990). Prior to the signing of the Nuclear Test Ban Treaty in 1963, many countries detonated their reserves of atomic weapons. This large release of $^{137}$Cs into the atmosphere led to global fallout, with deposition into lakes and wetlands that concentrated fallout into a distinct layer corresponding to the time of deposition. It was generally assumed that little natural circulation of $^{137}$Cs occurred in the sediment column, with some sites even showing distinction between peaks of $^{137}$Cs released in the 1959 and 1963 detonation periods (Feijtel, DeLaune, & Patrick, 1988; Ritchie & McHenry, 1973). However, a recent review of $^{137}$Cs-dated sediments from salt marsh environments shows that the mobility of $^{137}$Cs may be much greater than previously estimated (Drexler, Fuller, & Archfield, 2018). Because $^{137}$Cs was not deposited evenly across the globe, areas which experienced less initial fallout have failed to register a distinct peak more and more frequently in the past two decades. Mobility of $^{137}$Cs and the amount of decay which $^{137}$Cs has undergone since 1963 decrease the reliability of $^{137}$Cs as a chronomarker, especially for areas that had low initial $^{137}$Cs fallout. The coast of California received lower rates of $^{137}$Cs fallout and thus experiences many of the issues of detection and mobility of $^{137}$Cs in sediments. When $^{137}$Cs is detectible, it is a useful indicator of average

accretion over the past 60 years. As there is large uncertainty associated with this method, $^{137}Cs$ is best used in conjunction with other measures of sediment accumulation.

The most frequent companion to $^{137}Cs$ for chronological purposes is $^{210}Pb$ (Oldfield et al., 1979). This indicator, rather than being a single horizon which is identified as corresponding to a date, relies on the radiometric decay of $^{210}Pb$ and observations from a stratigraphic collection of sediment samples to calculate the age of sediment down a column and is often a more robust method to some of the uncertainty associated with $^{137}Cs$. $^{210}Pb$ naturally occurs as a decay product from two sources: 1) within the sediment column as a decay product of uranium, and 2) within the atmosphere as a decay product of radon. Atmospheric $^{210}Pb$ is deposited during precipitation, enriching surface sediments *in situ* as well as via deposition of $^{210}Pb$-enriched sediments in runoff. These two sources of $^{210}Pb$ mean that there is an expected background, or supported, level of $^{210}Pb$ in all sediment ($^{210}Pb_{supp}$), but for sediments at the surface excess $^{210}Pb$ ($^{210}Pb_{ex}$) arrives from the atmosphere and runoff. When sediments are buried and cut off from the source of $^{210}Pb_{ex}$, all $^{210}Pb$ in the sediment column decays at the same rate. However $^{210}Pb_{supp}$ is replaced in the sediment column, remaining at an equal level, while $^{210}Pb_{ex}$ can be observed decaying to zero. $^{210}Pb$ dating works by measuring $^{210}Pb$ activities in multiple sediment horizons from the surface to the depth at which $^{210}Pb_{ex}$ is no longer detectable. An estimation of the background level of $^{210}Pb_{supp}$ then allows for calculation of sediment accumulation based on the known rate of radioactive decay for $^{210}Pb_{ex}$.

Two common linear models are applied to calculate the age of the sediment column (Appleby & Oldfield, 1978). The first is the Constant Initial Concentration (CIC) model which assumes that the initial concentration of $^{210}Pb$ deposited on the surface is constant throughout time and holds the rate of accretion constant. The second model, the Constant Rate of Supply

(CRS) model, assumes that there is a constant level of $^{210}$Pb in all sediment being added to the marsh surface and any increases in concentration indicate an increase in sediment mass being added to the surface, or a change in the rate of sediment accretion. When modeling salt marsh accretion, the CRS model is more frequently employed because of this ability to vary the rate of sedimentation (Sanchez-Cabeza & Ruiz-Fernández, 2012). The CRS model has been used to calculate all accretion rates measured by $^{210}$Pb reported in this study.

Another radiometric dating method which is occasionally used to determine accretion rates in salt marshes is $^{14}$C dating. This method relies on radioactive decay of naturally occurring $^{14}$C in biological material. $^{14}$C is created in the atmosphere due to solar bombardment of nitrogen. Plants and animals then absorb $^{14}$C into their tissues while they actively exchange carbon with the atmosphere. Once the organism dies, the exchange with the atmosphere halts and the amount of $^{14}$C is fixed it its tissues. The amount of $^{14}$C in organic material will correspond to the approximate time over which that organism has been undergoing radioactive decay, with calibration for changes in the atmospheric level of $^{14}$C over time. $^{14}$C dating is effective time periods of 40,000 to 200 years before present. For samples over 40,000 years old, the length of approximately seven half-lives of $^{14}$C, the concentration of $^{14}$C is too low for accurate age estimates. And in the past 200 years, fossils fuel combustion and detonation of atomic weapons released or generated $^{14}$C in the atmosphere, altering the naturally occurring atmospheric $^{14}$C concentration. Therefore, as the initial concentration of $^{14}$C in recent biologic material is unpredictable, $^{14}$C dating is not effective for samples less than 200 years old.

Using $^{14}$C to measure sediment accretion presents a challenge regarding the timespan of observation. Sediment records which cover more than 200 years of accretion have undergone substantial organic matter decay and sediment compaction. This results in measures of accretion

much lower than rates of accretion which are taken over portions of the sediment record not yet subject to long-term decay and compactions processes. $^{14}C$ dates however can reveal some information about the age of a salt marsh as well as how much decay and compaction has taken place over the past several hundred or thousand years. When combined with $^{137}Cs$ and $^{210}Pb$ dates, a long-term age-depth model can be constructed for the sediment column, allowing for a reconstruction of any significant changes in deposition rates.

## 2.3 Methods

### *2.3.1 Review of Published Accretion Rates*

Using the Web of Knowledge, I searched for '"accretion rate" AND "salt marsh"' and returned 53 results published from 1994 to 2019. From these papers, all reported accretion rates were recorded with relevant locations and methods used. But, for ease of analysis, an average reported rate of accretion was calculated and minimum and maximum reported rates were calculated for each study without separation of data by site attributes or methods used (for studies which used multiple methods). For salt marsh sites on the US Pacific Coast, additional accretion data was gathered from known sources. Data for the Pacific Coast were averaged for each site and each method, not averaged by study as was done for the global analysis, for a total of eight entries from three different studies (Buffington, 2017; Callaway et al., 2012; Mudie & Byrne, 1980). All data were summarized to calculate average accretion rate by scale (continent, region, state, location) with standard errors (Appendix Table 2.1). A subset of studies which relied on only one method to measure accretion were used to compare reported accretion rates by method of measurement with a one-way analysis of variance (ANOVA) and post-hoc Tukey test (Figure 2.2).

### *2.3.2 Site Descriptions*

Large salt marsh complexes in California are primarily located in the San Francisco Bay area or the Humboldt Bay in the northern part of the state. However, there are many small salt marshes along the outer coast. For this study, I selected three salt marshes from Humboldt Bay, two salt marshes from the San Francisco Bay area, two salt marshes from the Northern and Central Outer Coast, and six salt marshes from Southern California (Table 2.1). All the marshes in the study are meso- to hypersaline. Salt marsh vegetation in California is fairly similar across the state. Distinct zonation can be observed in some salt marsh sites based on abiotic tolerances for salinity and inundation as well as interspecific competition (Pennings & Callaway, 1992; Zedler, 1977). Salt marshes in California are also characterized by the degree of human impact. Over 75% of native salt marsh habitat has been drained, reclaimed, or destroyed through human activities since 1800 (Stein et al., 2014). Much of the remaining habitat is preserved either through the Clean Water Act or as wildlife refuges for the benefit of migratory birds (Zedler & Kercher, 2005). There are several endangered species which are endemic to California salt marshes including birds such as the Ridgeway's Rail (*Rallus obsoletus*) and Belding's Savannah Sparrow (*Passerculus sandwichensis*) as well as some native plants like the Salt Marsh Bird's Beak (*Cordylanthus maritimus*).

The steep geomorphology of the Pacific coast and the history of habitat loss and population growth in California have resulted in very limited habitat within the tidal frame. Salt marsh habitat may span multiple horizontal kilometers along the East and Gulf coasts whereas the same vertical elevation change in California occurs in 10s to 100s of meters. Terrestrial sediment delivery, especially for marshes in Southern California, often arrives via rare, large precipitation events. It is not unusual that the majority of terrestrial sediments may be delivered

in one storm over the course of a decade. California marshes are also more frequently the geologic remnant of large estuaries with once sediment-rich waters which sustained their growth until damming, channelization, infilling, or diversion of rivers and creeks in the late 19th and 20th century (Brownlie & Taylor, 1981). Pacific coast geomorphology, the naturally erratic freshwater sediment delivery, and hydrologic modification by humans has resulted in comparatively small salt marshes which rely largely on sediment resuspension and marine sediment sources to maintain vertical accretion.

#### 2.3.2.1 Humboldt Bay

Humboldt Bay is the second largest bay on the coast of California and was once the site of 28 $km^2$ of salt marsh habitat (Barnhart, Boyd, & Pequegnat, 1992). The region has mild, dry winters and cool, wet summers with very little annual seasonality. Unlike San Francisco Bay, Humboldt Bay has no large freshwater tributaries and is fed only by Jacoby Creek, Freshwater Creek, and Salmon Creek which collectively drain an area about 578 $km^2$ in size. Precipitation events drive runoff in the creeks and sloughs that feed Humboldt Bay. The bay itself was likely formed as sea levels rose following deglaciation between 15 – 5 thousand years ago and the valleys from those three small creeks were joined together (Barnhart et al., 1992). At times in the past Mad River discharged into Humboldt Bay (likely forming what is presently known as Mad River Slough) but for the past 2 to 3000 years or more there has been no connection between Mad River and Humboldt Bay. Limited freshwater input to the bay means that the majority of sediment for salt marsh habitat must come from bay or marine sources.

Tidal marsh habitat in Humboldt was drastically reduced in the late 19th and early 20th centuries after European colonization. Settlers arrived after 1850 and began to dyke and drain marshland for agricultural land and pasture. The Northwestern Pacific Railroad finished

construction in 1901 around the bay and, along with the construction of the Pacific Coast Highway in 1927, served to dyke much of the remaining marshland. Currently, there are approximately 4 $km^2$, or 14% of the original tidal marsh, remaining in Humboldt Bay (Barnhart et al., 1992). Other human impacts to marshes in Humboldt Bay include the introduction of *Spartina densiflora*, a South American variation of the native *Spartina foliosa*, most likely by the timber trade between Chile and Humboldt. This invasive *S. densiflora* displaces native *S. foliosa* and *S. pacifica* with much larger and more competitive seeds. It occupies most of the mid-marsh elevations in Humboldt Bay and has been shown to increase below-ground biomass in sandy soils to expand potential available habitat (Castillo, Grewell, Pickart, Figueroa, & Sytsma, 2016), but actually shows lower net primary productivity than native vegetation (Lagarde, 2012). Low and high marsh areas typically are dominated by *Salicornia pacifica*. Treatment for the eradication of *S. densiflora* is ongoing (Pickart, 2012).

Four salt marshes in Humboldt Bay were selected for sediment coring. In the northern bay (Arcata Bay), Mad River Slough occupies what once would have been where Mad River discharged into Humboldt Bay. Mad River Low lies at the mouth of the slough on the edge of Arcata Bay and is mostly a low marsh plain dominated by *S. densiflora* (Appendix Figure 2.1). The Mad River High site occupies and island slightly upstream within the slough, although it is still tidal and saline. Dominant vegetation on the Mad River High site is *Distichlis spicata* and *Frankenia grandifolia* likely due to its higher position within the tidal frame. Sites in the South Bay of Humboldt also are also islands within the bay entrance of two separate sloughs: White Slough (Appendix Figure 2.2) and Hookton Slough (Appendix Figure 2.3) are both dominated by *Salicornia pacifica.*

#### 2.3.2.2 San Francisco Bay

The San Francisco Bay is the largest bay on the west coast of North America and once had an estimated 1400 $km^2$ of tidal marshlands (Atwater et al., 1979). Mean annual temperature is slightly higher in San Francisco Bay than it is in Humboldt Bay, but the region still experiences cool, wet winters with mild, dry summers. Reclamation, conversion of tidal marshland into salt ponds, and mining drastically transformed San Francisco Bay tidal marshes over the past century and a half, with some estimating 90 – 95% losses in the original marsh habitat and approximately 75 $km^2$ of new marshes built from sedimentation arriving from goldmining and farming (Atwater et al., 1979). Like Humboldt Bay, San Francisco Bay likely formed with SLR following deglaciation. The Sacramento and San Joaquin river valleys filled to the east, with South San Francisco Bay filling slightly later. Once SLR decreased, marshes began to fill in these large bays until there was proportionally more area of tidal marsh than open water. There is significant geologic evidence of subsidence in the Bay Area because of regional tectonics (Atwater et al., 1977) which continues to affect many of the salt marshes in the area today (Watson, 2004).

There are a mix of salt, brackish, and freshwater wetlands in San Francisco Bay. I selected two sites in the Bay which are old and relatively undisturbed salt marsh in the bay (Byrne et al., 2001; Watson, 2004), because of freshwater input from streams and seasonal runoff, have salinities ranging from nearly fresh up to 30 parts per thousand but are mainly dominated by salt marsh species such as *S. pacifica* and *S. foliosa*. The Petaluma River discharges into the San Francisco Bay from the north. Petaluma salt marsh (Appendix Figure 2.4) fringes the edge of the Petaluma River where it enters into San Pablo Bay. Petaluma marsh is dominated by *S. pacifica* and *D. spicata* at the highest elevations and a mix of *S. foliosa* and

*Schoenoplectus spp.*. In the South Bay, Triangle Marsh (Appendix Figure 2.5) fringes Coyote Creek as it enters into the bay not far from the mouth of the Guadalupe River. Triangle Marsh is dominated by a mix of *S. pacifica and S. foliosa* with *Schoenoplectus spp.* growing along the channels. This marsh once was part of a much larger marsh, known as Alviso Salt marsh, which was drained and is now used for salt evaporation pans. A commuter railway, constructed not far from Triangle Salt marsh, and the San Jose Sewage Treatment facility, built upstream from the salt marsh, have likely impacted the sedimentation regime and productivity of this salt marsh over the past several decades (Watson, 2004). Approximately 100 cm of subsidence occurred in the area of Triangle Marsh from 1920 to 1970 due to hydrologic pumping, followed by about 5 mm $yr^{-1}$ of uplift in the 1990s as groundwater levels rebounded (Watson, 2004).

#### 2.3.2.3 Northern and Central Outer Coasts

Northern and Central California outer coastal salt marshes experience similar climate as those marshes in San Francisco Bay, but they are distinguished from these marshes by their size and position on the outer coast. Most salt marshes on the outer coast of California formed at the mouth of estuaries and are protected by small bays and lagoons. The topographic relief of the California coast means that salt marsh species generally cannot establish without some sort of protection from the tide. These conditions result in isolated pockets of salt marsh which are about 1 $km^2$ in size or even less.

North of San Francisco Bay, Bolinas Lagoon (4.4 $km^2$) is protected by a sand spit which is the remnants of what was once likely an estuary (Appendix Figure 2.6; Giguere, 1970). In the late 20$^{th}$ century, there was some concern that increased sedimentation due to Redwood logging of the slopes surrounding Bolinas Lagoon was causing infilling. However studies of the sediment

record indicate that increased sediment rates were most likely driven by subsidence associated with the 1906 earthquake along the San Andreas Fault. This would have led to a vertical displacement of approximately 45 cm which would have increased rates of erosion from the surrounding areas and increased deposition in the lagoon. Increased area in the tidal prism due to the drop, however, meant that these increases in sedimentation would not lead to infilling of the lagoon (Byrne et al., 2005). Much of the drainage into Bolinas Lagoon arrives from small gulches which drain the 44 $km^2$ watershed, with half of the freshwater input arriving from Pine Gulch Creek, a permanent tributary. Salt marsh habitat is dominated by *S. pacifica* and *D. spicata* with some *S. foliosa*.

South of San Francisco Bay, Morro Bay is another small lagoon protected by a sand spit with approximately 2 $km^2$ of deltaic salt marsh habitat where Los Osos Creek and Chorro Creek enter the bay (Gerdes, Primbs, & Browning, 1974). The two creeks have a large drainage basin of approximately 200 $km^2$ (Appendix Figure 2.7). Historically, Morro Bay was a natural bay and received freshwater input from Morro Creek, Chorro Creek and Los Osos Creek. Morro Creek was diverted around the bay in the 20$^{th}$ century. The Army Corps of Engineers closed the northern entrance to the lagoon in 1936, and now only a single entrance to the bay remains. Dredging occurred in the mid 20$^{th}$ century to create a harbor in the lagoon. The salt marsh at Morro Bay is dominated by *S. pacifica* and is one the three sites in this study (Mad River Low, Morro, and Mugu) which do not have any *S. foliosa* present.

#### 2.3.2.4 Southern California

Southern California salt marshes have a relatively different climate from those marshes in the central and northern part of the state. Summers are warmer and dry and winters are mild and

moist, but not as wet as to the north. Annual precipitation for some sites is less than half of precipitation for more northerly sites. This often leads to extended periods of hypersalinity, especially in the high marsh (Zedler, Covin, Nordby, Williams, & Boland, 1986). I selected six salt marsh sites in Southern California for analysis.

Mugu Lagoon (Appendix Figure 2.8) receives freshwater input from Calleagus Creek and has 1 $km^2$ of salt marsh habitat. Like Morro Bay, the salt marsh area is dominated by *S. pacifica* and has little *S. foliosa* present at the site (Onuf, 1987). Mugu Lagoon was a true estuary before the channelization of Calleagus Creek in the late $19^{th}$ century (MacDonald, 1976). The watershed of Calleagus Creek is primarily agricultural and has delivered large amounts of sediment, fertilizer, and pesticides into Mugu Lagoon. Seal Beach (Appendix Figure 2.9) is a lagoon south of Los Angeles which was once part of the Santa Ana and San Gabriel River estuaries (Brownlie and Taylor, Stein 2007), but both rivers were channelized and diverted around the Seal Beach salt marsh in the $20^{th}$ century (Brownlie & Taylor, 1981). Seal Beach therefore has no freshwater input. The watershed of Seal Beach is densely urbanized, with little to no available habitat for landward migration. Additionally, because of water and oil withdrawal in the region, the land around the marsh is subsiding at a rate of about 4.4 mm $yr^{-1}$ (Bawden, Thatcher, Stein, Hudnut, & Peltzer, 2001). Upper Newport Bay (Appendix Figure 2.10) approximately 20 km south of Seal Beach similarly is subsiding at a rate of about 2.4 mm $yr^{-1}$ (Bawden et al., 2001). Newport Bay is fed by the San Diego Creek from a watershed of 320 $km^2$. The bay is the remnants of what once was a canyon before it was inundated by rising seas. Prior to European settlement, there was no large river which drained into the bay and San Diego Creek emptied into an ephemeral lake which was prevented from draining into the ocean due to a ridge along the bay. As agriculture developed in the region, San Diego Creek was diverted to serve as drainage for

irrigation starting in 1915 and expanding with agricultural growth throughout the early- to mid-20th century. The channels created in this process are eroding rapidly and have necessitated frequent dredging of Newport Bay as a result (Trimble, 2003). The marsh in Newport Bay is found along the edges of the creek, with a majority of the salt marsh area sheltered from the outer coast in the upper bay. *S. pacifica* and *S. foliosa* are both present and dominate the high and low elevations of the marsh, respectively.

Mission Bay (Appendix Figure 2.11) is a very small (<0.1 $km^2$) salt marsh which is likely the remnants of the San Diego River Estuary. As sedimentation increased in Mission Bay following cattle grazing after European occupation, the Army Corps of Engineers channelized and diverted the flows of the San Diego River to bypass Mission Bay in 1956. This marsh hosts *S. pacifica* and *S. foliosa*. Finally, the marsh at Tijuana River Estuary (Appendix Figure 2.12) is a large complex with no major embayment that is more of an intermittent estuary than a true estuary, as streamflow of the Tijuana River is highly variable (Zedler, Nordby, & Kus, 1992). The salt marsh can be divided into the southern, restoration salt marsh sites and the remaining northern arm of the original estuary complex, which is where I collected sediment cores. In the late 20th century, the main estuary channel was closed to tidal influence and the estuary suffered from several periods of hypersalinity before tidal flushing was reestablished. Tijuana River's watershed is approximately 4,500 $km^2$, most of which is Mexico. The marsh is co-dominated by *S. pacifica* and *S. foliosa.*

### *2.3.3 Study Design*

At each of the 13 salt marsh sites examined in this study, at least two sediment cores were taken. Coring sites were selected with the aim of capturing elevation differences in the salt

marsh; change in dominant vegetation type, with *S. foliosa* being indicative of lower elevations and *S. pacifica* being indicative of higher elevations, was used to differentiate low elevation habitat from high elevation while in the field. Handheld GPS locations were taken using a Garmin GPSMAP® 62s with an average of 9 m accuracy. These GPS positions were compared to coastal digital elevation models (DEMs) produced by the NOAA's National Centers for Environmental Information (NCEI) to obtain estimates of relative elevation differences of site locations (see page 27 for references). At each site, dominant vegetation types were identified and described. Sediment cores were taken using a Russian Auger, which minimizes compaction during the coring process. Sediment cores were taken in one meter lengths and extracted in the field. A preliminary core description was made and then verified later in laboratory analysis. Cores were then wrapped in plastic wrap and aluminum foil before being transported to UCLA where they were stored in a cold room at 4ºC until analysis. Most cores were refrigerated within 48 hours, although due to transportation time, some cores from Northern California may have been stored in a cool location for up to one week before being refrigerated.

### *2.3.4 Stratigraphic Analysis*

Sediment cores were subsampled at one centimeter intervals and loss-on-ignition (LOI) was conducted. Samples of one cubic centimeter were taken using a syringe barrel, dried in an oven at 110 ºC for at least 12 hours before being weighed for bulk density ($g/cm^3$; BD). Samples were then ignited at 550ºC for 4 hours, re-weighed for organic matter (SOM) loss (Heiri, Lotter, & Lemcke, 2001). An average value for BD and SOM was calculated for each core over the first meter of depth or, for cores which were less than one meter in length, to the maximum core depth.

### *2.3.5 Gamma Counting*

Based on estimates of known accretion rates for California salt marshes, a sampling strategy was designed for each core which aimed to capture the 1963 $^{137}$Cs peak as well as capture $^{210}$Pb activity from the surface down to depths where $^{210}Pb_{supp}$ was stable. For the first round of samples, approximately eight to ten individual samples were selected. If it was not certain that the first round of sampling had reached the level of $^{210}Pb_{supp}$ or, if there was a need for higher resolution sampling based on the returned activities, a second round of 2 – 4 samples extended the record further down the core as needed or filled gaps in the record. For each sample taken, approximately 2 – 6 $cm^3$ (depending on sediment density and availability) was measured for radioactivity. After samples were extracted, they were dried in an oven at 110ºC for 24 hours and then ground using a mortar and pestle. Powdered sample was placed into centrifuge tubes of 1.5 cm outer diameter to a minimum height of 2 cm. Most samples taken from the top 10 cm of sediment cores were highly organic and had low dry mass, making the gamma readings of these samples particularly difficult.

Samples were processed for $^{137}$Cs and $^{210}$Pb activities at Queen Mary University (QMU), University of Southern California (USC), and three cores were processed only for $^{137}$Cs activity at Core Scientific International (CSI). For sample tested at QMU, sediment was sealed in plastic tubes using epoxy. For sediments processed at QMU and USC, two weeks were allowed to pass before gamma counting began which allowed for radioactive equilibrium to develop between in situ $^{226}$Ra and decay products used to estimate $^{210}Pb_{supp}$. Raw activities were reported from each lab (Appendix Table 2.2). $^{137}$Cs dates were calculated by identifying an interval of the sediment core which was most likely to contain the year 1963 (defined by the measurements just above and just below the peak measurement). A minimum possible accretion rate and maximum

possible accretion rate were then obtained. Accretion rates from $^{137}Cs$ were calculated as the mean of these accretion rates. CRS modeling was performed at QMU and USC. No significant difference was found between accretion rates measured by different labs, although raw activities for $^{137}Cs$ and $^{210}Pb$ were significantly higher for samples measured at USC and CSI than activities at measured at QMU possibly due to differences in equipment used to measure radioactivities (t-test, 95% confidence; Appendix Figure 2.13).

### *2.3.6 Radiocarbon Dating*

Samples for $^{14}C$ dating were extracted by splitting sediment cores and extracting visible macrofossils with tweezers or wet-sieving small sections of sediment. Plant matter was extracted and visually identified as aboveground matter to avoid dating roots which can be much younger than the deposited sediments in which they are found. Because of uncertainties from the reservoir effects, or the affect that absorption of carbon from local marine sources which are not at equilibrium with contemporaneous atmospheric $^{14}C$ levels, dating of carbonate macrofossils from bivalves and gastropods was only preformed in the absence of plant macrofossils. Any bivalve or gastropod shells were identified to *Genus* level when possible, as species characteristics of coastal bivalves and gastropods can affect the proportion of atmospheric and marine carbon sources absorbed into shells and will influence the reservoir effect (Holmquist et al., 2015). All plant and shell samples were washed in deionized water and dried in a 60ºC oven for 6 – 24 hours, depending on the size.

All $^{14}C$ samples were processed at the UC Irvine Keck Radiocarbon Lab. Samples were washed in HCl before humic acids were removed using NaOH to the point where no more humic acids were produced and the solution appeared clear. Samples were then washed once more with

HCl and dried. Dry samples were placed in quartz tubes along with 60 mg of cupric oxide and a small section of silver wire, added to adsorb non-carbon combustibles, which were then vacuum sealed and combusted for 12 hours at 900ºC to produce $CO_2$ gas. Combusted $CO_2$ gas was isolated and baked onto graphite before being measured using accelerated mass spectrometry (AMS). Radiocarbon years were calibrated into calendar years using INTCAL 2013 (Reimer et al., 2013) with Calib software (Stuiver & Reimer, 1993) and published estimates for reservoir effects (Holmquist et al., 2015). Uncalibrated radiocarbon results are reported in Appendix Table 2.3.

Accretion rates from calibrated dates were estimated by dividing the depth at which the sample was extracted by its median age estimate. If multiple samples were dated from the same core, accretion rates were calculated from the surface, not between age steps; like the comparison between accretion measured by $^{137}$Cs and measured by $^{210}$Pb, multiple $^{14}$C dates from the same core then act as repeated estimates of a single parameter. This was done to avoid erroneous accretion estimates when $^{14}$C ages were not linear (resulting in negative accretion rates between points) and as a means to compare with $^{137}$Cs and $^{210}$Pb accretion rates, which also are measured from the surface.

### *2.3.7 Modeling Accretion*

For each core, data were gathered on site characteristics including: mean annual temperature (MAT), mean annual precipitation (MAP), elevation interpolated using core GPS locations from digital elevation models (DEMs) from NOAA's National Centers for

Environmental Information[1] and high-resolution LIDAR-corrected DEMs where available (Buffington, Dugger, Thorne, & Takekawa, 2016), diurnal tidal range, the historical rate of SLR (nearby NOAA tide gauge average rates of SLR for their total record), historical rates of subsidence, dominant vegetation, average BD, and average SOM (Table 2.1; "Climate Data Online," 2019; "NOAA Tides & Currents," 2019. Station and tide gauge name and location, along with corresponding data, for each site can be found in Appendix Table 2.4. All statistical analyses were done using open-source R software (RC Team, 2013).

Accretion rate data generated in this study were separated by method of measurement ($^{137}$Cs, $^{210}$Pb, and $^{14}$C) and compared to historic rates of SLR from NOAA tide gauges as well as the sum of SLR and rates of local subsidence, defined as relative SLR (RSLR) in this analysis. As anywhere from one to 14 different individual measures of vertical accretion were taken from locations with the same rates of sea level change, accretion rates were averaged by sea-level change for analyses. Akaike's information criteria (AIC), with lower values indicating better model performance (Thorne, Elliott-Fisk, Wylie, Perry, & Takekawa, 2014), were used to evaluate linear and polynomial model fits, with a maximum of third order polynomials to avoid over-interpolation of data.

To test which independent site variables have the greatest impact on vertical accretion rates in this dataset, forward and backward stepwise multiple regression was performed using the site characteristics listed above. Performance of multiple regression models was compared using AIC. A unique regression was made for data from each method used ($^{137}$Cs, $^{210}$Pb, and $^{14}$C) for

[1] (*Eureka, California 1/3 Arc-second MHW Coastal Digital Elevation Model*, 2016; *Orange County, California 1/3 arc-second NAVD 88 Coastal Digital Elevation Model*, 2016; *Port San Luis, California 1/3 arc-second MHW Coastal Digital Elevation Model*, 2016; *San Diego, California 1/3 Arc-second NAVD 88 Coastal Digital Elevation Model*, 2016; *San Francisco Bay, California 1/3 arc-second MHW Coastal Digital Elevation Model*, 2016; *Santa Monica, California 1/3 arc-second MHW Coastal Digital Elevation Model*, 2016)

both the linear and multiple regressions. For each final model chosen, the distribution of residuals was checked for normality and a plot of residuals versus predicted values was checked for bias and heteroscedasticity.

## 2.4 Results

### *2.4.1 Trends in Published Accretion Rates*

A review of recently published sediment accretion rates from around the globe shows that accretion in brackish and salt marshes averages at 5.9 ± 0.6 mm $yr^{-1}$ (Appendix Table 2.1). Compared with global eustatic sea level trends over the past century, this rate reflects that most salt marshes accrete sediment at a rate almost double the rate of eustatic SLR (~3 mm $yr^{-1}$). Asian, South American, African and Australian salt marshes were not well-represented in this review, a reflection of the fact that much of the published research into salt marshes has occurred in Europe and North America. In the US, the north- and southeast regions make up over 70% of the studies used in this review. The southeast, represented by salt marshes in Texas through North Carolina, has a highest average rates of sediment accretion (6.6 ± 1.2 mm $yr^{-1}$), likely due to local rates of SLR two times or more the rate of eustatic SLR. The northwestern US has sediment accretion averages near the accretion rates seen in the northeastern US marshes, although the northwestern coast is also underrepresented in the dataset. Accretion rates in California from published literature and this study average at 5.6 ± 0.8 mm $yr^{-1}$ and are the lowest for all regions, save one study from a marsh in Central America.

Analysis of published accretion rate data by method (marker horizons, $^{137}Cs$, $^{210}Pb$, and $^{14}C$) show that mean accretion rate values decrease with increasing observation period. Mean estimates range from 9.4 ± 8.72 mm $yr^{-1}$ for marker horizon data to 3.2 ± 3.6 mm $yr^{-1}$ for $^{14}C$

measured accretion rates (Figure 2.2). A one-way ANOVA of published accretion data by method used to collect the data show that accretion rates measured by marker horizons, which span timeframes on the order of decades, tend to be higher than accretion rates measured by $^{210}Pb$ and $^{14}C$, but means do not vary significantly ($p = 0.20$ and $p = 0.22$, respectively). The same test conducted on data from this study shows that accretion rates measured by $^{137}Cs$ have slightly higher means than accretion rates measured by $^{210}Pb$ and $^{14}C$, although a post-hoc Tukey test reveals that the effect size is much smaller for California salt marshes than for the global dataset (Appendix Figure 2.14).

### *2.4.2 Sediment Accretion in California*

Average accretion measured in this study across all California sites was $3.28 \pm 0.2$ mm $yr^{-1}$ (Table 2.2), a little over half the published accretion rates from the state. Many of the California studies obtained for this meta-analysis report high accretion rates from storm deposits (Cahoon, Lynch, & Powell, 1996) or due to local subsidence (Watson, 2004), which may explain some of the difference between published accretion means and mean accretion in this study.

Regional mean accretion increases moving south to north in the state (Figure 2.3). An analysis of this study's accretion rates with published rates for the Pacific coast of the lower 48 states in the US shows that accretion generally increases from south to north. Across all sites, intra-marsh accretion is higher in the lowest and mid elevations of the marsh compared to the high elevations of the marsh. This bimodal trend can be seen quite clearly when plotting accretion by elevation extracted from LIDAR-corrected DEMs relative to NAVD88 (Buffington et al., 2016). Elevations between 1.2 – 1.5 m have a large range of accretion rates, but generally show increased accretion in this zone of what is likely maximum plant productivity and sediment

trapping (Figure 2.4a). Categorical classification of salt marsh relative elevation made in the field based on observations of vegetation, however, show higher rates of accretion in the low marsh (Figure 2.4b), although the effect is not significant (ANOVA, 95% confidence). While these low areas are more frequently dominated by *Spartina* spp. in the salt marshes of California, there is little difference in accretion rates measured in *Spartina*-dominated marsh areas compared to *Salicornia*-dominated marsh areas, the vegetation more typical in higher elevations (Figure 2.4c). There is, however, an increased amount of accretion seen in marshes which are dominated by invasive *S. densiflora* compared *S. foliosa,* but the increase is not statistically significant (ANOVA, 95% confidence).

### *2.4.3 Accretion Rates, SLR, and RSLR*

Using polynomial and linear regression, this study indicates California accretion rates are highest where there are moderate levels of RSLR and have the most positive linear response to higher rates of both SLR and RSLR in low marsh elevations. Measures of vertical accretion compared to RSLR show strong non-linear variability ($^{137}$Cs, $R^2 = 0.72$; $^{210}$Pb, $R^2 = 0.31$; and $^{14}$C, $R^2 = 0.27$ respectively), but polynomial and linear relationships between all methods of measuring accretion and SLR generally have weak correlations (Figure 2.5). Polynomial regressions preform slightly better for SLR compared to accretion. But polynomial relationships between accretion rates and SLR best describe this data. These comparisons indicate accretion rates are highest when rates of RSLR are between 2 – 6 mm $yr^{-1}$, especially for short-term measures of accretion from $^{137}$Cs and $^{210}$Pb.

Method of measurement does appear to have some influence on the predicted relationship with rates of SLR. The non-linear trend between $^{137}$Cs dated accretion measures, the method with the shortest observation period, and RSLR is strongest in comparison to non-linear trends for

other methods of measuring accretion. However linear and non-linear relationships between $^{14}C$ measured accretion, with the longest observation period, and SLR are of comparable strength to $^{137}Cs$ linear trends with SLR. The relationship between $^{210}Pb$ dated accretion rates and SLR, however, was weakest both for linear and non-linear regression, but a non-linear trend similar to the strong trend between $^{137}Cs$ and RSLR can be seen when comparing $^{210}Pb$ accretion data to RSLR.

While non-linear trends have good explanatory power for this dataset, for all methods and measures of sea level change linear models had lower AIC values than any polynomial fit. This is likely due to a lack of complete representation of potential rates of SLR in the dataset leading to over-interpolation by polynomial regressions. Linear regressions between RSLR and accretion rates can be improved by sorting data into relative elevation categories (high, mid, and low). Stronger linear trends then emerge in the lowest elevations of the salt marsh, with RSLR having the greatest positive impact on $^{210}Pb$ accretion rates ($R^2 = 0.38$; $p = 0.057$, Table 2.3).

### *2.4.4 Factors Which Control Accretion Rates*

Forward and backward stepwise multiple regression indicate elevation, diurnal tidal range, SLR, subsidence, SOM content, and MAT are the factors with the most significant effect on accretion rates measured by different methods (Table 2.4). Compared to all models, the final model of accretion obtained from step-wise regression of $^{210}Pb$ accretion measurements and site parameters explains the most variability; accretion from $^{210}Pb$ is a factor of the diurnal tidal range and SLR ($R^2 = 0.52$; $p < 6.0 \times 10^{-6}$). The final model for environmental controls on accretion measured by $^{14}C$ has the next most explanatory strength ($R^2 = 0.22$; $p = 0.001$) and indicates MAT, SLR, subsidence, and SOM content are the best predictors for $^{14}C$ accretion

rates. $^{137}$Cs measured accretion is best predicted by elevation within the salt marsh, but overall model performance is weakest for these data ($R^2 = 0.07$; $p = 0.07$). These step-wise regression models show that there is a considerable amount of variability in rates of accretion which is not well-captured by MAT, MAP, elevation, diurnal tidal range, RSLR, dominant vegetation, average BD, or average SOM alone.

## 2.5 Discussion

Salt marsh accretion rates in the state of California are lower than regional US and global accretion rates from salt marshes for both published accretion data and data produced in this study. Accretion rates are, however, comparable to rates of RSLR for the coast of California. Accretion is highest in salt marsh elevations from 1.2 m to 1.5m, or for those elevations categorized as 'low' in the field. There is little difference in mean accretion rates for measurements taken in *Salicornia*-dominated habitat in comparison to *S. foliosa*-dominated habitat, but invasive *S. densiflora* habitat present in the San Francisco and Humboldt Bays have higher, though not statistically significant, mean accretion rates than areas with native vegetation. Non-linear trends between RSLR and accretion indicate that accretion is most robust at rates of RSLR between 2 mm $yr^{-1}$ and 6 mm $yr^{-1}$. Accretion in low elevations of salt marshes is most responsive to SLR in comparison to accretion rates from mid and high elevation categories. Elevation, tidal range, rate of SLR, MAT, and SOM content have the most significant contribution to variability seen in accretion rates in this study, but many of these site- or region-level environmental characteristics do not fully capture the drivers of variability in accretion rates.

### *2.5.1 Trends in Inter-Marsh Accretion for California*

California salt marshes are on average maintaining accretion rates roughly at or slightly higher than local rates of SLR, similar to most accretion rates seen in the meta-analysis. There is an increase in mean accretion rate from south to north in the state, which is seen also in review data from the entire US Pacific coast. Average accretion rates of 7.3 ± 0.4 mm yr-1 (n = 6) are reported from sites on the outer coast of the state of Washington, over double the average rates in Southern California from this study. The northwest Pacific coast and Northern California accretion rates and SLR trends are fairly comparable with published accretion rates and SLR from the US Northeast coast. Central California and Southern California, however, seem to show regionally unique average accretion rates that are the lowest for the continental US and generally lower than eustatic SLR.

While the mean accretion rate is low for the state of California, the range of accretion in California salt marshes points to the potential capacity of salt marshes to accelerate accretion in response to different conditions. For instance, Triangle Marsh in the South San Francisco Bay has the highest average accretion rate as well as the single highest reported rate of accretion, with one core showing 12 mm yr-1 of accretion based on $^{210}$Pb dating. These high estimated rates of accretion are not only seen in the $^{210}$Pb dates observed over the past century, but an estimated 6.4 mm yr$^{-1}$ and 6.3 mm yr$^{-1}$ of accretion was measured by $^{14}$C dating in the other two cores from this site over the past 2 – 4,000 years by Watson (2004). Triangle Marsh experiences the highest rates of RSLR seen in this database because of subsidence (Watson, 2004), likely contributing to higher accretion. This also holds true for the salt marsh at Bolinas Lagoon, where an estimated 45 cm of elevation was lost in the 1906 rupture of the San Andreas Fault. Accelerated accretion rates in response to this sudden drop were maintained throughout the 20$^{th}$ century and into the

21st (Byrne et al., 2005). Published data from Southern California using marker horizon data following storm events have even recorded up to 85 mm of vertical accretion in one year over areas where flooding deposited sediment and less than 1 mm in areas of the same marsh which were not in the path of floodwaters (Cahoon et al., 1996). These rates, while unusual for California, are not unusual for many of the large, estuarine systems observed around the globe that regularly see accretion rates on the magnitude of 10s of mm $yr^{-1}$. So while mean accretion in the state may be lower than in other regions, instances of high accretion are comparable to other salt marsh systems.

### *2.5.2 Trends in Intra-Marsh Accretion for California*

Mean accretion is highest in California salt marsh sites from 1.2 to 1.5 m in elevation relative to NAVD88, however elevations below 1.2 m and above 1.8 m are poorly represented in the dataset. The elevation zone with the highest accretion rates is also the zone with the widest range of accretion rates. This analysis indicates that while salt marsh habitat may be at an elevation which is favorable to accretion, there are other site-level factors which may ultimately determine the capacity for sediment accretion such as the availability of sediment or distance to the nearest tidal channel. Marshes of Humboldt Bay, the Outer Coast, and San Francisco Bay are also poorly represented in this analysis because they lack corresponding high-resolution elevation data used in analysis. All data were analyzed to observe trends in sediment accretion with relative elevation. Those coring sites which were classified as low elevation showed higher, though not significantly higher, accretion rates than cores taken in other elevation zones. This corresponds with high accretion means for quantitative elevation.

Dominant species' change also has been cited as a potential factor which may modify accretion rates, but this accretion database does not show that dominant species have a

significant effect on controlling accretion rates. *S. pacifica* and *S. foliosa* exhibit distinct zonation in California salt marshes, leading to productivity maxima for each species at different relative elevations; *S. foliosa* is most productive in frequently inundated low elevations whereas *S. pacifica* has its highest productivity in higher elevations with higher salinity (although productivity decreases during periods of hypersalinity). The net effect of this competitive zonation results in high productivity in low and high elevations where each plant is most suited to environmental conditions, with the lowest productivity in the ecotone where environmental conditions are less favorable for either species (Mahall & Park, 1976). For that reason, there is little difference in productivity between these two species and no significant difference in accretion rates for habitat dominated by one or the other.

Invasive *S. densiflora*, however, does show higher aboveground primary productivity than *S. folisa* and *S. pacifica*. But productivity for *S. densiflora* in Humboldt Bay has been linked to lower net ecosystem productivity for invaded habitats in comparison to native species because of low belowground production (Lagarde, 2012). The slightly higher mean accretion in sites dominated by *S. densiflora*, therefore may be an artifact of this species occurring where accretion rates are higher (driven by other site factors) rather than a clear indication that *S. densiflora* drives higher production, but more investigation into the impact invasive species have on accretion rates is needed.

### *2.5.3 California Salt Marsh Accretion and SLR*

Salt marsh sediment accretion does not show a strong positive relationship with the rates of SLR in this dataset, but polynomial regression reveals that accretion has a maximum at rates of RSLR between 1.2 to 1.5 mm $yr^{-1}$ and is lower than rates of RSLR above and below that range. This relationship has been observed and modeled for salt marshes and is the result of

ecogeomorphic feedbacks leading to an equilibrium elevation where plant productivity and sediment trapping are maximized (Morris et al., 2002). As this dataset has few samples from sties with RSLR between 1.2 – 1.5 mm $yr^{-1}$, further empirical analysis should focus on sites within this zone to verify that California salt marshes display this typical salt marsh ecosystem behavior.

It should also be noted that the poor linear relationship between SLR, RSLR, and accretion rates could also be caused by inaccurate estimates of SLR and RSLR due to the methodology employed for this analysis. Rates of SLR used in this analysis are from NOAA tide gauges which may not be near enough to salt marsh sites to accurately reflect the rates of SLR experienced by the salt marsh site. Additionally, rates of SLR in from the NOAA tide gauges are from the total historic record from each gauge and have not been directly matched with the time frame of accretion observation in this study. Rates of RSLR that are used in regressions reported in this dataset may also not correctly reflect the exact rate of SLR and subsidence seen at the site as rates of subsidence are estimated from subsidence over the general region and not measured in the marsh itself.

Working under the assumption that SLR and subsidence rates used in this study are accurate indicators of environmental conditions, however, linear analysis of mean site accretion rates compared to rates of SLR and RSLR provide historical context for the response of accretion at individual sites to mean SLR or RSLR. For this analysis, I have used only $^{137}Cs$ and $^{210}Pb$ accretion rates in an attempt to minimize the effect of different time periods of observation between accretion rate data and environmental data. Plotting mean site accretion by rates of sea level change, sites which have historic accretion rates higher than, at, or below the rate of SLR or RSLR can be identified. Average rate of SLR and RSLR for each site shows that there are two

sites accreting faster than both rates, three sites accreting only faster than rates of SLR, and six sites which are accreting slower than both measures. These sites have been classified as having historically high, marginal, or low rates of accretion relative to SLR and RSLR (Figure 2.6). Two sites (Mad River High and Mugu Lagoon) have not been included in this analysis because only one measure of accretion rate measured by $^{137}Cs$ or $^{210}Pb$ was obtained from these sites.

Sites which are accreting at rates faster than the rate of SLR from the nearest tide gauge as well as faster than rates of RSLR include: Morro Bay and Bolinas Lagoon. Petaluma Marsh, Mission Bay, Tijuana River Estuary, Upper Newport Bay, Hookton Slough, and Mad River Low are all sites which accrete sediment slower than the rates of SLR alone, experience no reported local subsidence, and may be keeping pace with SLR trends, but have been classified as having historically marginal accretion rates in comparison to SLR. Seal Beach, Triangle Marsh, and White Slough are accreting sediment faster than the NOAA tide gauge SLR but slower than rates of RSLR and are therefore have historically marginal rates of accretion mostly due to high rates of local subsidence, although they do exhibit increased rates of accretion in response to higher RSLR. Upper Newport Bay, Hookton Slough, and Mad River Low are sites which are accreting well below the rates of SLR measured by NOAA tide gauges, experiencing higher rates of RSLR because of subsidence, but show little sign of increased accretion which would keep pace with these increases in water levels. These sites therefore have been classified as having historically low accretion rates relative to SLR.

While these comparisons between sites are useful to contextualize current system status, these past behaviors are not a prediction of future vulnerability to accelerated SLR. Site-level studies are required to determine what specific factors have contributed to past system behavior and if those conditions are likely to change in the future. Parameters more-closely related to

accretionary processes, such as suspended sediment content and productivity, may be more important in driving long-term accretion trends than even mid-scale processes like local rates of SLR. Further comparison between sites which have had historically high accretion in comparison to sites which have had historically low accretion is an important next step to reveal possible strategies for adaptive management. All sites, regardless of past rates of SLR, should continue to be monitored and compared into the future to better understand how the relationship between SLR and vertical accretion affects salt marsh vulnerability.

### *2.5.4 Controls on Accretion in California Salt Marshes*

Using forward and backward stepwise regression to compare environmental variables to accretion rates measured by each method individually, the most consistent predictor in a multiple regression of environmental conditions and vertical sediment accretion across all methods of measuring accretion is SLR, although the effect size is quite small (Table 2.4). Diurnal tidal range is the variable that has the largest effect on $^{210}$Pb-measured accretion and the variable with the largest effect size of all variables across all methods of measuring accretion. Prediction of $^{210}$Pb accretion using tidal range and the rate of SLR is also the model which preforms best in comparison to $^{137}$Cs- and $^{14}$C-measured accretion rates ($R^2 = 0.56$, compared to $R^2 = 0.07$ and $R^2 = 0.27$ for $^{137}$Cs and $^{14}$C respectively). MAT, subsidence, SLR, and SOM content were selected as variables which explain the most variability in $^{14}$C accretion rates, with MAT and SLR having the largest effect sizes. Overall, $^{147}$Cs model performance is poor and only elevation was selected by stepwise regression for the final model, although there is a significant correlation between $^{137}$Cs accretion rates and diurnal tidal range. Rates of SLR were not significantly correlated with $^{137}$Cs accretion rates.

Considering the poor linear relationships between SLR and accretion rates seen in Figure 2.5, it is not surprising that SLR has a small effect size on overall accretion rates and is not selected as a significant predictor of $^{137}$Cs accretion rates. The lack of relationship between SLR and $^{137}$Cs, as this is the method with the shortest observation period which most closely resembles the observation period of SLR data, may be an indication that with modern acceleration of SLR the relationship between SLR and rates of accretion is changing throughout the state. This could be the result of some sites not keeping pace with modern rates of SLR, as well as the result of sites like Bolinas Lagoon and Morro Bay exhibiting much higher rates of accretion without increased rates of SLR. It is also important to note that $^{137}$Cs measurements also have increased uncertainty in California (Drexler et al., 2018) and poor agreement between modern accretion rates and rates of SLR should be verified by other short-term observation methods, like marker horizons and sediment elevation tables. Further analysis is needed to determine if there is, indeed, a change in the current behavior of sediment accretion in response to SLR in comparison to how this relationship has functioned in the past.

Because $^{137}$Cs accretion measurements have the shortest observation period, elevation, as measured at the surface coring location, may have a larger impact on accretion in the uppermost part of the core. This would mean that $^{137}$Cs rates are quite sensitive to intra-marsh variability in accretion rates. The negative correlation between accretion and elevation, not only for $^{137}$Cs accretion rates, but for $^{210}$Pb and $^{14}$C rates as well, reinforces the finding of the highest accretion rates in the lower elevations of the salt marsh.

The impact of tidal range on accretion rates is a well-documented phenomena. Increased tidal range is associated with increases in the range of depths which are suitable for high biomass production. This allows for greater stabilization of the salt marsh platform to sea level changes

(Kirwan & Guntenspergen, 2010). Most of the salt marshes studied in this analysis are micro-tidal (tidal range < 2 m), except Triangle Marsh and the marshes in Humboldt Bay. Triangle Marsh is the site with the highest reported values of accretion, as measured by $^{210}$Pb, which may explain why tidal range is such a significant predictor for that method. Both Humboldt Bay and Triangle Marsh also deal with higher rates of local subsidence, so it is difficult to separate out the effects of increased tidal range and increased rates of local SLR.

The model for $^{14}$C accretion rates is the only multiple regression model which selected a MAT, SOM content, and subsidence as a predictors of vertical accretion. Much of salt marsh accretion is driven by plant productivity, and thus higher rates of productivity should correspond to higher rates of accretion. Salt marshes from the San Francisco Bay have area shown strong, positive correlations between SOM and accretion measured by $^{210}$Pb and $^{137}$Cs (Callaway et al., 2012). But, in this analysis, SOM content is slightly negatively correlated (correlation coefficient = -0.02) with accretion rates measured by $^{14}$C. Because $^{14}$C-measured accretion rates cover a much larger timespan than the previous results, the negative relationship observed in this dataset is more likely to be a reflection SOM decay or compaction of sediment with time. Only accretion measured by $^{210}$Pb shows a positive correlation with SOM content, although it is not significant. All methods, however, show a positive correlation with BD, indicating that for this dataset the mineral component of sedimentation may drive higher accretion. The inclusion of MAT as a negatively correlated predictor in this dataset may be indication that there is an effect of increased decay rates with increased temperatures leading to lower accretion rates (Kirwan & Blum, 2011), but as there are many compounding factors which lead to higher accretion rates in the northern Pacific coast, such as tidal range and higher rates of RSLR, further analysis is needed to verify this effect. Subsidence has a negative impact on $^{14}$C accretion rates, as well as a

negative but not significant impact on $^{210}Pb$ rates, but a small, positive effect on $^{137}Cs$ accretion rates. Although subsidence can compound rates of accelerated SLR and lead to salt marsh drowning, as occurs along the US Gulf coast, but subsidence in some California salt marshes have been cited as drivers of increased sediment through the creation of accommodation space within the tidal frame (Byrne et al., 2005).

Overall, multiple regression analysis of environmental characteristics with sediment accretion reinforces the findings that the highest rates of accretion occur within low marsh elevations and indicates that site-level impacts, like tidal range and rates of subsidence, are important drivers of accretion but may act differently across different time frames. There is some evidence that the relationship between accretion and SLR has changed in the most recent period of accelerated SLR, but more investigation is needed.

### *2.5.5 Vertical Sediment Accretion and Salt Marsh Vulnerability to SLR*

Monitoring past accretion provides an estimate of the historic ecosystem function useful for parameterizing models to project the capacity for salt marshes to respond to accelerated SLR in the future. But past rates of sediment accretion alone are poor predictors of future rates. Not only is it difficult to predict how accretion may respond to changes in rates of SLR based on past system behavior, system functionality may also change with changing climate. The impacts of climate change on salt marshes are very hard to predict. There is evidence that productivity of marsh species may increase with elevated levels of $CO_2$ from fossil fuel release (Cherry, McKee, & Grace, 2009; Langley & Megonigal, 2010) which may increase rates of accretion. But there is also evidence that increased decomposition from increased temperatures may offset productivity gains from higher temperatures and increased $CO_2$ (Kirwan & Blum, 2011). Accretion rates may

also vary due to management choices, such as adding sediment either through re-establishment of historic sediment sources (Edmonds, 2012) or additions of sediment to the salt marsh plain itself (Croft, Leonard, Alphin, Cahoon, & Posey, 2006; Thorne, Freeman, Rosencranz, Ganju, & Guntenspergen, 2019). Monitoring the ability of a salt marsh to keep pace with SLR therefore needs to take a multi-pronged approach through monitoring in situ changes in sediment availability, sediment deposition, elevation change, local SLR, and vegetation to use along with baseline data generated in this and other studies for ecosystem vulnerability and process models.

This study shows California salt marshes have lower mean accretion than global accretion rates, identifies the low marsh as habitat which has the highest rates of accretion, shows that salt marsh accretion has a complex, nonlinear relationship with SLR and RSLR, and highlights the importance of elevation, diurnal tidal range, SLR, subsidence, SOM content, and MAT on vertical accretion rates. Data from this study are useful as baseline data for future use in ecosystem vulnerability and process models which may help stakeholders and researchers identify research and management priorities which support promotion of vertical sediment accretion as a means of adaptation to SLR.

## 2.6 Figures

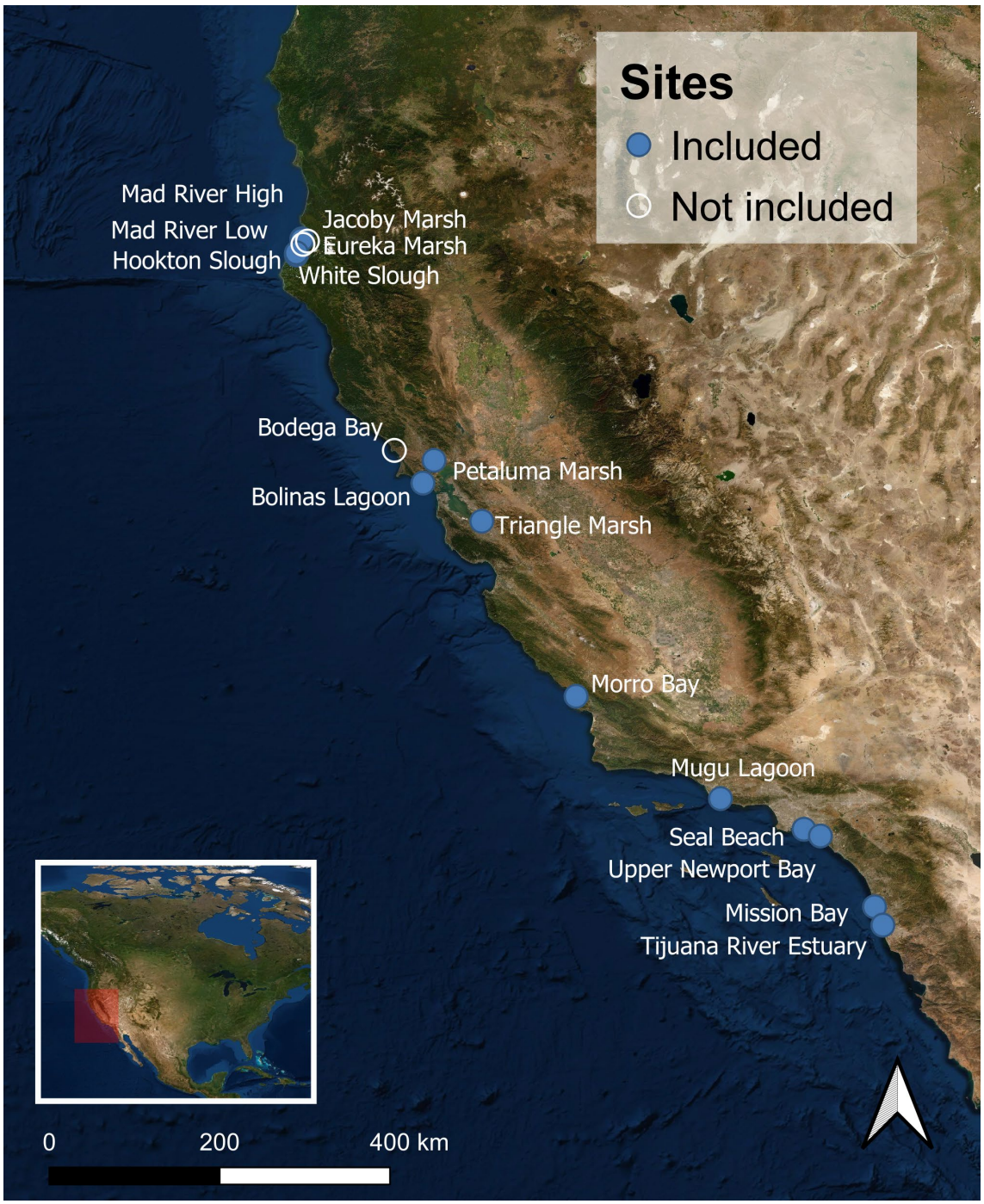


**Figure 2.1 Site Map**

This map depicts all sites cored in the duration of this project. Sites which were not included in the analysis but exist in the core database are indicated by white circles. Basemap is ESRI World Imagery available through Open Street Map (OSM).

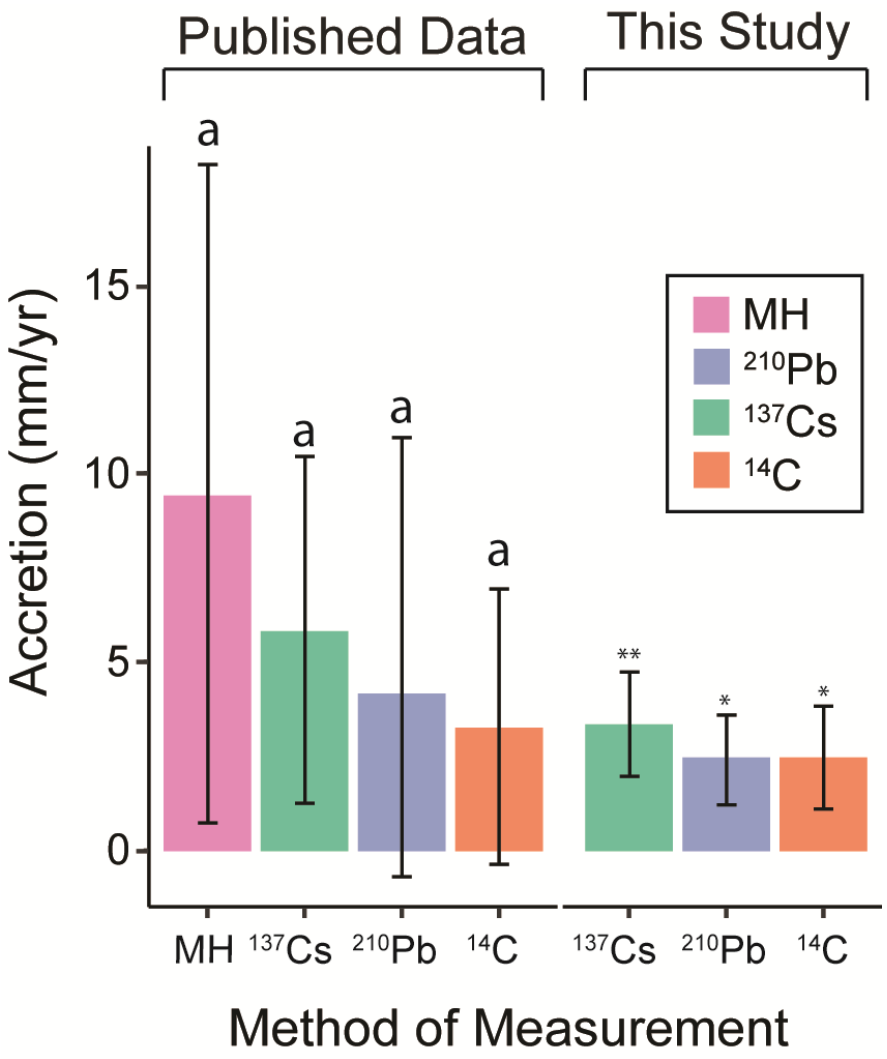


**Figure 2.2 Accretion Rates by Method**

Comparison of vertical sediment accretion rates by method of collection for published data from around the globe reviewed in this chapter and from data generated in this study. Means which share a letter are not significantly different for published data (ANOVA, 95% confidence). Means which share the same number of asterisks are not significantly different for data in this study (ANOVA, 95% confidence).

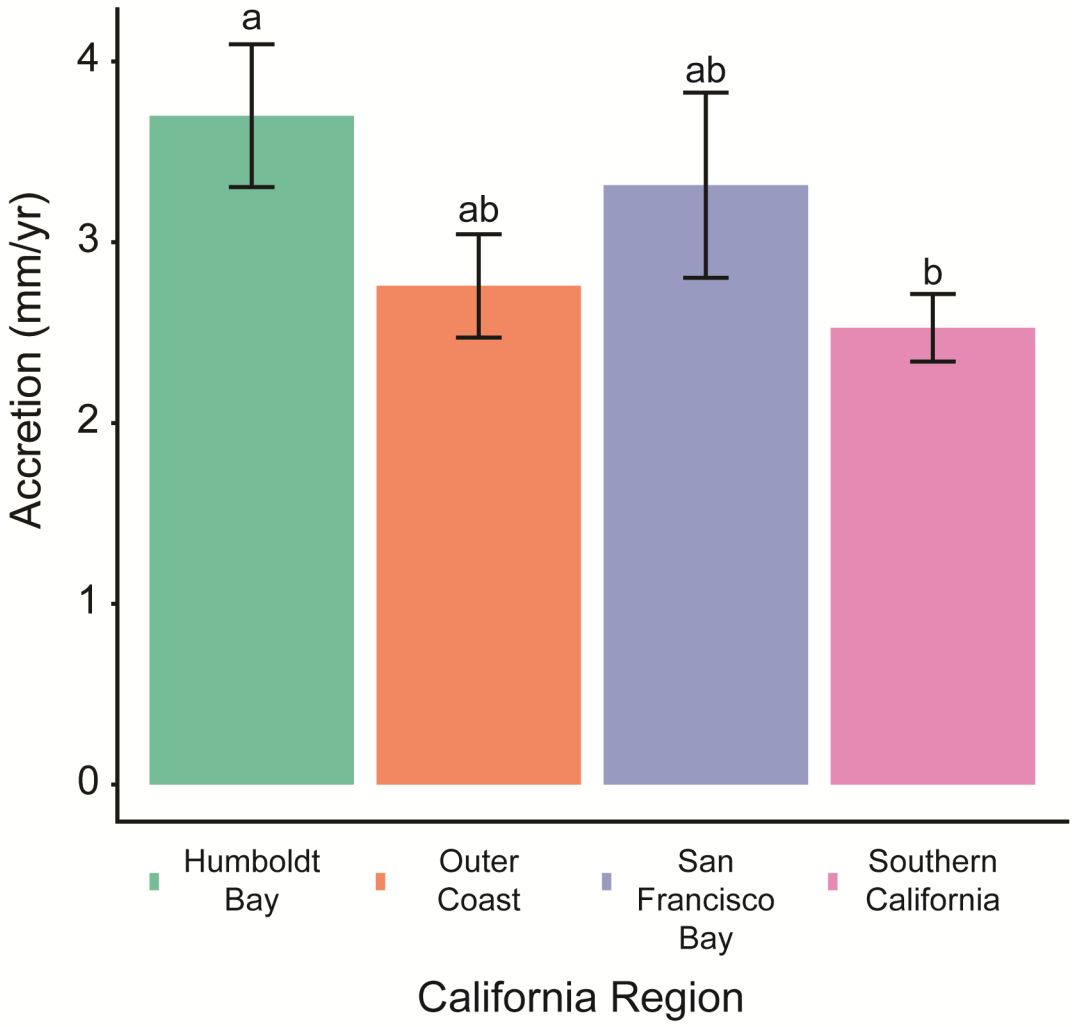


**Figure 2.3 Average Accretion by California Region**

Average regional accretion rates for this study with standard deviations. Means which share a letter are not significantly different (ANOVA, 95% confidence).

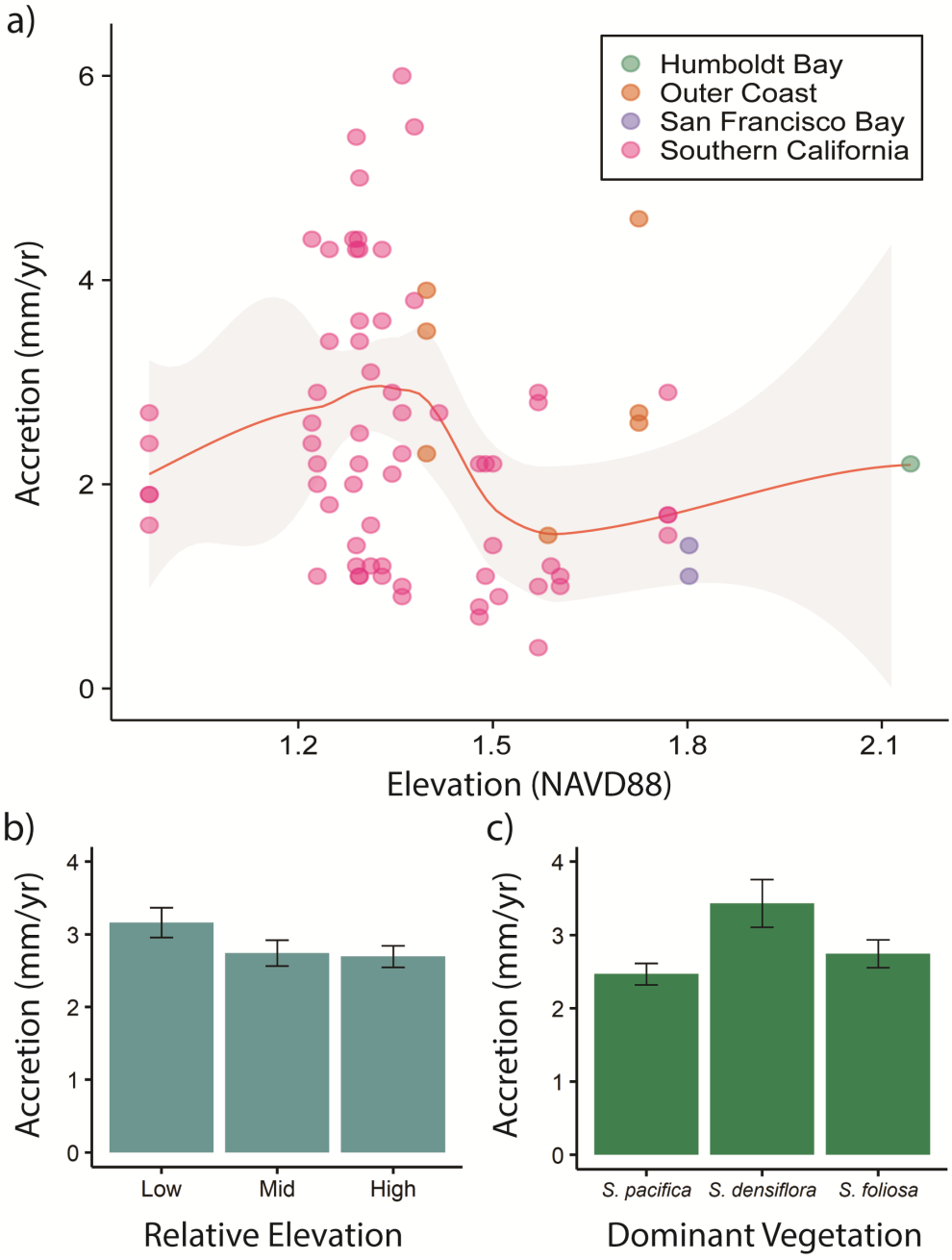


**Figure 2.4 Accretion by Elevation and Dominant Vegetation**

This figure depicts (a) variability in accretion rates over elevation extracted from NCEI DEMs using GPS core locations. Data are smoothed with a loess fit and the 95% confidence interval is shaded in grey. Average accretion rates are plotted by (b) relative elevation descriptions made in the field and (c) dominant vegetation with standard errors.

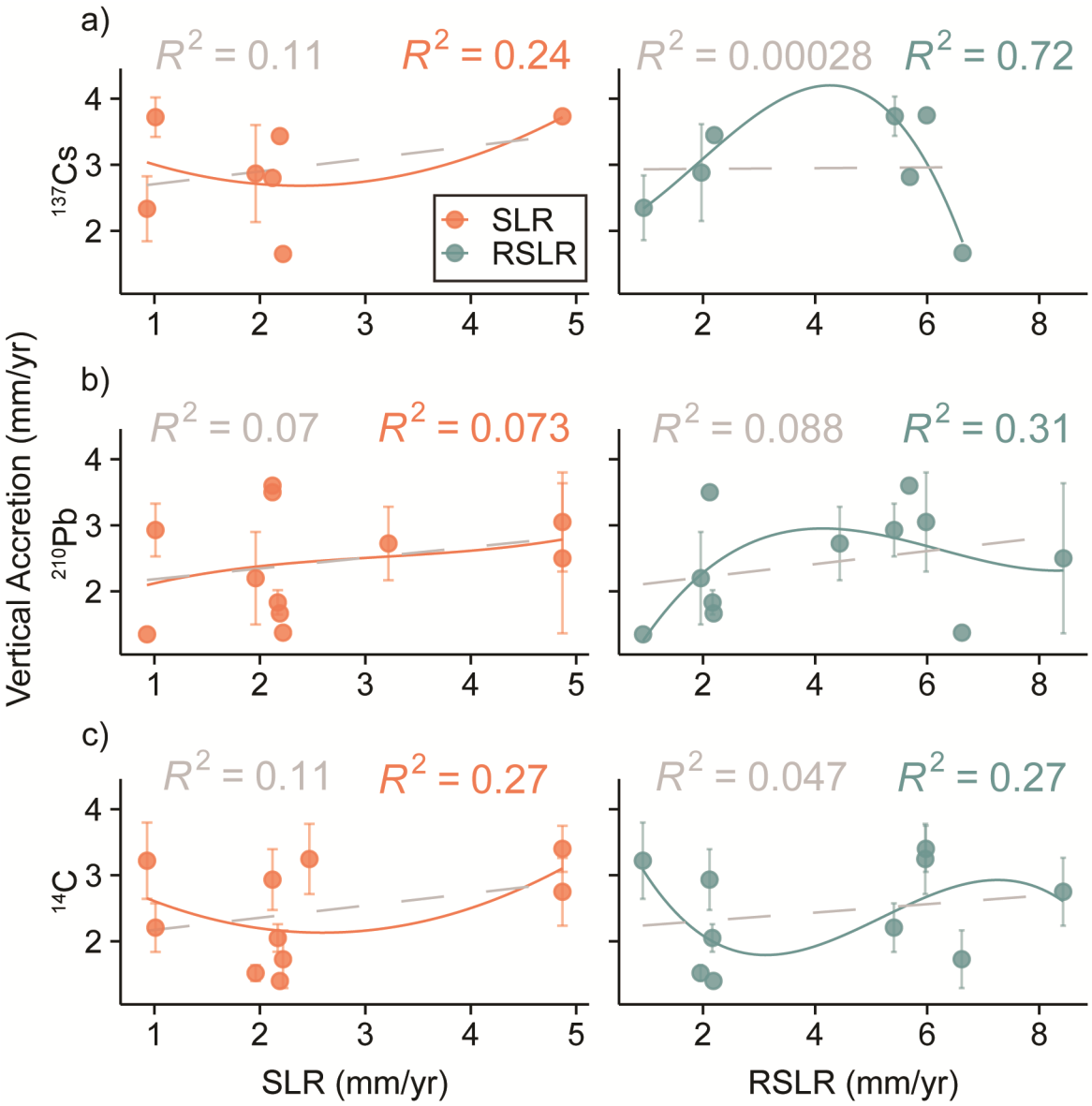


**Figure 2.5 SLR, RSLR, and Vertical Accretion**

SLR and RSLR are compared with vertical accretion rates from sites analyzed in this study sorted by method of measurement: a) $^{137}$Cs, b) $^{210}$Pb, and c) $^{14}$C. Measures of vertical accretion rates from sites with the same rate of SLR or RSLR are averaged with error bars representing standard deviations. The dotted, grey line on each plot shows the linear regression each set of variables and $R^2$ values are shown at the upper left of each plot in grey. Polynomial regressions and $R^2$ values (upper right) are color-coded by sea level change rates. Third-order polynomial regressions were used for the relationships between SLR and $^{210}$Pb measured accretion and all relationships with RSLR. Relationships between SLR and $^{137}$Cs and SLR and $^{14}$C are second-order polynomials to prevent interpolation where data are sparse at rates of SLR between 3 – 5 mm/yr.

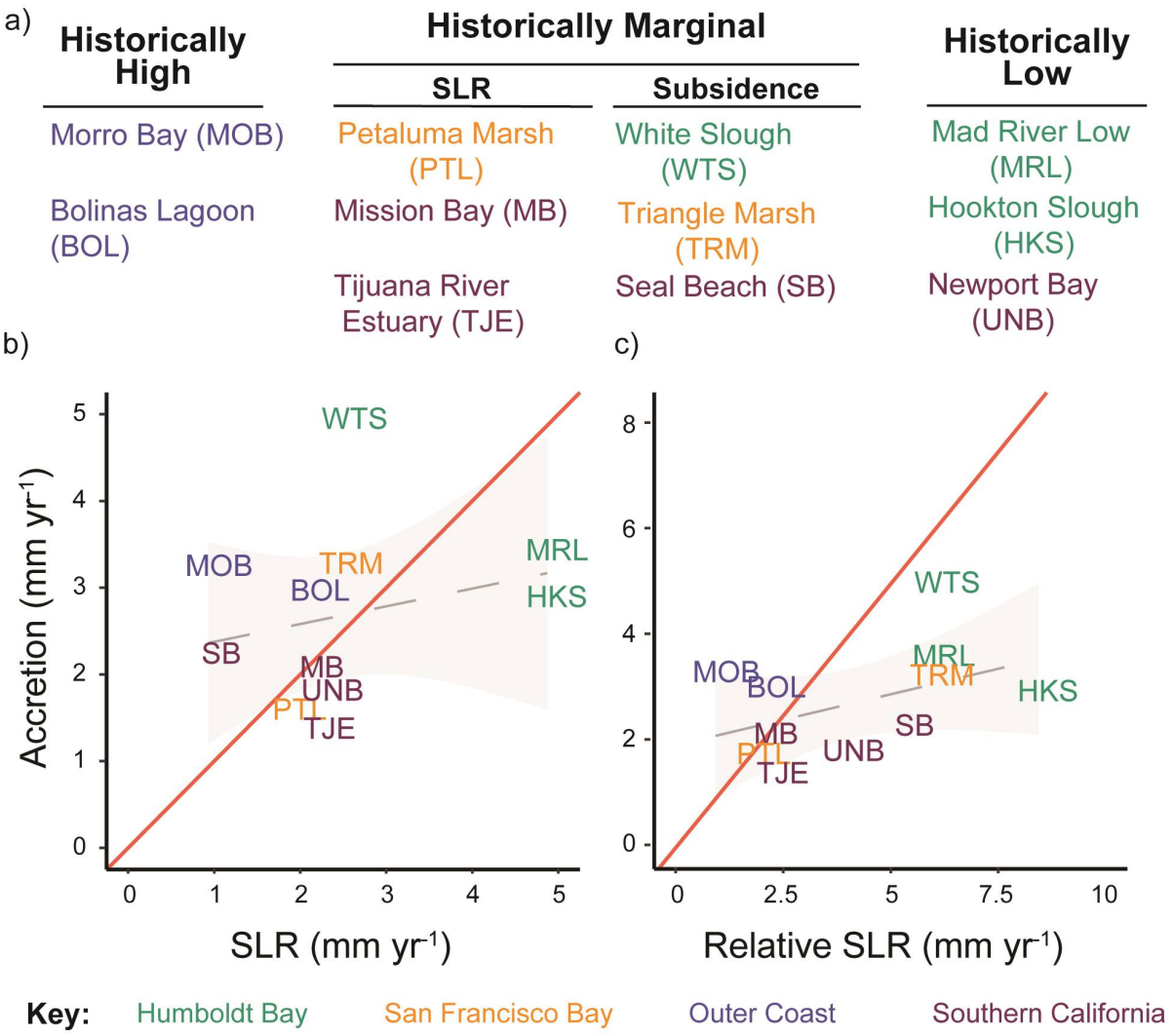


**Figure 2.6 Site-by-Site Comparison of Accretion and SLR**

Average accretion rates by site are compared to rates of SLR from nearest NOAA tide gauges (SLR) and the sum of rates of SLR and subsidence (Relative SLR). Sites are colored according to the region of California where they are found. Based on the comparisons between SLR and accretion and RLSR and accretion, sites have been ranked as having accretion rates that are (a) "Historically High", "Historically Marginal", and "Historically Low". A 1:1 line comparing SLR and Relative SLR to accretion rates is drawn in solid red on each plot. Sites which are above the 1:1 line in both plots are "Historically High", below the 1:1 line in both plots with no subsidence are "Historically Marginal" due to SLR, below the 1:1 in only the RSLR plot are "Historically Marginal" because of subsidence, and below the 1:1 line in both plots are "Historically vulnerable". Regressions between (b) SLR and accretion and (c) RSLR and accretion are seen in the dotted grey lines with a 95% confidence interval shaded in grey.

## 2.7 Tables

**Table 2.1 Site Characteristics**

| | Site | n | Tidal Range (m) | MAT (ºC) | MAP (mm) | Historic SLR (mm/yr) | VLS (mm/yr) | Dominant Vegetation |
|---|---|---|---|---|---|---|---|---|
| **Humboldt Bay** | *Mad River High* | 1 | 2.09 | 12 | 264 | 4.87 ± 0.90 | 2.11 | *D. spicata, F. grandifolia* |
| | *Mad River Low* | 2 | 2.09 | 12 | 264 | 4.87 ± 0.91 | 1.11 | *S. densiflora* |
| | *White Slough* | 2 | 2.09 | 12 | 264 | 3.5 ± 0.9 | 3.56 | *S. pacifica, S. densiflora* |
| | *Hookton Slough* | 2 | 2.09 | 12 | 264 | 4.87 ± 0.91 | 3.56 | *S. pacifica, S. densiflora* |
| **San Francisco Bay** | *Petaluma Marsh* | 3 | 1.85 | 15 | 160 | 1.96 ± 0.18 | -- | *S. pacifica, Schoenoplectus* |
| | *Triangle Marsh* | 3 | 2.7 | 15 | 98 | 2.47 ± 1.62 | 3.5 | *S. foliosa, S. pacifica, Schoenoplectus* |
| **Outer Coast** | *Bolinas Lagoon* | 3 | 1.76 | 13 | 334 | 2.12 ± 0.88 | -- | *S. foliosa, S. pacifica* |
| | *Morro Bay* | 4 | 1.62 | 15 | 122 | 0.93 ± 0.38 | -- | *S. pacifica* |
| **Southern California** | *Mugu Lagoon* | 4 | 1.65 | 15 | 76 | 3.22 ± 1.66 | 1.22 | *S. pacifica* |
| | *Seal Beach* | 10 | 1.67 | 18 | 68 | 1.01 ± 0.23 | 4.4 | *S. foliosa, S. pacifica* |
| | *Upper Newport* | 5 | 1.67 | 18 | 77 | 2.22 ± 1.04 | 2.4 | *S. foliosa, S. pacifica* |
| | *Mission Bay* | 5 | 1.62 | 16 | 83 | 2.17 ± 0.27 | -- | *S. foliosa, S. pacifica* |
| | *Tijuana River* | 5 | 1.74 | 17 | 73 | 2.19 ± 0.18 | -- | *S. foliosa, S. pacifica* |

For each of the 13 salt marsh sites in this study, the number of sediment cores (n), diurnal tidal range, mean annual temperature (MAT) and mean annual precipitation (MAP), historic rate of SLR, vertical land subsidence (VLS), and dominant vegetation are reported. Information on sources for climate data, SLR data, and VLS data can be found in Appendix Table 2.4.

**Table 2.2 Mean Accretion by Site and Method**

| | Site | Mean Accretion (mm $yr^{-1}$) | | | |
|---|---|---|---|---|---|
| | | $^{137}$Cs (n) | $^{210}$Pb (n) | $^{14}$C (n) | All |
| **Humboldt Bay** | *Mad River High* | 2.2 (1) | - | - | 2.2 (1) |
| | *Mad River Low* | 4.5 ± 0.7 (2) | 3.1 ± 0.8 (2) | 3.4 ± 0.3 (4) | 3.6 ± 0.3 (8) |
| | *White Slough* | 5.1 ± 0 (2) | 3.6 ± 0.8 (2) | 2.9 ± 0.6 (5) | 3.5 ± 0.5 (9) |
| | *Hookton Slough* | 3.2 ± 0.4 (2) | 2 ± 1.6 (2) | 4.9 ± 1.4 (7) | 4.1 ± 1 (11) |
| **San Francisco Bay** | *Petaluma Marsh* | 2.9 ± 0.7 (3) | 2.2 ± 0.7 (3) | 1.5 ± 0.1 (5) | 2.1 ± 0.3 (11) |
| | *Triangle Marsh* | - | 8.1 ± 2.2 (3) | 3.2 ± 0.5 (11) | 4.3 ± 0.8 (14) |
| **Outer Coast** | *Bolinas Lagoon* | - | 3.5 (1) | 2.9 ± 0.5 (6) | 3 ± 0.4 (7) |
| | *Morro Bay* | 2.3 ± 0.5 (3) | 1.4 ± 0.9 (2) | 3.2 ± 0.6 (5) | 2.6 ± 0.4 (10) |
| **Southern California** | *Mugu Lagoon* | 5.5 (1) | 2.7 ± 0.6 (4) | - | 3.3 ± 0.7 (5) |
| | *Seal Beach* | 3.7 ± 0.3 (10) | 2.9 ± 0.4 (7) | 2.2 ± 0.4 (14) | 2.9 ± 0.2 (31) |
| | *Upper Newport* | 1.7 ± 0.6 (2) | 1.4 ± 0.3 (4) | 1.7 ± 0.4 (7) | 1.6 ± 0.3 (13) |
| | *Mission Bay* | 4.6 ± 2.5 (3) | 1.8 ± 0.2 (3) | 2.1 ± 0.2 (6) | 2.6 ± 0.6 (12) |
| | *Tijuana River* | 3.4 ± 1.4 (3) | 1.7 ± 0.5 (3) | 1.4 ± 0.5 (3) | 2.2 ± 0.6 (9) |
| **All** | | **3.54 ± 1.75 (32)** | **2.83 ± 2.16 (32)** | **2.72 ± 1.8 (73)** | **2.93 ± 1.9 (141)** |

Site-by-site mean accretion rates with standard errors by each method of measuring accretion and across all methods.

**Table 2.3 Regression Results for Accretion and RSLR**

| Method | All Elevations | Relative Elevation | | |
|---|---|---|---|---|
| | | ***High*** | ***Mid*** | ***Low*** |
| $^{137}Cs$ | 0.039 (n=30) | 0.039 (n=16) | 0.089 (n=6) | 0.024 (n=4) |
| $^{210}Pb$ | 0.111 (n=34) * | 0.161 (n=14) | 0.09 (n=8) | 0.381 (n=8) |
| $^{14}C$ | 0.001 (n=26) | 0.196 (n=11) | 0.05 (n=4) | 0.27 (n=7) |
| $^{137}Cs$ & $^{210}Pb$ | 0.115 (n=39) * | 0.141 (n=18) | 0 (n=9) | 0.276 (n=8) |

Significance codes : *** $p < 0.001$, ** $p < 0.01$, * $p < 0.05$

Results of linear regression ($R^2$ values) for comparison of vertical accretion rates to Relative SLR (SLR + subsidence) for all sites in the database compared by method of measuring accretion and relative elevation of the coring location in the salt marsh.

**Table 2.4 Step-Wise Multiple Regression of Environmental Variables and Accretion**

| | $R^2$ | f | p | Coefficient | Estimate Std. | Error | t value | |
|---|---|---|---|---|---|---|---|---|
| $^{137}$Cs | 0.04 | 1.29 | 0.3 | Intercept | 3.12 | 0.58 | 5.36 | *** |
| | | | | Rate SLR | 0.23 | 0.22 | 1.06 | |
| $^{210}$Pb | 0.56 | 18.89 | *** | Intercept | -6.85 | 1.65 | -4.16 | *** |
| | | | | Diurnal Tidal Range | 5.87 | 0.95 | 6.15 | *** |
| | | | | Rate SLR | -0.55 | 0.24 | -2.14 | ** |
| $^{14}$C | 0.27 | 6.14 | *** | Intercept | 13.08 | 2.29 | 5.70 | *** |
| | | | | MAT | -0.58 | 0.12 | -4.79 | *** |
| | | | | Rate SLR | -0.69 | 0.24 | -2.92 | ** |
| | | | | Subsidence | -0.33 | 0.12 | -2.79 | ** |
| | | | | Average OM | -0.06 | 0.04 | -1.50 | |

Significance codes : *** $p < 0.001$, ** $p < 0.01$

Results of stepwise multiple regression for accretion rates with all data as well as separated by method.

## 2.8 Appendix

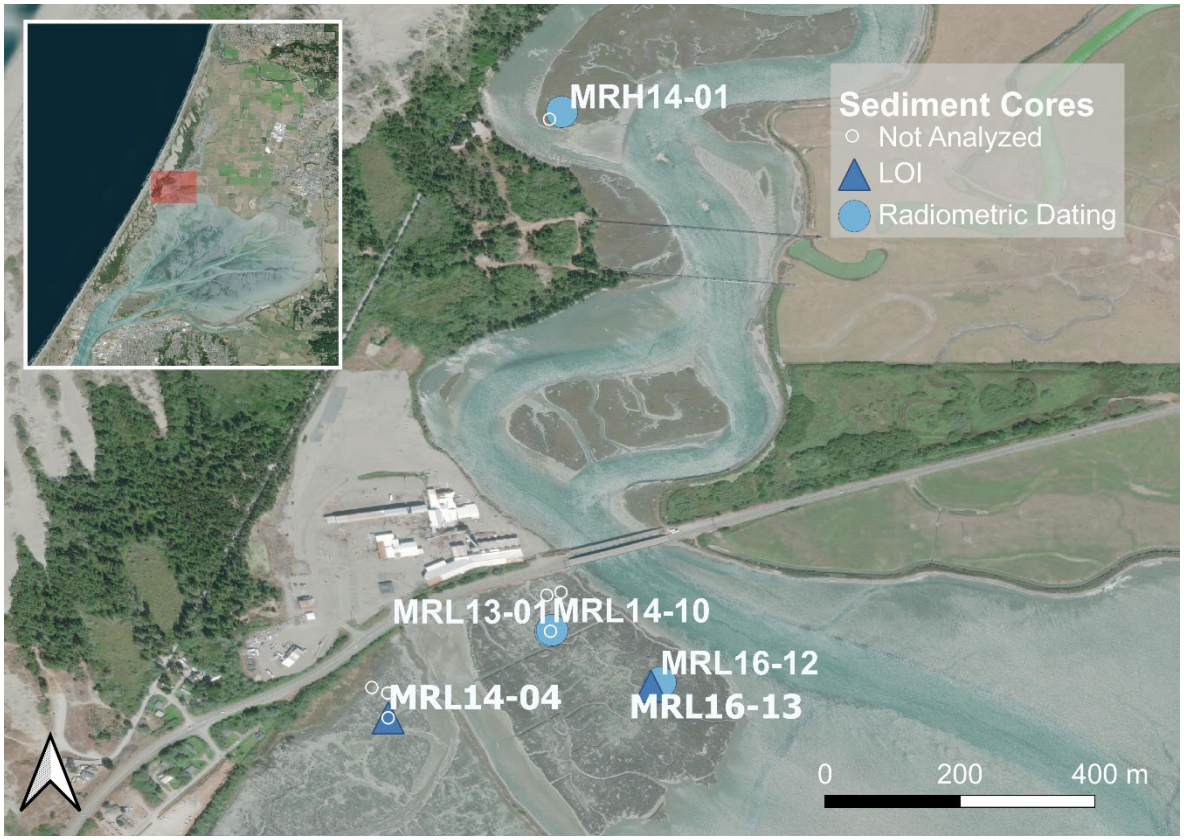


**Appendix Figure 2.1 Site Map: Mad River High & Low**

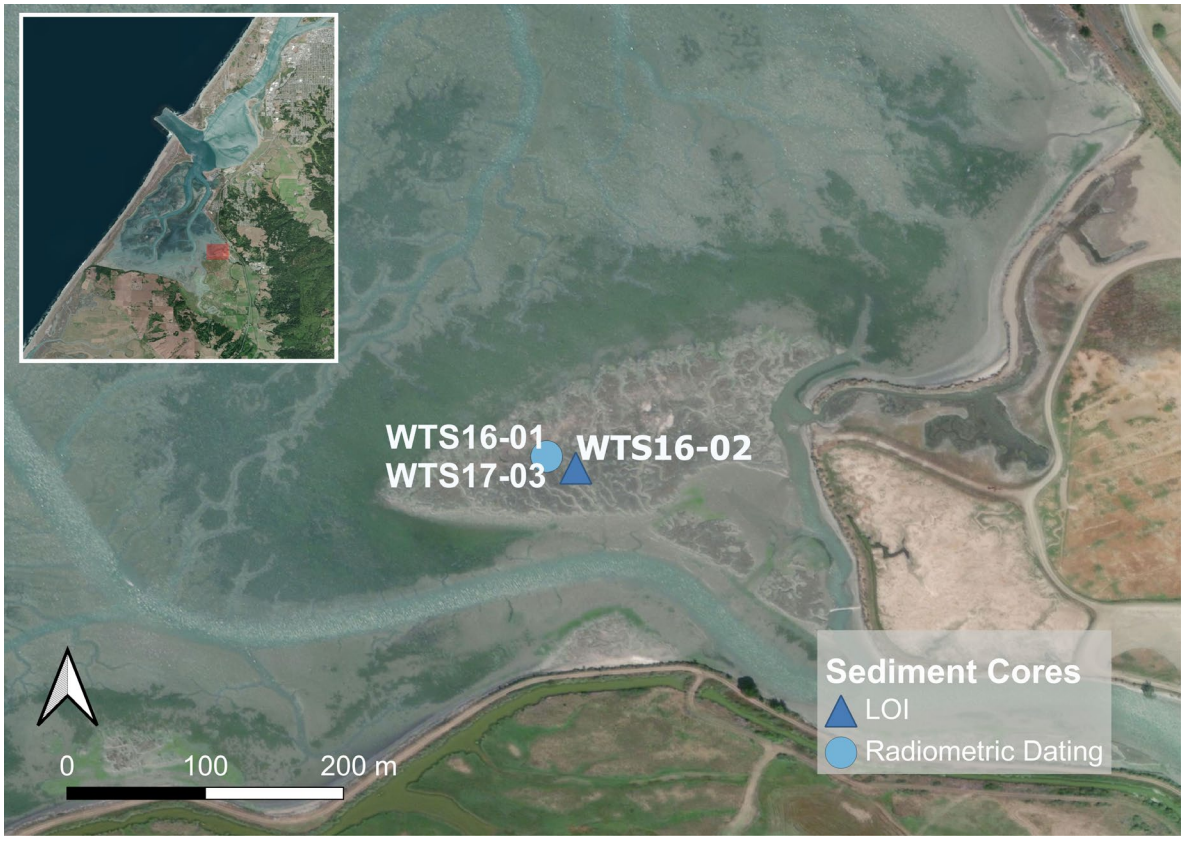


**Appendix Figure 2.2 Site Map: White Slough**

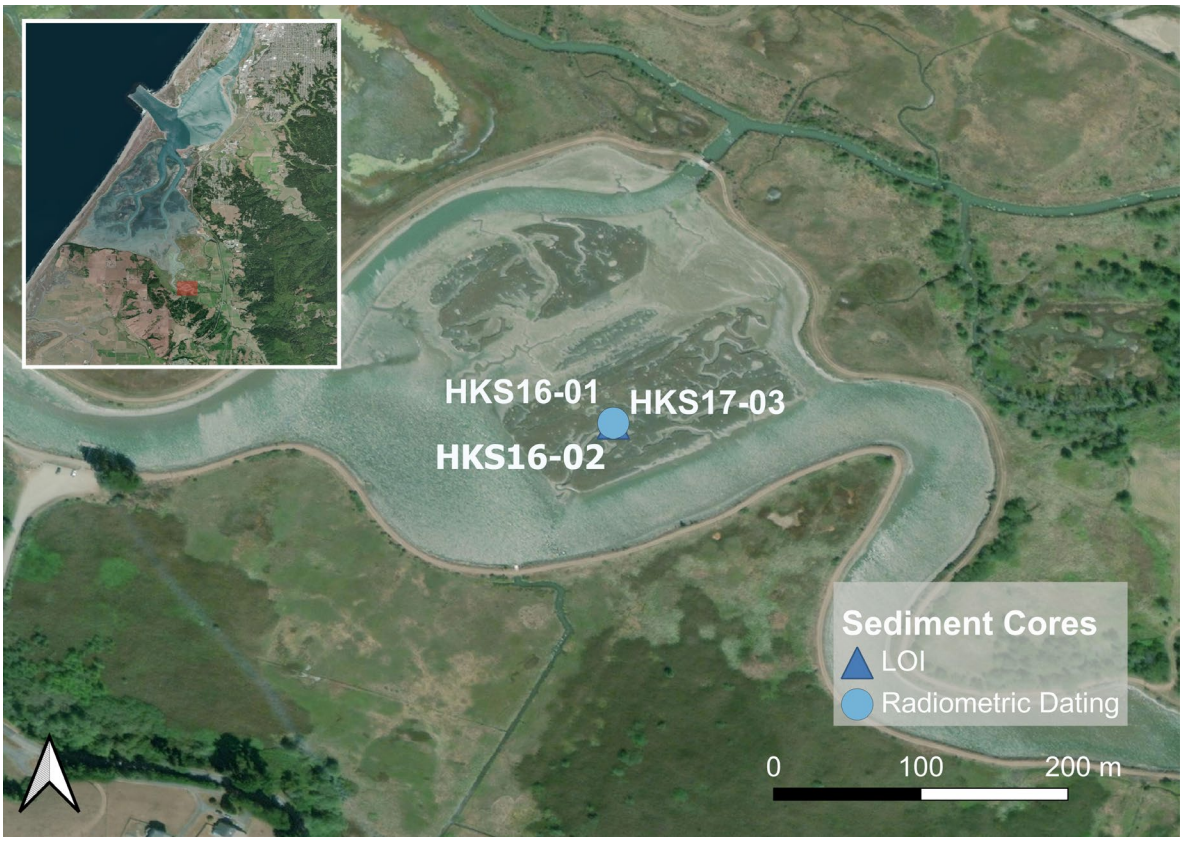


**Appendix Figure 2.3 Site Map: Hookton Slough**

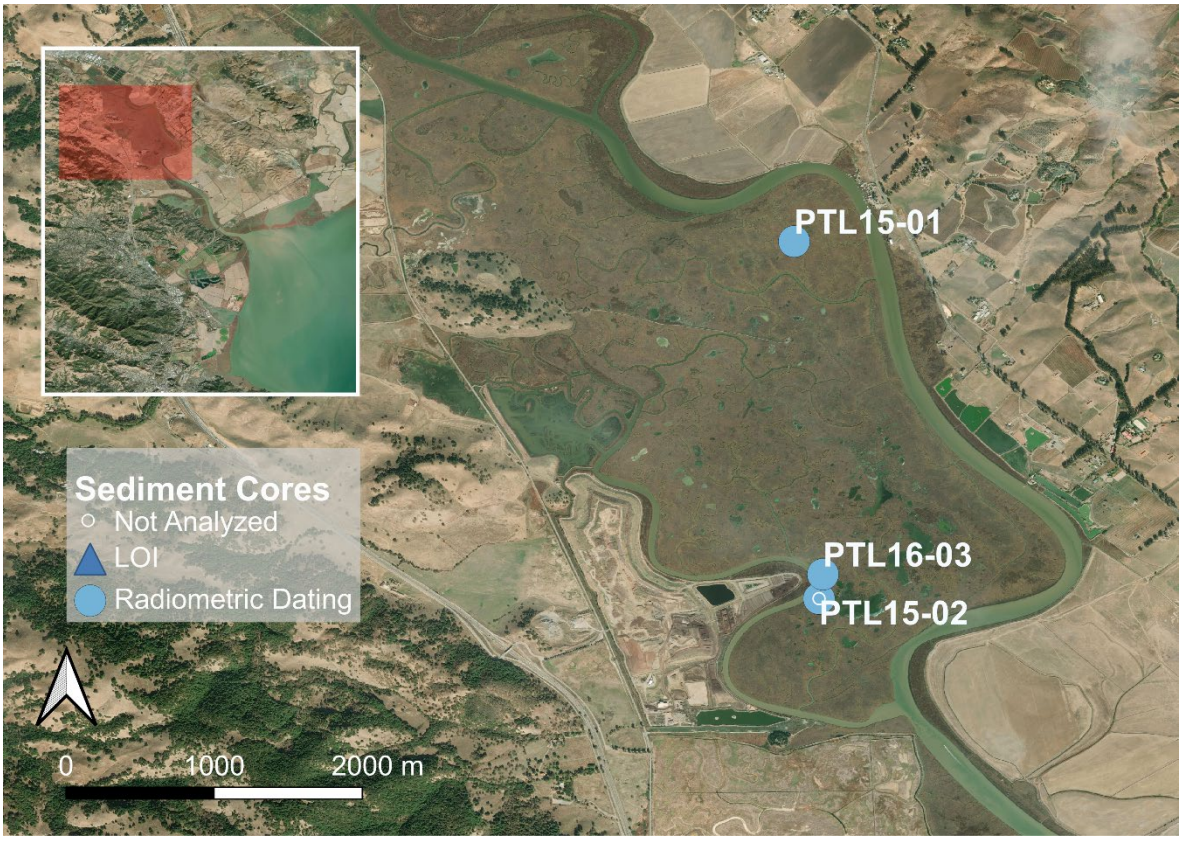


**Appendix Figure 2.4 Site Map: Petaluma Marsh**

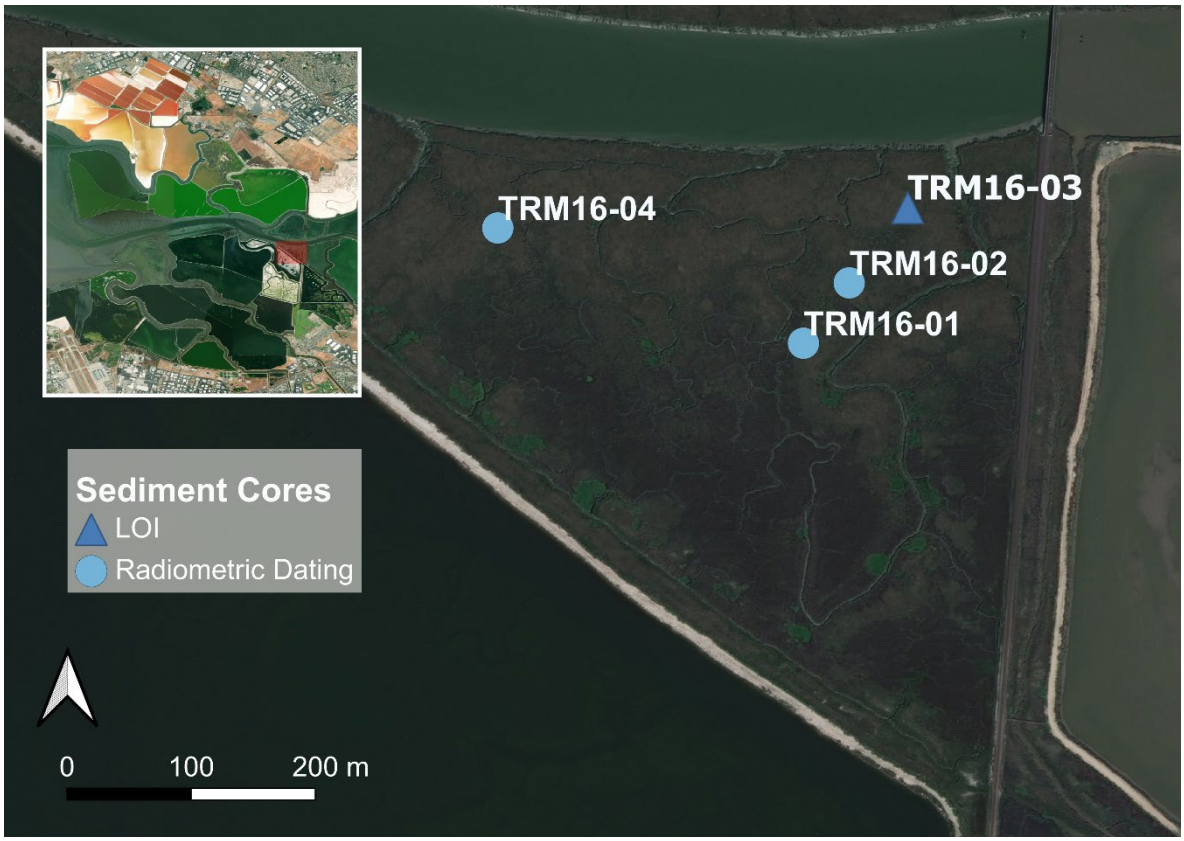


**Appendix Figure 2.5 Site Map: Triangle Marsh**

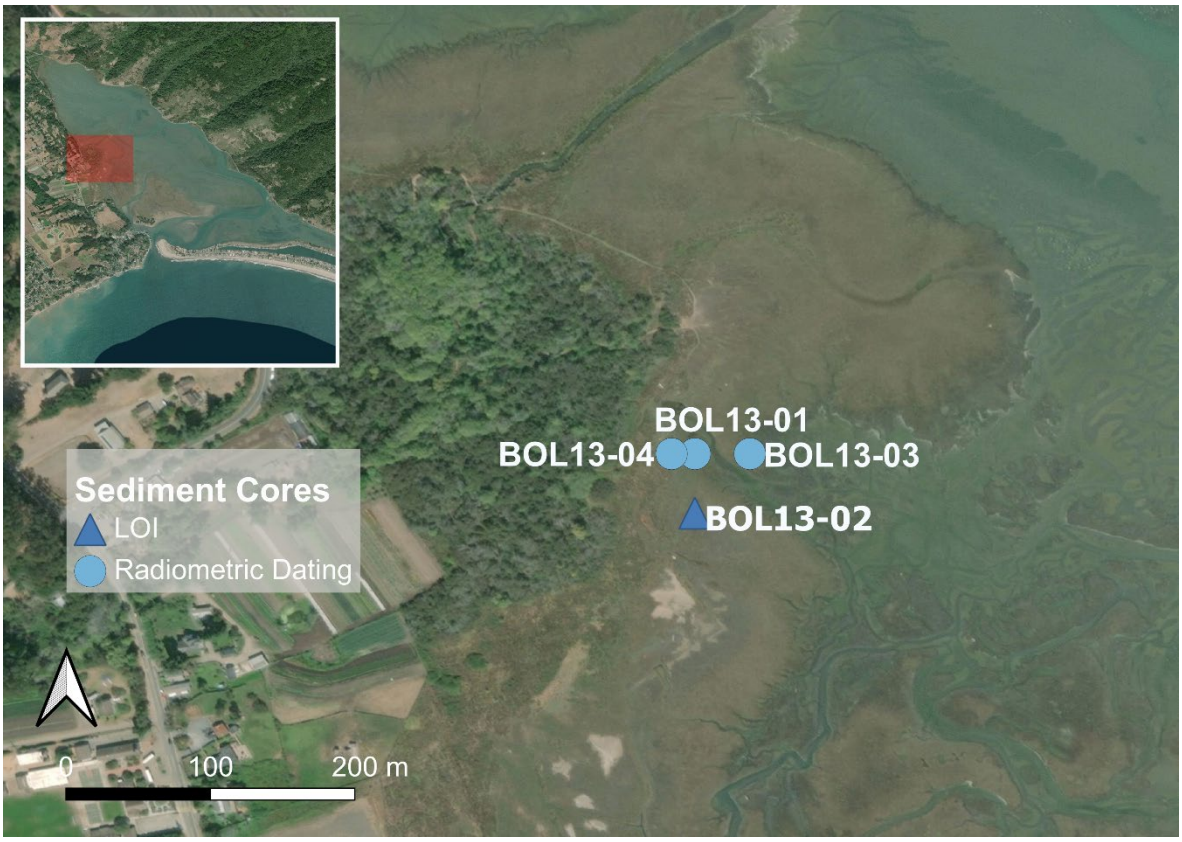


**Appendix Figure 2.6 Site Map: Bolinas Lagoon**

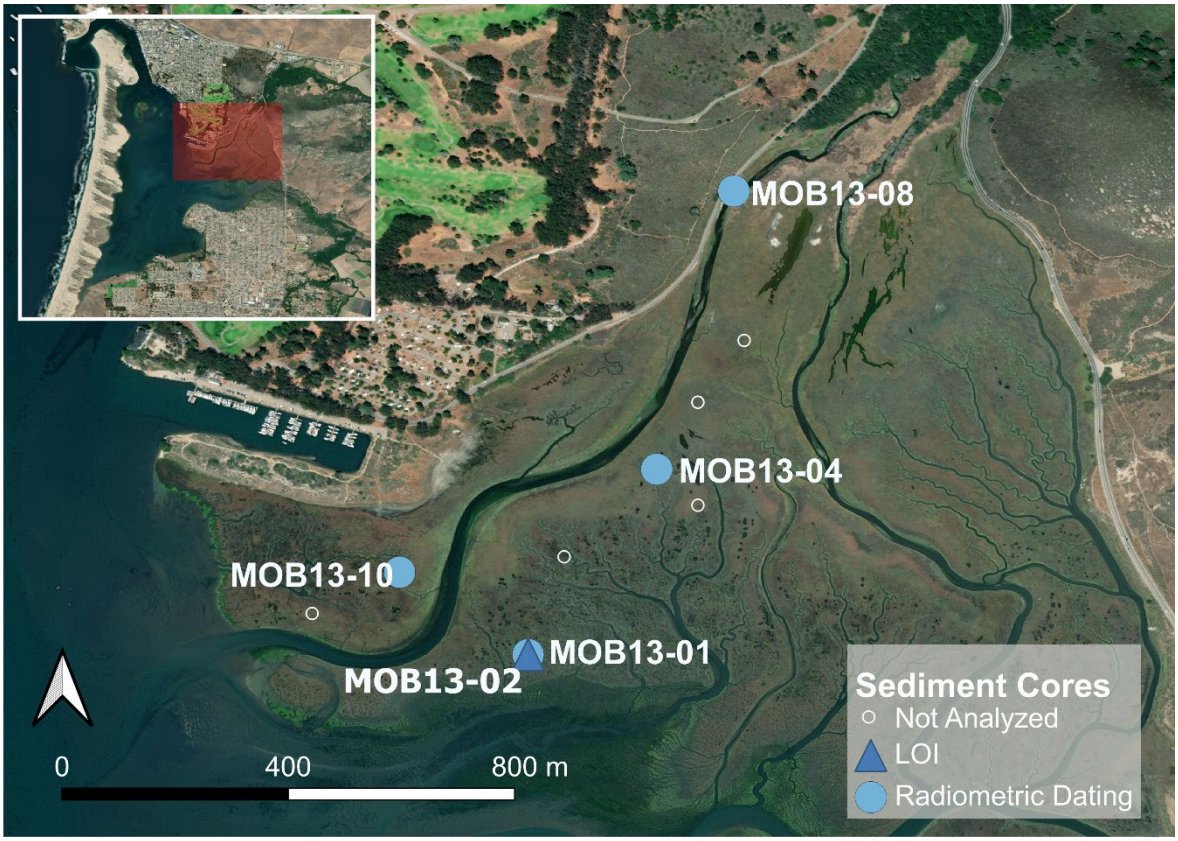


**Appendix Figure 2.7 Site Map: Morro Bay**

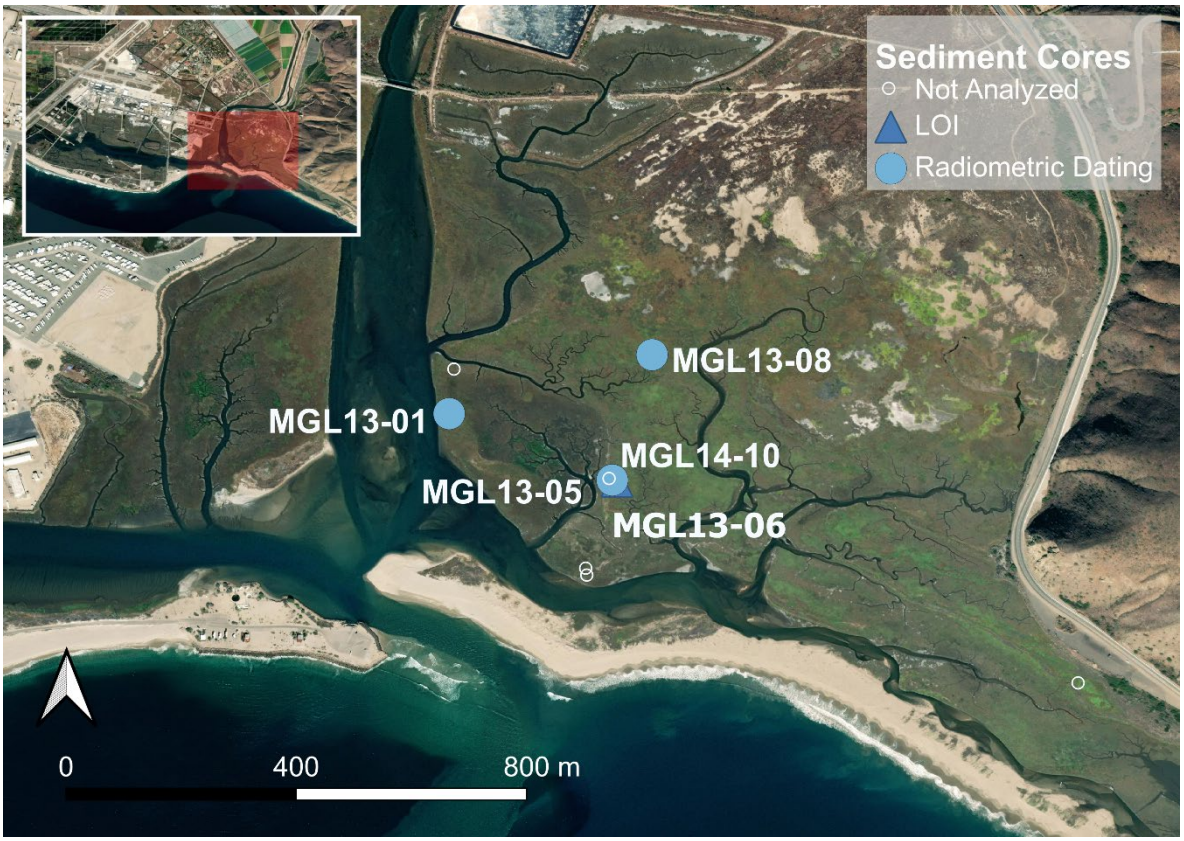


**Appendix Figure 2.8 Site Map: Mugu Lagoon**


**Appendix Figure 2.9 Site Map: Seal Beach**

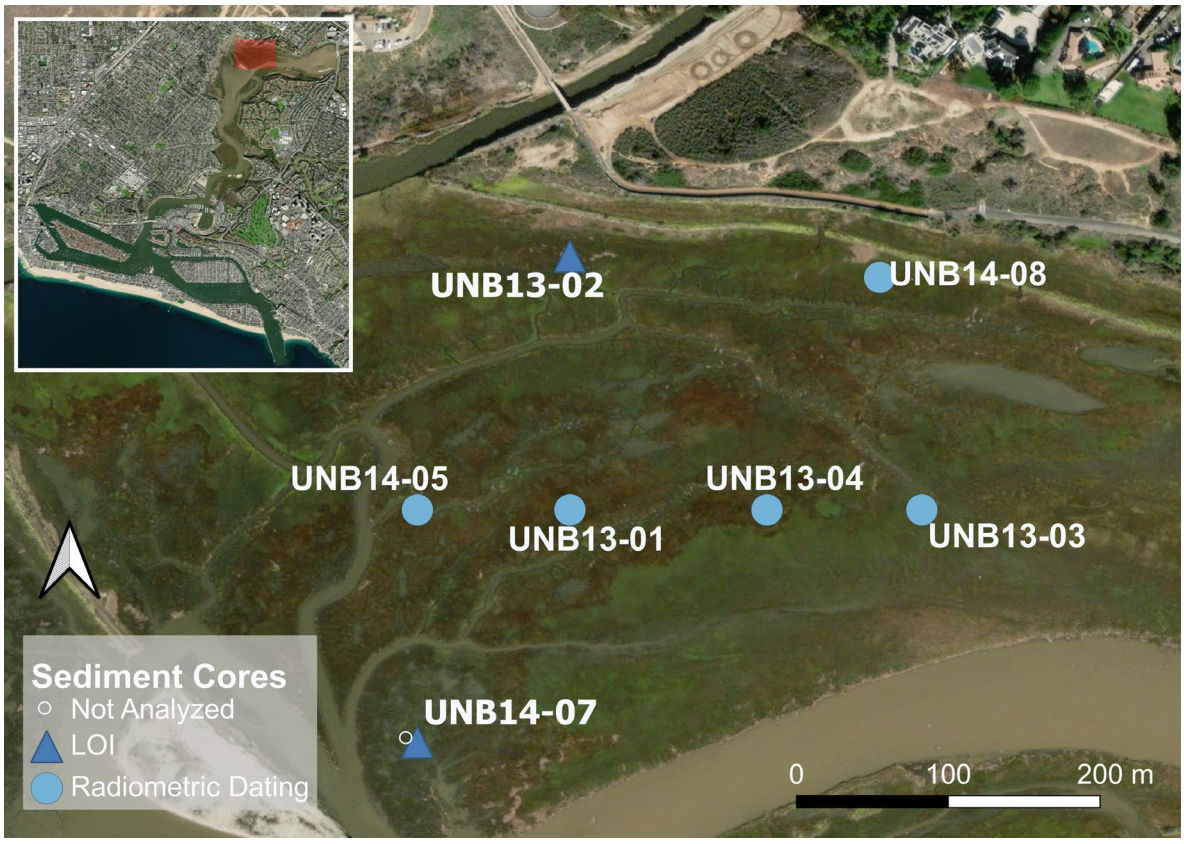


**Appendix Figure 2.10 Site Map: Upper Newport Bay**

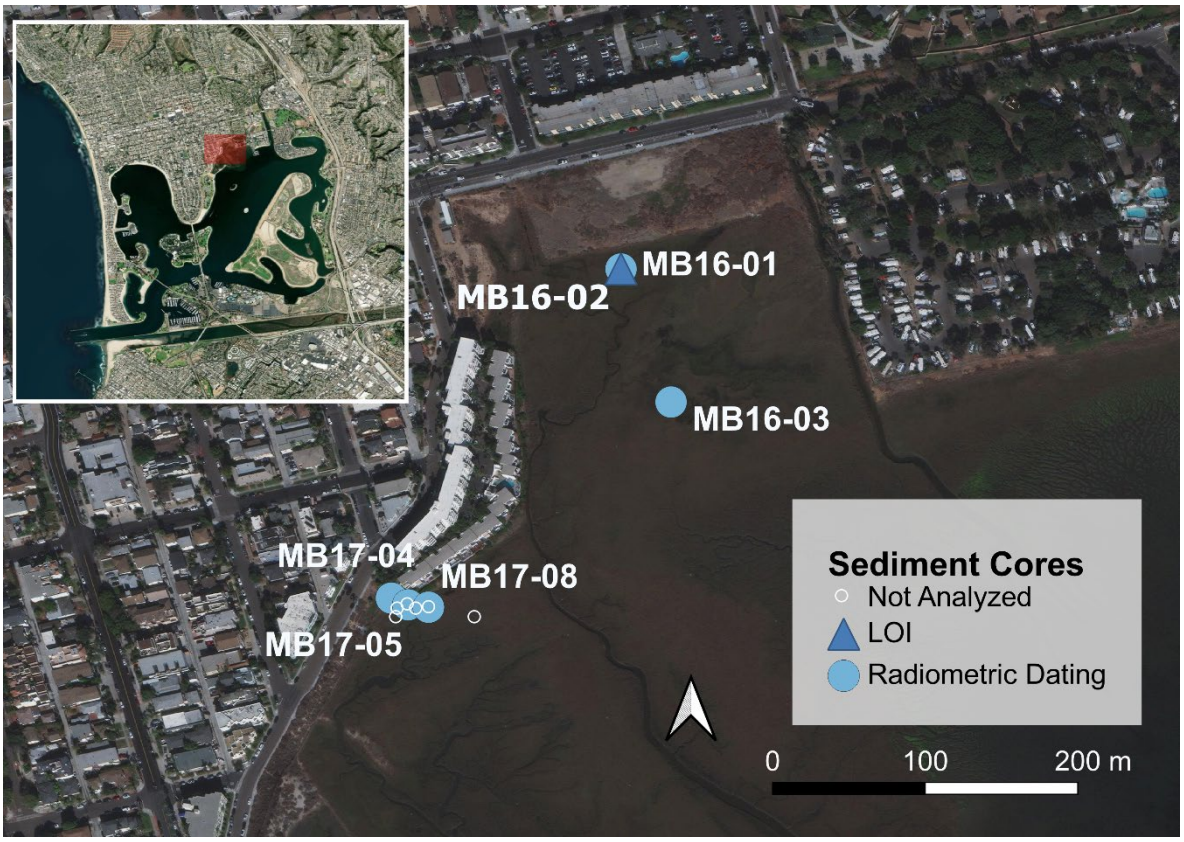


**Appendix Figure 2.11 Site Map: Mission Bay**

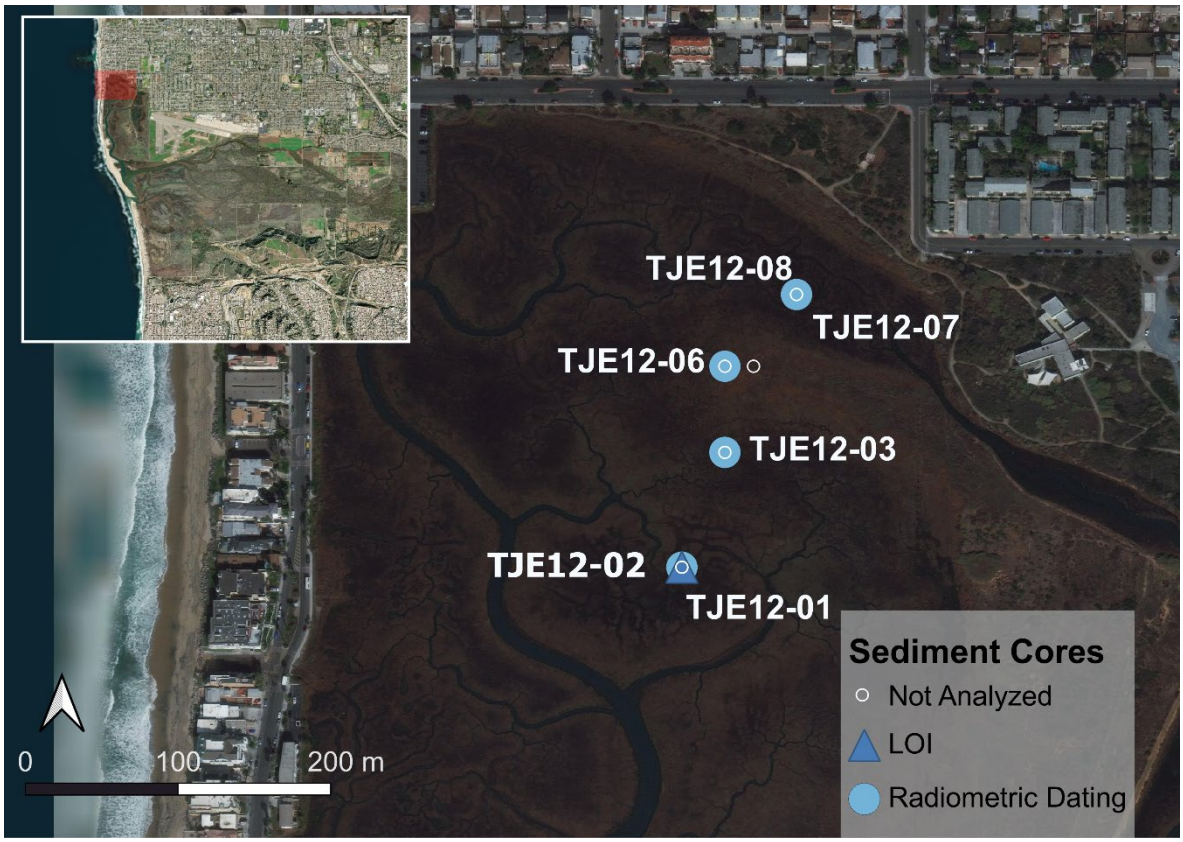


**Appendix Figure 2.12 Site Map: Tijuana River Estuary**

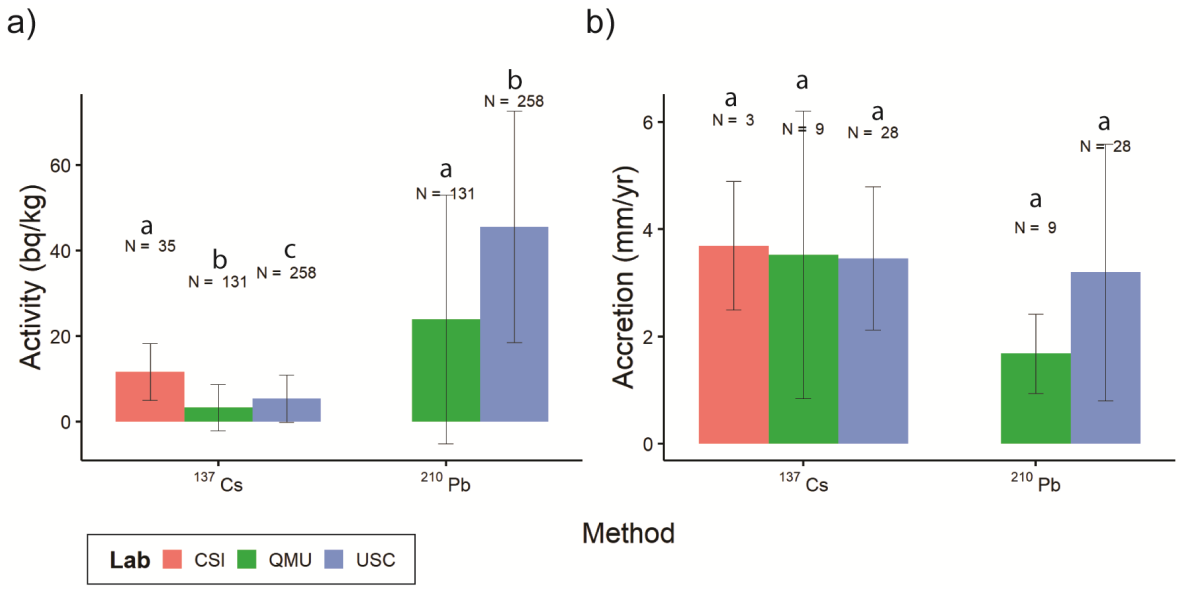


**Appendix Figure 2.13 Interlab Comparison for Gamma Detection**

Samples tested at Core Scientific International (CSI), Queen Mary University (QMU), and University of Southern California (USC) are compared based on (a) raw $^{137}$Cs and $^{210}$Pb activity and (b) core-level accretion rates. Measurement of raw radioactivites vary significantly (t-test; $p < 0.05$) between all laboratories. There is no significant difference (t-test; $p > 0.05$) between accretion rates measured between labs. Means which are not significantly different are indicated by shared letters.

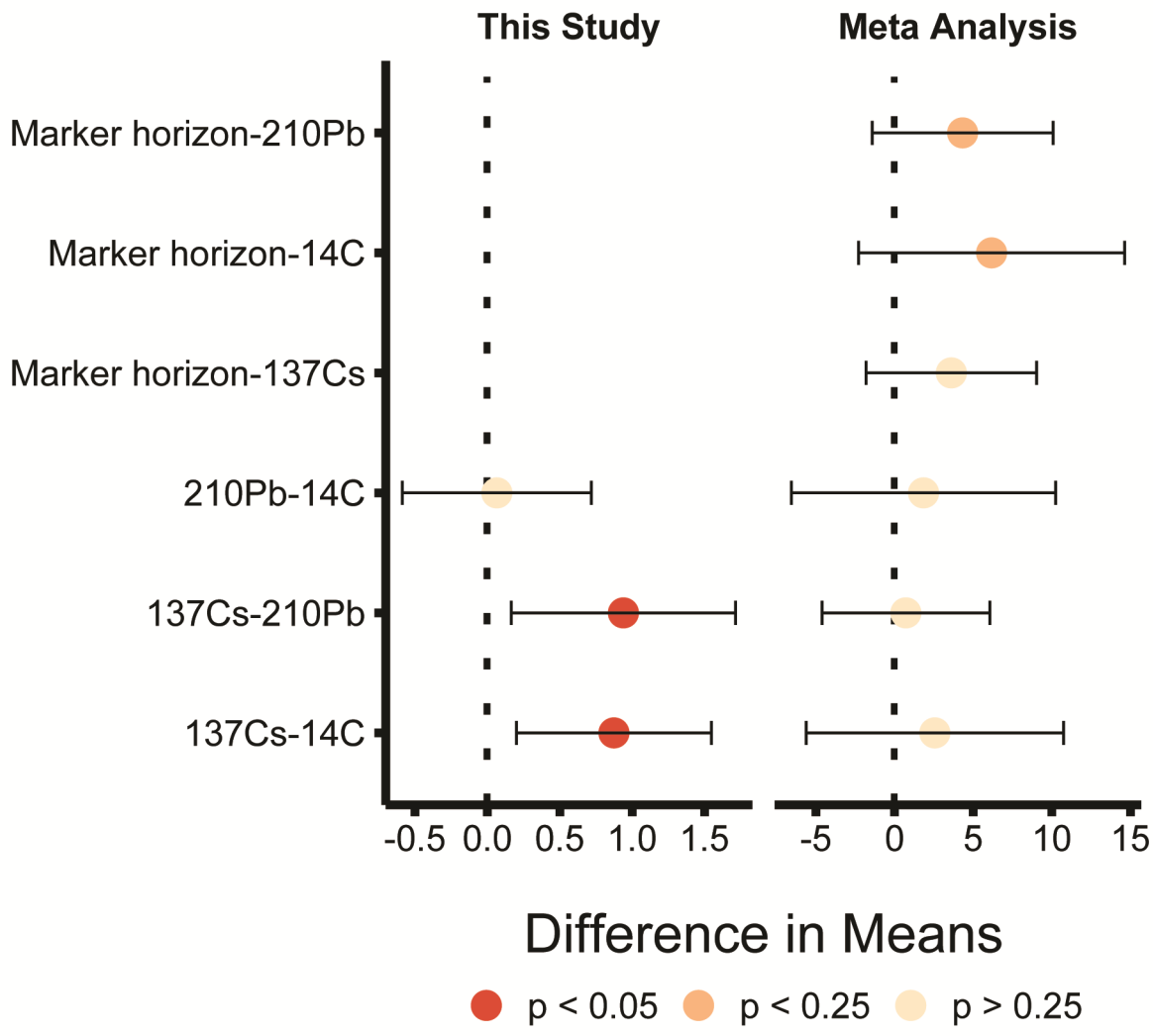


**Appendix Figure 2.14 Difference of Mean Accretion Rates by Methods**

Results of a one-way ANOVA show estimated difference in means for accretion rate data measured by different methods. Data from this study as well as published data (Meta Analysis) were analyzed.

**Appendix Table 2.1 Summary of Global Accretion Rates**

| Region | n | Accretion (mm/yr) | Range |
|---|---|---|---|
| **Asia** | 3 | 24.7 ± 1.7 | 0.96 - 54 |
| **Central America** | 1 | 3.1 | 4 - 10.3 |
| **Europe** | 19 | 8.2 ± 1.4 | 0.3 - 38.1 |
| **North America** | 51 | 4.6 ± 0.5 | 0 - 85 |
| **United States** | 49 | 4.7 ± 0.5 | 0 - 85 |
| Northeastern US | 21 | 4.7 ± 0.6 | 0 - 24 |
| Northwestern US | 4 | 4.7 ± 0.9 | 1.6 - 8 |
| Southeastern US | 15 | 6.6 ± 1.2 | 0.26 - 30 |
| Southwestern US | 9 | 3.9 ± 0.7 | 0.1 - 85 |

Summary of review of mean published accretion rates and ranges by global region and US region

**Appendix Table 2.2 $^{137}$Cs and $^{210}$Pb Activities (preview)**

| lab | date | sitecode | year | corecode | upper_ depth | lower_ depth | 210pb_ bqkg | 210pb_ bqkg_err |
|---|---|---|---|---|---|---|---|---|
| USC | Jan-17 | HKS | 2016 | HKS16-01 | 1 | 2 | 73.61 | 14.06 |
| USC | Jan-17 | HKS | 2016 | HKS16-01 | 3 | 4 | 71.84 | 9.89 |
| USC | Jan-17 | HKS | 2016 | HKS16-01 | 7 | 8 | 63.19 | 8.87 |
| USC | Jan-17 | HKS | 2016 | HKS16-01 | 15 | 16 | 35.54 | 6.21 |
| USC | Jan-17 | HKS | 2016 | HKS16-01 | 19 | 20 | 39.16 | 6.04 |
| USC | Jan-17 | HKS | 2016 | HKS16-01 | 27 | 28 | 24.22 | 7.49 |
| USC | Jan-17 | HKS | 2016 | HKS16-01 | 33 | 34 | 39.90 | 8.42 |
| USC | Jan-17 | HKS | 2016 | HKS16-01 | 37 | 38 | 14.06 | 6.45 |
| USC | Jan-17 | HKS | 2016 | HKS16-01 | 39 | 40 | 27.35 | 8.23 |
| USC | Jan-17 | HKS | 2016 | HKS16-01 | 47 | 48 | NA | NA |
| USC | Jan-17 | HKS | 2017 | HKS17-03 | 3 | 4 | 69.46 | 8.08 |
| USC | Jan-17 | HKS | 2017 | HKS17-03 | 7 | 8 | 62.34 | 6.58 |

Above is a preview of the datasheet containing raw $^{137}$Cs, $^{210}$Pb, $^{226}$Ra, $^{214}$Pb, $^{214}$Bi, and/or $^{241}$Am activities with reported errors from University of Southern California (USC), Queen Mary University (QMU), and Core Scientific International (CSI) laboratories. If labs reported calculated values of $^{210}Pb_{ex}$, those values are also shown here. All 'NA" values correspond either to activities not measured by that specific laboratory or samples for which activities were not successfully measured. These data are available in their entirety as an Excel sheet appendix to this manuscript.

**Appendix Table 2.3 Radiocarbon Results**

| Region | Site | Core | Depth (cm) | UCI AMS # | $^{14}$C Age (BP) |
|---|---|---|---|---|---|
| Humboldt Bay | *Mad River Low* | MRL13-01 | 124 - 125 | 191925 | 245 ± 15 |
| | | MRL13-01 | 145 - 146 | 210740 | 645 ± 20 |
| | | MRL13-01 | 153 - 154 | 210739 | 420 ± 70 |
| | | MRL13-01 | 172 - 173 | 148359 | 415 ± 20 |
| | | MRL13-01 | 22 - 23 | 138996 | -3550 ± 25 |
| | *White Slough* | WTS16-01 | 93 - 94 | 183283 | 360 ± 25 |
| | | WTS17-03 | 124 - 125 | 193503 | 135 ± 20 |
| | | WTS17-03 | 277 - 278 | 193504 | 565 ± 20 |
| | | WTS17-03 | 348 - 349 | 193505 | 330 ± 20 |
| | | WTS17-03 | 348 - 349 | 193505 | 2875 ± 20 |
| | | WTS17-03 | 393 - 394 | 210742 | 4560 ± 150 |
| | | WTS17-03 | 436 - 437 | 193506 | 595 ± 20 |
| | *Hookton Slough* | HKS16-01 | 94 - 95 | 183284 | -20 ± 20 |
| | | HKS17-03 | 148 - 149 | 193500 | 230 ± 20 |
| | | HKS17-03 | 203 - 204 | 210743 | 1250 ± 45 |
| | | HKS17-03 | 243 - 244 | 193501 | 1065 ± 20 |
| | | HKS17-03 | 295 - 296 | 210744 | 1505 ± 20 |
| | | HKS17-03 | 371 - 372 | 193502 | 1395 ± 25 |
| San Francisco Bay | *Petaluma* | PTL15-02 | 1106 - 1107 | 191918 | 130 ± 15 |
| | | PTL15-02 | 1169 - 1170 | 183280 | -310 ± 15 |
| | | PTL15-02 | 232 - 233 | 183277 | 1645 ± 15 |
| | | PTL15-02 | 410 - 411 | 183278 | 2390 ± 30 |
| | | PTL15-02 | 600 - 601 | 191917 | 4700 ± 60 |
| | | PTL15-02 | 651 - 652 | 183279 | 3895 ± 25 |
| | | PTL15-02 | 987 - 988 | 191919 | 4695 ± 15 |
| | *Triangle Marsh* | TRM16-01 | 162 - 163 | 210745 | 1105 ± 25 |
| | | TRM16-01 | 245 - 246 | 185584 | 295 ± 30 |
| | | TRM16-01 | 282 - 283 | 185585 | 1805 ± 15 |
| | | TRM16-01 | 332 - 333 | 210746 | 1745 ± 30 |
| | | TRM16-01 | 386 - 387 | 210747 | 1790 ± 100 |
| | | TRM16-02 | 148 - 149 | 210748 | 325 ± 40 |
| | | TRM16-02 | 240 - 241 | 185586 | 350 ± 15 |
| | | TRM16-02 | 324 - 325 | 183281 | 875 ± 15 |
| | | TRM16-02 | 426 - 427 | 185587 | 1345 ± 15 |

**Appendix Tab 2.3 (cont'd)**

| Region | Site | Core | Depth (cm) | UCI AMS # | $^{14}$C Age (BP) |
|---|---|---|---|---|---|
| San Francisco Bay | *Triangle Marsh* | TRM16-02 | 510 - 511 | 183282 | 1905 ± 15 |
| | | TRM16-02 | 538 - 539 | 210749 | 3310 ± 110 |
| Outer Coast | *Bolinas* | BOL13-01 | 140 - 141 | 138967 | 815 ± 20 |
| | | BOL13-01 | 46 - 47 | 138990 | 160 ± 25 |
| | | BOL13-01 | 54 - 55 | 148353 | 130 ± 20 |
| | | BOL13-03 | 54 - 55 | 138969 | 430 ± 20 |
| | | BOL13-03 | 96 - 97 | 138970 | 695 ± 20 |
| | | BOL13-04 | 83 - 84 | 148372 | 850 ± 20 |
| | *Morro Bay* | MOB13-04 | 267 - 268 | 128221 | 825 ± 15 |
| | | MOB13-04 | 73 - 74 | 148356 | -340 ± 20 |
| | | MOB13-08 | 111 - 112 | 128207 | 1180 ± 15 |
| | | MOB13-08 | 150 - 151 | 128222 | -275 ± 15 |
| | | MOB13-08 | 196 - 197 | 128208 | 830 ± 15 |
| | | MOB13-08 | 55 - 56 | 128223 | 190 ± 60 |
| | | MOB13-10 | 196 - 197 | 128210 | 995 ± 15 |
| Southern California | *Mugu Lagoon* | MGL13-05 | 66 - 67 | 124539 | -190 ± 15 |
| | | MGL13-08 | 67 - 68 | 128219 | -285 ± 15 |
| | *Seal Beach* | SB14-01 | 106 - 107 | 139000 | 640 ± 60 |
| | | SB14-01 | 59 - 60 | 138999 | 335 ± 20 |
| | | SB14-05 | 129 - 130 | 139003 | 255 ± 20 |
| | | SB14-05 | 272 - 273 | 139004 | 2010 ± 25 |
| | | SB14-05 | 293 - 294 | 148362 | 2395 ± 20 |
| | | SB15-06 | 98 - 99 | 183285 | 340 ± 15 |
| | | SB15-11 | 109 - 110 | 168443 | 1060 ± 15 |
| | | SB15-11 | 173 - 174 | 183286 | 870 ± 40 |
| | | SB15-14 | 103 - 104 | 168444 | 900 ± 20 |
| | | SB15-14 | 106 - 107 | 168445 | 1025 ± 15 |
| | | SB15-16 | 90 - 91 | 168446 | 925 ± 15 |
| | | SB15-20 | 165 - 166 | 168449 | 1620 ± 60 |
| | | SB15-20 | 190 - 191 | 183288 | 865 ± 20 |
| | | SB15-20 | 295 - 296 | 183289 | 640 ± 15 |
| | *Upper Newport Bay* | UNB13-01 | 47 - 48 | 128212 | -1270 ± 15 |
| | | UNB13-01 | 96 - 97 | 128213 | 1410 ± 15 |
| | | UNB13-03 | 478 - 479 | 128215 | 5465 ± 15 |
| | | UNB13-03 | 64 - 65 | 148373 | 195 ± 20 |
| | | UNB14-05 | 118 - 119 | 138976 | 635 ± 20 |
| | | UNB14-05 | 296 - 297 | 138977 | 2620 ± 20 |
| | | UNB14-08 | 103 - 104 | 148363 | 2620 ± 80 |

**Appendix Tab 2.3 (cont'd)**

| Region | Site | Core | Depth (cm) | UCI AMS # | $^{14}$C Age (BP) |
|---|---|---|---|---|---|
| Southern California | *Upper Newport Bay* | UNB14-08 | 107 - 108 | 148376 | 615 ± 20 |
| | | UNB14-08 | 162 - 163 | 138982 | 875 ± 20 |
| | | UNB14-08 | 49 - 50 | 138981 | -1075 ± 20 |
| | *Mission Bay* | MB17-05 | 109 - 110 | 191928 | 335 ± 15 |
| | | MB17-05 | 143 - 144 | 191929 | 915 ± 15 |
| | | MB17-05 | 147 - 148 | 191930 | 1070 ± 15 |
| | | MB17-08 | 129 - 130 | 191932 | 700 ± 15 |
| | | MB17-08 | 166 - 167 | 191933 | 760 ± 15 |
| | | MB17-08 | 70 - 71 | 191931 | 335 ± 15 |
| | *Tijuana River Estuary* | TJE12-03 | 53 - 54 | 128226 | -980 ± 50 |
| | | TJE12-07 | 130 - 131 | 115842 | 1575 ± 20 |
| | | TJE12-07 | 64 - 65 | 138974 | 550 ± 20 |
| | | TJE12-08 | 141 - 142 | 115843 | 1610 ± 30 |

Results from radiocarbon dating of biologic material reported as uncalibrated $^{14}$C age before present (BP).University of California, Irvine AMS identification numbers are listed.

**Appendix Table 2.4 Climate and Tidal Metadata**

| Site | MAT (°C) | MAP (mm) | NOAA Climate Station ID | Station Latitude | Station Longitude | Dirunal Tidal Range (m) | SLR (mm $yr^{-1}$) | NOAA Tidal Gauge |
|---|---|---|---|---|---|---|---|---|
| Mad River High<br>Mad River Low<br>White Slough<br>Hookton Slough | 11.6 | 264.16 | USW00024213 | 40.77 | -124.22 | 2.09 | 4.87 ± 0.91 | 9418767, North Spit |
| Petaluma | 14.6 | 159.77 | USC00046826 | 37.81 | -122.47 | 1.85 | 1.96 ± 0.18 | 9414290, San Francisco |
| Triangle | 15.4 | 97.54 | USC00046144 | 37.51 | -122.21 | 2.70 | 2.47 ± 1.62 | 9414523 Redwood Cit |
| Bolinas | 13.4 | 334.01 | USC00046370 | 38.00 | -122.97 | 1.76 | 2.12 ± 0.88 | 9415020, Point Reyes |
| Morro Bay | 14.8 | 122.43 | USC00045866 | 35.17 | -120.75 | 1.62 | 0.93 ± 0.38 | 9412110. Port San Luis |
| Mugu Lagoon | 15.2 | 76.45 | USW00093111 | 34.35 | -119.44 | 1.65 | 3.22 ± 1.66 | 9411270, Rincon Island |
| Seal Beach | 18.2 | 68.07 | USW00023129 | 32.72 | -118.27 | 1.67 | 1.01 ± 0.23 | 9410660, Los Angeles |
| Upper Newport Bay | 17.8 | 76.71 | USW00093184 | 33.60 | -117.88 | 1.67 | 2.22 ± 1.04 | 9410580, Newport Beach |
| Mission Bay | 16.4 | 83.31 | USC00047741 | 32.87 | -117.26 | 1.62 | 2.17 ± 0.27 | 9410230, La Jolla |
| Tijuana River Estuary | 16.9 | 72.9 | USW00093115 | 32.71 | -117.17 | 1.74 | 2.19 ± 0.18 | 9410170, San Diego CA |

This table shows the metadata for site environmental characteristics.

# 3. Improving Blue Carbon Estimates: Best Practices for Quantifying Uncertainty in Loss-on-Ignition

## 3.1 Abstract

Coastal vegetated habitats, although small in areal extent, store carbon in their soils at rates higher than many terrestrial environments (Mcleod et al., 2011). This coastal carbon sink is frequently referred to as blue carbon. Most reported values of blue carbon storage and sequestration are based on estimates of soil organic carbon (SOC) derived from loss-on-ignition (LOI). But LOI methodology and, importantly, conversions of LOI-derived estimates of soil organic matter (SOM) into SOC vary widely. This chapter presents a short review of the uncertainties and errors associated with LOI-based estimates of SOC. The magnitude of uncertainties and errors in laboratory protocol and the conversion between SOM and SOC are quantified from published sources and empirically tested using a database of salt marsh sediment samples from the California coast. Review and empirical tests indicate that, although standardization of LOI protocol is difficult because of inherent differences in soil properties, data generators and users can take simple, cost-effective steps to estimate common sources of error such as random laboratory error (less than 2%), measurement of inorganic carbon (generally less than 10%), or measurement of non-carbon elements (generally less than 30%). The largest source of error for blue carbon estimates is the conversion of SOM to SOC, with different conversion equations resulting in up to 50% difference in estimates of SOC across ecosystem types and up to 15% within California. Comparing region-specific conversion equations with constructed conversion equations for use in California salt marshes, I contend that careful reporting of LOI protocol, conversion methods, and publication of raw LOI data are the most

crucial steps to reduce uncertainty, error, and incompatibility in global blue carbon estimates from LOI.

## 3.2 Introduction

Since 2009 the identification of blue carbon as a carbon sink provided by coastal vegetated habitats (CVHs) such as seagrasses, mangroves, and salt marshes has galvanized much research aiming to quantify and project carbon stocks and fluxes (Nellemann et al., 2009). The storage and longevity of carbon in these systems is primarily due to rapid burial in anaerobic soils, like in freshwater wetlands, as well as the reduced soil conditions from added sulfates which decrease the loss of carbon via methane production (Mitra, Wassmann, & Vlek, 2005). Current estimates show that salt marshes, mangroves, and seagrass ecosystems accumulate carbon at rates between 18 to 1,713 g C $m^{-2}$, faster by an order of magnitude or more than terrestrial forest ecosystems (Mcleod et al., 2011). Therefore, while CVHs are geographically limited in area, a potential 10.2 Tg C $yr^{-1}$ are sequestered in these systems (Ouyang & Lee, 2014) and estimates of storage of greater than 10,000 Tg C – about one-third of annual global greenhouse gas emissions[2] – have been made (Chmura, Anisfeld, Cahoon, & Lynch, 2003).

The interest in carbon storage as an ecosystem service and demand for detailed carbon budgets for potential sinks requires improved accuracy of measurements and estimates at the local to the global level (Chmura, 2013). Researchers and stakeholders are presented with the dual challenge of obtaining the most accurate data for their own study and purposes while also maintaining data standards which will comply with global standards for comparisons. While methodologies are being developed to bring blue carbon values to carbon markets (American Carbon Registry, 2017; Verified Carbon Standard: A Global Benchmark for Carbon, 2015), there are not yet any accepted global standards for methods of measurement and estimation. Top-down

[2] Global emissions estimated at 37.1 gigatonnes $CO_2$ for 2018 (Global Carbon Project, 2018)

measurements such as flux towers and remote sensing of carbon stocks are in development and are extremely limited in spatial distribution and in terms of temporal span of measurement (Baldocchi, 2014; Yan et al., 2008). Most of our current knowledge of the carbon cycle in CVHs is from bottom-up measurements of soil carbon which are extrapolated outwards to regional and global estimates (Chmura et al., 2003; Holmquist et al., 2018; Ouyang & Lee, 2014). These bottom-up measures are often less expensive and more easily obtained, making this a more accessible option for researchers and stakeholders in developing nations where blue carbon data are in high demand. Yet considerable uncertainty in large-scale estimates of stocks and fluxes then arises from combining data from multiple sources, estimating and propagating error from the site level up to global scale.

Quantification of soil carbon content alone has been done in many ways (Table 3.1), often with methodological variability even within methods. In effort to reduce method variability, many papers have been published comparing the accuracy and precision of different methodologies (Ball, 1964; Campos C., 2010; Frangipane, Pistolato, Molinaroli, Guerzoni, & Tagliapietra, 2009; Konare et al., 2010; Wright, Wang, & Reddy, 2008), discussing the potential errors and difficulties associated with each (Heiri et al., 2001; Hoogsteen, Lantinga, Bakker, Groot, & Tittonell, 2015) and providing recommendations based on these experiments. But recommendations from some authors may be in direct contradiction to others. For instance some recommend that combustion of soil for measurement of organic content should be conducted at low temperature combustion for long duration (Ball, 1964) while others advise shorter, higher temperature treatments (Heiri et al., 2001). Some of this disparity may be explained by authors working with different soils and ecosystems; for instance, researchers working to quantify blue carbon in the calcareous soils of the Everglades need to avoid overestimating blue carbon content

by combustion of inorganic carbon (IC) at high temperatures (Wright et al., 2008). Whereas, researchers working in non-calcareous sediments following similar protocols may ultimately underestimate blue carbon content due to incomplete combustion of recalcitrant soil types (Byers, Mills, & Stewart, 1978). In short, methodological variability arises from a real difference in performance of methods across soil types. Therefore, while standardization of the methods of measuring soil carbon might reduce some of the uncertainty in global-scale blue carbon data syntheses, standardization will not reduce the inherent uncertainty arising from comparisons of different soil types with different errors and uncertainties associated with standardized methods. So then, how can researchers most effectively measure blue carbon in individual studies while ensuring data will be suitable for global comparisons?

This chapter reviews literature on soil organic matter (SOM) and soil organic carbon (SOC) measurement within and outside the blue carbon community in order to create a decision-making structure for scientists, managers, and stakeholders regarding the use of loss-on-ignition (LOI) as a method of estimating SOC. First, I present a review of the methods of LOI and how it has been employed within the blue carbon community. Then, using sediment from six coastal marshes on the coast of California, I test the effects of temperature, treatment time, clay content, and carbonate content on the use of LOI to estimate carbon content in salt marsh soils. I use this dataset to construct a region-specific SOM-SOC conversion equations and compare these with existing conversion equations using a database of SOM values generated in Chapter 4 to estimate the effect different conversion equations have on mean estimates of SOC and carbon stocks. Finally, based on literature and data analysis, I make recommendations for conducting LOI, quantifying uncertainty and errors, and creating soil-specific SOM-SOC conversion equations to ensure estimates are accurate and scalable to global meta-analyses. I present this as a potential

standard way for data creators and data users to make the best, most-informed choices about data collection and selection to ensure global accuracy and comparability. I conclude that careful reporting of all methodologies and estimation of study uncertainty are the most important steps researchers must take when generating or utilizing blue carbon data.

### *3.2.1 LOI as a Method of Estimating Carbon in Soils*

Many methods of measuring SOC exist (Table 3.1). Generally, measurement has taken place in the lab and relies on the combustion of SOM into $CO_2$ gas by wet or dry methods. Then, either the $CO_2$ product or remaining soil fractions are measured by mass, volume, or chemical properties. Using spectrometry, there are some methods of estimating SOC either in the field or remotely, however these methods are in their development and are not cost-efficient for the majority of data creators and users (Nayak et al., 2019). LOI is often chosen for estimates of SOC because, relative to other methods, it is fast, inexpensive, and reliable. LOI has been tested in comparison to wet and dry combustion methods across many different soil types and ecosystems with positive results (Abella & Zimmer, 2007; Byers et al., 1978; Campos C., 2010; Craft, Seneca, & Broome, 1991; Dean, 1974; Frangipane et al., 2009; Ghabbour, Davies, Cuozzo, & Miller, 2014; Goldin, 1987; Hoogsteen et al., 2015; Howard & Howard, 1990; Kamara, Rhodes, & Sawyerr, 2007; Luczak, Janquin, & Kupka, 1977; Ranney, 1969; Ratnayake, Seneviratne, & Kulasooriya, 2007; Salehi, Beni, Harchegani, Borujeni, & Motaghian, 2011; Wang, Li, & Wang, 2011). Testing a range of sediment types from coastal and terrestrial ecosystems, Wang et al. (2011) used principle components analysis (PCA) to show that LOI, thermogravimetric analysis (TGA), and the Walkley Black method (WB) all fall within acceptable ranges for measuring SOC, with some deviations for individual samples measured by WB. The WB method uses a mix of dichromate and sulfuric acid to combust $CO_2$ and generates

hazardous waste. This reaction is known to underestimate SOM, particularly from carbon in the recalcitrant pool. This method, while correctable and reliable, has fallen out of widespread use mostly because of the cost of dichromate and the disposal of hazardous waste. Correlation between LOI and the WB method is strong in many studies with $R^2$ values of above 0.9 (Kamara et al., 2007), but because there can be variability in the effectiveness of the method by soil type, other studies report lower correlations (Konare et al., 2010). Therefore the expense and the risk of incomplete combustion with the WB method has led many to choose LOI as a more suitable alternative.

Dry combustion methods are used for processes such as gas chromatography and spectrometry. These processes, rather than calculate the loss of weight due to $CO_2$ combustion, directly measure the $CO_2$. The main challenge with either of these processes is the differentiation between IC and SOC. There is no method which can separate inorganic from organic $CO_2$, so the only two options are to be certain that all $CO_2$ generated is from organic sources or to separately quantify IC and subtract that value from total carbon. Most researchers accomplish this by removing sources of IC from their samples before combustion. Methods of doing so, including acid treatments, can risk the removal of SOC during the process. Acids can also leave deposits on samples or remove inorganic portions of soil which can lead to incorrect mass estimates and damage to equipment used during combustion and measurement. So while removal of IC is essential for calcareous soils, the error from accidental removal of SOC during treatment must be assessed against the error of over-estimation of SOC due to IC content.

Regardless of the difficulties of separating SOC from IC, because chromatographic and spectrometric methods directly measure the $CO_2$ produced by combustion of SOC, using temperatures that ensure full combustion of even the most recalcitrant carbon, these methods are

often held as the most accurate measure of SOC with the least opportunity for error from misidentification of non-carbon content as SOC. The drawbacks of chromatographic and spectrometric methods are the expense of the equipment, need for training, and processing time for samples (Konare et al., 2010; Konen, Jacobs, Burras, Talaga, & Mason, 2002). But because LOI shows high correlation with these methods (Abella & Zimmer, 2007; Ball, 1964; Craft et al., 1991; Frangipane et al., 2009; Ghabbour et al., 2014; Howard & Howard, 1990; Konare et al., 2010; Konen et al., 2002; Wang et al., 2011; Wright et al., 2008), it is often used as a cost-effective, time-saving method for obtaining estimates of SOM with subsequent conversion into SOC using correction factors or correction equations.

Despite how well LOI performs in most comparison studies, there are many critiques of the process. Most notably, LOI has been called qualitative by some (Santisteban et al., 2004). This critique may be fair on the assumption that LOI directly measures SOM, but LOI is not a direct measure of SOM. Rather is a statistical estimate base on a correlation between LOI and SOM (Heiri et al., 2001). Furthermore, although SOM itself is not always evenly correlated with SOC in all systems, these statistical estimates can be tailored to fit ecosystem parameters. For instance, because older, more humified samples with less SOM show a different SOM-SOC relationship than younger, SOM-rich samples, a quadratic expression is often used to capture some of the higher SOC values associated with higher values of SOM (Callaway et al., 2012; Craft et al., 1991). But because LOI is two steps removed from a direct measurement of SOC, many assumptions must be made along the conversion of LOI to SOM to SOC. For that reason, the most important step which any generator of blue carbon estimates from LOI can take is to carefully report all procedural steps and assumptions made during the LOI process as well as during the conversion of LOI data to SOC estimates.

### *3.2.2 Sources of Error and Uncertainty*

Error and uncertainty in LOI can be attributed to three broad categories: laboratory error, error from natural variability, and error from conversion of SOM to SOC. There is a large literature on LOI methodology. The potential magnitude of error and uncertainty introduced by errors and uncertainties from these three sources have been estimated across many soil types. I review these studies and present a summary of potential errors, magnitude of effects, and provide best practice recommendations to address known errors and uncertainties (Table 3.2).

#### 3.2.2.1 Sample Preparation

Because many practitioners of LOI come from different disciplines, the methods for collecting soil samples, preparing samples, and selecting a sample size can vary widely. Many of the initial estimates of blue carbon stocks and fluxes were made using soil cores collected to 0.5 m depth (Chmura et al., 2003). Extrapolating these estimates, which likely contain a large portion of root mass depending on the system, to the maximum depth of the carbon pool or using these values to project future carbon sequestration likely will be biased due to this position in the root zone (Bai et al., 2016). Yet continuous sampling from a soil core shows that there is considerable variability in carbon values throughout the carbon pool. Sampling from a soil core must therefore aim to capture the real variability in the system while minimizing the amount of sampling and subsampling required.

The question of bulk sampling or contiguous sampling leads to some very different methods of preparing soils for LOI. Bulk samples are often homogenized, ground, and sieved at 2 mm. While there is little evidence to show that grinding samples has an influence on measurement of carbon values (Houba, Chardon, & Roelse, 1993), there is not any research

which compares un-sieved versus sieved samples or compares homogenized versus contiguous sampling. Some efforts are underway to determine the most efficacious sampling strategy to reduce labor but to accurately estimate the carbon pool, but the influence of belowground biomass and sieving has not fully been investigated.

After samples are collected and prepped, there is still some variability in sample size with LOI. Bulk sediments frequently are measured in large masses (>10 g) whereas others will randomly subsample small samples (<1g) repeatedly to get an estimate of variability. Hoogsteen et al. (2015) examined the standard deviation of replicate samples sized from 0.15 g to 20 g and found that as sample size increased, standard deviations between replicates decreased. For this reason, they recommend a minimum sample size of 2g. They conclude that the variability is both a factor of the natural variability within soils, but also may be related to the capacity for smaller, less-air-filled samples to heat in comparison to the heating capacity for larger samples. However, Wang et al. (2011) caution that large sample sizes can lead to incomplete combustion due to a lack of surface area and recommend sample sizes from 1g to 2g.

#### 3.2.2.2 Laboratory Error

Studies which have looked at comparisons between different laboratories measuring the same set of samples using varied protocols overall have found relatively small differences (Heiri et al., 2001). Most of these differences may be due to different oven temperatures and treatment times. Others have discussed the possibility of different lab equipment having uneven heating; Hoogsteen et al. (2015) tested the effect of pre-heating furnace air before samples were placed in the furnace and found no significant difference. However, differences of up to 2% weight loss can be seen between samples near the center of furnaces compared to those at the edges (Heiri et al., 2001) and the standard deviation between same-sample tests was decreased when samples

nearest to the furnace door were rotated half-way through treatment (Hoogsteen et al., 2015). These small differences in protocol may be negligible for many samples which have percent SOM measures greater than 50%, but can make large differences for samples low in SOM.

Other differences in protocol which may create small differences in mass loss measurements include failure in preventing condensation of water on samples during cooling by not allowing samples to cool in a desiccator. There have not been any studies which have tested for differences in mass based on the length of time samples were allowed to cool, but this, like pre-heating of the furnace, is likely to have negligible impacts. Handling samples is another similar area of some uncertainty surrounding laboratory protocol. Because there is the possibility of transfer of oils during movement of crucibles by hand, many labs have standardized using tongs to move crucibles during weighing. However, there is no empirical evidence which shows that this has an effect on the ultimate mass estimate. Other labs have also used crucibles with lids compared to open-top crucibles, which might be one possibility to keep temperatures more even between crucibles or may reduce air-flow to samples. This latter change which may affect the heating of the crucible itself would likely have a greater contribution to any error, like furnace position or sample rotation, but errors would likely be in a similar range of about 2%.

Many of the above sources of error are best described more simply as the random error associated with different laboratories conducting research. Heiri et al. (2001) conducted a large inter-lab comparison and found that reported measurements of standard samples ranged from 1 – 4% across labs. While many of these differences are small and have not been shown to cause significant differences on ultimate estimates of SOM in samples, many researchers have called for a more rigorous standard of reporting lab-specific protocol, especially concerning the type of oven and any protocol surrounding crucible rotation during treatment (Hoogsteen et al., 2015).

Standardization of all lab protocol is one way to decrease the possible error introduced by these small differences, but because it is impossible to eliminate all differences, good reporting of lab protocol and more participation in inter-lab comparison studies will be the best way to quantify and control for sources of lab error in SOM estimates.

#### 3.2.2.3 Temperature

LOI operates on the principles of TGA; because components of the soil oxidize at different temperature points, the difference in mass between these temperature points is used as a proxy for components which burn off at the specific temperature. While these principles have been tested and show very good accuracy (Frangipane et al., 2009; Ghabbour et al., 2014; Wang et al., 2011), there is still some overlap between oxidation temperatures of soil component parts. This overlap of combustion temperatures means that both the composition of the soil and the temperature chosen will determine the possible biases that estimates of SOM from LOI may suffer from.

The first component of the soil to be released is water retained in the soil and, potentially, structural clay water. Water is released from 25 – 190°C (Ghabbour et al., 2014). With sediments that are rich in clay, it is possible that structural water loss from clay will continue to occur even at higher temperatures (Ball, 1964). At temperatures from 200 – 450ºC the majority of mass loss is attributable to more biologically available SOC (Frangipane et al., 2009). These pools of carbon, mainly made up of soil litter and fulvic acids, can be seen to make up two distinct peaks in some TGA (Ratnayake et al., 2007). For soils which may be older and more humified, the sequestered portion of carbon may not, however, be released until temperatures of 450 – 650ºC are reached (Frangipane et al., 2009; Ghabbour et al., 2014). Temperatures greater than 500ºC

are known to release some IC fractions (Hirota & Szyper, 1975), although the bulk of IC will be lost at temperatures from 650 – 1000ºC (Dean, 1974). For this reason, studies which have focused more on labile carbon pools or geologically younger sites have encouraged the use of temperatures lower than 450ºC to avoid the potential release of IC and structural clay waters which might also be released at high temperatures (Ball, 1964). Lower temperatures, however, risk incomplete combustion of recalcitrant SOC in samples (Frangipane et al., 2009; Ranney, 1969). For that reason, the paleolimnology community have adapted to the standard temperature of 550ºC to ensure full combustion and increase comparability between sites (Heiri et al., 2001), as lake sediments have very humified organic contents. Wang et al. (2011) support the conclusion that lake and marine sediments may require temperatures of 500ºC or greater, and note that temperatures can even be reduced to 475ºC for most wetland, riverine, estuarine, and canal sediments. While these guidelines are broadly applicable, the individual site characteristics should be taken into consideration before the selection of a temperature of combustion.

#### 3.2.2.4 Exposure Time

Exposure time also leads to uncertainties surrounding estimates of SOC from LOI. For samples that are clay- or carbonate-rich, longer exposure times can lead to increased losses of non-SOC components especially, although not exclusively, at higher temperatures. Longer exposure times at lower temperatures may avoid some of the risk of oxidation of non-SOC components, but also likely runs the risk of incomplete combustion of SOC. Studies looking into the efficiency of SOC combustion recommend higher temperatures for relatively short durations. Heiri et al. (2001) found that 98% of pure graphite samples combust after 5 hours of treatment at 550°C, but when samples of mixed soils were tested a plateau of mass loss was reached by approximately 4 hours of treatment. After the 4 hour window, mass losses of less than 1% were

recorded up to 64 hours likely due to the loss of structural clay water or other volatile soil components. For this reason, Heiri et al. (2001) recommend that a combustion time of 4 hours be used. This recommendation is still not standardized throughout the literature however, likely because comparisons between datasets are only possible when similar methods are used. For instance, Hoogsteen et al. (2015) uses a treatment time of 3 hours at 550ºC in order to make a comparison with structural clay water loss estimates made by Houba et al. (1993).

#### 3.2.2.5 Inorganic Carbon

Calcium carbonate ($CaCO_3$) is common in coastal vegetated soils, especially in regions where the substrate is Ca-rich. All methods of quantifying carbon can potentially include this and other sources of IC in estimates of SOC. Most carbonates are oxidized at temperatures higher than 400ºC, therefore low combustion temperatures during LOI can reduce the influence of carbonates, although at these lower temperatures more resistant SOC may not completely combust (Abella & Zimmer, 2007; Hirota & Szyper, 1975). For sites with low carbonate content and older, more humified carbon, the incomplete combustion of SOC may have an equal if not larger effect than the combustion of carbonates at temperatures below 550°C (Table 3.2).

Pre-treatment of sediments with acid, such as HCl, can be used to remove IC before analysis of SOC, however, SOC is not completely resistant to acid and can result in the loss of 10 – 44% of the SOC (Byers et al., 1978). For non-calcareous sediments with less than 5 – 10% carbonate, loss of SOC from acid pre-treatment is likely a larger margin of error than the error associated with the measurement of IC, and, for this reason, acid pre-treatment is not recommended for sites with less than 10% carbonate contents. A standard error of ± 2% carbon may be applied to account for potential IC, or, rather than risk the loss of SOC through removal

of carbonates, the direct measurement of Ca can serve as an estimate of total $CaCO_3$ under the assumption that all IC is from $CaCO_3$ (Dean, 1974; Salehi et al., 2011). Wright et al. (2008) found that direct measures of Ca content in soils enabled them to better constrain the relationship between LOI and SOC in soils with 1 – 34% Ca contents. Their method works particularly well for soils with low SOC and high Ca values, meaning that sites with low carbonate content may find Ca a weak predictor of IC making the standard estimate of error from IC a more robust estimate. Likely this reflects that IC comes from a non-$CaCO_3$ source determined by regional geology.

#### 3.2.2.6 Clay Content

One of hardest uncertainties to control for in the LOI is the loss of structural water from minerals and clays. Structural water stored in minerals can be released at temperatures from 100 - 1000ºC depending on the species of mineral, which means that temperature or duration of treatment cannot control for this process. Sun et al. (2009) presents potential structural water loss (SWL) from 17 common minerals found in soils which might be useful as estimators of possible weight loss, but soil composition must be known in order to accurately take advantage of this information. Also, because LOI temperatures are often below temperatures required to fully combust structural water in clays, it is impossible to say if SWL has completely occurred and will be proportional to the composition of clay in the sediments. For many sites which have less than 10% clay content, a simple estimate of 2 – 5% mass loss due to SW at temperatures greater than 500ºC has been used, as most clays contain about 5 – 9% water (Ball, 1964; Dean, 1974). Samples which may contain higher amounts of clay that might lose structural water from 200ºC can be held at ~105ºC for 24 hours to de-water clays, however there is a small chance that SOM will be removed even at such low temperatures. Other species of clays, such as kaolinite, can

lose as much as 20% of its weight in water at temperatures from 450-600ºC. Gibbsite has been observed to lose 35% of its weight at temperatures of only 300ºC (Wang et al., 2011). In cases where the substrate is clay-rich, especially rich in species which are known to release more clay water, more attention needs to be paid to the potential error from SWL.

#### 3.2.2.7 Error from Non-Carbon Elements

Some weight lost during LOI or other procedures to measure carbon cannot be attributed to either organic or inorganic carbon or SWL from clays. This weight loss is frequently ascribed to volatile materials, such as salts, which may oxidize during the heating process. While it may be difficult to determine the precise elements or minerals responsible for this weight loss, it is most likely that low-clay sites which have large losses not attributable to organic or inorganic carbon are seeing losses from Fe, Mn, Al, or Mg oxides. Sutherland (1998), working in a basalt-rich site, noted that weight losses were correlated with particle size as well as the presence of Fe, Mn, and Mg elements in the samples and concluded that oxides not associated with clay were losing water during the heating process. This has also been observed with minerals such as goethite and gibbsite which may lose water at temperatures greater than 450°C (Sutherland, 1998). Additionally, sites that are rich in Fe, Mg, or Mn in the presence of $CaCO_3$ may decrease the temperature needed to combust $CaCO_3$.

It is also important to note that not all weight loss from IC will be attributable to Ca-associated carbonates. In the case of Siterite, magnesite, rhodochrosite, combustion can occur at between 425 – 520°C and this is something to consider when trying to attribute error to non-carbon and non-SWL sources (Weliky, Suess, Ungerer, Muller, & Fischer, 1983). If there are large inconsistencies between losses that cannot be attributed to either of the former error source,

an analysis of the elemental composition of a subset of samples may allow for some insight into what types of volatile substances are causing additional weight loss not already accounted for in the mode.

#### 3.2.2.8 Error and Uncertainty in Conversion Rates

After obtaining an estimate of SOM from LOI, much error and uncertainty in blue carbon stocks can be introduced based on the method that researchers use to convert SOM to SOC. SOM is composed of many elements which oxidize at high temperatures including SOC, structural clay water, volatile salts, IC, and all elements associated with the combustible materials. This means that the percent SOM in a sample is an over-estimate of SOC in the sample. In some soil science communities, a standard conversion factor was used to transfer between SOC and SOM with the estimate that SOM was composed of roughly 51 – 58% SOC (Howard & Howard, 1990). However further examination shows that there is considerable variability in the amount of carbon which contributes to SOM based on individual site conditions (Howard & Howard, 1990; Konare et al., 2010; Santisteban et al., 2004; Spain, Probert, Isbell, & John, 1982). Creating an individualized SOM-SOC conversion equation for each site has further revealed that the percent of SOC in SOM also depends on the amount of SOM. Samples which have less than 5% SOM consistently show a different SOM-SOC relationship across sites, likely due to the dominance of IC in elemental measurements of carbon used to describe the relationship (Wright et al., 2008).

## 3.3 Methods

### *3.3.1 Loss on Ignition*

To test the effect of temperature and treatment time on weight lost during ignition, a subset of 50 samples was collected from cores taken from six salt marsh sites along the California coast (Mad River Low, Bolinas Lagoon, Petaluma Marsh, Mugu Lagoon, Seal Beach, and Mission Bay; site descriptions can be found in Chapter 2). Stratified random sampling was used to ensure even distribution of samples with regard to estimated percent OM, on samples tested previously (Chapter 4). Each sample represented a 1 – 2 cm interval of a core and four cubic centimeter samples were taken (using a graduated syringe barrel) from each interval. Samples were placed in pre-weighed ceramic crucibles, weighed before dehydration, and then dried in an oven at 90ºC for at least 12 hours and re-weighed to obtain bulk density (BD; $g/cm^3$). Crucibles were moved with tongs to avoid changes in weight. Three of the four sets of samples then underwent LOI treatments at 450ºC, 500ºC, and 550ºC respectively in a Fisher Scientific Isotemp Muffle Furnace. Samples were cooled for 30 minutes in a desiccator and weighed at each of the following time steps: 1, 2, 3, 4, 5, 6, 7, 8, 12, and 24 hours. The fourth set of samples was ground into a powder using a mortar and pestle, re-weighed and then were treated for LOI at 550ºC with weights taken at the timesteps described previously and are referred to as 550°Cg, hereafter.

### *3.3.2 Particle Size Analysis*

A cubic centimeter sample was taken from each of the 50 samples used in the previous sampling, wrapped in plastic, bagged and sent to the USC Fullerton Paleooceanography and Paleotsunami Lab for particle size analysis. There, samples were boiled in a 30% solution of

$H_2O_2$ until effervescence ceased, indicating organic matter had been removed. Particle size for each sample was then measured by a Malvern Mastersizer Particle Size Analyzer. Three measurements were taken from each sample and the mean of those estimates was used for analysis. Particle size measures were divided into the following classes: sand (> 0.05 mm), silt (0.004 – 0.05 mm), and clay (< 0.004 mm).

Mean clay content for each sample was compared to mean SOM content as estimated by LOI conducted at 450°C, 500°C, 550°C, and 550°Cg using a linear model to check for potential release of structural clay water for samples with higher clay content and at higher combustion temperatures.

### *3.3.3 Elemental Analysis*

Using the same subset of 50 samples in previous analyses, 50 additional one cubic centimeter samples were extracted and measured for elemental carbon. A random stratified subset of 30 samples (based on estimated carbonate content from LOI at 950°C) were selected for acid pre-treatment with 8 randomly selected replicate samples. All 50 samples were tested without pretreatment for acid removal with 8 randomly selected samples for duplicate analysis. This created a database of 96 samples with a group of untreated samples (n = 50, 8 replicates) and a paired group of acid treated samples (n = 30, 8 replicates).

For acid-treated samples, approximately 10 mL of 6N hydrochloric acid (HCl) was added to each sample and stirred until effervescence stopped. Samples were then centrifuged and acid was decanted and sediments were rinsed in deionized water until pH had reached neutral. Once pH had returned to neutral (after about 6 water rinses), sediment was dried at 60°C for 24 hours. Then approximately 12 – 15 mg of sample from each acid-treated and untreated sample was

wrapped in a tin capsule. Samples were run on a Thermo Delta V Advantage mass spectrometer in continuous flow mode coupled to an Elementar vario ISOTOPE Cube Elemental Analyzer (EA) via a Thermo Conflo IV. Weight percent carbon values were calculated using a peak area calibration based on the homogeneous Costech Acetanilide standards run every 10 – 12 samples (Schimmelmann et al., 2009). Calculations of raw isotope values were performed with Isodat 3.0 software. Reproducibility of standards is ≤0.2‰ (1σ).

Estimated SOC values were plotted against SOM values obtained in LOI for each temperature treatment grouped by acid treated and untreated samples. A second-order polynomial regression was made for each group within each treatment and $R^2$ values were calculated to estimate strength of the relationship.

### *3.3.4 Effect of SOM-SOC Correction Equation*

Published correction equations from salt marsh studies were compared to correction equations in this study, using only SOC measures from untreated samples. A dataset of SOM measurements generated for California salt marshes in Chapter 4 of this dissertation was used to analyze how the use of different conversion equations affected estimates of mean SOC and estimated total carbon stock for the state of California. Total carbon stock for the state of California was calculated using mean BD from the same dataset and the sum of area classified as 'Estuarine and Marine Wetland' from publically accessible shapefiles created by the National Wetlands Inventory (NWI) mapping project Version 2, Surface Waters and Wetlands (*National Wetlands Inventory—Wetlands Project, Version 2*, 2019).

## 3.4 Results

### *3.4.1 Effect of Temperature and Duration on LOI*

Average percent SOM and percent IC estimated by LOI at the temperature steps and 950°C are shown in Figure 3.1. The effect of temperature and duration of treatment are correlated, as lower temperature treatments for longer durations return similar values of LOI to lower temperatures for shorter or longer durations. The majority of the differences between treatment temperatures are negligible by the 8 hour mark. Differences between treatments of 450ºC and 500ºC are, at most, 10% lower than treatments of 550ºC or 550ºCg sediments. There is very little difference between treatments at 550ºC and treatments of the same temperature with ground sediments.

### *3.4.2 Effect of Clay Content*

Mean clay content for samples in the dataset was 15 ± 7 % with a maximum site mean clay content of 22.4 % at Bolinas Lagoon. In the same site, the single maximum clay content for the database was 56.8 % Table 3.4. Linear regressions between percent clay content and percent SOM content have low explanatory power for percent SOM values generated from LOI conducted at all temperatures and treatments (Figure 3.2). LOI treatments at higher temperatures show marginally higher $R^2$ values than LOI conducted at 450°C, with the highest $R^2$ value at 0.06 for LOI conducted at 550°C on samples ground before treatment.

### *3.4.3 Effect of Acid Treatment on SOM-SOC Conversion Equations*

SOC values measured for acid treated and untreated sediments are found in Table 3.5. Acid treatment of samples increased mean SOC estimates from 9.0 ± 6.8 % in untreated samples to 16.5 ± 7.9 % for acid treated samples. This reduced R-squared values for all temperatures and

treatments. Regressions between untreated SOC samples and SOM values from LOI conducted at 450°C as well as 500°C performed best out of all temperatures and treatments ($R^2 = 0.96$; Figure 3.3). Regressions for higher temperature LOI treatments and for comparisons between all LOI treatments and acid treated SOC measures still show strong correlation between SOM and SOC, with the lowest $R^2$ of 0.9 for the regression between 550°Cg samples and acid-treated SOC samples.

### *3.4.4 Effect of SOM-SOC Conversion Equations on SOC*

Conversion equations generated in this study are compared to those used across different soil types and within coastal wetlands in Figure 3.4. References for all conversion equations from published literature that were analyzed in this study can be found in Appendix Table 3.2. Commonly used regressions in the wetlands community, and the regression used in this dataset, are shown in Figure 3.4a and equations are described in Table 3.6. Using the SOM database in Chapter 4, a comparison of conversion equations from selected published sources in salt marsh sites and this study return mean estimates of SOC that range from 3.5 to 5.09 %. All means are significantly different (ANOVA; 95% confidence). Conversion equations which are most significantly different are those from the Craft et al. (1991) and the Keller et al. (Keller et al., 2015) study. The conversion equation generated from LOI at 450°C is most similar to the conversion equation for San Francisco Bay salt marshes by Callaway et al. (2012) and Craft et al. (1991). The conversion equation published by Keller et al. (2015) using soils from restored salt marshes in Southern California is most similar to curves generated from LOI at 550°C and 550°Cg.

While the effect size of different conversion equations on mean SOC estimates may be small, these tiny differences can have large effects at regional scales. Using a BD value of 0.72 g

$cm^{-3}$, an estimate of 592.3 $km^2$ of salt marsh in the state of California, and these values of SOC obtained from different conversion equations, stock values for the state vary from 14.9 – 21.7 Tg C.

## 3.5 Discussion

### *3.5.1 Review of LOI Protocol*

There are several steps which researchers may take to make the selection process behind LOI protocol more transparent and maximize the efficiency of combustion. Based on a review of published literature and empirical tests, recommendations for best practice methods are made in Table 3.2. For laboratory-specific, or random error, conducting tests on samples to maximize combustion of SOM and minimize combustion of non-SOM components, using standard materials as reference, replicating samples, and participation in interlab comparison studies will be most effective to reduce error or uncertainty. Estimation of IC and clay content should be conducted and correction factors should be used in conversion equations, if appropriate. For sites with the potential large errors from these sources, additional treatments should be carefully monitored and reported; correction may need to be made based on the potential for losses of SOM.

Conversion rates between SOM and SOC throughout different soil types have ranged from 0.2 to 0.58 (Appendix Table 3.1) and have mostly taken the form of linear regressions (Appendix Table 3.2). These regressions also reflect that based on the transformation of SOM to SOC, values could over- or underestimate percent carbon in soils by up to 50% or more. Transparency in methods of converting estimates of SOM into SOC as well as reporting of raw

LOI data along with any publication will make the largest contribution to reducing error and uncertainty and increasing the suitability of data for secondary users.

### *3.5.2 LOI as a Measure of SOC in California Salt Marsh Soils*

#### 3.5.2.1 Impact of Temperature, Duration, and Homogenizing Sediments on LOI

Empirical tests to determine the optimal temperature and duration for treatment of sediment samples in California salt marshes show that temperatures greater than 500°C result in weight losses about 10% more than lower temperatures for the first 5 hours of combustion. This is likely due to the presence of recalcitrant carbon in salt marsh soils and indicates that higher combustion temperatures are needed to ensure full combustion. At 8 hours of combustion, differences between temperature treatments are mostly within about 5% of total weight loss and are likely negligible. For temperature treatments above 450°C, a plateau is reached by about the four hour mark, likely indicating full combustion and continued time may only increase the release of non-carbon elements (Heiri et al., 2001). Lower temperature treatments do not reach this plateau until about 8 – 12 hours into treatment, indicating that longer treatment times may be needed for lower temperatures. Percent weight loss for ground sediments exceeds 100%, indicating that sample was lost during the treatment and indicating that the increase seen from 550ºC without grinding sediments to 550ºC with grinding sediments may be the influence of sample loss during transfer of crucibles in and out of the furnace (Table 3.3).

#### 3.5.2.2 Impact of Clay Content on LOI

The overall effect of SWL due to clay content is relatively low for California salt marsh samples, although some samples have clay content greater than 50%. Regressions of percent clay content compared to percent SOM show that there is little relationship between the two variables

for all temperatures ($R^2 < 0.06$) and indicate that weight loss in sediments of high clay content is, at most, equal to about 1% for every 4% SOM (Figure 3.2.). Most samples also show estimated losses from IC determined by combustion at 950°C of less than 10%. Losses at this temperature are fairly even across samples treated for LOI at 500°C and above, indicating that samples treated at 450°C may not have achieved full combustion of SOM and these elevated estimates of IC contain the recalcitrant portion of SOM as well.

#### 3.5.2.3 Impact of Acid Treatment on Measurement of SOC

LOI at temperatures of 950°C indicate that most sediments in California salt marshes have little carbonate content, although there are notable outliers such as samples from Seal Beach (Table 3.3). After acid treatment to remove carbonates, however, % total carbon estimates were higher than for samples which had not been treated for carbonates (Table 3.5). This is likely the effect of water rinses following acid treatment. This step is needed to prevent acid from dissolving SOC after IC is removed and to protect equipment during combustion. However, there is a risk of rinsing away non-carbon acid soluble portions of the soil matrix resulting in inaccurate weights and leading to an over-estimation of total carbon for samples. This risk, along with the risk of dissolving SOC during acid treatment, introduces a large amount of uncertainty, especially for samples which likely have very small risks of error from carbonate release during combustion.

Although acid treatment did not effectively separate IC from SOC in this experiment, regressions between LOI at all temperatures and treatments in comparison to acid treated estimates of SOC are still relatively robust (Figure 3.3). However, there is some indication – especially for treatments at higher temperatures – that increases in estimated SOC for acid treated samples disproportionately affect samples high in SOM. As this is where most of the

variability is introduced into the SOM-SOC conversion, treating California salt marsh samples with acid to remove SOC is likely less effective than any error which is introduced from carbonate combustion during LOI.

#### 3.5.2.4 SOM to SOC Conversion Equations for California

A comparison of the regressions commonly used in salt marsh carbon studies shows that the ratio of SOC to SOM in this database is equal to or slightly higher than published equations at low values of SOM and lower than published equations at higher values of SOM. Low values of SOM often have a very different SOC content than samples with higher SOM, which is why much of the salt marsh community has adapted quadratic equations to model this relationship. This means that with higher SOM values, sample differences between conversion equations may range from 10 – 15%. There is still very good agreement between published conversion equations and results from this study, underlining the reliability of LOI as an estimation of SOC and the similarity between salt marsh soils in comparison to conversion equations which have been constructed for soil samples in other ecosystem types.

There is very little clear impact of LOI temperature selection on regressions between SOM and SOC (Figure 3.3). However, temperature differences have the largest impact on how well regression equations perform at low values of SOM. Some studies have suggested using separate regression equations for low-SOM and high-SOM samples to capture the different behavior of these sample types, but more analysis is needed to assess how this would impact overall estimates.

Use of published conversion equations and equations produced in this study to convert SOM values from the database generated in Chapter 4 show that there are relatively similar estimates of mean SOC for the state of California made by all conversion equations (range: 3.5 –

5.09%). Standard deviations of these samples are also similar, with the exception of the equation published by Keller et al. (2015), which is the only equation which does not pass through the origin and has a c coefficient (Table 3.6). All of the mean estimates of SOC are statistically different for the Chapter 4 dataset (ANOVA; 95% confidence), but for a randomly generated dataset, only conversion equations from Keller et al. (2015) and this study (550°Cg) are significantly different. Effect size of these differences, however, is very small (post hoc Tukey test; Appendix Figure 3.1).

While these differences seem small, an extrapolation of mean SOC values to the state scale shows that estimates of total carbon stock to 1 m depth range from 14.9 TgC – 21.7 TgC. This extrapolation assumes standard values of bulk density (mean BD taken from Chapter 4) and standard accretion rates (mean accretion taken from Chapter 4), as well as standard SOC and uses an estimate of tidal marsh area in the state of 592.3 $km^2$ (see Chapter 4). Given that these are large assumptions and analysis which takes variability in those parameters may reduce differences between correction curves, the small differences in conversion equations have a significant impact on state-level carbon stock estimates. For that reason, further analysis is needed to assess at what level (site, region, ecosystem type) a new correction equation is needed.

### *3.5.3 Best Practices for Laboratory Protocol*

Sediment sampling protocol within the marsh should aim to capture the range of SOC values within their study site, both horizontally and vertically, and beware of extrapolating SOC values from the root zone, where SOC has not yet gone through its decay process, deeper into the marsh. To ensure there is no sampling bias in individual LOI samples, the size of samples should be kept to 1 – 4 g, as samples smaller than 1g have demonstrated larger standard deviations

(Hoogsteen et al., 2015) and samples larger than 4g risk incomplete combustion (Heiri et al., 2001; Houba et al., 1993). Random lab error should be captured through the use of replicate samples to measure standard deviations, especially between samples at different positions in the furnace. Rotation of samples during treatment is recommended. The measurement of standard samples should be conducted regularly. The inclusion of blank samples or samples of pure graphite might also inform operators about the accuracy of mass balance results, especially in the light of condensation and evaporation of water within crucibles themselves, or efficiency of carbon combustion (although pure graphite samples may not combust in similar ways to soil carbon).

If there is prior knowledge about the age and state of SOC in the site, the amount of IC and potential for release of structural water, selection of temperature and duration can be made based this knowledge with the decision-making reported as part of methodology. If there is no prior knowledge about soil contents, it is recommended that a small batch of test samples be combusted at different temperatures for different durations and then, if possible, tested for the presence of SOM following combustion. This will enable a more informed decision regarding combustion temperature and will allow for an estimation of error due to incomplete combustion, regardless of temperature chosen. Even if SOM cannot be quantified following combustion, testing different soil types for ideal combustion temperature and duration should be a part of LOI protocol and reported along with any SOC results as justification for methodological choices.

To control for interlab variability, best practice methods are to carefully and thoroughly report all LOI protocol. This includes equipment specifications such as furnace and crucible type as well as mass balance accuracy and calibration. Protocols should include if air is pre-heated as well as how long crucibles are cooled before weighing, if a desiccator is used, and if samples are

moved by hands or tongs. Finally efforts should also be made to make more interlab comparisons and create estimates of lab accuracies, such as the study by Heiri et al. (2001). These comparisons not only allow for the estimation of random error due to lab-specific protocol by secondary data users, but such efforts can also increase lab accuracy and accountability in regards to how well their individual protocol compares to other labs preforming the same methodologies. Examples of this already exist in the soils community through the North American Proficiency Testing Program (NATP) which facilitates the exchange of standardized samples for testing between labs. These collaborative efforts also may encourage more labs to adopt standard LOI protocols, without serving as gatekeepers or creating barriers for the creation of data and inclusion of data through different LOI methodology.

### *3.5.4 Best Practices for Quantifying Error from non-SOC*

After accounting for error which might be attributable to lab protocol and random error, the inherent error in the LOI process needs to be assessed. This is the error associated with combustion of IC, clay water, and other non-carbon elements. If IC and clay content are known and are not likely to contribute significant error, prior studies have used standard error estimates of 2-5% for loss of clay water (Dean, 1974; Salehi et al., 2011). These assumptions, along with measures of IC and clay, should be reported along with SOC estimates.

When there is less prior information about IC, clay content, or the potential combustion of volatile elements, one possible method to estimate the non-SOC combustible parts of the soil is to remove the SOM portion of the soil either through treatment with $H_2O_2$ or bleach and then conduct LOI (Mook & Hoskin, 1982). If this is conducted on a subset of samples that can give a more accurate estimate of the error in the sample set associated with SWL and non-SOM

combustion. This process may not give a completely accurate picture for sites with recalcitrant carbon which may not be fully removed by $H_20_2$ or bleach treatments.

To target only the error due to SWL, tests of the correlation between the clay fraction of sediments measured by particle size analysis (PSA) and LOI can be used as an estimate of error due to clay water. If clay is determined to be a large source of error for a particular site or set of samples, Luczak et al. (1977) suggests that sorting of sediments according to size class may first be done before conducting LOI. This then isolates the SWL to only the clay fraction and could allow for a better estimation of SOM in some soils. Targeting the loss due to IC can be done in the same manner by testing for correlation between IC content in soils, measured either through a calcimeter or other methods, and the SOM.

### *3.5.5 Best Practices for Creating Soil-Specific Correction Factors*

When converting from SOM to SOC, the use of standard conversion factors is highly discouraged. There is very little research which supports a standard conversion factor and single conversion factors do not capture the underlying variability in the SOM-SOC relationship. The amount of carbon which contributes to SOM will depend on the organic source, its age and decay state, and the associated non-organic elements in the soil matrix. Using a correction equation which shows the change in SOC with the change in SOM shows that there is often a significant difference in that relationship for highly mineral rich sediments which have less than 5 – 10% SOM. Additionally, there is substantial variability in these equations between ecosystem and soil types. It is currently recommended that each study should conduct dry combustion on a subset of samples to create its own correction equation, although published correction equations can be used where cost and access prohibits this analysis provided raw data

are published and methods are transparent. When possible, correction equations should account for variability in the SOM-SOC relationship with percent SOM, age or decay state of carbon, depth of sample, and/or particle size. The use of multiple conversion equations, especially for SOM-poor samples, has been shown to increase the accuracy of the conversion and, for sites rich in clay or rich in IC, the inclusion of these variables in the conversion equation has also been shown to increase accuracy (Wright et al., 2008).

### *3.5.6 LOI for Blue Carbon*

LOI is an efficient, cost-effective method which enables rapid, bottom-up estimates of blue carbon for salt marsh sediments. Although there are many differences in methodology and assumptions made in the process, the majority of these sources of error and uncertainty can be quantified and accounted for in the eventual conversion of estimated SOM to SOC. This chapter presents estimates of error and uncertainty for soil sampling strategies, laboratory protocol and interlab variability, losses due to non-carbon elements such as structural clay water and IC, and variability in conversion rates between SOM and SOC. The vast majority of error and uncertainty is related to this latter step in the process. While best practices have been presented to reduce error and uncertainties in each step of the LOI process, the single most important step that scientists and data generators can make is to provide access to raw data as well as full transparency in the LOI process and conversion equation. In this way, data will be most useful for global synthesis studies and any incompatibilities in between methodologies can be accounted for at larger scales.

## 3.6 Figures

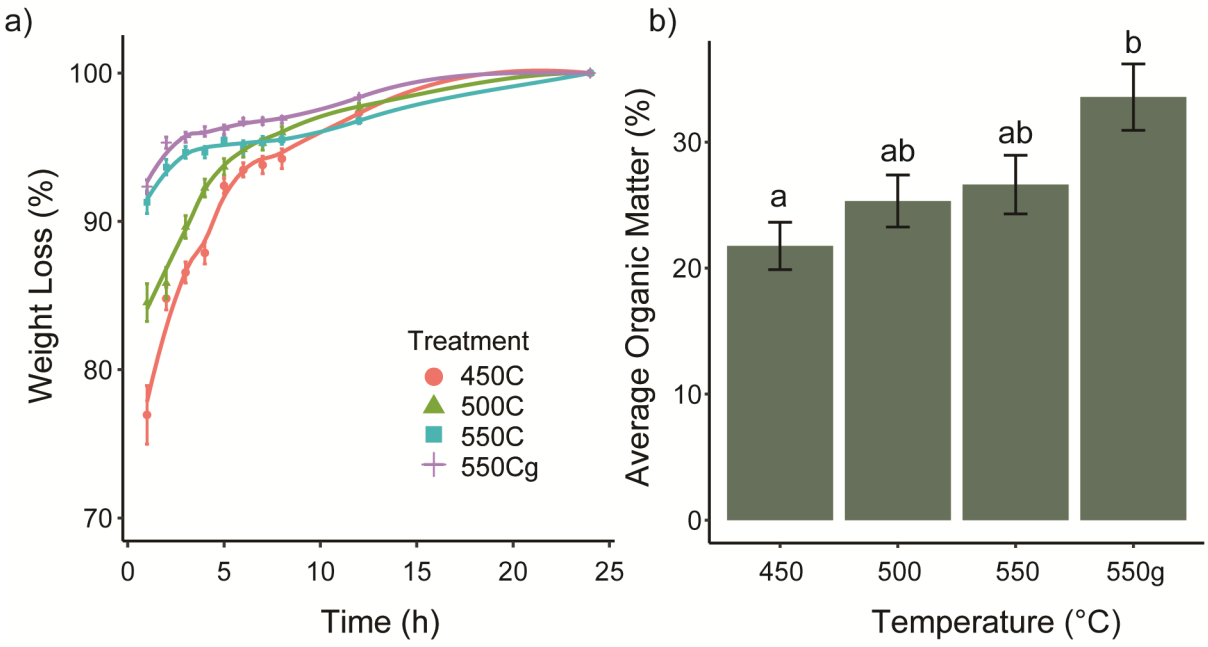


**Figure 3.1 Effect of Temperature and Duration of LOI**

The average weight loss (%) for each treatment temperature is plotted with standard errors and a loess fit (a). The average weight loss for each temperature at 8 hours is shown with standard errors (b); means which share a letter are not significantly different (ANOVA, 95% confidence).

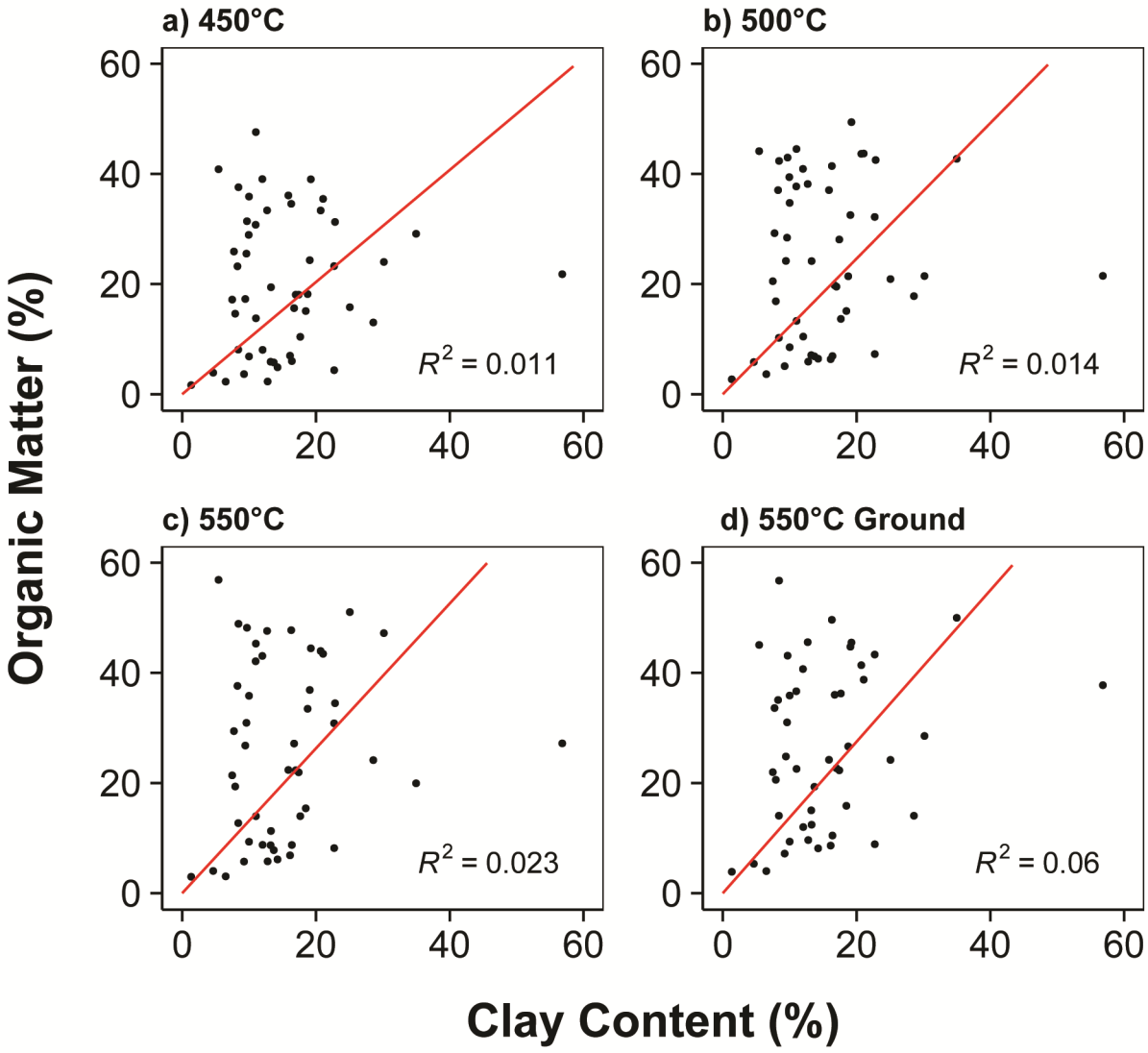


**Figure 3.2 Effect of Clay Content**

Organic matter content (%) is plotted against percent clay content for 50 sediment samples taken from California salt marsh sediments for LOI protocols using different temperatures and methodologies. Linear regressions and $R^2$ values are shown.

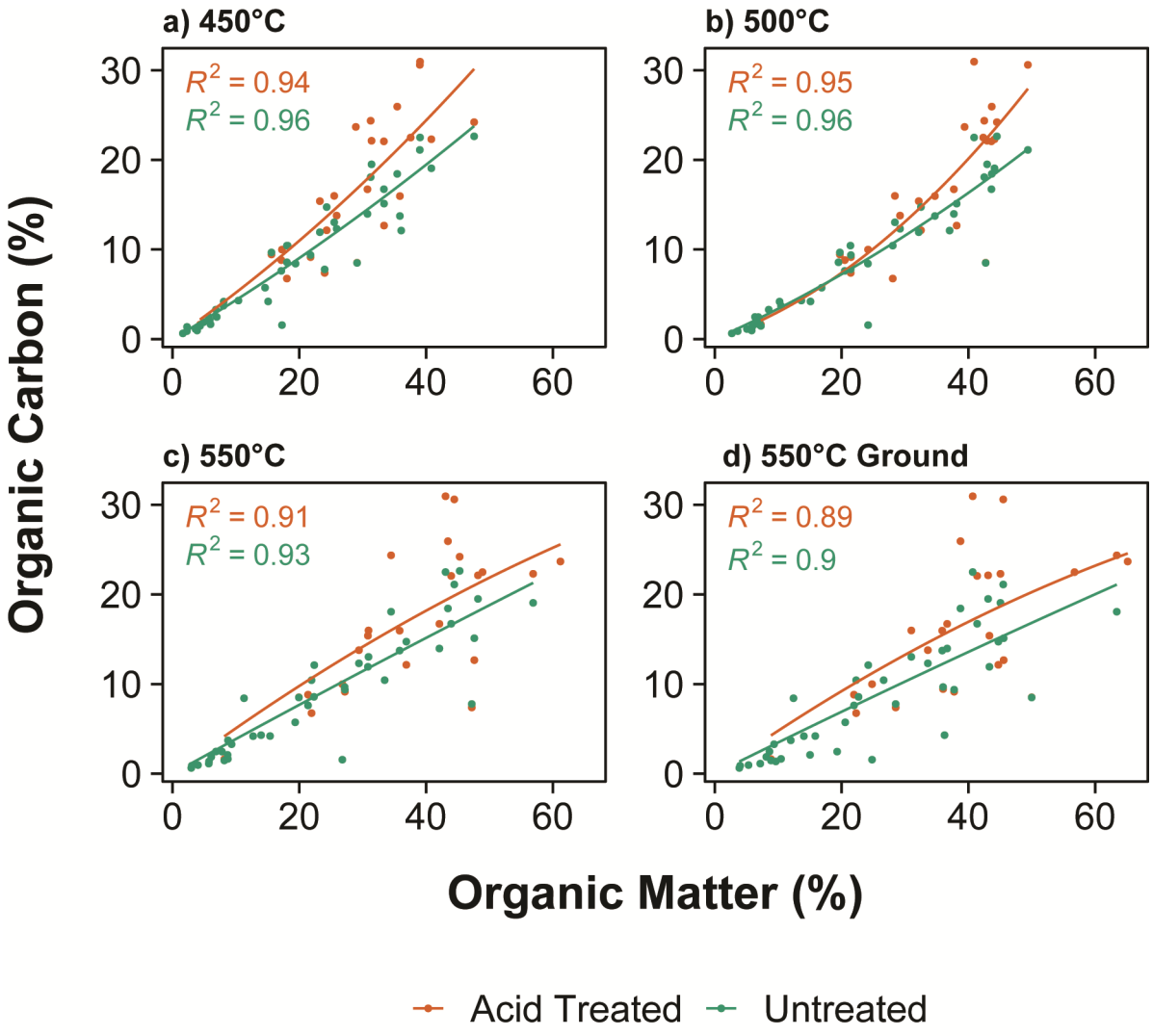


**Figure 3.3 Effect of Carbonate Removal on SOC Estimates**

Percent organic carbon content is plotted by percent organic matter grouped by samples which were acid treated to remove carbonates and those which were not. Regression and $R^2$ values are shown.

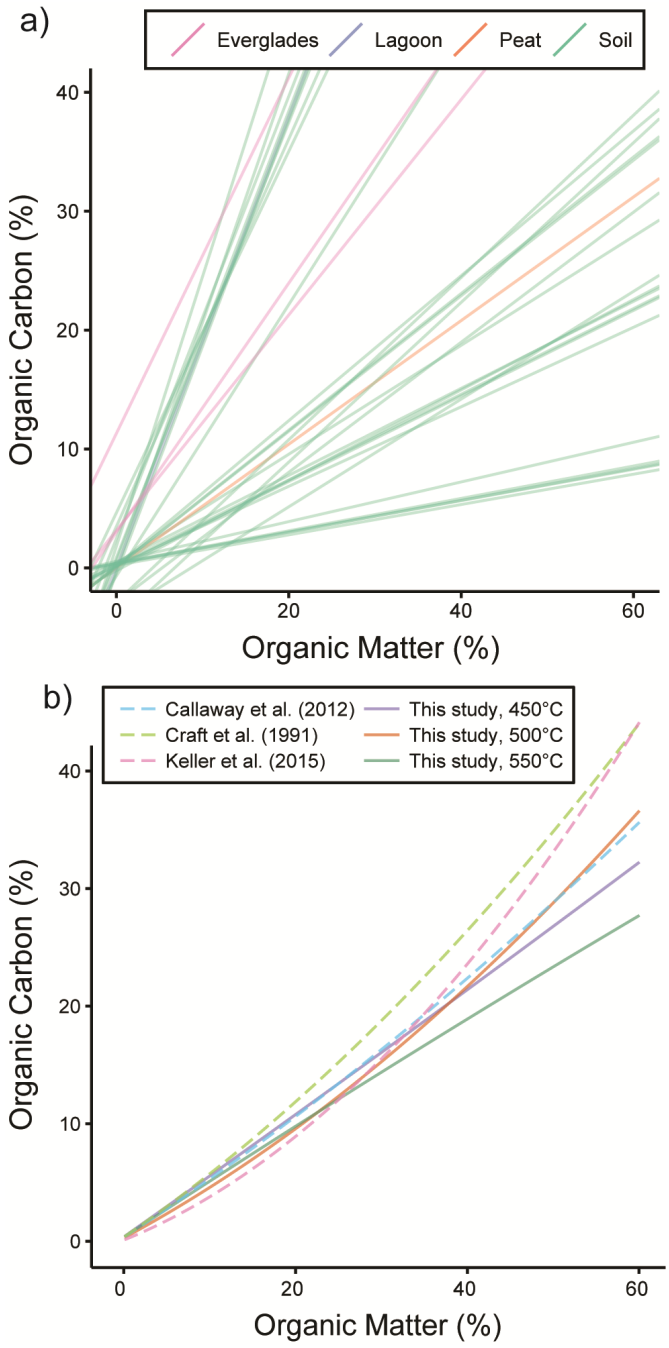


**Figure 3.4 SOM to SOC Conversion equations**

Linear correction equations from published sources across soil types are plotted (a). Quadratic correction equations from published sources using salt marsh sediments (dotted lines; Callaway et al. 2012; Craft et al. 1991; Keller et al. 2015) are compared to corrections equations generated in this study (solid lines).

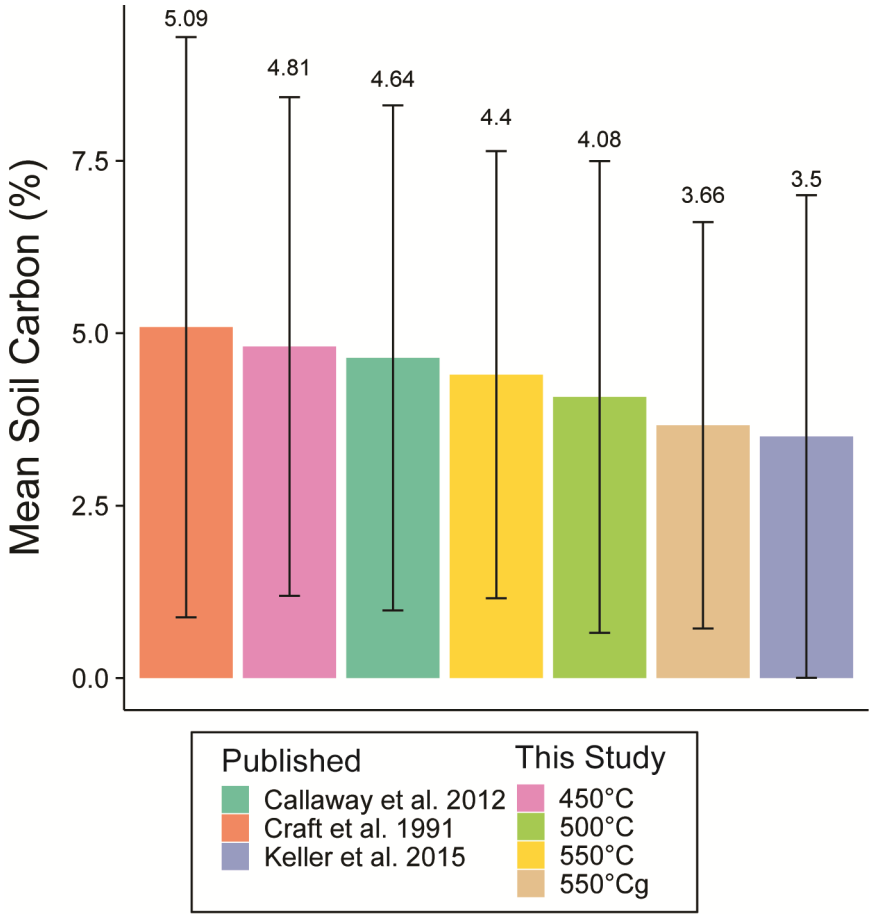


**Figure 3.5 Effect of Correction Equation on Mean SOC Estimates**

Average soil organic carbon (SOC) was calculated for a database of soil organic matter (SOM) values generated in Chapter 4 using published correction equations and corrections equations from this study. Mean SOC values are shown above error bars showing standard deviation.

## 3.7 Tables

**Table 3.1 Methods of Determining SOC Content**

| Method | Measurement Type | Pros | Cons |
|---|---|---|---|
| ***Dry Combustion*** | | | |
| *LOI* [1,2,3] | Gravimetric | Accessible, reliable, inexpensive | Non-standardized methods, errors associated with clay water, IC and volatiles |
| *Thermogravimetric Anallysis (TGA)* [4,5,6] | Gravimetric | Accurate, standard | Access, expensive |
| *Elemental Analysis* [7,8,9] | Gas Chromatography, Spectrometry | Accurate, replicable | Access, expensive, error from IC |
| ***Wet Combustion*** | | | |
| *Walkley-Black (WB)* [10,11] | Titrimetric | Reliable | Expensive, hazardous, error from refractory carbon and Fe/Mn |
| ***Non-Combustion*** | | | |
| *Soil Fractionation* [6,12] | Physical or Chemical | Differentiates carbon pools | Complex, time-intensive |
| *Diffuse reflectance spectroscopy* [13] | Spectrometry | Reliable, less labor-intensive, in-situ and remote applications | Expensive, inaccessble, untested |

Sources: [1]Dean (1974), [2]Heiri et al. (2001), [3]Hoogsteen et al. (2015), [4]BenDor and Banin (1989), [5]Ghabbour et al. (2014), [6]Frangipane et al. (2009), [7]Matejovic (1993), [8]Bhatti and Bauer (2002), [9]Konare et al. (2010), [10]Walkley and Black (1934), [11]Kamara et al. (2007), [12]Ratnayake et al. (2007), [13]Nayak et al. (2019)

This table compares pros and cons for each method of measuring SOC.

**Table 3.2 Sources of Error in LOI, Estimated Magnitude, and Recommendations**

| Sources of Errors | Risks | Magnitude of Error | Sources | Recommendations |
|---|---|---|---|---|
| **Sample Preparation** | | | | |
| *Sampling depths < 20cm* | Over-estimation of SOC in active root zone | ~ 30% | Bai et al. (2016) | Sample below root zone; Sample sizes from 1 - 4 g; measure SD of replicate samples |
| *Sample sizes < 2 g* | Increased inter-sample variability, overestimation of carbon | 2 - 3 % | Hoogsteen et al. (2015), Wang et al. (2011) | |
| *Sample size > 4 g* | Incomplete combustion due to lack of surface area | 2% or greater | Wang et al. (2011) | |
| *Non-ground, un-homongenized samples* | Increased inter-sample variability; incomplete combustion | likely < 2% | This study | |
| *Ground, homogenized samples* | Sample losses | < 1 - 2 % | Houba et al. (1993), This study | |
| **Laboratory Error** | | | | |
| *Random error (inter-lab)* | Lab-specific errors | 1 - 4% | Heiri et al. (2001) | Inter-lab comparison studies; include standard samples with each batch; estimate SD of replicate samples |
| *Furnace type/Pre-heating* | Inconsistent/irregular heating leading to combustion variability | Insignificant | Hoogsteen et al. (2015) | |
| *Furnace placement* | Increased inter-sample variability | 2% | Heiri et al. (2001), Hoogsteen et al. (2015) | |
| *Sample rotation* | Increased inter-sample variability | < 3% | Hoogsteen et al. (2015) | |
| *Crucible handling* | Under- or over estimates of mass losses (e.g. addition of oils from handling crucibles, different levels of combustion with lids, etc.) | Insignificant | Heiri et al. (2001) | |

**Table 3.2 (continued)**

| Sources of Errors | Risks | Magnitude of Error | Sources | Recommendations |
|---|---|---|---|---|
| **Temperature** | | | | |
| *< 400°C* | Incomplete Combustion | ~ 10 % with shorter exposure times | Frangipane et al. (2009), Ranney et al. (1969), This study | Conduct a test to ensure full combustion; <450ºC for carbonate and clay rich sediments; >500ºC for humified samples |
| *400° - 500°C* | Release of SCW; incomplete combustion of more humified matter | 2 % - 10% or more in clay rich sediment | Ghabbour et al. (2014), Frangipane et al. (2009), Heiri et al. (2001) | |
| *500° - 600°C* | Release of SCW and IC | 2 - 10% + depending on sediment type | Hirota & Szyper (1975) | |
| **Exposure time** | | | | |
| *< 1 hr* | Incomplete Combustion | 2% - 10% for temperatures < 500°C | Heiri et al. (2001), Hoogsteen et al. (2015), Smith (2003) | Conduct a test to ensure full combustion at chosen temperature to minimize exposure time |
| *1 - 4 hrs* | Inter-lab differences | Insignificant at temperatures > 450°C | Heiri et al. (2001), this study | |
| *12 hrs +* | Release of SCW, IC, non-carbon elements | ~ 1 % | Heiri et al. (2001) | |
| **Inorganic Carbon** | | | | |
| *Carbonate Removal (HCl)* | Removal of SOC | 10 - 44% | Byers et al. (1978) | |
| *Samples of < 10% Carbonate* | Combustion of IC at high temperatures | 2 - 5% | Dean (1974), Salehi et al. (2004) | Measure IC content; use correction factor or remove IC for samples >10% |
| *Samples of > 10% Carbonate* | Combustion of IC at high temperatures | >10% | Abella and Zimmer (2007), Dean (1974), Frangipane et al. (2009), Heiri et al. (2001), Hirota & Szyper (1975) | |

**Table 2 (continued)**

| Sources of Errors | Risks | Magnitude of Error | Sources | Recommendations |
|---|---|---|---|---|
| **Clay Content** | | | | |
| *Sites with < 10% Clay* | Release of SCW from 100° - 1000°C | 2 - 5% | Howard and Howard (1990), Ball (1964), Craft et al. (1991), Dean (1974) | Measure clay content; check for presence of high SWL species; use correction factor |
| *Sites with > 10 % Clay* | Release of SCW from 100° - 1000°C | Up to 30 % | Mook and Hoskin (1982), Sun et al. (2009), Davies (1988) | |
| **Non-carbon Elements** | | | | |
| *Sites with Fe, Mn, Al, or Mg oxides* | Release of structural waters above 450°C | 3 - 10% | Sutherland (1998) | Check for weight losses not explained by IC or SWL from clay; use a correction factor; measure elemental composition of sediment |
| *Goethite and Gibbsite* | Release of structural waters above 400°C | ~ 35% | Davies (1974) | |
| *Siterite, Magnesite, rhodochrosite* | Release of structural waters between 425°C - 520°C | 1 -10 % | Weliky et al. (1983), Heiri et al. (2001) | |
| Other | Misc. losses depending on sediment type | 2 - 20% | Howard (1965), Mook and Hoskin et al. (1982) | |
| **Conversion Rates** | | | | |
| *Sites with < 5 % OM* | Overestimation of carbon due to IC release | 2 - 5% | Bojko and Kabala (2002), Craft et al. (1991), Ghabbour et al. (2014) | Construct region- and site-specific conversion factors/equations with carbon measuremnts from EA on a subset of samples |
| *Standard conversion rates* | Over- or underestimates of carbon based on site-specific LOI-SOM-SOC relationships | Up to 50% | Howard (1965), Howard and Howard (1990), Konen et al. (2002), Santisteban et al. (2004), Spain (1982), | |

This table presents risks associated with errors and uncertainties in the LOI process, the potential magnitude of influence on weight loss as a % weight loss attributed to the specified effect, references, and recommended avenues for avoiding or accounting for the specified errors.

**Table 3.3 Average SOM and Carbonate Content Estimated from LOI**

| | Sites (n) | Mad River Low (12) | Bolinas Lagoon (6) | Petaluma Marsh (12) | Mugu Lagoon (2) | Seal Beach (16) | Mission Bay (2) |
|---|---|---|---|---|---|---|---|
| **Soil Organic Matter (%)** | *450°C* | 11.8 ± 2.9 | 25 ± 2.6 | 8.4 ± 3.2 | 5.9 ± 1 | 28.6 ± 2.7 | 23.6 ± 9.8 |
| | *500°C* | 14.1 ± 3.1 | 32 ± 3.5 | 10.3 ± 3.2 | 7.5 ± 1 | 33.4 ± 2.7 | 25.7 ± 12.4 |
| | *550°C* | 12.1 ± 1.9 | 35.6 ± 3.3 | 11.7 ± 4.5 | 7.7 ± 1.6 | 38 ± 3.4 | 30.8 ± 16.8 |
| | *550°Cg* | 14.7 ± 1.8 | 39.9 ± 3.1 | 12.8 ± 5.3 | 8.7 ± 0.6 | 36.9 ± 3.5 | 34.1 ± 11.5 |
| **Carbonate Content (%)** | *450C* | 4.4 ± 0.2 | 7.5 ± 0.6 | 4 ± 0.9 | 3.6 ± 0.1 | 36.4 ± 29.6 | 8.8 ± 0.8 |
| | *500C* | 2.4 ± 0.1 | 3.8 ± 0.4 | 2.3 ± 0.6 | 1.4 ± 0.1 | 4.6 ± 0.3 | 4.4 ± 1.5 |
| | *550C* | 2.7 ± 0.1 | 5.5 ± 0.7 | 2.9 ± 0.7 | 1.6 ± 0 | 5.7 ± 0.5 | 8.5 ± 4 |
| | *550Cg* | 2.5 ± 0.1 | 4.2 ± 0.5 | 2.1 ± 0.4 | 1.3 ± 0.2 | 4.1 ± 0.5 | 6.2 ± 2.8 |

The results of LOI performed on 50 samples across multiple sediment cores taken at six California salt marshes with standard errors. Number of samples from each site is indicated by (n). LOI was performed at temperatures of 450°C, 500°C, 550°C, and 550°C on samples ground by mortar and pestle before treatment (550°Cg). Percent SOM is the weight lost on ignition at each temperature. Weight loss for samples of each treatment subsequently ignited at 950°C are used as estimates of carbonate content.

**Table 3.4 Average Particle Size by Site**

| Region | Sites | (n) | Sand (%) | Silt (%) | Clay (%) |
|---|---|---|---|---|---|
| Northern California | Mad River Low | 12 | 10.6 ± 2.4 | 73.7 ± 2.1 | 15.5 ± 1 |
| | Bolinas Lagoon | 6 | 8.3 ± 2.8 | 69.2 ± 2.6 | 22.4 ± 1.6 |
| San Francisco Bay | Petaluma Marsh | 12 | 40.3 ± 12.6 | 41.3 ± 7.3 | 18.3 ± 8.6 |
| | Mugu Lagoon | 2 | 5.7 ± 1.8 | 82 ± 0.3 | 12.1 ± 2.1 |
| Southern California | Seal Beach | 16 | 10.5 ± 1.2 | 79.9 ± 0.9 | 9.5 ± 0.6 |
| | Mission Bay | 2 | 9.6 ± 5.4 | 78.5 ± 6.2 | 11.9 ± 0.8 |
| | All sites | 50 | 14 ± 12 | 72 ± 16 | 15 ± 7 |

The results of particle size analysis on 50 samples across multiple sediment cores taken at six California salt marshes with standard errors. Number of samples from each site is indicated by (n).

**Table 3.5 SOC for Acid Treated and Untreated Soil Samples**

| Site | n | Acid Treated (%) | n | Untreated (%) |
|---|---|---|---|---|
| Mad River Low | 2 | 4.19±3.63 | 12 | 4.7±4.01 |
| Petaluma Marsh | 9 | 17.32±8.6 | 11 | 12.88±5.29 |
| Bolinas Lagoon | 6 | 9.15 | 5 | 3.12±3.72 |
| Mugu Lagoon | 0 | - | 2 | 2.58±1 |
| Seal Beach | 12 | 18.92±6.47 | 12 | 12.99±7.1 |
| Mission Bay | 1 | 12.67 | 1 | 15.12 |
| **All** | **30** | **16.52±7.94** | **43** | **7.94±9.07** |

Results of elemental analysis of samples acid treated for removal of carbonates and untreated samples are summarized by site and for all samples with standard deviations.

**Table 3.6 California SOM-SOC Conversion Equations**

| Sample Locations | LOI Temperature (°C) | Hours | a | b | c |
|---|---|---|---|---|---|
| *North Carolina* [1] | 450 | 8 | 0.0025 | 0.4 | 0 |
| *San Franciso Bay* [2] | 450 | 8 | 0.001217 | 0.3839 | 0 |
| *Southern California* [3] | 400 | 10 | 0.0048 | 0.23 | -0.11 |
| *California* [4] | 550 | 1-24 | 0.00026 | 0.389 | 0 |
| *California* | 500 | 1-24 | 0.00231 | 0.315 | 0 |
| *California* | 450 | 1-24 | 0.000172 | 0.417 | 0 |
| *California* | 550g | 1-24 | 0.0013 | 0.297 | 0 |

[1]Craft et al. (1991), [2]Callaway et al. (2012), [3]Keller et al. (2015), [4]This Study

LOI treatments and conversion equation coefficients are shown for studies from salt marsh habitats. All equations are quadratic ($SOC = aLOI^2 + bLOI + c$)

## 3.8 Appendix

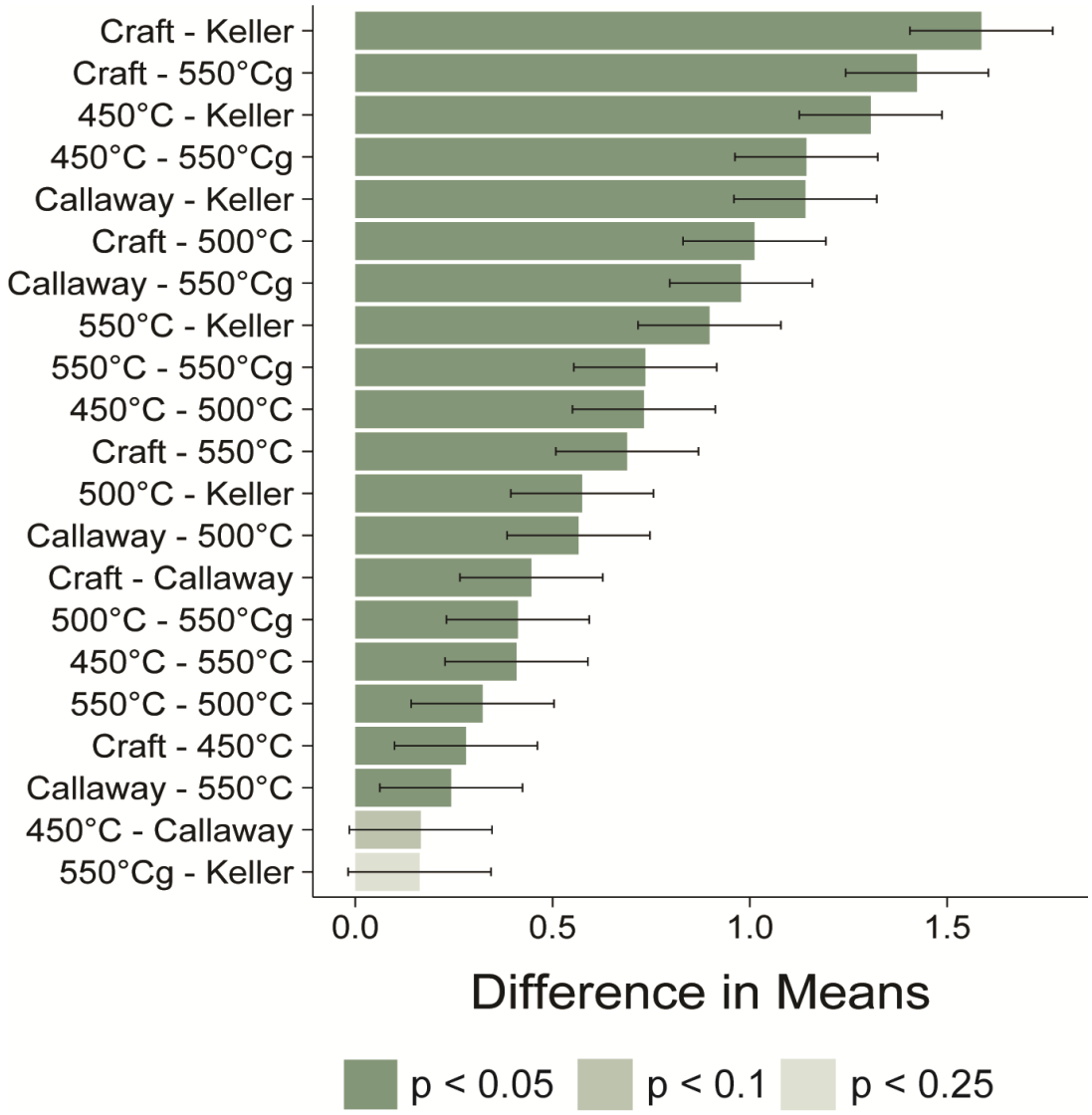


**Appendix Figure 3.1 Effect Size of Different Salt Marsh Correction Equations on Mean SOC**

The effect of different salt marsh conversion equations on mean SOC is estimated with a post-hoc Tukey test. Significance levels are indicated by color.

**Appendix Table 3.1 Published Organic Matter-Organic Carbon Conversion Factors**

| Soil Type | Converstion Factors Used | References |
|---|---|---|
| Peat | 0.5 | Tolonent et al (1992), Kauppi et al. (1997) |
| Peat | 0.517 | Gorham (1991) |
| Peat | 0.52 | Clymo et al. (1998) |
| Peat | 0.56 | Botch et al. (1995) |
| Peat | 0.57 | Botch et al. (1995) |
| Peat | 0.3 - 0.58 | Bhatti and Bauer (20020 |
| Peat | 0.5 | Howard (1965) |
| Salt Marsh | 0.22 - 0.52 | Lord (1980); Nixon (1980); Bowden (1984); Morris and Whiting (1986); Craft et al (1988b) |

This table shows the range of published SOM-SOC conversion factors used in the peat and salt marsh soil communities

**Appendix Table 3.2 Published Soil Organic Matter Soil Organic Carbon Regressions**

| Reference | Ecosystem | Depth | Method | $R^2$ | Slope | Intercept | c | Type |
|---|---|---|---|---|---|---|---|---|
| Ball (1964) | *North Wales Soil* | Surface | Tinsley | 0.99 | 0.48 | 1.87 | NA | linear |
| Ball (1965) | | Surface | Tinsley | 0.99 | 0.46 | 0.40 | NA | linear |
| Bhatti & Bauer (2002) | *Canada, peat* | 1m | CHN | | 0.52 | 0.00 | NA | linear |
| Callaway et al. (2012) | *CA Marshes* | 1m | EA | 0.99 | 0.00 | 0.00 | 0.38 | quadratic |
| Campos (2010) | *Tropical Cloud Forest, Mexico* | Surface | EA | 0.96 | 0.45 | -3.92 | NA | linear |
| | | Surface | WB | 0.88 | 0.55 | -2.90 | NA | linear |
| Craft et al. (1991) | *NC Salt Marsh* | 30cm | EA | 0.99 | 0.40 | 0.00 | 0.00 | quadratic |
| Frangipane et al. (2009) | *Venice Lagoon* | 1 m | EA | 0.93 | 1.90 | 0.00 | NA | linear |
| Ghabbour et al. (2014) | *CO Soils* | Surface | EA | 0.91 | 0.57 | 0.09 | NA | linear |
| | | Surface | EA | 0.83 | 0.38 | -0.23 | NA | linear |
| Howard & Howard (1990) | *Gley* | 20cm | EA | 0.52 | 1.52 | 4.64 | NA | linear |
| | *Base-deficient brown earth* | 20cm | EA | 0.77 | 1.63 | 3.48 | NA | linear |
| | *Brown podzolic* | 20cm | EA | 0.84 | 1.86 | 2.47 | NA | linear |
| | *Base-rich brown earth* | 20cm | EA | 0.95 | 2.27 | 1.82 | NA | linear |
| | *Podzol* | 20cm | EA | 0.98 | 2.09 | -0.23 | NA | linear |
| | *Peaty Podzol* | 20cm | EA | 0.98 | 1.83 | 0.87 | NA | linear |
| | *Peaty gley* | 20cm | EA | 0.98 | 1.89 | 0.61 | NA | linear |
| | *Hill peat* | 20cm | EA | 0.71 | 1.91 | -0.46 | NA | linear |
| Konare et al. (2010) | *Sahel, West Africa* | 60 cm | WB | 0.89 | 0.36 | 0.06 | NA | linear |
| | | 60 cm | EA | 0.80 | 0.33 | 0.17 | NA | linear |
| | | 60 cm | EA | 0.69 | 0.13 | 0.22 | NA | linear |
| | | 60 cm | EA | 0.89 | 0.36 | 0.20 | NA | linear |
| | | 60 cm | EA | 0.74 | 0.37 | 0.46 | NA | linear |
| | | 60 cm | EA | 0.68 | 0.17 | 0.56 | NA | linear |
| | | 60 cm | EA | 0.70 | 0.14 | 0.40 | NA | linear |
| | | 60 cm | EA | 0.73 | 0.13 | 0.34 | NA | linear |
| | | 60 cm | EA | 0.74 | 0.13 | 0.38 | NA | linear |
| Konen et al. (2002) | *North Central US* | Surface | EA | 0.94 | 1.14 | -0.68 | NA | linear |
| | | Surface | EA | 0.94 | 0.67 | -4.54 | NA | linear |
| | | Surface | EA | 0.98 | 0.57 | 0.10 | NA | linear |
| | | Surface | EA | 0.97 | 0.68 | -2.87 | NA | linear |
| | | Surface | EA | 0.98 | 0.61 | 0.19 | NA | linear |
| Wang et al. (2011) | *FL Sediments* | 210cm | TGA | 0.99 | 1.05 | 2.99 | NA | linear |
| | | 210cm | EA | 0.96 | 0.91 | 3.16 | NA | linear |
| | | 210cm | WB | 0.65 | 1.50 | 11.31 | NA | linear |
| | | 210cm | TGA | 0.98 | 0.95 | 0.55 | NA | linear |
| Wright et al. (2008) | *Everglades* | 30cm | EA | 0.96 | 0.44 | 55.80 | NA | linear |

This table shows references for SOM-SOC regression equations used in Figure 3.3.

# 4. California Salt Marsh Blue Carbon

## 4.1 Abstract

Salt marsh blue carbon has been proposed as an opportunity for the state of California to invest in mitigation of climate change through the preservation and restoration of salt marsh area. However, this chapter shows that salt marshes in the state annually sequester only about 0.08% of one year's state-wide greenhouse gas emissions and store about 23% of one year's annual emission in their soils (estimated from 2016 emissions data). With carbon market values of $15 per metric tonne of $CO_2$ equivalent, state-wide annual sequestration is worth about $4.8 million with $1.4 billion total carbon stock protected in California salt marsh soils. I content that blue carbon storage and sequestration is small in comparison to annual greenhouse gas emissions in California and would not present a significant avenue of climate mitigation for the state. But protection of the almost $1.5 billion stored value of carbon, as well as myriad other ecosystem services provided by salt marsh habitat, should be a priority for managers and stakeholders. This chapter provides baseline estimates of carbon storage and sequestration for 13 salt marsh sites along the California coast and examines the factors which lead to higher rates of carbon sequestration and storage in order to preserve functionality of the salt marsh carbon sink in the face of climate change. Average rates of sequestration across the state are 148.56 ± 121.78 g C $m^{-2}$ $yr^{-1}$ with the large part of sequestration occurring in the low marsh elevations and northern part of the state. Environmental and site variables reveal that many of the factors which contribute most to higher rates of sediment accretion – like larger tidal ranges and higher rates of sea-level rise – are those factors which contribute more to increased rates of carbon sequestration. Finally, the state's larger salt marshes in San Francisco Bay and Humboldt Bay

contribute most to carbon sequestration and stock by virtue of their relative size and higher rates of sediment accretion. For this reason, the two most effective ways to increase carbon sequestration are the preservation and expansion of salt marsh area and increase in sediment accretion or carbon burial rates.

## 4.2 Introduction

The term blue carbon was coined in 2009 to describe the sequestration and storage of carbon in coastal habitats such as tidal marshes, mangroves, and seagrasses (Nellemann et al., 2009). Although these coastal zones are limited in area, they store carbon at rates higher than terrestrial forests and therefore have been proposed as a potentially globally significant pathway for carbon storage. Current estimates of annual sequestration have great uncertainty based on poor estimates of total area covered by these habitat types, but they show coastal vegetated habitat may sequester up to 0.008% of annual global emissions[3] in a single year according to estimates with higher area cover (Mcleod et al., 2011). While this overall contribution climate mitigation is relatively insignificant, interest in quantifying carbon stocks and fluxes in these habitats for use in carbon markets to fund habitat protection and restoration projects has inspired much research into carbon cycling in coastal ecosystems (Table 4.1; Bear, 2017; Chmura, 2013; Chmura et al., 2003; Hopkinson et al., 2012; Ouyang & Lee, 2014; Vanderklift et al., 2019). These studies have found that salt marshes, mangroves, and seagrasses are play a small but active role in the global carbon cycle through the removal of $CO_2$ by vegetation, anaerobic decay of organic matter into recalcitrant forms of carbon, and burial for hundreds to thousands of years (Mitra et al., 2005).

California is within the temperate zone and once had large expanses of salt marsh habitat along its outer coasts and within the San Francisco Bay. This habitat has been reduced by up to 75% in Southern California (Stein et al., 2014) and 80% or more in the San Francisco Bay (Atwater et al., 1979) because of human land-use change following European colonization. Even

[3] Global emissions estimated at 37.1 gigatonnes $CO_2$ for 2018 (Global Carbon Project, 2018)

so, there is significant interest in the value of these remaining salt marshes and the potential for restored marshes to sequester and store carbon (Callaway et al., 2012). Published studies show that carbon sequestration in the San Francisco Bay on average is 79 g C $m^{-2}$ $yr^{-1}$, which is less than half of the reported global average of 210 – 240 g C $m^{-2}$ $yr^{-1}$ (Chmura et al., 2003; Ouyang & Lee, 2014). Even with these lower rates of sequestration, the potential for climate mitigation through the preservation and expansion of this salt marsh area is of great interest. Early feasibility assessments for the use of carbon credit programs to fund protection and restoration project show that the current price of carbon will not completely cover costs for small restoration projects, but there is potential for large restoration projects or for projects to become feasible as carbon prices increase (Bear, 2017).

Additionally, the degradation or loss of 1 $km^2$ of tidal marsh habitat has been shown to re-release an estimated 0.1 Mt $CO_2$ from the top meter of the soil column. Salt marshes in the San Francisco Bay and along the outer coast of California have been collecting carbon stores for approximately 4 to 6,000 years or more (Atwater et al., 1979). The loss of this habitat and release of 6,000 years of stored carbon would not only contribute further to increased temperatures but would also mean the loss of other ecosystem services that salt marshes provide to California, such as water filtration, nurseries for fisheries, and storm surge protection (Barbier et al., 2011; Costanza et al., 1997). Even if carbon credits for funding ecosystem protection and restoration is not currently a feasible option, the protection of carbon stores and marsh habitat is a priority for the state due to the other myriad ecosystem services provided by coastal wetlands (Barbier et al., 2011) and as part of the states' efforts to reduce overall emissions. Protection of coastal salt marsh habitat is already of great concern to the state due to potential habitat loss from accelerated sea-level rise (SLR) caused by climate change. Rates of projected SLR based on

IPCC climate change scenarios will result in habitat change and potential losses of all tidal marsh habitat by the end of the 21st century for the state of California under high SLR scenarios (Thorne et al. 2018). Habitat loss will likely release stored carbon and have a positive feedback on increased global temperature, leading to more habitat loss. For this reason, marketization of blue carbon has been proposed as one way to not only fund the protection of this habitat but also to offset the negative consequences of salt marsh habitat loss.

Protecting blue carbon stocks and incorporating wetland carbon storage into carbon markets both will require the measurement and quantification of current carbon stocks and sequestration potential for California. Carbon stock in salt marshes is preserved mostly in sediments, although active above- and below-ground biomass layers contribute to carbon stocks as well. Collection of sediments through sediment coring and measurement of soil carbon content has been conducted in some areas of the state (Callaway et al., 2012; Keller et al., 2015, 2012), but the expansion of the geographic range of this dataset will provide further information on variability within and between salt marshes in the state. Sediment cores can also be dated to obtain sediment accretion rates which then, with soil carbon content data, can be used to calculate rates of sequestration over the past hundred or more years. This data, paired with biomass surveys and carbon flux data, lay the foundation for describing the carbon cycle of a salt marsh system. If the ecosystem service of carbon storage is to be protected, or valued on the carbon market, these data are the first step to an ongoing quantification and monitoring process.

This chapter uses estimates of carbon content made from loss-on-ignition (LOI) of 61 sediment cores from 13 salt marshes along the coast of California for quantification of carbon stocks. Carbon sequestration rates are then calculated for these same sites using accretion rate measured from 32 of 61 cores. Estimates of total carbon stock and sequestration rates for the

entire state of California are compared to published estimates of global stocks and sequestration rates. Using this database, I assess:

1) Where is the most carbon stored within marshes and between salt marshes in California?
2) What abiotic and biotic factors control carbon storage and sequestration across the state of California?
3) What is the total amount of carbon sequestered annually, total stored, and potential monetary value?
4) How can carbon storage be maximized?

This work responds to interest in the potential of blue carbon credits to promote climate mitigation, habitat protection and restoration in the state of California. These data serve as baseline estimates for the potential ecosystem service value of these sites but much more work will be needed to assess the potential for blue carbon accreditation in the state. Effects of climate change and accelerated SLR on the carbon stock and carbon sequestration of salt marshes are uncertain, but loss of habitat will inevitably lead to loss of carbon sequestration potential and release stored carbon back into the atmosphere. Regardless of the potential market value of carbon storage and sequestration, the protection of salt marsh habitat in California is an essential priority for preservation of carbon stores, continued mitigation of climate change through sequestration, as well as protection of all other ecosystem services salt marshes provide.

## 4.3 Methods

### *4.3.1 Site Descriptions*

The database for this chapter contains 61 sediment cores across 13 sites and spans 8.3 degrees latitude. Individual sites are represented by 3 to 12 cores. Site descriptions can be found

in Table 2.1. Mean annual temperature (MAT) ranges from 12ºC (Humboldt Bay) to 18ºC (Long Beach) and mean annual precipitation (MAP) varies from 73 mm $yr^{-1}$ (Tijuana River) to 264 mm $yr^{-1}$ (Humboldt Bay; "Climate Data Online," 2019). Each salt marsh is represented by core samples from the low and high elevations of the marsh, with overall elevation (extracted from the National Center for Environmental Information (NCEI) coastal digital elevation models (DEMs) based on latitude and longitude of core locations recorded in the field; see page 27 for references) ranging from 0.97 m (Mission Bay) to 2.144 m (Mad River High). Diurnal tidal range varies from 1.62 m (Mission Bay) to 2.15 m (Triangle Marsh) and rates of SLR range from less than 1 mm $yr^{-1}$ (Morro Bay) to almost 5 mm $yr^{-1}$ (Humboldt Bay; "NOAA Tides & Currents," 2019). Humboldt Bay, Bolinas Lagoon, Triangle Marsh, Mugu Lagoon, Seal Beach, and Upper Newport Bay all have experienced land subsidence either from tectonics or oil and water extraction (Bawden et al., 2001; Hansen et al., 2003; Poland & Ireland, 1988; State Coastal Conservancy and Coastal Ecosystems Institute of Northern California, 2015; Watson, 2004). Salt marsh environments vary from those, like Point Mugu, which are dominated by *Salicornia pacifica* to the northern sites in Humboldt Bay which have been invaded by *Spartina densiflora*. Detailed site descriptions can be found in Chapter 2 (pages 16 - 23).

Salt marsh area for each salt marsh site as well as total salt marsh area in the state was calculated by watershed as the sum of area classified as 'Estuarine and Marine Wetland' using publically accessible shapefiles from the National Wetlands Inventory (NWI) mapping project Version 2, Surface Waters and Wetlands (*National Wetlands Inventory—Wetlands Project, Version 2*, 2019). As all salt marshes in Humboldt Bay are in the same watershed, only one area estimate has been used for those four sites and all measured values are averaged between the four Humboldt sites for watershed-level estimates.

### *4.3.2 Carbon Content and Sequestration Rates*

Core collection and sediment analysis for LOI is described in Chapter 2 (pages 23 - 25). LOI estimates of soil organic matter were converted to estimates of soil organic carbon using the conversion equation generated in Chapter 3 for LOI conducted at 550°C, as this was the temperature used during preparation of all samples.

To calculate the carbon content of sediment (g C $cm^{-3}$), bulk density (BD) measured during LOI was multiplied by percent carbon obtained from the conversion equation. An estimate of carbon storage for each salt marsh was made by multiplying the average carbon content of the top meter of sediment in all cores taken at the site by the total area of the salt marsh and assuming one meter of carbon stock for the entire marsh. The rate of sediment accumulation for each sediment core was measured using $^{137}Cs$ and $^{210}Pb$. The average accretion rate from each of these methods was calculated for each sediment core and used as the rate of sediment accumulation. If a core was not successfully dated with $^{137}Cs$ or $^{210}Pb$, an average site accumulation rate from the other cores measured in this database was used (Appendix Table 4.1).

Measured carbon content for each cubic centimeter of the sediment core was multiplied by the average accumulation rate for that sediment core or for the site and area was increased to one square meter to obtain estimated rates of sequestration (g C $m^{-2}$ $yr^{-1}$). Average rates of sequestration taken from each core were averaged with all cores taken at the site and used as the long-term average sequestration rate for the site.

### *4.3.3 Environmental Controls on Sequestration in California*

Sequestration rates, accretion rates, bulk density, organic matter content, carbonate content, dominant vegetation, and relative elevation for each core were compared with site

parameters including MAT and precipitation, historic rate of SLR, historic subsidence, and diurnal tidal range in a principle component analysis (PCA). Categorical variables were converted to dummy variables (dominant vegetation and relative elevation). The effect of each parameter on the dataset was plotted with the length of arrow and color representing its contribution to variability (Figure 4.6a). A screeplot was used to determine the number of factors which described most of the variability in the dataset (Appendix Figure 4.1). Individual core datapoints were plotted in Figure 4.6b and a 95% confidence interval ellipse indicates the four different studied regions of the California coast (Humboldt Bay, San Francisco Bay, the Outer Northern and Central Coasts, and Southern California) with arrows drawn for the parameters which contributed to most of the variability. Loadings for all core and site parameters are seen in Table 4.3.

### *4.3.4 Estimated Ecosystem Service Value by Watershed*

Using area of Estuarine and Marine Wetland measured by the NWI for each watershed in which sediment cores were sampled multiplied by average annual sequestration rate for all cores within that watershed, an estimate of annual sequestration (Mg C $yr^{-1}$) was obtained. Assuming one meter depth of storage for all wetland area within each watershed, an estimate of total storage in the watershed was calculated (Tg C). Errors for both of these values are calculated based on the standard error associated with core estimates of annual sequestration or carbon content.

The estimated ecosystem service value for annual sequestration and total storage was calculated assuming an estimated $15 per metric tonne $CO_2$ equivalent ($CO_2e$), a standard measure of the effect one metric tonne of $CO_2$ has on the climate system (Boden, Marland, &

Andres, 2017). $CO_2$ contains one molecule of carbon and two molecules of oxygen, so the weight of $CO_2$ is equivalent to ~ 0.27 g of carbon. Because of this, annual sequestration and total storage were first divided by 0.27 to obtain an estimate of $CO_2e$. This value was multiplied by $15 per metric tonne to obtain dollar value estimates of the ecosystem service value of carbon sequestration and storage for each watershed in which sediment cores were taken. An estimate of total sequestration and storage (using average sequestration and carbon content from all cores in this study) was also calculated.

## 4.4 Results

### *4.4.1 Trends in Soil Carbon in California Salt Marshes*

Bulk density of sediments in the dataset ranges from 0.1 – 2.3 g $cm^{-3}$ and averages at 0.74 ± 0.73 g $cm^{-3}$ (reported errors are standard deviations). Sites on the Outer Coast and in Southern California tend to have higher bulk densities than those sites which are found within the two larger bays in the state. Mad River Low, on the edge of Humboldt Bay, has BD in the range of marshes on the outer coasts while Seal Beach has BD more reminiscent of the marshes found within bays (Table 4.1). BD shows a typical non-linear relationship with SOM where, as BD decreases, SOM increases (Figure 4.1).

Average carbon content in California salt marshes sediments is 4.50 ± 3.26% and ranges from less than 1% to 21% carbon. Within individual sediment cores, average carbon content of the top 25 cm of the sediment column is double that of the bottom 25 cm (Figure 4.2). Although the range of percent carbon content is fairly wide for the dataset, over 50% of the data falls within the 2.2 – 6.0 % carbon range. Individual site average percent carbon content varies between 2.6 – 8.6 %. Mugu Lagoon has the lowest average percent carbon content (2.55 ±

2.12%) and Petaluma Marsh in San Francisco Bay has the highest average percent carbon content (8.58 ± 4.02%). Sites in the northern part of the state tend to have higher percent carbon content in salt marsh sediments, however there are sites with percent carbon content values lower than the statewide mean (Mad River Low) in northern California and sites higher than the mean in Southern California (Seal Beach).

Carbon content shows non-linear trends over elevation, with mid elevations of salt marshes in California exhibiting the highest observed average values of percent carbon content (5.10 ± 3.91%). Low elevation salt marsh area has slightly higher carbon content than the high elevations (4.37 ± 2.68 % and 3.83 ± 2.88%, respectively). Mid elevations, however, have the most variability in carbon content. A loess fit of carbon content by elevation of the salt marsh core taken (relative to NAVD88), shows max carbon content in sediments from 1 – 2 m elevation, but individual core average carbon content reveals that this fit contains many cores taken in these mid elevations which do not show a significantly higher percent carbon content than cores taken in the lowest elevations or highest elevations (Figure 4.3). Higher average carbon content in the mid elevations is driven primarily by several cores within this range that have particularly high carbon content taken from Seal Beach and Triangle Marsh.

### *4.4.2 Trends in Carbon Sequestration in California*

Average carbon sequestration in California is 148.56 ± 121.77 g C $m^{-2}$ $yr^{-1}$. This average is slightly higher than the previously reported averages estimated from San Francisco Bay area of 79 g C $m^{-2}$ $yr^{-1}$ (Callaway et al., 2012), and average sequestration in the San Francisco Bay sites studied in this dataset is much higher at 206.38 ± 131.40 g C $m^{-2}$ $yr^{-1}$. Carbon sequestration at each site is a factor of both percent carbon content in sediment and the accretion rate at the site. While there is little variability in the percent carbon content across sediments, there are larger

differences in the average carbon sequestration rates across sites, and even between sediment cores within the same site which may have different rates of accretion. Figure 4.4 displays the average percent carbon content, rate of accretion, and rate of sequestration for cores sorted by relative elevation (High, Mid, and Low) and each region of California. Higher rates of accretion tend to drive higher rates of carbon sequestration. This becomes more apparent when comparing the percent carbon content of the Mid and Low elevation marshes to their rates of sequestration; although the mid marsh tends to have higher percent carbon content, higher accretion rates in the low marsh lead to higher rates of sequestration. Similarly, looking at trends of sequestration across California regions, there is little difference between the average carbon content across Humboldt Bay, the Outer Coast, and Southern California. But lower rates of sediment accretion in Southern California lead to significantly lower sequestration in this region than in either of the bays in the northern part of the state.

Although percent carbon content has a smaller impact on overall sequestration, the contribution of SOM to sediment is positively correlated with sequestration rates (Figure 4.5; $R^2 = 0.55$; $p < 8.5x10^{-12}$) while BD is negatively correlated with sequestration ($R^2 = 0.34$; $p < 8.3x10^{-7}$). The rate of sediment accretion also has a significant positive effect on sequestration ($R^2 = 0.39$; $p < 3.5x10^{-8}$).

### *4.4.3 Environmental Controls on Sequestration*

PCA of core variables (elevation, dominant vegetation, accretion rate, subsidence, average BD and SOM, and sequestration) and site characteristics (MAT and precipitation, rate of SLR, tidal range, area) identified MAT, the rate of SLR, marsh area, tidal range, and MAP as the principal components which contributed most to 25% of variance in the whole dataset described

by the first dimension (Table 4.3). SLR, marsh area, tidal range, and MAP are positively associated with sequestration, while MAT has a negative association. BD contributes most to the second principal dimension, and has a negative association with sequestration, explaining and additional 19.7% of the variance in the in the dataset. Dominant species differences are the primary contributions to the third dimension and relative elevation effects contribute to over 25% of variance explained by the $4^{th}$ and $5^{th}$ dimensions. These first five dimensions explain a cumulative total 75.4% of the variance.

The relative importance of these variables in contribution to rates of carbon sequestration can be seen by the close association of accretion rates, tidal range, low marsh elevations, and marsh area (Figure 4.6a). High marsh elevations, carbonate content, and BD are negatively associated with carbon sequestration. Sediment cores in Humboldt Bay and San Francisco are more closely clustered with factors associated with higher sequestration, while marshes of the Outer Coast and Southern California have a more negative association. *S. densiflora* is more closely associated with sequestration, but contributes significantly less to variance than dominant native species types. *S. pacifica* and *S. foliosa* are associated with the third dimension of the PCA and are negatively associated with one another. *S. pacifica* is closely associated with subsidence..

Individual core sites plotted in dimensional space cluster together and show that salt marshes of Southern California and the Outer Coast are significantly different than those marshes of Humboldt Bay (Figure 4.6b). Salt marshes in the San Francisco Bay area are distributed widely in dimensional space and have similarities to all regions in the dataset. Higher MAP and higher BD are most characteristic of marshes in Southern California. The marshes of Humboldt are very similar to those of the San Francisco Bay, but while both regions see high

SLR, have larger tidal ranges, and have larger areas, marshes of San Francisco have the highest rates of accretion and sequestration likely driven by higher SOM content and rates of accretion.

### *4.4.4 Total Salt Marsh Storage and Annual Sequestration in California*

Total salt marsh annual sequestration for California is 87,993 ± 959 Mg C $yr^{-1}$ and total storage estimated to one meter depth is 27 ± 0.3 Tg C for the state (Table 4.4). Calculation of total sequestration and storage for each watershed in the dataset shows that the marshes of San Francisco Bay and Humboldt Bay make, by far, the largest contribution to annual sequestration and total carbon storage in the state. San Francisco Bay watersheds, represented here by only marshes in the South Bay and San Pablo Bay, account for over half of the state-wide estimated annual sequestration (about 32,000 Mg C $yr^{-1}$) as well as make up almost half of the storage for the state (~16 Tg C).

### *4.4.5 Ecosystem Service Value of California Salt Marshes*

State-wide, salt marshes carbon sequestration is valued at $4.8 to $4.9 million based on a carbon credit value of $15 per metric tonne $CO_2e$. Value estimates for storage range from $1.46 billion to $1.49 billion dollars (Table 4.5). Error from these estimates derives from the standard deviation of average soil carbon content and annual sequestration rates for cores in this study. Error does not account for differences in carbon sequestration or storage between or within salt marshes, nor does it account for error in estimation of salt marsh area or depth of carbon stock.

## 4.5 Discussion

### *4.5.1 Where is Carbon Stored in California Salt Marshes?*

The majority of carbon in California salt marsh soils is stored in the top 25 cm of the soil column. About one-half of the total percent soil carbon in the top 25 cm is lost by the time soil reaches depths greater than 75cm in the salt marsh column. This is likely due to a combination of decay of organic matter over time, but also a factor of the limitation on soil carbon density. Soil carbon density has been shown to average at about 0.027 g C $cm^{-3}$ for the continental US (Holmquist et al., 2018). Therefore, increases in percent carbon of soils reflect more of a change in overall density of the soil, or the amount of organic material compared to mineral material. This maximum concentration of carbon means that the increased percent soil carbon seen in these top 25 cm is most likely in labile and easily decayed soil carbon pools. The same holds true for the increased percent soil carbon values seen in the mid marsh. Mid-elevations are typically where salt marsh vegetation find equilibrium with sea-levels and productivity is maximized. Increased productivity is what likely leads to higher SOC in these areas. However, increases in productivity does relatively little to increase long-term rates of sequestration and without high rates of carbon burial.

Increases in the rate of sequestration and potential storage can, however, be achieved through increases in sediment accretion alone, or increases in sediment accretion and SOC. The more rapidly carbon in the active soil layer is buried and no longer subject to decay, the more of the originally-deposited carbon will remain in the soil carbon. This is the mechanism which drives higher rates of sequestration in the low salt marsh elevations, as well as Humboldt Bay and San Francisco Bay. So while the higher SOM and sediment accretion are correlated with

higher rates of overall sequestration in this study, salt marsh habitat and salt marsh sites with higher rates of sediment accretion are those which ultimately sequester and store more carbon on the site- or region level. Accumulation of carbon in the anaerobic environment is what allows salt marshes to store carbon, and the increase of this variable is most important to maintain and increase sequestration rates overall.

### *4.5.2 What are the Environmental Controls on Salt Marsh Storage and Sequestration?*

Because of this close relationship between carbon sequestration and rates of sediment accretion, many of the most important environmental variables affecting the rate of sequestration are related to rates of accretion. Higher rates of SLR, larger tidal ranges, and *S. foliosa* habitat are all factors which are associated with high sediment burial rates. SLR and large tidal ranges increase the frequency of flooding and bring in the mineral material for *S. foliosa* to trap and use to build up the marsh platform. MAT was the factor with the largest effect in this dataset and was negatively associated with sequestration. The negative association with sequestration rates and annual temperature, although possibly an indication of increased rates of SOM decay with increased temperatures (Kirwan & Blum, 2011), may be more closely related to the fact that the salt marshes in Southern California – where temperatures are higher – have very different hydrologic conditions and thus lower rates of sediment accretion and burial of carbon. This relationship between temperature and rates of carbon storage merits much more study, especially considering increased temperatures to come with climate change.

Finally, a singly important parameter which increases carbon sequestration and carbon storage is simply salt marsh area. Salt marshes in San Francisco Bay and Humboldt Bay have much higher carbon stocks and sequestration rates because they cover a larger area. Because of

the large impact of increased area on carbon sequestration and storage, this study indicates that the single most important priority for the salt marsh blue carbon sink is simply preserving the salt marsh area which exists currently and restoring salt marsh habitat lost over the past 200 years.

### *4.5.3 How Much Carbon do California Salt marshes Sequester and Store?*

Based on average annual sequestration and carbon content of sediment cores in this study, the salt marshes of California sequester 0.08 Tg C $yr^{-1}$ and store an estimated 27 ± 0.3 Tg C in their soils. Compared to annual California emissions[4], each year salt marshes sequester 0.08% of annual emissions. This means that salt marshes in California would not make a significant contribution to annual emission remissions for the state. And, as stored carbon in salt marsh soils is equal to 23% of state-wide greenhouse gas emissions, the release of $CO_2$ from salt marshes would have only a moderate effect on state-wide emissions. Overall California salt marshes have very limited potential to make an impact on California greenhouse gas emissions. But this is not due to any significantly lower carbon storage or sequestration in California salt marshes compared to salt marshes around the US or the globe. This study finds an average carbon density of 0.024 g $cm^{-3}$, which is the similar average density calculated by recent models for all coastal marshes in the continental US (Holmquist et al., 2018) as well as other empirically-obtained estimates of carbon density for the state (Bear, 2017). Instead, the modest impact is primarily due to the limited area of salt marshes remaining in the state. If California salt marsh area was returned to its pre-European-contact extent, annual sequestration would be about 0.09% of emissions and storage would make up 31% of annual emissions. This increase in area by ~33%,

[4] California emissions for the year 2016 estimated as 429 Tg $CO_2e$ (Boden, Marland, & Andres, 2017)

however, still demonstrates that the global-scale impacts of carbon storage and sequestration in salt marshes are fairly small due to the small area which they occupy.

At a market value of $15 per metric tonne $CO_2e$, California salt marshes annually sequester about $4.8 – 4.9 million and store $1.4 billion in carbon. This means the ecosystem service value of annual sequestration in all salt marshes is very modest, while the value of storage in these habitats is of slightly higher economic significance. This study indicates that the incentive to protect the value of carbon stock is more likely to present an opportunity for economic investment in salt marsh habitat than the value of annual carbon sequestration. It is also important to emphasize that carbon sequestration and storage in salt marshes is only one of many different ecosystem services that are provided by salt marsh habitat, and these estimates of value do not fully encompass all of the benefits society gains from salt marsh habitat through water filtration, nurseries for fisheries, coastal protection, recreation, and aesthetic, cultural, or intrinsic values.

While carbon cycling in salt marshes may play a globally small role, tracking carbon cycling through a salt marsh is still of great interest to the scientific community, ecosystem managers, and stakeholders in terms of habitat function, resiliency, and vulnerability. There are still many areas of uncertainty regarding aspects of salt marsh carbon cycling which are not accounted for in these estimates. As all estimates only account for the current soil carbon pool, there is no account of carbon storage and sequestration occurring in aboveground biomass of the ecosystem. Additionally, these annual rates of sequestration are estimated from average rates of sequestration over the first meter of the sediment column. Annual sequestration measured at the surface of the sediment is much higher as well as the rate of decay and release of carbon back into the atmosphere. The flux of carbon in and out of this active layer of the soil column could,

therefore, be quite different from the average rates of sequestration measured over timeframes of 50 to 100s of years of accumulation.

Additionally, state-level estimates made using mean estimates of SOC may underestimate total stocks for the state due to the differences in mean SOC between California regions. Site-level analysis indicate that some salt marsh sites, especially larger salt marsh sites with higher mean SOC, contribute more to state-wide carbon stocks than others. The two watersheds studied in San Francisco Bay contain 42% of salt marsh area in the state and account for 71% of state-wide sequestration and 59% of the storage. Humboldt Bay contains 11% of the salt marsh area for the state. It contributes a consistent 12% of annual state-wide sequestration and maintains 12% of the state-wide storage. The studied salt marshes of the Outer Coast and Southern California coast make up an additional 11% of the annual sequestration, 12% of the storage, and covers 14% of the area. Calculations of sequestration and stock by site using the sites studied in this analysis represent 69% of the total area of California salt marsh stocks and account for 90% of mean state-wide sequestration estimates and 83% of mean stock estimates for the state. However, it is likely that the remaining 31% of salt marsh area in the state which was not studied in this review sequesters more than the 10% of the state-wide budget and stores more than 17% of carbon stocks based on site- and region-specific calculations in this study, especially because much of that area is within the San Francisco Bay.

Finally, studies of carbon cycling and efforts to use blue carbon credits to protect and restore ecosystems must also include evaluations of how carbon sequestration and storage will change under climate change conditions. Active salt marsh carbon stocks and functions will be subject to the effects of climate change, including increased $CO_2$ levels, nitrification, increased temperatures, and accelerated SLR which will inevitably affect the way carbon moves through

the system. Increased $CO_2$, nitrification, and higher temperatures may increase above- or below-ground biomass production in some species and may also lead to elevation changes (Cherry et al., 2009). These effects may, at first, increase the pace at which carbon is stored, but the increased carbon burial is not likely to be able to keep pace with the rate of SLR towards the latter 21$^{st}$ century and may actually increase the potential for release of carbon (Kirwan & Mudd, 2012). Increased temperatures are also associated with increases in microbial activity which may change the rate of decay and offset some of the added biomass and from elevated $CO_2$ (Foote & Reynolds, 1997; Kirwan & Blum, 2011). In sum, while these past rates of sequestration may inform the potential for future sequestration, monitoring of rates of sequestration and climate change impacts to salt marshes will be critical for quantifying the net effect, import or export, of carbon from these systems as they change through the next century.

### *4.5.4 What Can be Done to Maximize Salt Marsh Carbon Storage and Sequestration?*

Preservation of current salt marsh habitat and functions should be the priority of all stakeholders and land managers interested in the use of salt marsh habitat for blue carbon storage. Accelerated SLR poses a huge risk to current salt marsh carbon stocks and losses of carbon from the top meter of salt marsh in the state would mean contributing years' worth of carbon accumulation back into the atmosphere. The main threat to salt marsh habitat from accelerated SLR is, however, the relative limits on salt marsh sediment accretion – the very process which is most important to driving carbon storage. Providing adequate sediment supply either through the restoration of sediment from dammed freshwater sources (Edmonds, 2012) or the addition of sediment to the salt marsh itself (Thorne et al., 2019) are both avenues of current research exploring how best to maintain salt marsh accretion with rising tides. But work on protecting salt marsh collapse, both from increased wave action from SLR as well as increased

storminess from climate change, has received less attention (Barnard et al., 2019; Schuerch et al., 2013). The potential for salt marsh restoration or allowing landward migration of salt marsh habitat as seas rise may allow for continued sequestration over the next decades – and may even increase early rates of sequestration as salt marshes establish – but it is uncertain if these new areas will perform in the same ways as well-established salt marsh (Callaway et al., 2012). And, even if marshes move inland, loss of carbon stocks on the seaward margin may result in a net export of carbon to the atmosphere. These are some of the questions and avenues of research which must be prioritized for the survival of salt marsh habitat in the 21$^{st}$ century and are the same questions that will help preserve and foster salt marsh sequestration of carbon for the state of California. Marketization of the ecosystem service value of carbon is one way this could be funded. But, given the modest contribution of salt marshes to annual carbon emissions and the low price of carbon, blue carbon may only be one among many ecosystem services which managers and stakeholders should prioritize.

## 4.6 Figures

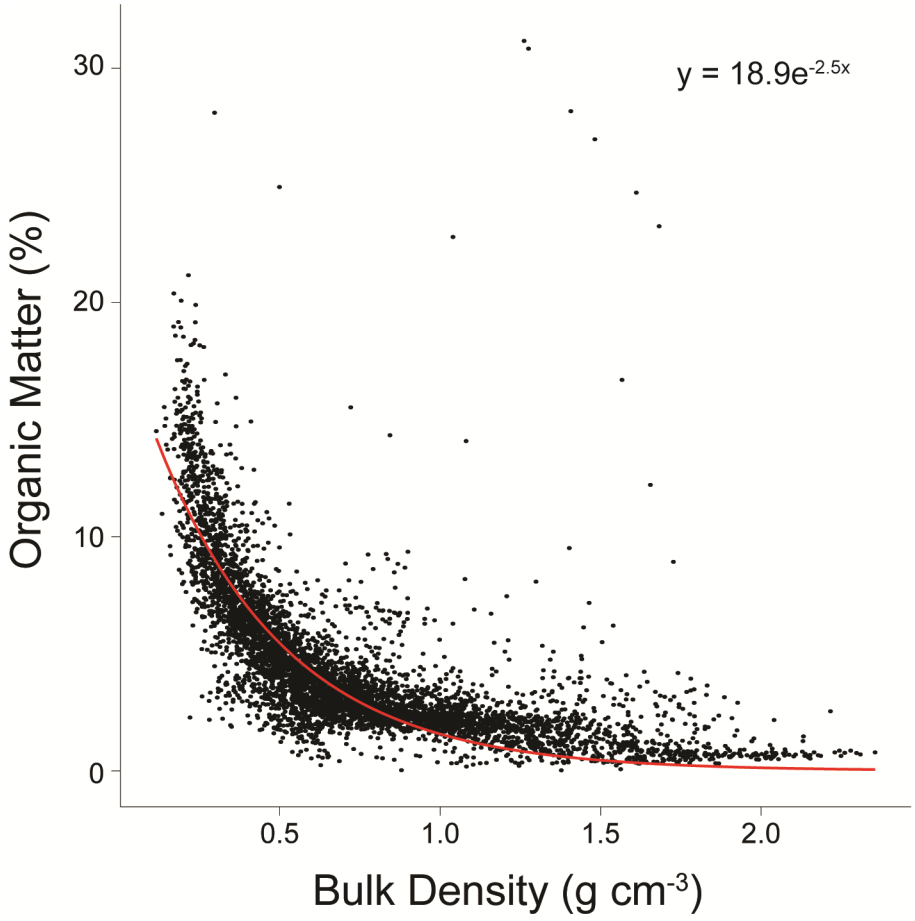


**Figure 4.1 Bulk Density versus Soil Organic Matter**

Percent soil organic matter decays exponentially with bulk density.

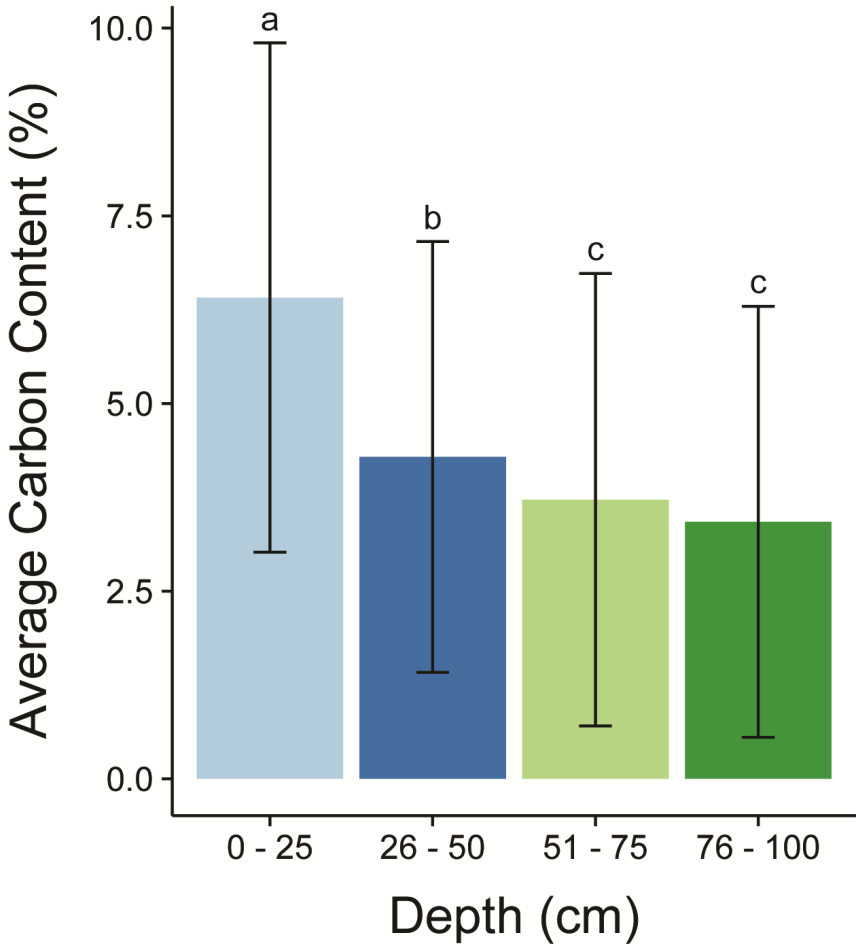


**Figure 4.2 Percent Carbon by Depth**

Percent carbon content averaged for all cores with standard deviation plotted by depth interval in the first meter of sediment. Means for depth intervals which share a letter are not significantly different (ANOVA; 95% confidence).

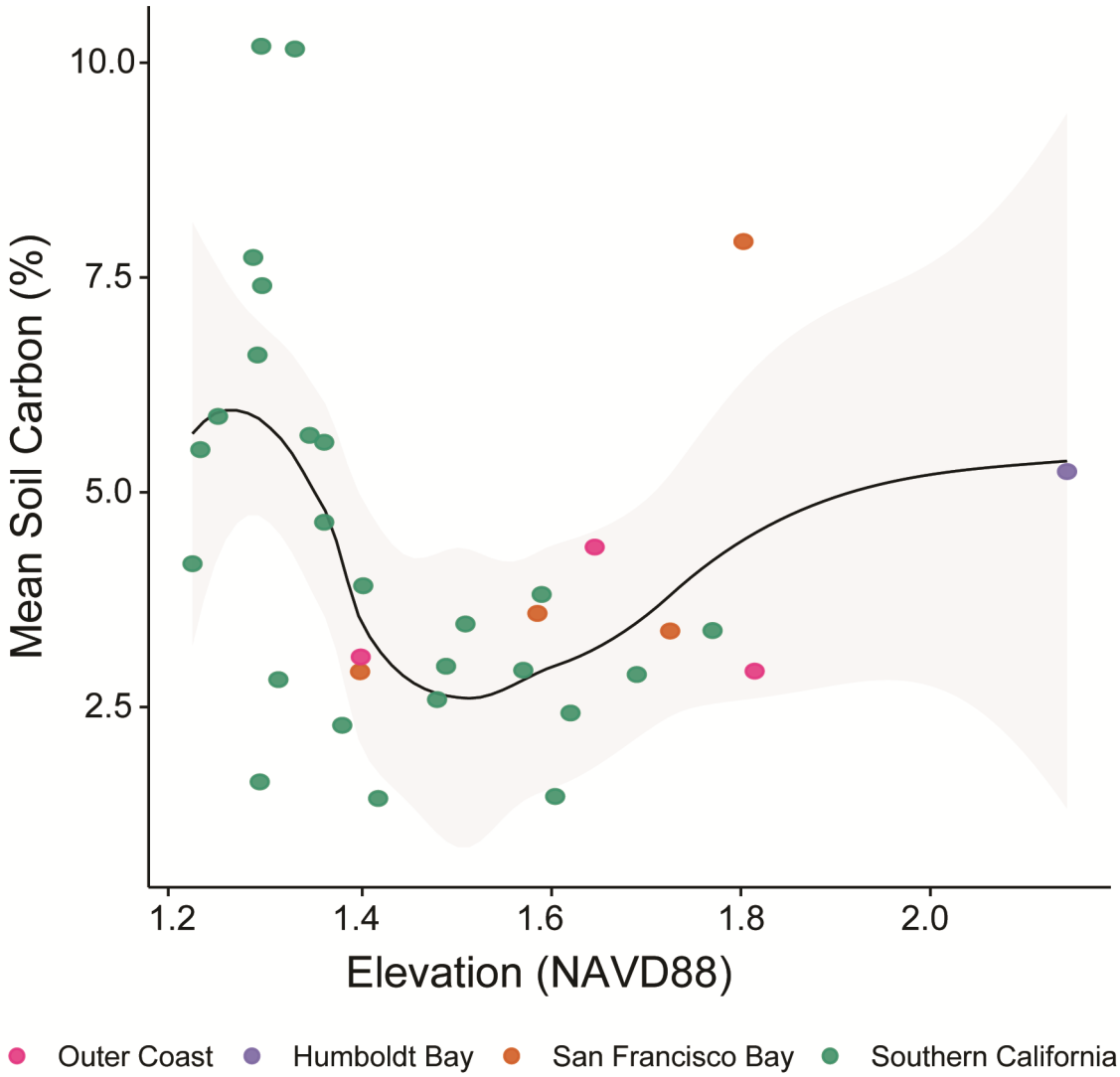


**Figure 4.3 Soil Carbon by Elevation**

Average soil percent carbon content for each core was plotted against elevation relative to NAVD88. A loess fit is seen with the 95% confidence interval shaded in grey.

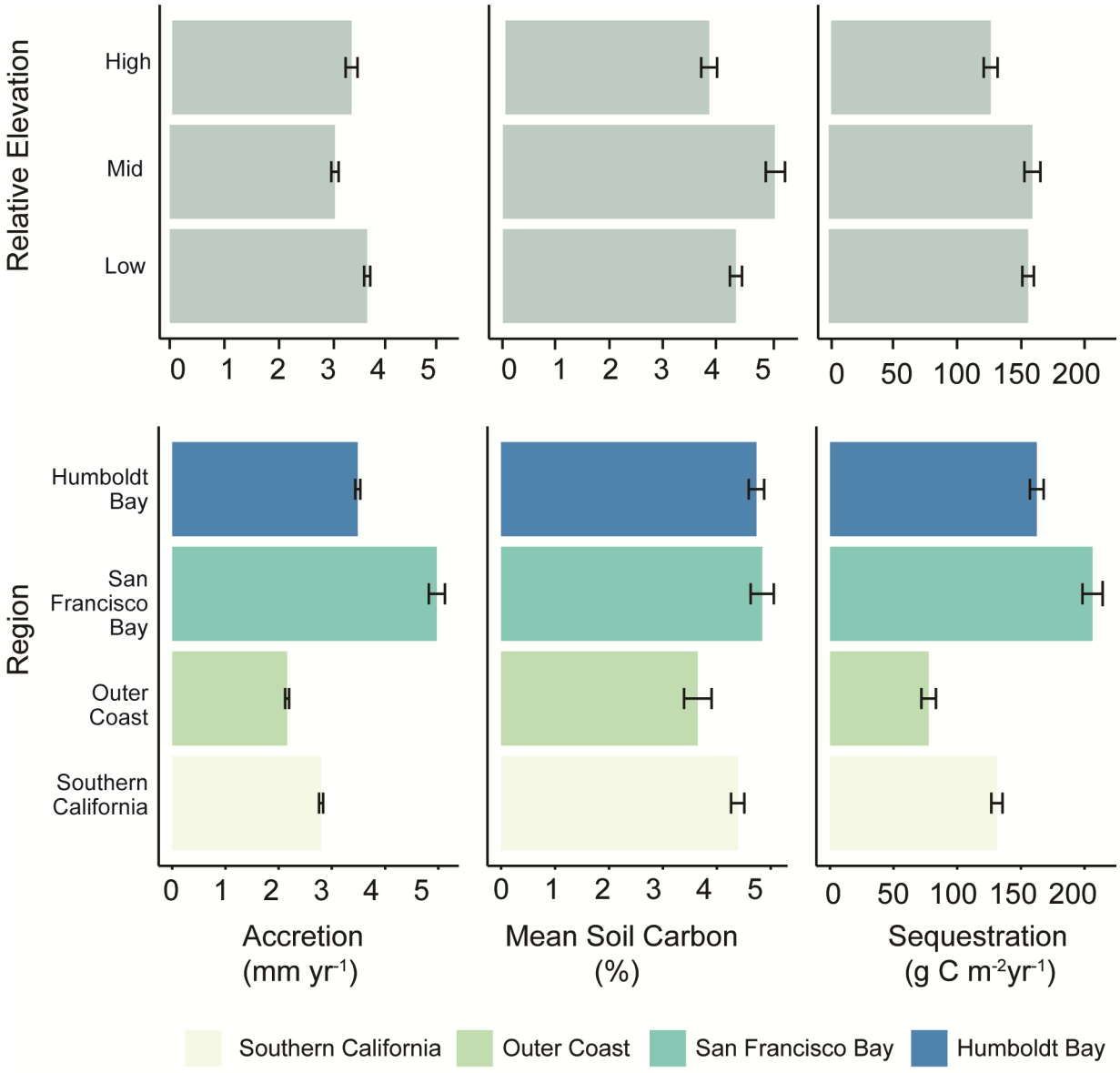


**Figure 4.4 Soil Carbon, Accretion and Sequestration in California Marshes by Region**

Average soil organic carbon content (%), average rate of accretion (mm $yr^{-1}$), and average sequestration (g C $m^{-2}$ $yr^{-1}$) were calculated with standard errors for relative elevations across the marsh (High, Mid, and Low) and regions in the state (Humboldt Bay, San Francisco Bay, the Outer Coast, and Southern California).

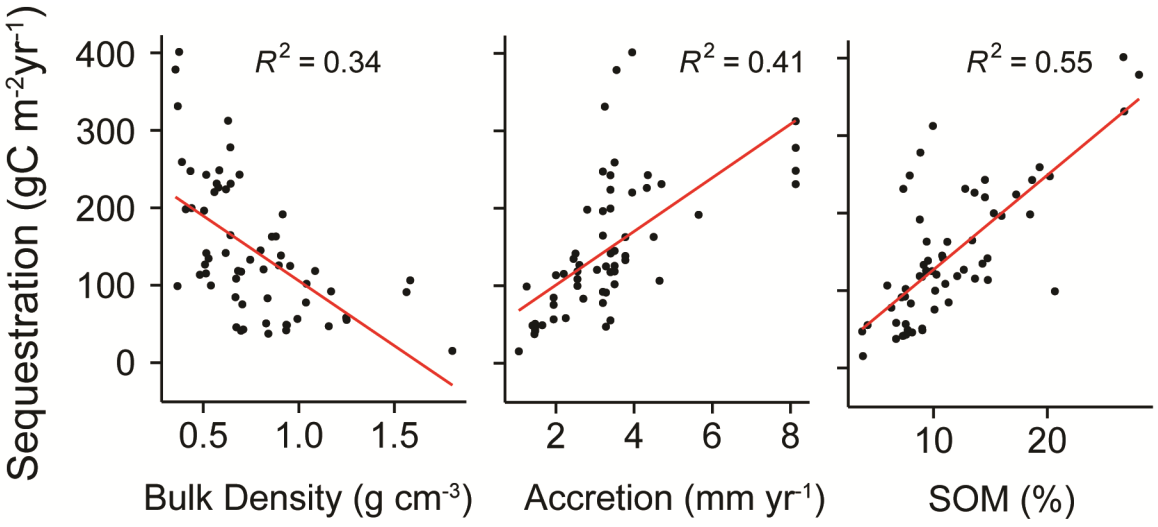


**Figure 4.5 Sequestration compared to Bulk Density, Organic Matter, and Accretion**

Linear Regressions between bulk density, organic matter, accretion rates, and carbon sequestration calculated for each core with $R^2$ values shown.

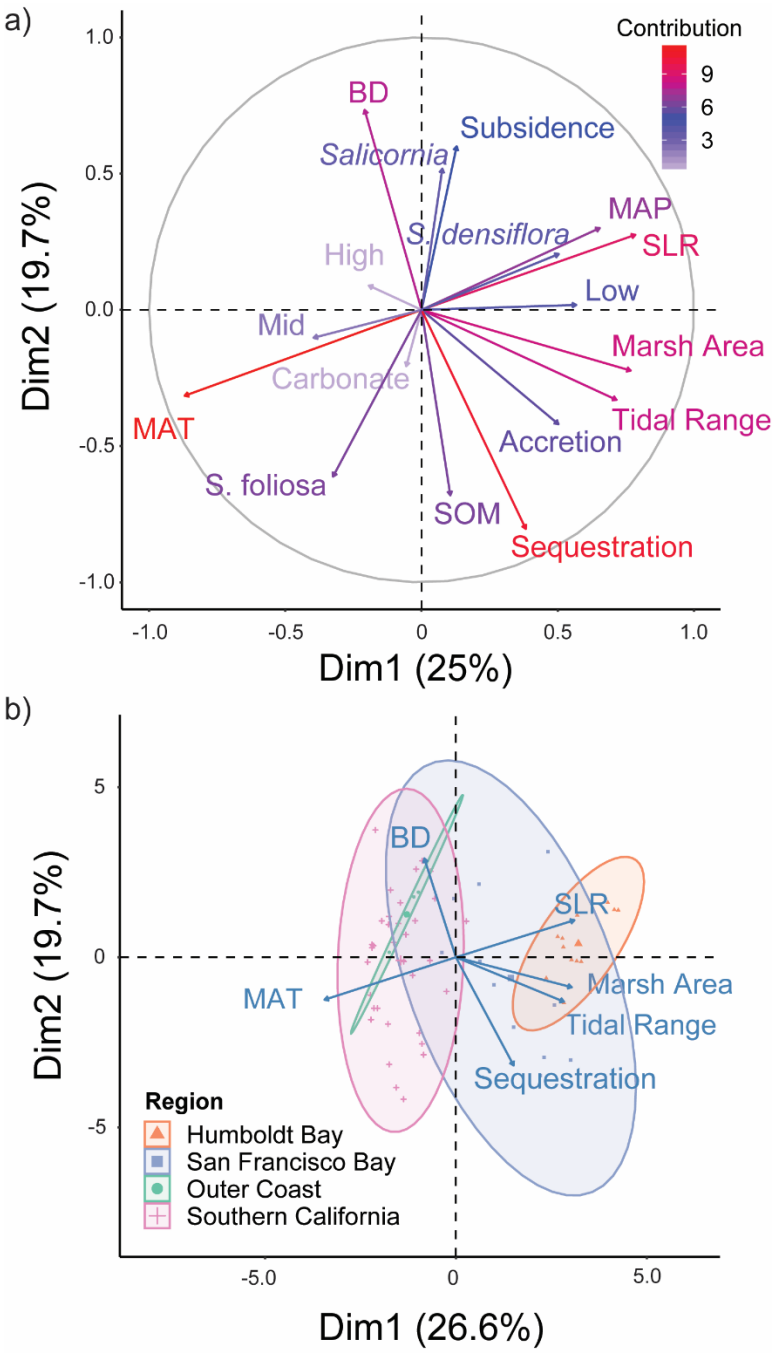


**Figure 4.6 PCA**

The results of PCA of data structure with (a) variables plotted with loadings represented by the length of arrow and contribution scaled by color, and with b) individual cores plotted in dimensional space colored by region with ellipses drawn around the 95% confidence interval for each region.

## 4.7 Tables

**Table 4.1 Comparison of Reported Carbon Storage and Sequestration Rates**

| Region | Global intertidal marshes[1] | Global salt marshes[2] | Global salt marshes[3] | NE Pacific[3] | NW Atlantic[3] | CONUS[4] | California[5] |
|---|---|---|---|---|---|---|---|
| *Area ($km^2$)* | - | 21,988 | - | - | - | 26,700 | 592.32 |
| *Carbon Density ($gCcm^{-3}$)* | - | 0.039±0.00 | - | - | - | 0.027 | 0.024±0.01 |
| *Sequestration Rate ($gCm^{-2}\ yr^{-1}$)* | - | 210±20 | 244± 6 | 179±45 | 172±18 | - | 148±2 |
| *Mean Annual Sequestration ($TgCyr^{-1}$)* | 49.2±37.8 | 42.6±4 | 10±1.1 | 0.36±0.03 | 1.3±0.3 | - | 0.09±0.00 |
| *Storage (TgC)* | - | 430† | - | - | - | 720†† | 27±0.3†† |

*[1] Hopkinson et al. (2012), [2] Chmura (2003), [3] Ouyang and Lee (2014), [4] Holmquist et al. Estimated depth of stocks are indicated as †0.5m and ††1m*

This table shows reported carbon density (g $cm^{-3}$), rates of sequestration (gC $m^{-2}$ $yr^{-1}$), total sequestration per year (Tg C $yr^{-1}$), area ($km^2$), and estimated total carbon storage (PgC) for three studies which report one or more of these parameters for global marsh area or for US coasts (Chmura 2003, Hopkinson et al. 2012, and Oyang and Lee 2014), and one study which estimates these parameters for the continental US (CONUS; Holmquist et al. 2019) compared to this study. Estimated area of intertidal marsh in California was obtained from the NWI sum of Estuarine and Marine Wetland.

**Table 4.2 Summary of Soil Characteristics by Site**

| Region | Site | Cores (n) | Accretion ($mmyr^{-1}$) | BD ($g\ cm^{-3}$) | SOC (%) | Sequestration ($gC\ cm^{-2}yr^{-1}$) |
|---|---|---|---|---|---|---|
| Humboldt Bay | *Mad River High* | 1 | 2.2 | 0.51±0.2 | 5.24±3 | 115±66 |
| | *Mad River Low* | 5 | 3.78±0.46 | 0.84±0.31 | 3.82±2.28 | 144±87 |
| | *White Slough* | 3 | 4.32±0.31 | 0.57±0.21 | 5.25±2.45 | 226±104 |
| | *Hookton Slough* | 3 | 2.6±0.49 | 0.5±0.15 | 5.57±2.33 | 146±73 |
| San Francisco Bay | *Petaluma Marsh* | 3 | 2.54±0.96 | 0.38±0.17 | 8.58±4.02 | 227±166 |
| | *Triangle Marsh* | 4 | 8.13±0 | 0.62±0.09 | 3.29±1.05 | 268±85 |
| Outer Coast | *Bolinas Lagoon* | 4 | 3.5±0 | 0.95±0.39 | 3.54±2.69 | 124±94 |
| | *Morro Bay* | 5 | 1.99±0.44 | 0.81±0.41 | 3.61±2.38 | 71±51 |
| Southern California | *Mugu Lagoon* | 4 | 3.81±0.67 | 1.38±0.37 | 2.55±2.12 | 96±84 |
| | *Seal Beach* | 12 | 3.26±0.41 | 0.53±0.3 | 6.46±3.96 | 213±141 |
| | *Upper Newport Bay* | 7 | 1.49±0.07 | 0.8±0.38 | 2.96±2.46 | 44±37 |
| | *Mission Bay* | 4 | 3.81±1.06 | 0.94±0.38 | 3.46±2.8 | 131±109 |
| | *Tijuana River* | 6 | 2.57±0.97 | 0.93±0.56 | 3.78±2.56 | 109±92 |
| **All** | | **61** | **3.31±1.65** | **0.74±0.41** | **4.5±3.27** | **148.56±121.78** |

Average accretion rates ($mm\ yr^{-1}$), bulk density (BD; $g\ cm^{-3}$), soil organic carbon (SOC; %), and sequestration ($gC\ cm^{-2}yr^{-1}$) for each site with standard deviations.

**Table 4.3 Results of PCA**

| | **Dim. 1** | **Dim. 2** | **Dim. 3** | **Dim. 4** | **Dim. 5** |
|---|---|---|---|---|---|
| **Prop. Of Variance:** | **25.0%** | **19.7%** | **12.6%** | **9.4%** | **8.5%** |
| **Total Variance:** | **25.0%** | **44.7%** | **57.4%** | **66.8%** | **75.4%** |
| MAT | **17.77** | 2.97 | 0.11 | 0.80 | 0.27 |
| SLR | 14.47 | 2.26 | 2.50 | 0.49 | 0.00 |
| Marsh Area | 13.84 | 1.48 | 5.42 | 2.84 | 1.30 |
| Tidal Frame | 12.03 | 3.25 | 0.08 | 14.05 | 3.95 |
| MAP | 10.05 | 2.69 | 0.00 | 3.24 | 2.89 |
| Low Elevation | 7.57 | 0.01 | 8.12 | 10.71 | 0.00 |
| *Spartina densiflora* | 5.96 | 1.25 | 1.21 | 1.71 | 3.82 |
| Accretion | 5.93 | 5.25 | 0.32 | 16.76 | 10.10 |
| Mid Elevation | 3.69 | 0.31 | 10.06 | 3.22 | 24.45 |
| Sequestration | 3.44 | **19.26** | 2.10 | 0.00 | 0.36 |
| *Spartina foliosa* | 2.48 | 11.15 | 16.21 | 0.00 | 0.05 |
| Bulk Density | 1.03 | 16.07 | 3.45 | 2.51 | 10.22 |
| High Elevation | 0.88 | 0.24 | 0.08 | **29.58** | **27.91** |
| Subsidence | 0.39 | 10.74 | 6.39 | 0.12 | 0.09 |
| OM | 0.26 | 13.80 | 8.08 | 12.43 | 3.81 |
| *Salicornia pacifica* | 0.14 | 8.00 | **21.55** | 0.50 | 0.58 |
| Carbonate | 0.07 | 1.27 | 14.32 | 1.04 | 10.21 |

Loadings from PCA analysis for the first five dimensions explaining a cumulative 75.4% of variance in the dataset. For each dimension, the percent value from the variable which contributes to most of the variability is indicated in bold.

**Table 4.4 Total Salt Marsh Carbon Storage and Sequestration for California**

| Region | Site | Marsh Area in Watershed ($km^2$) | Sequestration in watershed (Mg C $yr^{-1}$) | Storage in first meter of Watershed (Tg C) |
|---|---|---|---|---|
| Humboldt Bay | *Mad River High*<br>*Mad River Low*<br>*White Slough*<br>*Hookton Slough* | 68 | 10,725 ± 5610 | 3.38 ± 1.79 |
| San Francisco Bay | *Petaluma Marsh* | 137 | 31,074 ± 22,742 | 12.23 ± 8.95 |
| | *Triangle Marsh* | 117 | 31,310 ± 9,945 | 3.85 ± 1.22 |
| Outer Coast | *Bolinas Lagoon* | 27 | 3,344 ± 2,538 | 0.96 ± 0.73 |
| | *Morro Bay* | 22 | 1,705 ± 1,188 | 0.79 ± 0.55 |
| Southern California | *Mugu Lagoon* | 13 | 1,074 ± 988 | 0.34 ± 0.31 |
| | *Seal Beach* | 5 | 1,067 ± 705 | 0.33 ± 0.22 |
| | *Upper Newport Bay* | 3 | 133 ± 111 | 0.09 ± 0.07 |
| | *Mission Bay* | 14 | 1,837 ± 1526 | 0.48 ± 0.4 |
| | *Tijuana River* | 3 | 327 ± 276 | 0.13 ± 0.11 |
| **State-Wide Salt Marshes** | | **592.32** | **87,993 ± 959** | **27 ± 0.3** |

This table shows the total sequestration (Mg C $yr^{-1}$) and storage (Tg C) to 1m depth for each watershed in which a salt marsh site was studied. Salt marsh area for each watershed was calculated as the sum of Estuarine and Marine Wetland within NWI HUC8 watersheds. For all marshes in Humboldt Bay within the same watershed average carbon content across sites was used to calculate total sequestration and storage for the Humboldt watershed. A total sum of Estuarine and Marine Wetland from NWI was used to estimate total marsh area in the state. The average carbon content from all sites in this study was used to calculate state-wide estimates of sequestration and storage.

**Table 4.5 Ecosystem Service Value of Carbon Sequestration and Storage**

| | | Millions of Dollars By Watershed | |
|---|---|---|---|
| | | **Annual Sequestration** | **Storage** |
| **Humboldt Bay** | *Mad River High*<br>*Mad River Low*<br>*White Slough*<br>*Hookton Slough* | 0.28 - 0.91 | 88 - 287 |
| **San Francisco Bay** | *Petaluma Marsh* | 0.46 - 2.99 | 182 - 1,177 |
| | *Triangle Marsh* | 1.19 - 2.29 | 146 - 282 |
| **Outer Coast** | *Bolinas Lagoon* | 0.04 - 0.33 | 13 - 94 |
| | *Morro Bay* | 0.03 - 0.16 | 13 - 74 |
| **Southern California** | *Mugu Lagoon* | 0 - 0.11 | 2 - 36 |
| | *Seal Beach* | 0.02 - 0.1 | 6 - 31 |
| | *Upper Newport Bay* | 0 - 0.01 | 1 - 9 |
| | *Mission Bay* | 0.02 - 0.19 | 4 - 49 |
| | *Tijuana River* | 0 - 0.03 | 1 - 13 |
| **All California** | | **4.84 - 4.94** | **1,460 - 1,492** |

Estimated dollar value in millions of dollars of carbon sequestration and storage by watershed of studied sites as well as average state-wide carbon sequestration and storage estimates. Range estimates come from standard deviation of carbon content or sequestration rates from measured cores.

## 4.8 Appendix

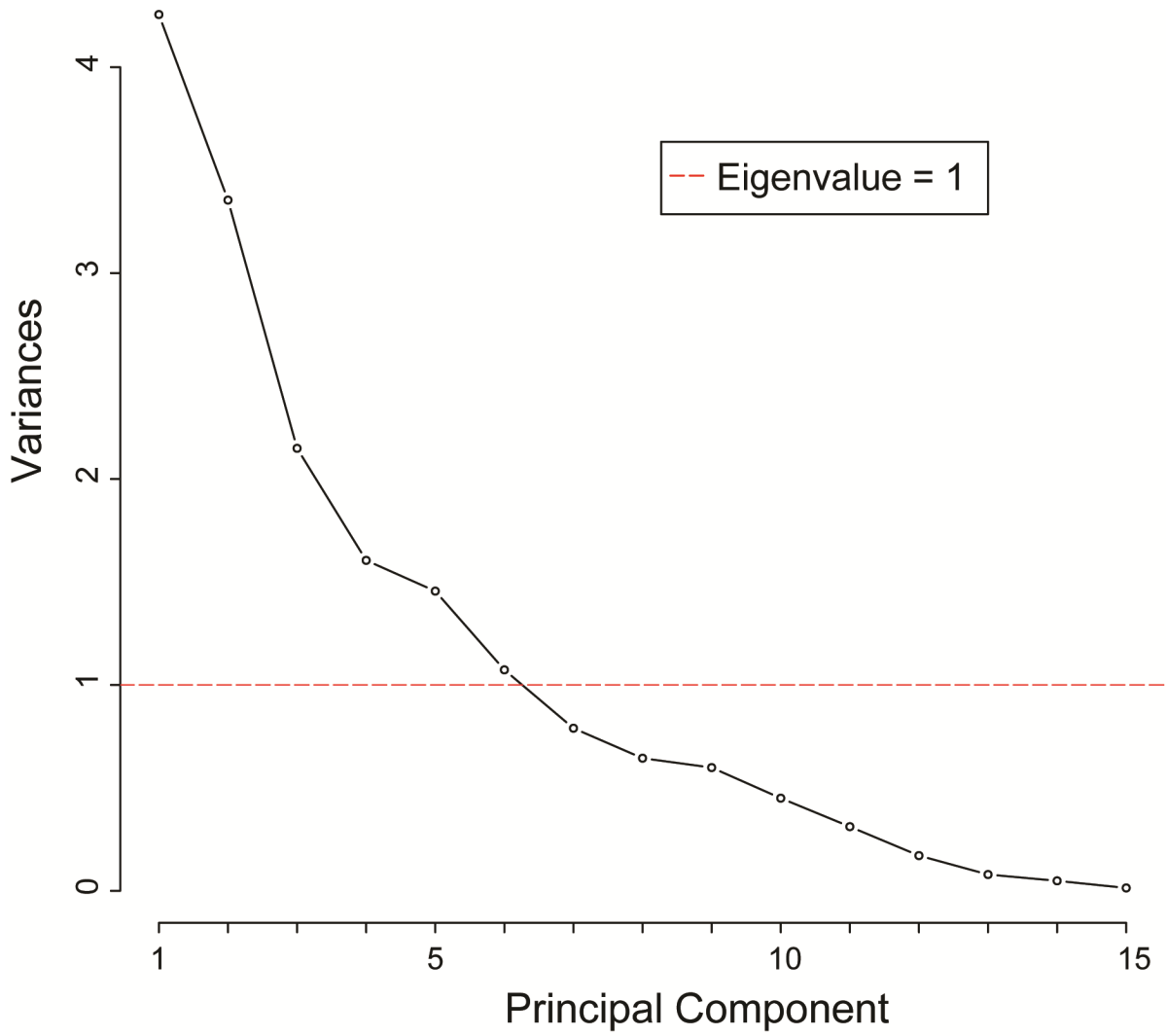


**Appendix Figure 4.1 Screeplot**

Screeplot of principal components with eigenvalue to indicate the number of factors which describe the majority of variance in the dataset.

**Appendix Table 4.1 Sediment Accretion Rates Used to Calculate Sequestration**

| Region | Site | Core | Accretion Rate (mm $yr^{-1}$) | Core or Site Average |
|---|---|---|---|---|
| Humboldt Bay | *Mad River High* | MRH14-01 | 2.2 | Site |
| | *Mad River Low* | MRL13-01 | 3.8 | Site |
| | | MRL14-04 | 3.8 | Site |
| | | MRL14-10 | 3.1 | Core |
| | | MRL16-12 | 4.5 | Core |
| | | MRL16-13 | 3.8 | Site |
| | *White Slough* | WTS16-01 | 2.0 | Core |
| | | WTS16-02 | 2.6 | Site |
| | | WTS17-03 | 3.2 | Core |
| | *Hookton Slough* | HKS16-01 | 4.7 | Core |
| | | HKS16-02 | 4.3 | Site |
| | | HKS17-03 | 4.0 | Core |
| San Francisco Bay | *Petaluma Marsh* | PTL15-01 | 1.3 | Core |
| | | PTL15-02 | 2.8 | Core |
| | | PTL16-03 | 3.6 | Core |
| | *Triangle Marsh* | TRM16-01 | 8.1 | Site |
| | | TRM16-02 | 8.1 | Site |
| | | TRM16-03 | 8.1 | Site |
| | | TRM16-04 | 8.1 | Site |
| Outer Coast | *Bolinas Lagoon* | BOL13-01 | 3.5 | Site |
| | | BOL13-02 | 3.5 | Site |
| | | BOL13-03 | 3.5 | Site |
| | | BOL13-04 | 3.5 | Site |
| | *Morro Bay* | MOB13-01 | 2.7 | Core |
| | | MOB13-02 | 1.9 | Site |
| | | MOB13-04 | 1.9 | Site |
| | | MOB13-08 | 1.9 | Site |

This table shows the sediment accretion rates used to calculate sequestration for each sediment core and indicates if each rate is measured for the individual core or if a site average accretion rates was used. Table continues on the next page.

**Appendix Table 4.1 (cont'd)**

| Region | Site | Core | Accretion Rate (mm $yr^{-1}$) | Core or Site Average |
|---|---|---|---|---|
| Southern California | *Mugu Lagoon* | MOB13-10 | 1.4 | Core |
| | | MGL13-01 | 3.3 | Site |
| | | MGL13-05 | 4.7 | Core |
| | | MGL13-06 | 3.3 | Site |
| | | MGL13-08 | 3.3 | Site |
| | *Seal Beach* | SB14-01 | 3.4 | Site |
| | | SB14-02 | 3.4 | Site |
| | | SB14-04 | 3.4 | Site |
| | | SB14-05 | 3.4 | Site |
| | | SB15-06 | 3.4 | Core |
| | | SB15-08 | 3.4 | Site |
| | | SB15-09 | 3.2 | Core |
| | | SB15-11 | 2.5 | Core |
| | | SB15-14 | 4.0 | Core |
| | | SB15-16 | 3.3 | Core |
| | | SB15-20 | 3.5 | Core |
| | | SB15-21 | 2.5 | Core |
| | *Upper Newport Bay* | UNB13-01 | 1.5 | Site |
| | | UNB13-02 | 1.5 | Site |
| | | UNB13-03 | 1.5 | Core |
| | | UNB13-04 | 1.7 | Core |
| | | UNB14-05 | 1.5 | Site |
| | | UNB14-07 | 1.5 | Site |
| | | UNB14-08 | 1.5 | Site |
| | *Mission Bay* | MB16-01 | 3.2 | Site |
| | | MB16-02 | 3.2 | Site |
| | | MB16-03 | 3.2 | Site |
| | | MB17-05 | 5.7 | Core |
| | *Tijuana River Estuary* | TJE12-01 | 2.6 | Site |
| | | TJE12-02 | 2.6 | Site |
| | | TJE12-03 | 2.3 | Core |
| | | TJE12-06 | 1.1 | Core |
| | | TJE12-07 | 2.6 | Site |
| | | TJE12-08 | 4.4 | Core |

# 5. Multiple Stressors Influence Salt Marsh Recovery after a Spring Fire at Mugu Lagoon, CA

## 5.1 Abstract

This paper presents the first record of fire in Pacific coast salt marshes; the 1993 Green Meadows Fire and the 2013 Camarillo Springs Fire burned an area of *Salicornia*-dominated salt marsh at Point Mugu, CA. These fires inspire concern about resiliency of ecosystems not adapted to fire, already threatened by sea-level rise (SLR), and under stress from extreme drought. We monitored vegetation percent cover, diversity, and soil organic carbon (SOC) in burned and unburned areas of the salt marsh following the 2013 Camarillo Springs Fire and used remotely sensed Normalized Vegetation Difference Index (NDVI) analysis to verify the *in situ* data. Two years following the fire, vegetation percent cover in burned areas was significantly lower than in unburned areas, with dominant-species change in recovered areas, and NDVI was lower than pre-fire conditions. Multi-year disturbance, such as fire, presents challenges for salt marsh resilience and dependent species, especially in sites facing multiple stressors. With anticipated higher temperatures, increased aridity, extreme drought, and higher frequency fires becoming a reality for much of the Pacific coast, this study indicates that fire in *Salicornia*-dominated marshes is a vulnerability that will need to be addressed differently from other grass- or reed-dominated marsh systems.

## 5.2 Introduction

In the past 200 years population growth and urbanization caused the destruction or conversion of an estimated 75% of the salt marsh habitat in California (Stein et al., 2014). According to recent ecosystem vulnerability models that use projected rates of sea-level rise (SLR) from the IPCC RCP 8.5 scenarios (Stocker et al., 2013) up to 99% of vegetated salt marsh habitat may be converted to tidal flats by 2100 (Doughty, Cavanaugh, Ambrose, & Stein, 2019; Thorne et al., 2018). These estimates do not include recent uncertainty surrounding continental ice sheet stability that could add an additional meter or more to sea-level rise projections in worst-case scenarios (Griggs et al., 2017) and result more rapid loss of salt marsh habitat; nor do they take into account some of the more dynamic, storm-, flooding-, and erosion- driven changes which will likely occur under anthropogenic climate change conditions (Barnard et al., 2019). Landward migration is the natural salt marsh response to increases in SLR, but many natural and human barriers may inhibit migration along the California coast (Kirwan et al., 2016; Pethick, 2001). The remaining salt marsh habitat which supports endangered species, such as the Belding's savannah sparrow (*Passerculus sandwichensis beldingi*), and provides a wealth of ecosystem services (Barbier et al., 2011; Chmura et al., 2003; Costanza et al., 1997; Powell, 1993), is therefore even more vulnerable to natural and human-caused stressors, which could further increase the rate of habitat loss.

Fire has not been documented as a natural stressor for Pacific coast salt marshes dominated by *Salicornia pacifica* (pickleweed). Although fire is relatively common in reed- or grass-dominated salt marshes (Nyman & Chabreck, 1995; Salvia, Ceballos, Grings, Karszenbaum, & Kandus, 2012), to date we found no peer-reviewed literature regarding incidents of fire in US Pacific coast or *S. pacifica*-dominated salt marshes. Salt marshes in the

California Mediterranean-type climate experience a fall-winter dormant season when above ground biomass is either dead or desiccated (Mahall & Park, 1976), conditions which would favor fire. Given California's winter rain regime, fires have historically been less frequent or intense in the late fall and winter, but rising temperatures and prolonged drought are producing a lengthened fire season in regions such as Southern California (Yoon et al., 2015). This longer fire season is further exacerbated by higher temperatures, drought, and increased population leading to greater fire risk for many areas (Westerling, Hidalgo, Cayan, & Swetnam, 2006). Such changes in fire regimes could mean that the risk of fire for *S. pacifica*-dominated salt marshes, too, is increasing.

The best comparison of fire in similar habitats are the marshes of the southeastern US. These marshes are often dominated by *Spartina spp.* (cordgrass) or *Schoenoplectus spp.* (bulrush) and have a well-established, seasonal fire regimes. Fire occurs naturally from lightening (Loveless, 1959), spontaneous combustion (Viosca, 1932), and as a management practice used by humans for several hundred years (Bickford, Needelman, Weil, & Baldwin, 2012; Kern & Shriver, 2014; Komarek, 1975; Lynch, 1941; O'Neil, 1949; Smith, 1942; Stewart, 1963; Uhler, 1944). Habitat managers use controlled burns to reduce wildfire as well as employ low-intensity burns to increase productivity and promote species diversity of both flora and fauna in Louisiana saline and brackish marshes (Gabrey & Afton, 2000), Chesapeake Bay brackish marshes (Kern & Shriver, 2014), and saline marshes on the coast of Argentina (Isacch, Holz, Ricci, & Martínez, 2004). Studies show that a one to five year return interval on controlled burning will continue to stimulate high productivity without negative ecosystem impacts in both freshwater systems dominated by *Spartina spp.* (Johnson & Knapp, 1993) and brackish systems with a mix of *Spartina spp.*, *Schoenoplectus spp.*, and *Distichlis spp*. (Flores, Bounds, & Ruby,

2011). For *Schoenoplectus spp.* and *Spartina spp.* marshes, biomass removal has been shown to be the most likely driver of increases in productivity (Bickford et al., 2012). Brackish salt marshes in Chesapeake Bay were even observed to have attained 100% vegetation recovery within a year of fire (Nyman & Chabreck, 1995).

The long-term effects of fire on soil or ecosystem function are not as well documented, even for salt marshes with a fire regime. Fire's effects on soil depends highly upon the intensity of the burn, the fate of ash, and the hydrology of the salt marsh immediately following the fire (Lynch, 1941; Nyman & Chabreck, 1995). For example, more intense burns that completely remove vegetation cover and damage or expose soils to direct solar radiation cause low soil moisture and further slow nutrient recovery of the soil (Salvia et al., 2012). Studies of soil dynamics show more severe and longer-lasting effects on soil organic matter (SOM) occur with greater burn intensity (Salvia et al., 2012), while soil dynamics after lower-intensity fires show an initial decrease in SOM followed by increased levels for nine months as vegetation recovers (Schmalzer & Hinkle, 1992). For this reason, occasional or managed burns have been used to stimulate growth and prevent more severe burning which might affect ecosystem services in the long term. But relatively few studies have documented how fire impacts ecosystem function or salt marsh resiliency over such time periods.

At the end of the peak spring growth period in May 2013 the Camarillo Springs Fire, which started from roadside ignition, burned approximately 24,000 acres of chaparral vegetation and a section of the high-elevation, infrequently-inundated salt marsh at Naval Base Ventura County Point Mugu ("Springs Fire Incident Information," 2013). The 2013 Camarillo Springs Fire occurred during a period of unusually extreme drought in California which started in 2012 (Griffin & Anchukaitis, 2014); a drought severe enough to have caused changes to the

geomorphologic function of nearby streams following the fire event (Florsheim, Chin, Kinoshita, & Nourbakhshbeidokhti, 2017). This pattern of burning is similar to that of the Green Meadows Fire that occurred in October 1993 and burned the same area of salt marsh at Point Mugu (Figure 5.1), although the Green Meadows Fire did not occur during a drought nor outside of the historic fire season. These events present evidence for a recurring pattern of burning in a *S. pacifica*-dominated salt marsh and indicate a need for better understanding of fire dynamics in Pacific coast salt marsh habitats, specifically in terms of vegetation recovery period and soil dynamics.

With so little information on the effects of fire in Pacific coast salt marsh ecosystems, we find the disturbance from the 2013 Camarillo Springs Fire provides an important case study and possible early warning of a new vulnerability for salt marshes facing multiple stressors along the Pacific coast. This paper combines field survey and remote sensing to assess the impact of the disturbance and track the recovery of salt marsh vegetation at Point Mugu after the 2013 Camarillo Springs Fire. Using a control-impact design, we evaluate percent cover *in situ* to assess vegetation recovery, species composition and diversity, and soil organic carbon (SOC). We assessed vegetation recovery remotely using Normalized Difference Vegetation Index (NDVI), which is positively correlated with estimates of percent cover (Purevdorj, Tateishi, Ishiyama, & Honda, 1998) and has been used to estimate vegetation recovery following fire (Díaz-Delgado, Lloret, & Pons, 2003). This study contributes to the understanding of salt marsh recovery from small-scale disturbance under drought-stressed conditions to identify future vulnerabilities for salt marsh ecosystems facing multiple stressors.

## 5.3 Methods

### *5.3.1 Study Site*

The vegetated salt marsh at the Naval Base Ventura County Point Mugu is located at 34.116 N, 119.116 W and covers approximately 1.09 $km^2$ (Onuf, 1987; Thorne et al., 2016). Calleagus Creek, channelized since the early 20th century, empties into the central basin of the salt marsh. Further human impacts on the salt marsh include the intensive agriculture of the surrounding region starting in the $20^{th}$ century (Onuf, 1987). The salt marsh is dominated by *S. pacifica*, and a host of other common Pacific coast salt marsh species such as *Distichlis spicata* (saltgrass), *Frankenia grandifolia* (alkali heath), *Jaumea carnosa* (fleshy jaumea), *Limonium californicum* (sea lavender), *Suaeda californica* (seablite), *Batis maritima* (saltwort), and *Distichlis littoralis* (shore grass). The ecotone between salt marsh and chaparral vegetation at Mugu Lagoon is commonly colonized by upland species such as *Baccharis pilularis* ssp. *consanguinea* (coyote brush) as well as exotic weeds such as *Brassica rapa* (mustard), *Ricinus communis* (castor bean), *Arundo donax* (giant reed), and *Polypogon monspeliensis* (rabbitsfoot grass).

Mugu Lagoon has a Mediterranean-type climate with mild temperatures and precipitation occurring during the winter and spring months. Temperature and precipitation normals as recorded by the NOAA station at Camarillo are 15.8°C with 38.7 cm rainfall (https://www.ncdc.noaa.gov/cdo-web/). The 1993 Green Meadows Fire occurred in a year where mean annual temperature was lower than station normals (14.4° C) and 94.5 cm rainfall was recorded, but particularly strong Santa Ana winds in October contributed to fire conditions (M. Reed & Alvarez, 1993). The Palmer Drought Severity Index (PDSI) for Ventura County during

1993 indicates that there was no drought for the 1992 – 1993 period. During this paper's remote sensing study period of March 2010 to May 2015, temperatures averaged 20.5°C and rainfall averaged 16.2 cm per year, an increase in temperature and reduction in annual precipitation from station normals. PDSI data from a 4X4 $km^2$ region centered at 34.108 N, 119.083 W show that there have been three periods of increasingly severe drought occurring since 2005 (Abatzoglou et al., 2017; Palmer, 1965; Appendix Figure 5.1). The drought in which the Camarillo Springs Fire occurred started in early 2012 and reached extreme status a month preceding the fire in April 2013. Extreme drought conditions continued throughout most of the study period, with only a brief interlude of severe-drought status during the rains in winter 2014.

### *5.3.2 Site Selection and Description*

Much of the area burned by the 2013 Camarillo Springs Fire inside the Mugu Lagoon reserve had been vegetated by upland transition species, such as *B. pilularis*, or covered by salt pans (some of which are outlined on the map in Figure 5.2). Although no published literature or grey literature exists pertaining to vegetation recovery following the 1993 Green Meadows Fire, this mix of upland, high marsh, and salt pan habitat in the Green Meadows burn area may be a remnant of recovery following that event. The site established in 2013 is located in the central basin of the Mugu Lagoon salt marsh, an area that had been dominated by *S. pacifica* before the Camarillo Springs Fire. Study transects occupy an area of burned salt marsh adjacent to unburned *S. pacifica*-dominated salt marsh. The study site is tidally-influenced habitat intersected by small tidal channels and suited for salt marsh species. However, the proximity of the salt pan northwest of transects (seen in Figure 5.2) indicates the study site sits at the upper limits of tidal reach. High resolution Digital Elevation Models (DEMs) produced by the United States Geologic Survey (Takekawa, Thorne, & California Landscape Conservation Cooperative,

2015) indicate that fire burned areas of marsh 1.72 to 2.53 m in elevation with plots occupying an area 1.7 – 1.8 m in elevation.

Establishment of the sampling plots and collection of data in the first survey took place on June 11, 2013, five weeks after the salt marsh burned. Seven 27 m-long transects (A – G) were established roughly perpendicular to the boundary between burned and unburned salt marsh. Transects were laid out on a grid with six meters between each. Because of a channel which bisects the plots, the two final transects (F and G) were located about 10 m east of transect E and slightly rotated to remain perpendicular to the burn edge. Along each transect four quadrats (0.25 $m^2$) were distributed evenly, totaling 28 study plots. Of those 28 plots, one quadrat located approximately one meter into unburned salt marsh vegetation marked the start of each transect, for a total of seven quadrats plots placed in unburned salt marsh area. Unburned plots were placed within green, undamaged vegetation with a small buffer of healthy vegetation at the edge of the burn zone to prevent edge effects. The remaining 21 plots were placed at equal intervals into the burned area, three per transect (Figure 5.2). All quadrats were marked with PVC piping for repeated sampling.

### *5.3.3 Percent Cover*

Nine times over the course of the two-year study period quadrats were photographed (Appendix Figure 5.2) and total vegetation percent cover and percent cover by species were estimated. Percent cover estimates were made consistently by the same researcher. Percent cover estimates totaled to 100% and did not separate canopy layers. Vegetation that was dormant was counted towards percent cover estimates, but vegetation that was browned or dead was not included in totals. For the initial surveys, the number of plant recruits, defined as sprouts from

seed, in each quadrat was counted. Recruits were counted only if the base of plant was within the quadrat. If multiple shoots were clearly associated with a single plant, only one recruit was recorded. *Salicornia pacifica* shoots were frequently the result of sprouting from remaining adult plant roots, making the enumeration of individuals difficult, and those sprouts were not included in the recruit count. *Salicornia pacifica* plants were counted only if they were separated by more than one centimeter, all *S. pacifica* shoots within one centimeter of each other were counted as a single individual. After the initial recruitment period in the fall of 2013, only percent cover estimates were made.

Percent cover estimates were first used to estimate recovery by comparing unburned and burned plots with a spline fit (unburned n=7, burned n=21; standard error; Figure 5.3a). Then percent cover in burned plots was separated by distance to test the effect of distance from unburned vegetation on recovery. A spline fit for each unburned salt marsh distance category, near (9 m distant), mid (18 m distant), and far (27 m distant), was used (n=7, standard error; Figure 5.3b).

### *5.3.4 Species Composition, Diversity, and Evenness*

Percent cover data by species was averaged for unburned and burned plots at each sampling period (Figure 5.3c and d). The Simpson's index of diversity (ID), an index which is not as sensitive to species richness as the Shannon diversity index (Nagendra, 2002), was used to compare species composition between plots and timepoints. Average Simpson's ID for unburned and burned plots was plotted by time and a simple linear regression was used to interpret species diversity change over time (Figure 5.4).

Nonmetric Multidimensional Scaling (NMDS) compared species composition between burned and unburned sites throughout the study period using the R package, Vegan (Oksanen, 2015; RC Team, 2013). Percent abundance of each species was transformed by taking the square root to reduce the influence of the most and least abundant groups. A distance matrix between sites was calculated using the Sorenson (Bray-Curtis) dissimilarity index. Sites were plotted in two-dimensional space with stress less than 0.15. A 95% confidence interval ellipse was drawn around burned and unburned sites and species variables were factor fitted to the NMDS major axes to examine structure of the data. Within burned and unburned sites, plots were connected in temporal order to elucidate any trends over time (Figure 5.5).

### *5.3.5 Soil Organic Carbon*

During the six vegetation surveys from June 2013 – April 2014, soil sampling for lab analysis took place. Three transects were analyzed for SOC, selected starting from A and measuring every other transect (A, C, and E). A 3 – 5 cm depth soil sample was extracted adjacent to the plot for a total of nine burned-area samples and three unburned-area samples. SOM was analyzed using loss on ignition (LOI). One cubic centimeter of sediment was dried, weighed, and burned in a furnace at 550°C for four hours (Heiri, Lotter, and Lemcke, 2001). Percent SOM was converted to an estimate of percent carbon using Eq. 1 taken from Craft et al. (1991) who described the relationship between organic matter determined from LOI and organic carbon measured by elemental analysis.

#### 5.3.5.1 Equation 1

$$\text{Organic C} = (0.40 \pm 0.01)\text{LOI} + (0.0025 \pm 0.003)\text{LOI}^2$$

Average organic carbon for unburned and burned plots was plotted with a standard error in Figure 5.6.

### *5.3.6 Remote Sensing*

A coastal salt marsh shapefile was obtained from the Pacific Institute, created as a filtered subset of wetlands below or within 100 m of mean higher high water (http://www.pacinst.org/reports/sea_level_rise), and was used to create shapefiles for Mugu Lagoon. Fire shapefiles for the 2013 Camarillo Springs Fire and the 1993 Green Meadows Fire were extracted from the CalFire Fire Perimeters Version 14_2 (http://frap.cdf.ca.gov/data/frapgisdata-sw-fireperimeters_download). The shapefile for Mugu was clipped using the shapefile of the 2013 Camarillo Springs Fire to create a burned area shapefile for analysis. This burned area shapefile (red shading on Figure 5.1) was used to do the following analysis.

NASA MODIS 16-day composite imagery (250 m spatial resolution MOD13Q1 tiles h08v04, h08v05, h09v04) were downloaded from NASA/USGS (https://lpdaac.usgs.gov/dataset_discovery/modis/modis_products_table/mod13q1) for March 2010 – April 2015 of Point Mugu and its surroundings. NDVI was calculated using a ratio of measured albedo (α) using MODIS spectral reflectance data:

#### 5.3.6.1 Equation 2

$$NDVI = \frac{\alpha_{0.86\mu m} - \alpha_{0.65\mu m}}{\alpha_{0.86\mu m} + \alpha_{0.65\mu m}}$$

Time series for NDVI was plotted using mean NDVI. Data were smoothed using a Savitzky-Golay filtering algorithm which uses a local polynomial least squares fit along a

moving window to smooth noisy data. This method of analysis for NDVI data was introduce by Chen et al. (2004) and has been shown to be effective in reducing noise introduced by cloud cover and atmospheric variability in MODIS time series. Because NDVI can respond to short-term temperature or precipitation events, regional temperature, precipitation, PDSI, and burned-area NDVI are compared in Figure 5.7. Contemporaneous temperature and precipitation data were obtained from the NOAA Climate Data Online website, station USW00023136 (https://www.ncdc.noaa.gov/cdo-web/). PDSI data were taken from a 4X4 $km^2$ region centered on 34.108N, 119.083W; data are a monthly self-calibrated timescale downloaded from the West Wide Drought Tracker webpage (Abatzoglou et al., 2017).

## 5.4 Results

### *5.4.1 Initial Sampling Period*

During initial sampling, one month following the 2013 Camarillo Springs Fire, unburned plots were estimated to have 100% cover, with a mix of *D. spicata*, *F. grandifolia*, and *S. pacifica;* in contrast, average estimated percent cover for plots located in burned areas was less than 1%, with seven of 21 plots devoid of vegetation. *Distichlis spicata* was the most prevalent species in the burned plots, having an average of 6.4 shoots per plot (range: 0 – 24; present in 12 of 21 plots) compared to an average of 0.3 shoots for *F. grandifolia* (range: 0 – 4; present in three of 21 plots) and average 0.4 shoots for *S. pacifica* (range: 0 – 4; present in three of 21 plots; Appendix Table 5.1).

SOC measured from soil samples taken adjacent to vegetation plots during the initial sampling showed SOC of 9.02 ± 2.84% in unburned plots and 7.83 ± 1.14% in burned plots (all

reported errors are standard errors). At the initial sampling, no significant difference between SOC was found between burned and unburned sites (Kruskal-Wallis test, $p = 1$).

### *5.4.2 Percent Cover*

Vegetation showed strong but incomplete recovery of percent cover within two years following the fire (Figure 5.3), with the most recovery taking place in the second year of the monitoring period (see Figure 5.3a). Average percent cover in unburned plots was 100 ± 0.5% for the duration of the study, with the exception of September 2014, when average percent cover in control plots was 95 ± 2%. One year after the fire, average percent cover in burned plots only reached 34 ± 4%. Vegetation experienced a large growth period the summer of 2014, and average percent cover of burned plots by September 2014 was 70 ± 6%, with three out of 21 plots observed at 100% cover. While winter rains from 2014-15 created a small reprieve from extreme to severe drought status (reflected in increased PDSI ; Appendix Figure 5.1), the last survey during May 2015 showed a similar average percent cover to the previous survey of 71 ± 5% and only one of 21 plots had retained 100% cover (Appendix Table 5.2). All sampling periods were significantly different in percent cover between burned and unburned sites (Kruskal-Wallis test, $p < 0.004$).

### *5.4.3 Spatial Recovery Pattern*

There was evidence of spatial patterning in vegetation recovery (Figure 5.3b). By March 2014, quadrats closest to the margin of unburned salt marsh habitat (approx. 9 m) had reached an average of 56 ± 8% cover compared to less than 25% cover in quadrats mid and far from unburned habitat (18 m and 27 m). The trend for higher recovery in the quadrats near to unburned salt marsh was maintained throughout the two-year monitoring period, with the final

monitoring period in May 2015 showing the closest quadrats having attained 88 ± 3% cover compared to 58 ± 13% and 68 ± 8% cover for the mid and the far plots respectively. There were significant differences in percent cover between all burned plots by distances from unburned salt marsh for January and August of 2013 and March and April of 2014 (Kruskal-Wallis test, $p = 0.07$, $p = 0.09$, $p=0.006$, $p = 0.017$, respectively). Significantly higher percent cover was observed in plots 9 m to salt marsh edge compared to only sites 27 m from unburned salt marsh during six of the nine sampling periods (Kruskal-Wallis test, June, August, and October 2013, March and April 2014, and May 2015).

### *5.4.4 Species Composition, Diversity, and Evenness*

For the majority of the study period the dominant species in all unburned quadrats was *S. pacifica* with an average cover of 67 ± 3% (Figure 5.3c). *Frankenia grandifolia* was the second most common species in unburned quadrats at 27 ± 3% cover. *Distichlis spicata* averaged 6 ± 2% cover during the study period, but generally did not represent more than 5% cover in unburned plots except for a sudden increase in September 2013 to 37 ± 17% cover followed by a drastic decrease to 1 ± 0% cover in the next month.

In burned quadrats *D. spicata* was the most prevalent colonizer and remained dominant in the burned area until the end of the study period where it represented on average 43 ± 8% of plots (Figure 5.3d). As in the unburned plots, *F. grandifolia* was the second most dominant species in burned plots. *Salicornia pacifica* recolonization of the burned area occurred quite slowly and remained low, compared dominance of *S. pacifica* in unburned plots. In spring 2015 *S. pacifica* reached a maximum of 32 ± 8% cover in burned plots, half of the estimated average percent cover in unburned areas.

Only three species were observed within the study plots, which is not unusual for Pacific coast salt marshes that typically show distinct vegetation zonation based on abiotic conditions and inter-specific competition (Pennings & Callaway, 1992). The Simpson's ID for the unburned plots therefore shows quite large fluctuations over the study period, likely due to the low species richness and seasonal changes in vegetation composition (Figure 5.4). However, a linear model of the change in Simpson's ID over time shows no overall trend ($R^2 = 0.01$; $p = 0.77$). In contrast, there is a positive linear trend in the species diversity over time in the burned plots ($R^2 = 0.68$; $p = 0.006$). The increase is not, however, due to an increase in the number of species present but rather the evenness of distribution, as seen in the percent distribution shown in Figure 5.3d.

NMDS shows that species composition is significantly different between burned and unburned sites throughout the entire monitoring period (95% confidence interval; Figure 5.5). NMDS axis 1 is positively correlated with *D. spicata* and negatively correlated with *S. pacifica*, and NMDS axis 2 is positively correlated with *F. grandifolia* (Table 5.1). The temporal trend in unburned plots is circular and shows very little change over the monitoring period, aside from the September 2013 increase in *D. spicata* noted previously. For much of the monitoring period the general trend in burned sites is positive along NMDS axis 2, indicating increased F. grandifolia in burned sites. In September 2014 and May 2015, points move negatively along NMDS axis 1, as *S. pacifica* begins to increase in relative abundance compared to D. spicata for burned plots.

### *5.4.5 Soil Organic Carbon*

Following the initial sampling period with slightly higher, but not significant, SOC levels in unburned plots, SOC showed no significant difference between burned and unburned plots throughout the study (Figure 5.6). Comparing average SOC between plots that had greater than 10%, greater than 20%, and greater than 30% cover to those that had less cover similarly showed no significant difference between means. Comparison between plots with higher cover than 30% was not possible as only one plot with greater than 40% cover was sampled for soil carbon. Average monthly values of SOC in all sites varied from 4.5 ± 0.4% to 9.0 ± 2.8% but had little temporal variability (Appendix Table 5.3).

### *5.4.6 Remote Sensing*

Remote sensing results echo the *in situ* observations, with a sustained period of suppressed NDVI values following the fire in 2013 and a slight recovery toward the beginning of 2015 (Figure 5.7). This period of low NDVI is distinct from any period before the fire, March 2010 to April 2013, where NDVI variability responds to positively to precipitation and negatively to temperature. NDVI values are depressed in spring of 2012 and 2013 compared to spring 2010 and 2011 as PDSI decreases and the region begins to experience moderate to severe drought. NDVI values are decreasing in April before the 2013 fire occurs, while temperature is high and precipitation is low. This drop coincides with the beginning of the extreme drought. Such a drop in NDVI indicates that pre-fire vegetation was unseasonably brown. After the fire in May 2013, NDVI values are not immediately at their lowest point but continue to decline until reaching their lowest point in July-August 2013. NDVI remains lower than any other dry season in this record until a precipitation event in winter of 2014, when increased mean NDVI likely

reflects the increase in percent cover seen during *in situ* surveys, and NDVI values more closely resemble values seen before the Camarillo Springs Fire.

## 5.5 Discussion

Vegetation monitoring following the 2013 Camarillo Springs Fire at Point Mugu shows fire produces a multi-year disturbance in a Pacific Coast salt marsh. Even two years after the fire occurred, percent cover and species composition of the burned area at Point Mugu show variation from unburned salt marsh conditions (Figure 5.8). We show that recovery is a multi-year process resulting in a shift in species evenness with a fine-scale geographic patterning favoring sites closest to unburned vegetation. The length of the recovery, comprising perhaps two to three breeding seasons, is particularly concerning in terms of impacts on endangered species, such as the Belding's savannah sparrow, with obligate salt marsh habitat requirements (Powell, 1993). The 20-year recurrence interval between the Green Meadows Fire and the Camarillo Springs Fire indicate that, while fire may not be a documented disturbance in *Salicornia spp.*-dominated salt marshes, *Salicornia* marshes are at risk from disturbance by fire, especially in climate change conditions.

The gradual vegetation recovery in this study appears to be different from the rapid recovery of grass- and reed-dominant marshes to near pre-fire conditions within one year. While more intensive soil or peat burns have been shown to result in damage to SOC stock or increased SOM from increased productivity following biomass removal, we do not find any evidence to show that the Camarillo Springs Fire altered SOC content of burned and unburned soil, indicating a need for further research to understand post-fire wetland soil conditions. This study finds that fire in Pacific coast salt marshes could have long-term effects on ecosystem resiliency

in terms of vegetation recovery time which can impact ecosystem functionality and dependent species. Therefore a more intensive management response following disturbance by fire, especially in the case of ecosystems facing multiple stressors, may be required for Pacific coast salt marshes compared to their East coast counterparts.

### *5.5.1 Vegetation Recovery Following Fire in Pacific Coast Salt Marshes*

Of particular concern for local ecosystem resiliency to fire is the slow recovery of the dominant vegetation type, *S. pacifica,* which serves as the species responsible for sediment trapping to maintain elevation increases with SLR because of the lack of *Spartina* at the site. *Salicornia pacifica* does not attain an average percent cover above 25% in burned areas compared to unburned averages which are consistently above 50% for entire study period. The slow recruitment of *S. pacifica* is also surprising given that a study in the nearby salt marsh at Tijuana River Estuary found recruitment of *Salicornia spp.* and *Suada esteroa* dominated, among eight other identified species including *F. grandifolia*, in bare areas of a restoration site (Lindig-Cisneros & Zedler, 2002). Moreover, seed banks of salt marshes in the San Francisco Bay area were shown to contain a majority *Salicornia spp.* seeds, with *F. grandifolia* and *D. spicata* comprising less than 2% of the seedbank each (Hopkins & Parker, 1984). Despite these previous studies showing *S. pacifica* recruits easily in Southern California salt marshes, recovery of *S. pacifica* following fire at Mugu was slow compared with other species.

The significantly higher recruitment observed in plots closest to unburned salt marsh suggests that recruitment following large disturbance events may be impeded by the distance to non-affected salt marsh habitat. Such effects may have been especially pronounced due to the seasonality of the 2013 Camarillo Springs Fire. Seed dispersal in Pacific coast salt marshes is

limited (Lindig-Cisneros & Zedler, 2002) but occurs primarily in winter (Morzaria-Luna & Zedler, 2007), so the seed bank would have been depleted for one entire growing season following the 2013 fire event. Observed spatial patterning could also be influenced by canopy removal causing increased solar radiation and loss of soil moisture. Those conditions would likely prevent *S. pacifica* and other salt marsh plants from establishing. The prevalence of *D. spicata* in recovered vegetation can also largely be attributed to its preference for disturbed sites (Bertness, 1991; Hopkins & Parker, 1984). Monotypic stands of *D. spicata* in the burned area and preference for sites closer to unburned salt marsh suggests a lack of seed availability and unsuitable environmental conditions in burned sites. Recovery could be accelerated by planting or seeding in areas that are disturbed.

The overall trend towards more species evenness seen from the Simpson's ID of burned areas is an indication of higher vegetation diversity in burned areas, but, with no difference in the number of species observed in burned and unburned sites, the effect of this change in composition may be quite minimal. Even so, this change in species evenness could have implications for ecosystem functionality. *Salicornia pacifica* is the main ecosystem engineer in the Mugu Lagoon salt marsh and its decrease in percent cover could result in less sediment trapping and slower elevation gain. Our results, showing that *S. pacifica* is the slowest of the three observed vegetation types to recover, would indicate that small disturbances such as a fire could have long-term impacts on marsh resiliency to accelerated SLR.

Moreover, as the study site represents a very small area of the total area burned, we think these results do not fully capture some of the changes in vegetation composition that resulted from the 2013 Camarillo Springs Fire. Expansion of *B. maritima* was observed near some of the denuded salt pans and large, monotypic stands of *Suaeda californica* were seen in some burned

areas above the frequently inundated tidal regions in the first year following the fire. These qualitative observations would point to higher rates of vegetation change following disturbance at upland-marsh transition zone which need to be explored further.

### *5.5.2 Soil Organic Carbon*

Results indicating no difference in mean SOC between vegetated and unvegetated soil conditions may be related to the slow revegetation and drought seen in the study. Schmalzer and Hinkel (1992) found that SOM increased in burned areas for nine months following a controlled burn in a mixed *Juncus roemerianus* and *Spartina bakeri* salt marsh, likely related to the increased productivity typically seen in bulrush and cordgrass marshes. No increase in SOC in burned sites at Mugu underscores that soil recovery, like vegetation recovery, is similarly slow at Mugu compared to marshes with documented burn records. Not all marshes show increased SOM following fire, however. Salvia et al. (2012) show fires occurring during a drought period in the Paraná River Delta in Argentina caused a decrease in SOC for a *Schoenoplectus californicus* and *Cyperus giganteus* marsh following burning which did not recover to SOC levels observed in unburned marsh during the year of monitoring. They conclude that recovery of vegetation and soil conditions largely depend upon the severity of the burn and the hydrological condition of the marsh. While the Camarillo Springs Fire does not appear to have been a high severity burn causing damage below the topsoil, low SOC (< 10%) may be more indicative of overall hydrological stress in both unburned and burned sites due to drought, rather than reflective of post-fire conditions. These very different wetland soil responses indicate a need for further research into how fire affects wetland soils with particular focus on hydrological conditions.

### *5.5.3 Multiple Stressors*

The influence of drought on salt marsh vegetation and post-fire recovery cannot be ignored. It is evident from NDVI that salt marsh vegetation was stressed due to climate conditions immediately before and during the recovery period. Drought in Southern California salt marshes has been linked to increased soil salinity (Zedler, 2010), which decreases recruitment in most salt marsh species (Shumway & Bertness, 1992). Seasonality and timing of precipitation can greatly influence recruitment success as well (Zedler, 2010). The Camarillo Springs Fire occurred in May and cut the 2013 growing season short. Plants would have been recruiting after winter rains, when seed banks were depleted, past the peak growing season, and may have seen a higher proportion of die-off due to continued drought and soil salinity stress as summer progressed. These factors – the drought and the seasonality of the disturbance – may have significantly hindered the recovery at Mugu Lagoon. And while we cannot separate these effects in this study, decreased moisture and a longer fire season are predicted to become the norm under climate change conditions.

Although data on browned or dead vegetation were not collected in this study, it is a factor which should be considered in future research which tracks marsh vegetation recovery following disturbance or during drought. Salt marsh dieback, observed across the continental US, was linked to drought through PDSI along the southeast and Gulf coasts (Alber, Swenson, Adamowicz, & Mendelssohn, 2008). The mechanisms which lead to sudden dieback are complex and often linked to interactive or additive stressors. Browned or dead cover will also affect soil conditions, such as sunlight receipt (Salvia et al., 2012), or waterflow across the site and could provide more insight into vegetative stress in recovery and control areas as well as provide an important parameter for further understanding of soil conditions.

Additionally, while there were no upland or non-marsh species in our direct study site, non-marsh species likely had an influence on recovery in other areas of the burn site. One year after the Camarillo Springs Fire, managers at Mugu started weed control for *B. rapa, R. communis, A. donax*, and others which had colonized the highest elevations in the burn area (personal communication, Valerie Vartanian). Many of these non-native or upland annuals have a competitive advantage over native high-elevation marsh and marsh peripheral vegetation in post-fire, disturbed soils (Zedler & Kercher, 2004). Evidence points to a positive feedback between fire and upland species in many ecosystems (Brooks et al., 2010). Upland plants may cause long-term ecological modification through changes to canopy structure and soil moisture, preventing native high-elevation marsh and marsh peripheral vegetation from reestablishing. The upland ecotone in salt marshes on the Pacific Coast serves as critical habitat for pollinator and bird species which support the biodiversity of the salt marsh (Callaway & Zedler, 2004) and the interaction between marsh and upland species will be a key issue in adaptation to accelerated SLR, as landward migration is the primary mechanism for salt marsh ecosystem adaptation to SLR (Kirwan et al., 2016). Repeated disturbances from fire and subsequent colonization by non-marsh species at the highest elevations of the marsh represents a secondary stressor on ecosystems already threated by SLR on the seaward margin with unknown long-term impacts on both marsh and upland transition zone ecology.

If climate change is increasing both the propensity of California salt marshes to burn and the length of time required for recovery it raises questions of salt marsh vulnerability to SLR as well as impact on ecosystem services, such as carbon storage in soils. Loss of remaining critical habitat will stress salt marsh biota, including listed species such as the Belding's savannah sparrow which might see local population collapse with habitat disturbances that impact two or

more breeding seasons. Careful monitoring of the impact of not only the fire itself but also the additional stressors to the salt marsh ecosystem is needed. While examples from the Gulf and East coast ecosystems can provide some guidance as to how long-term recovery of ecosystem processes like accretion and carbon storage may progress after fire, the timing of the recovery in *S. pacifica*-dominated systems may result in vastly different outcomes. Multiple disturbances to salt marsh ecosystems have proven complex for ecosystem health and management (Martone & Wasson, 2008; Zedler, 2010). The Green Meadows and Camarillo Springs Fires highlight the need for ecosystem level management in the face of multiple environmental stressors, particularly in the face of accelerated SLR.

### *5.5.4 Recommendations*

Given the serious implications of slow recovery of salt marsh species following fire, we recommend intensive monitoring and analysis of future fire disturbance in Pacific salt marshes, especially those dominated by *S. pacifica.* Such analysis should include the effects of vegetation denudation on sediment accretion rates, salt marsh elevation, and soil dynamics in addition to monitoring rate and composition of revegetation. Monitoring the interaction between non-marsh vegetation and native salt marsh plant revegetation should also occur, especially in the high-elevation marsh, as the impact of fire on this ecotone has not been documented before. Particular attention should be paid to multi-year disturbances of habitat critical for endangered species. In such cases of long-term disturbance on salt marsh ecosystems facing multiple, additive stressors, comprehensive ecosystem-wide monitoring will be needed to guide recovery efforts. With threats from accelerated SLR and urbanization, long-term disturbance from fire could have significant impacts on the resiliency of salt marsh habitat in the future.

## 5.6 Figures

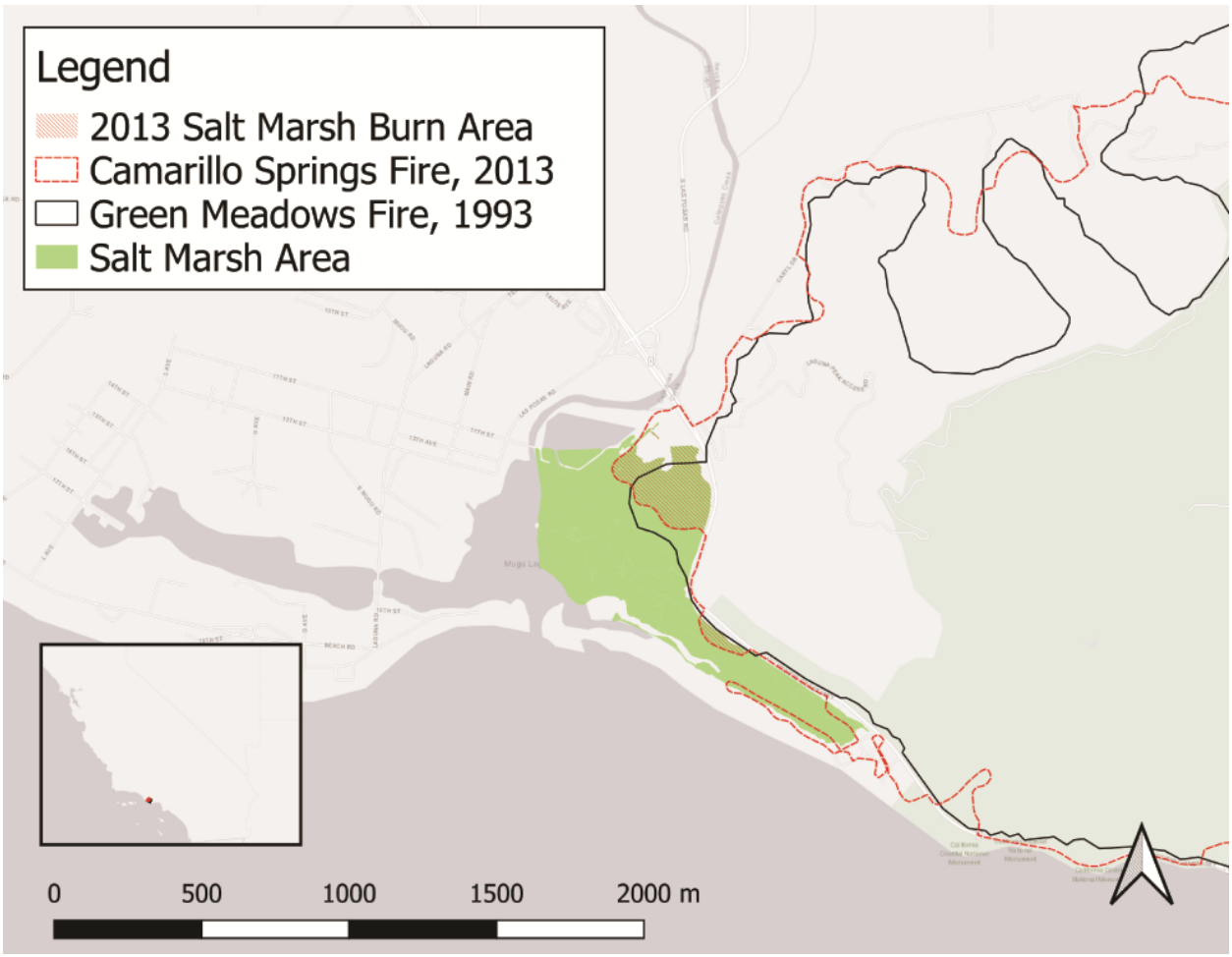


**Figure 5.1 Area Map Showing Fire Extent**

Map of the 1993 Green Meadows Fire and 2013 Camarillo Springs Fire extent at Mugu Lagoon. Wetland outline was obtained from The Pacific Institute shapefile of wetlands below or within 100 m of mean higher high water, fire perimeters were obtained from CalFire Fire Perimeters Version 14_2 and basemap is open source ESRI Gray (light).

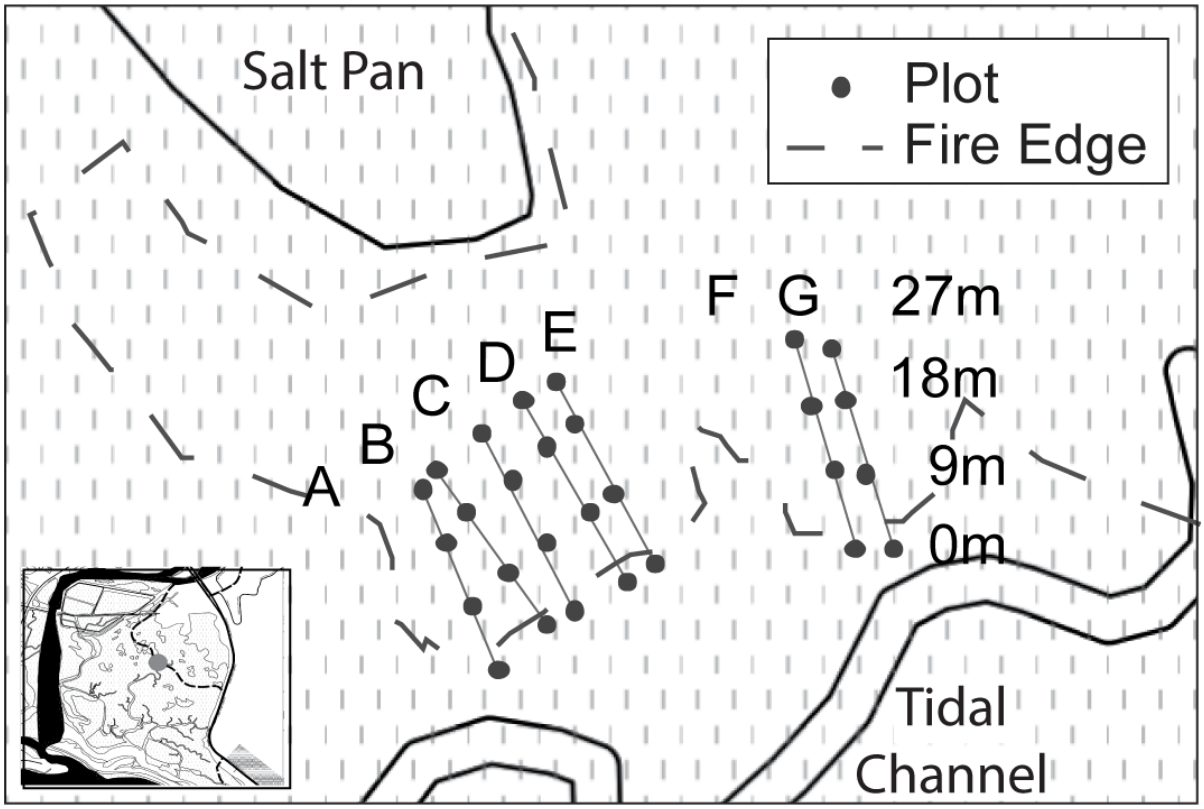


**Figure 5.2 Map of Study Site**

Site map depicting the seven transects, A to G from left to right. Dots on each transect indicate the 21 quadrats in burned areas (three on each transect) and seven quadrats in unburned areas (one quadrat on each transect). Wetland outline was obtained from The Pacific Institute shapefile of wetlands below or within 100 m of mean higher high water, fire perimeters were obtained from CalFire Fire Perimeters Version 14_2 and basemap is open source in QGIS from OpenStreetMap.

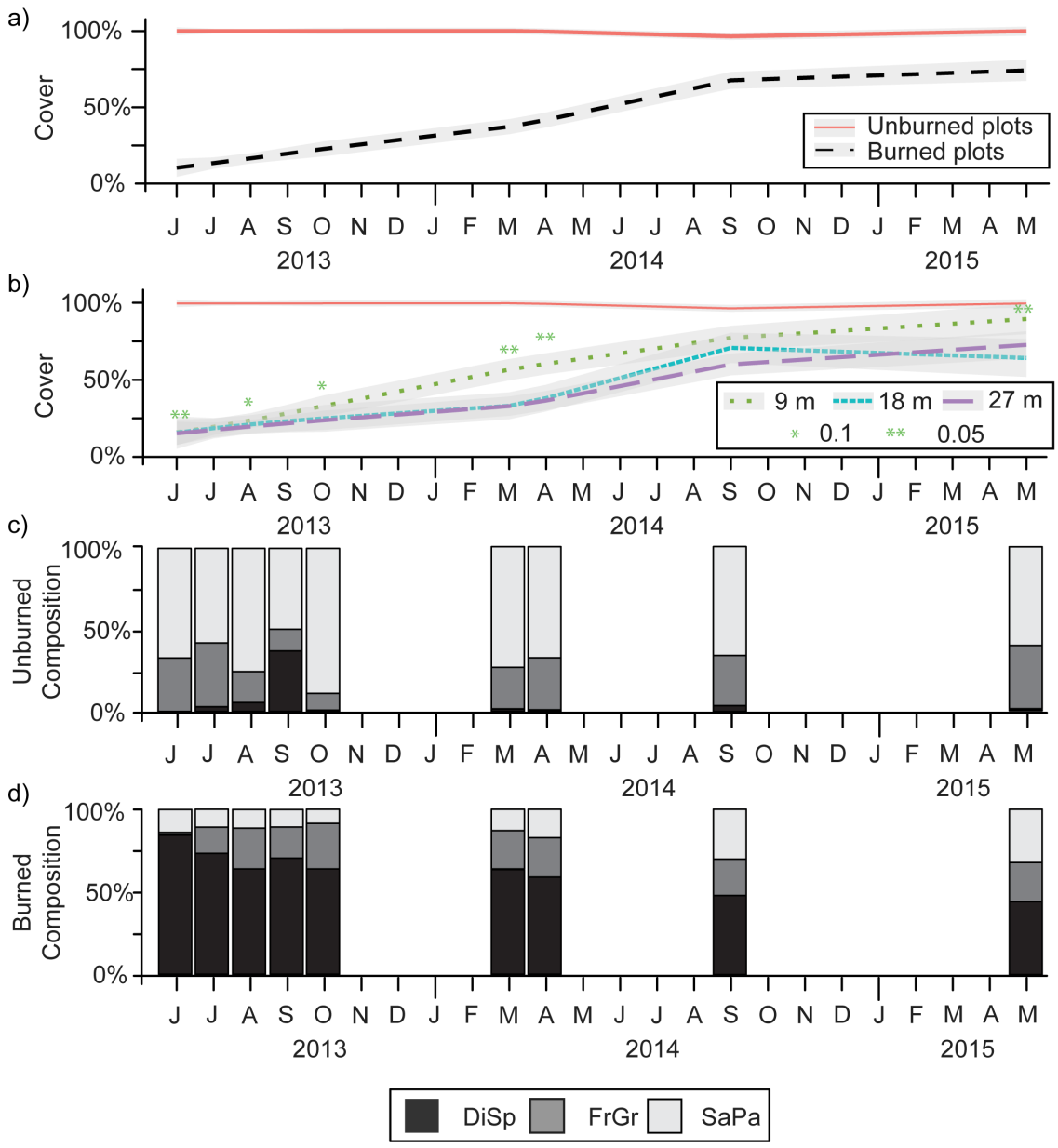


**Figure 5.3 Vegetation Percent Cover and Species Composition**

Vegetation for the study period of June 2013 – May 2015 seen as (a) a spline fit of percent cover for all unburned (solid line) and burned (dashed line) quadrats with shaded standard error, (b) a spline fit of percent cover in unburned quadrats with percent cover in burned plots sorted by distance, with shaded standard error, and asterisks indicating significance levels of difference in recovery between plots 9 m from unburned marsh compared to plots 27 m from unburned marsh, (c) average unburned quadrat species composition as a percentage of cover present, and (d) average burned quadrat species composition as a percentage of cover present (c and d are plotted out of 100% to make species differences visible for those time periods which have less than 10 % cover, and they do not reflect relative cover between time periods or treatments).

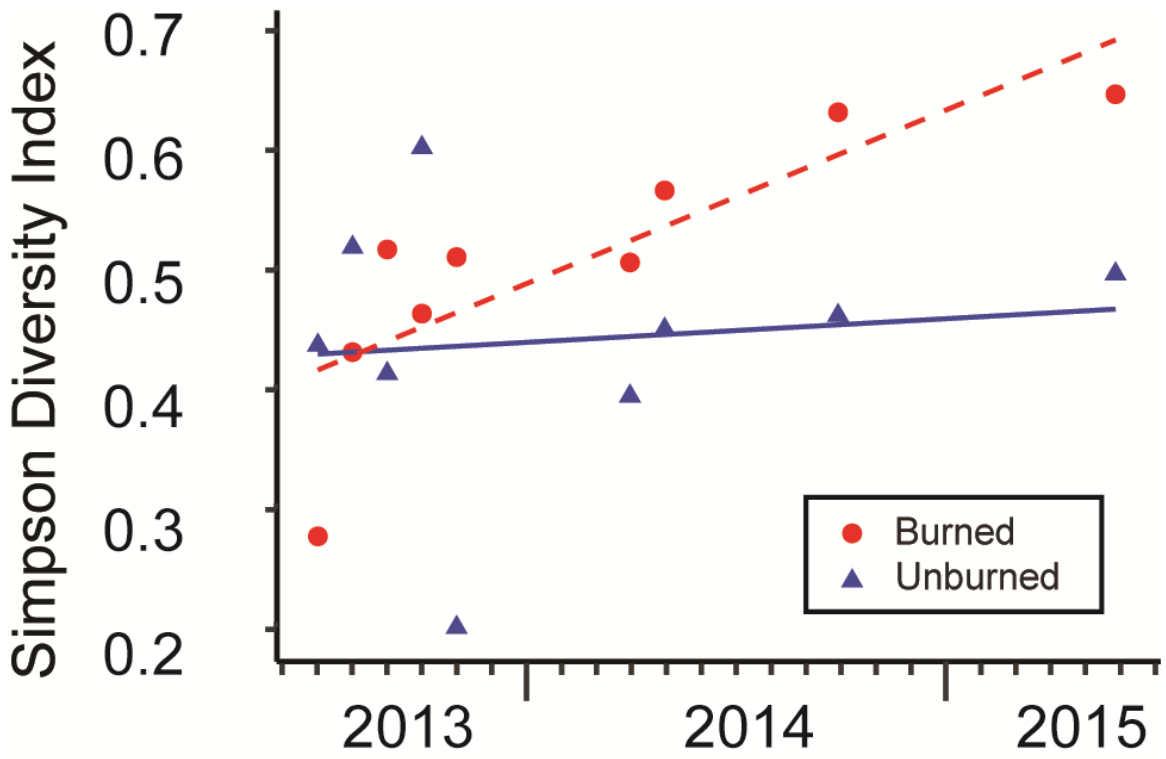


**Figure 5.4 Simpson's Diversity Index**

Simpson's Diversity Index (ID) averaged for burned and unburned plots for each observation during the study period with linear trendlines. Unburned plots show no trend in Simpson's ID ($R^2 = 0.01$; $p = 0.77$) while burned plots show a slight increase in Simpson's ID over time ($R^2 = 0.68$; $p = 0.006$).

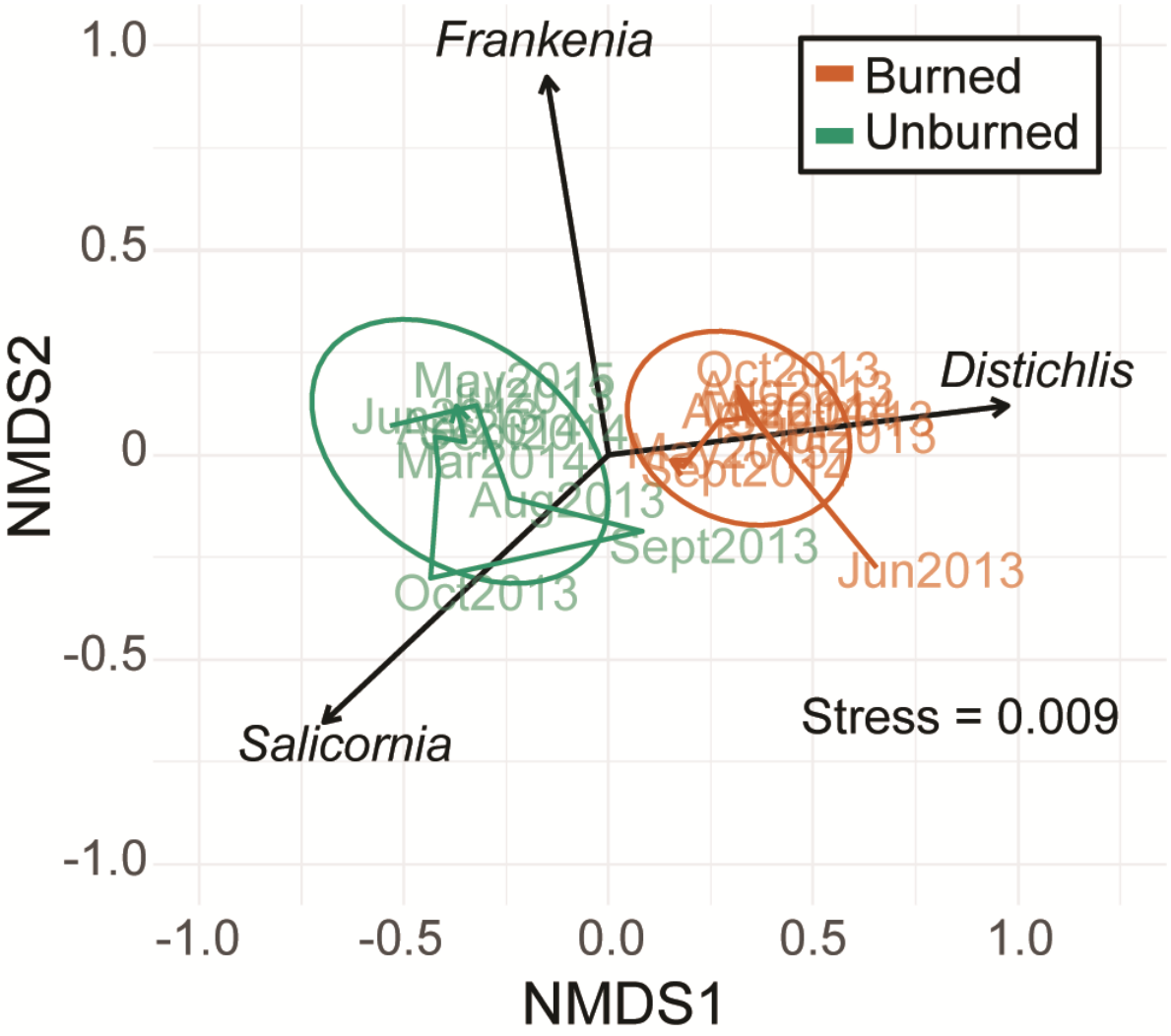


**Figure 5.5 NMDS Plot for Axes1 and 2 of Species Composition**

Species composition for all timepoints was plotted using non-metric multidimensional scaling (NMDS). Stress value was 0.009. Ellipses indicate the 95% confidence interval of burned and unburned plot positions in non-dimensional space. Species variables were fitted to NMDS axes and are plotted with arrows. Timepoints were connected by a line for burned and unburned plots and show trends in species composition over the duration of the study.

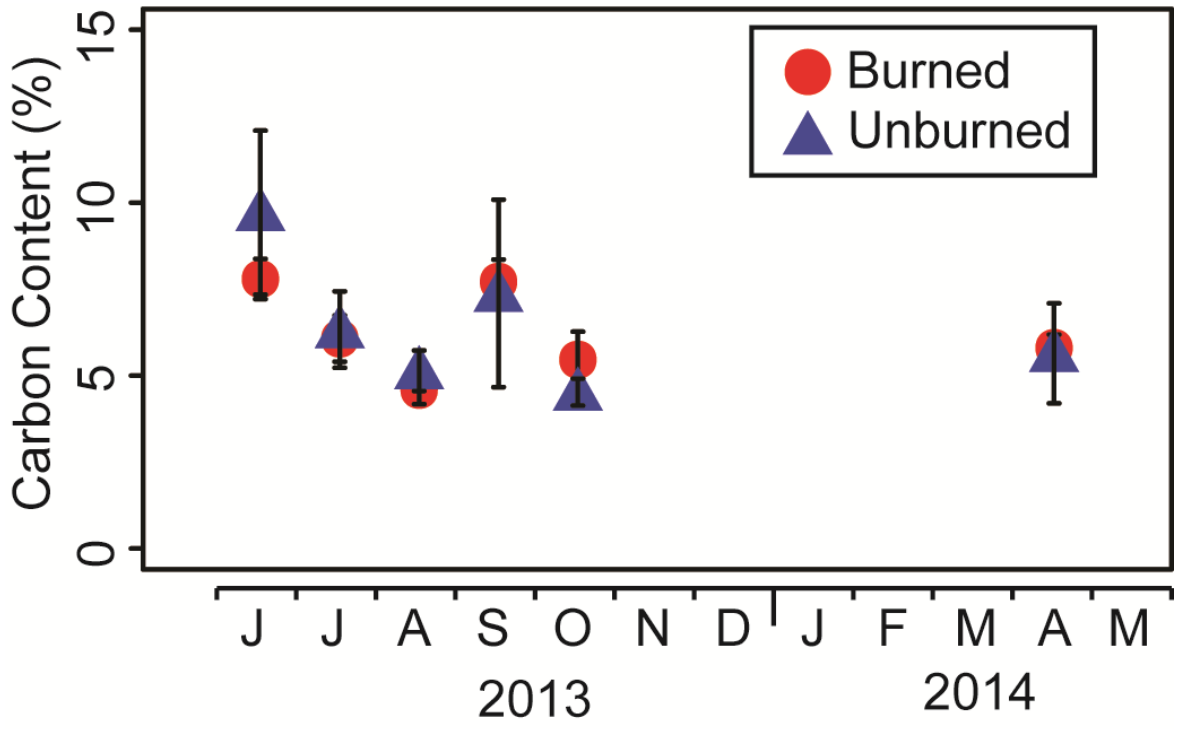


**Figure 5.6 Soil Organic Carbon**

Average soil organic carbon (SOC) for unburned and burned plots from June 2013 to May 2014. Error bars show one standard error.

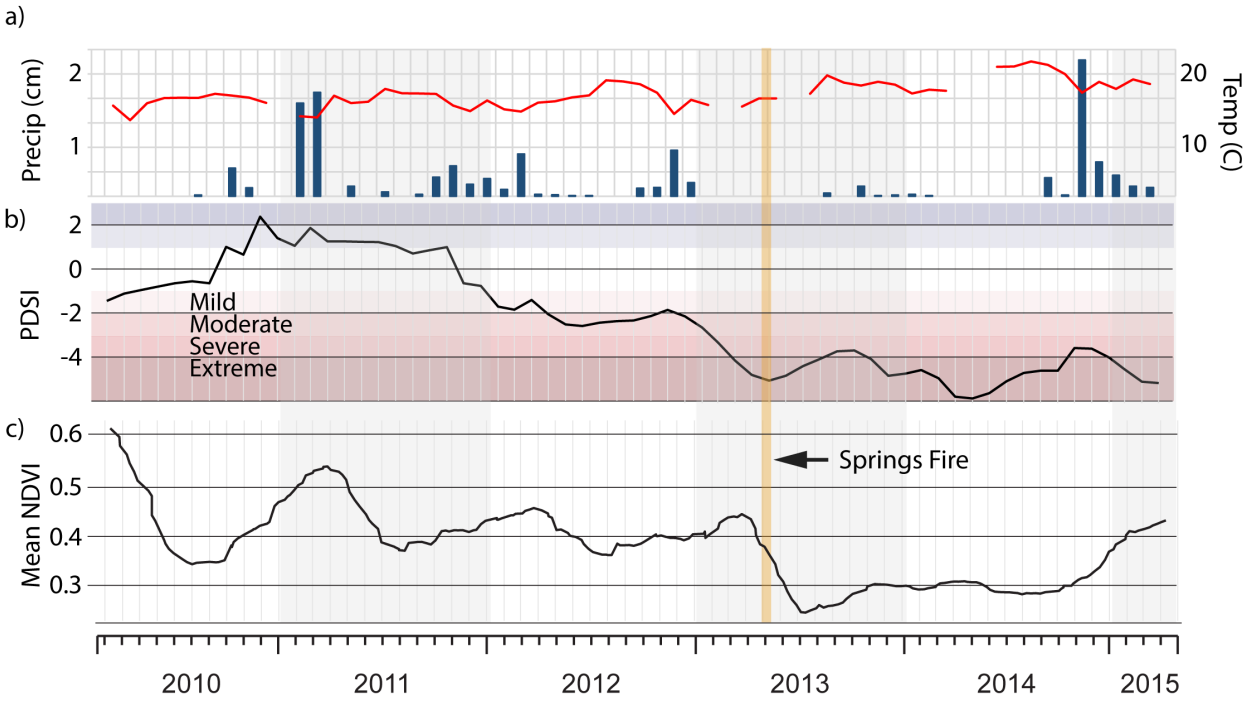


**Figure 5.7 Temperature, Precipitation, PDSI, and NDVI**

Remote sensing analysis for the period of March 2010 to April 2015 with a) average temperature and precipitation at nearest NOAA weather station (Mugu Lagoon), b) PDSI, and c) a Savitzky-Golay filter of mean NDVI.

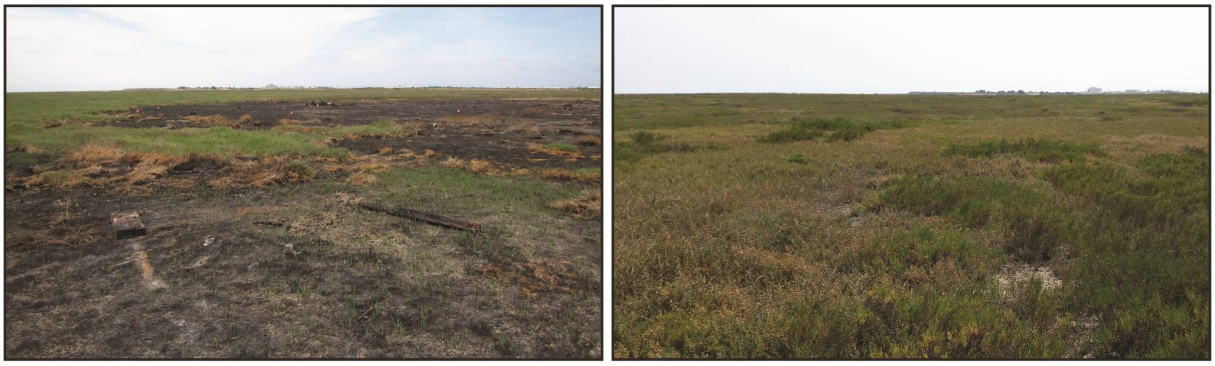

June 2013 May 2015

**Figure 5.8 Pictures of Study Site Following Fire and During Recovery**

Two photos taken looking east over the study site. The first was taken in June 2013 about one month following the Camarillo Springs Fire (photo credit: Richard Ambrose). The second was taken during the final survey in May 2015 (photo credit: Lauren Brown).

## 5.7 Tables

**Table 5.1 NMDS Results**

| | MDS1 | MDS2 | r2 | p |
|---|---|---|---|---|
| *Distichlis* | 0.99246 | 0.1226 | 0.9639 | <0.001 |
| *Frankenia* | -0.1616 | 0.98685 | 0.8745 | <0.001 |
| *Salicornia* | -0.7293 | -0.6842 | 0.9106 | <0.001 |

Results of species variable fitting of NMDS for burned and unburned plots.

## 5.8 Appendix

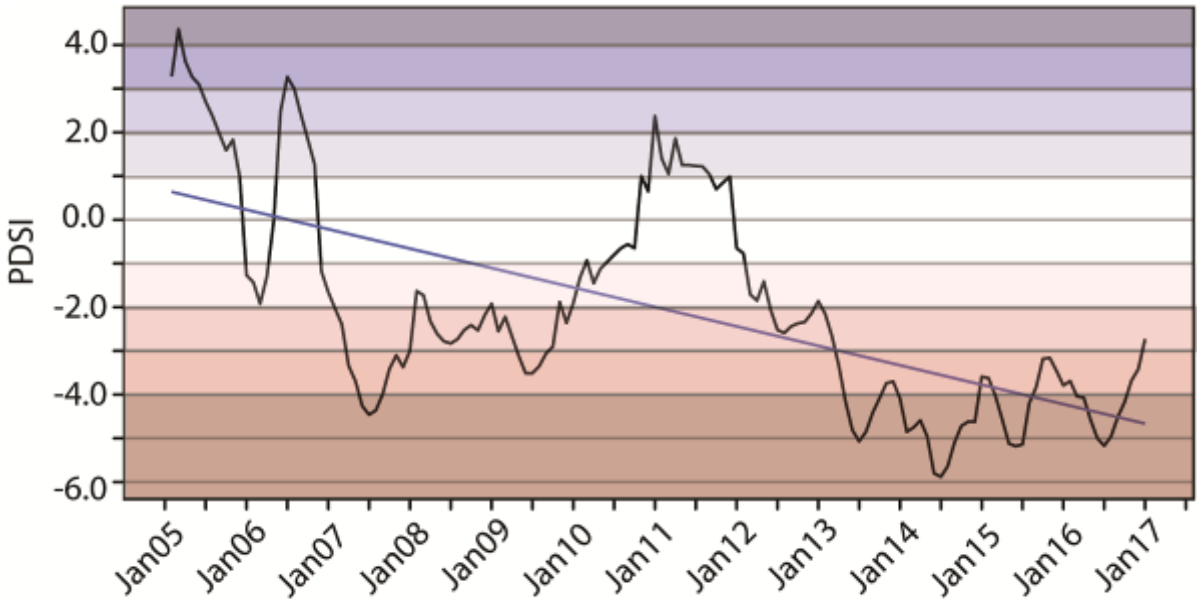


**Appendix Figure 5.1 PDSI Timeseries with Trendline**

PDSI data obtained from the West Wide Drought Tracker webpage (Monitoring & Scales, 2017) for the Point Mugu Lagoon area from January 2005 to January 2017 showing a negative trend.

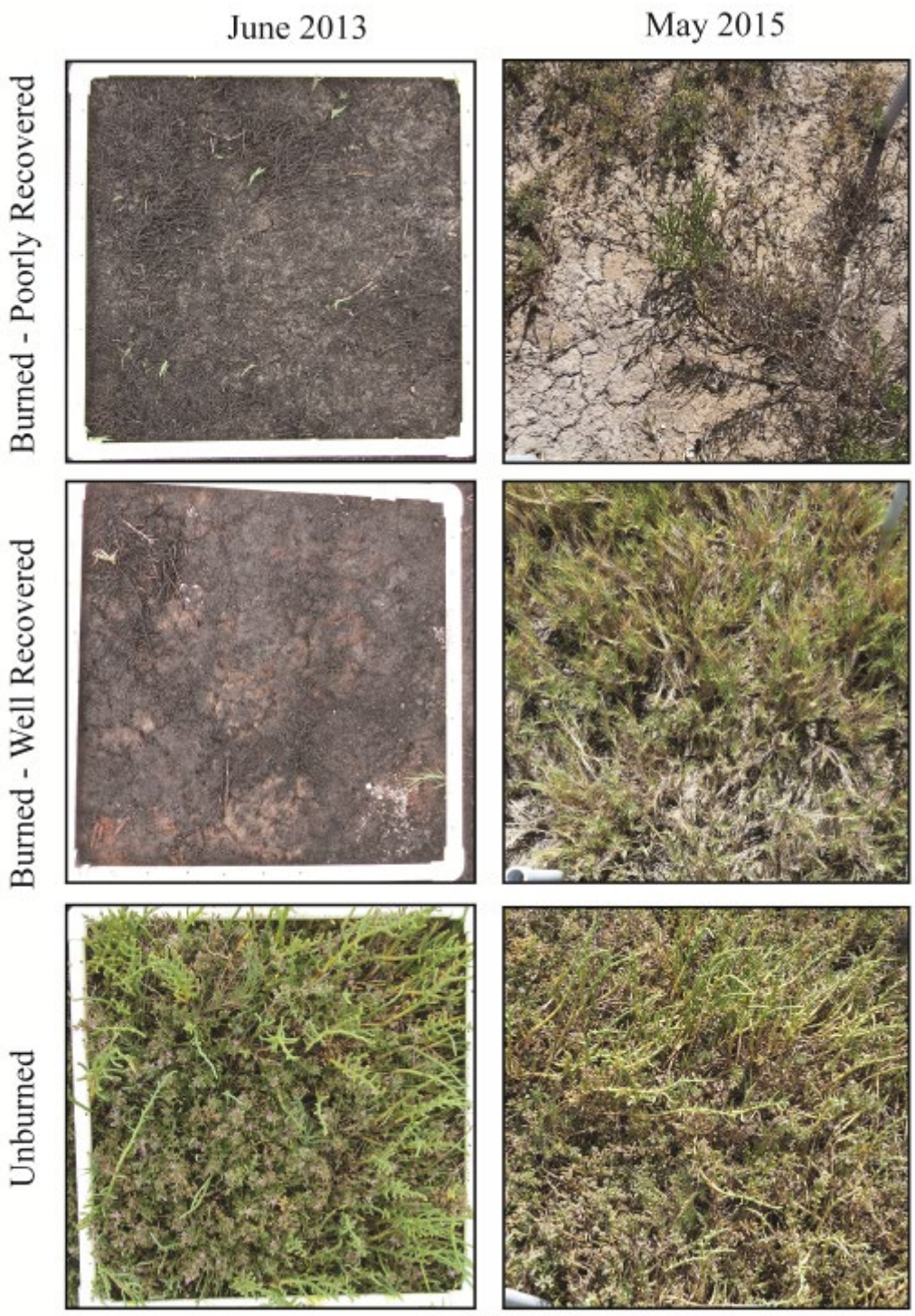


**Appendix Figure 5.2 Photos of Plot Recovery**

Photographic examples of vegetation recovery from June 2013 to May 2015 for examples of poorly- and well-recovered burned plots as well as change in an unburned plot (photos: L. Brown)

**Appendix Table 5.1 Average Shoots Counted in 2013**

| | Disp | Frgr | Sapa |
|---|---|---|---|
| **Jun** | 6 ± 8 | 0 ± 1 | 0 ± 1 |
| **Jul** | 20 ± 20 | 3 ± 6 | 2 ± 4 |
| **Aug** | 16 ± 18 | 8 ± 18 | 1 ± 3 |
| **Sept** | 20 ± 21 | 5 ± 7 | 2 ± 5 |
| **Oct** | 17 ± 18 | 5 ± 7 | 2 ± 4 |

Average new shoots counted in burned plots for 2013 with standard errors.

**Appendix Table 5.2 Percent Cover and Species Distribution Averages**

| | Year | 2013 | | | | | 2014 | | | 2015 |
|---|---|---|---|---|---|---|---|---|---|---|
| | Month | Jun | Jul | Aug | Sept | Oct | Mar | Apr | Sept | May |
| Unburned Cover (%) | **Mean** | 100 ± 0 | 100 ± 0.4 | 100 ± 0.4 | 100 ± 0 | 100 ± 0 | 100 ± 0 | 100 ± 0.8 | 95 ± 5 | 100 ± 0 |
| | **Max** | 100 | 100 | 100 | 100 | 100 | 100 | 100 | 100 | 100 |
| | **Min** | 100 | 99 | 99 | 100 | 100 | 100 | 98 | 65 | 100 |
| | **Disp** | 0 ± 0 | 4 ± 4 | 7 ± 7 | 37 ± 17 | 1 ± 0 | 1 ± 1 | 1 ± 1 | 3 ± 2 | 2 ± 1 |
| | **Frgr** | 32 ± 10 | 38 ± 12 | 19 ± 5 | 14 ± 4 | 10 ± 5 | 25 ± 10 | 32 ± 11 | 30 ± 8 | 38 ± 13 |
| | **Sapa** | 68 ± 10 | 58 ± 13 | 74 ± 5 | 50 ± 18 | 89 ± 5 | 73 ± 10 | 67 ± 11 | 67 ± 8 | 60 ± 14 |
| Burned Cover (%) | **Mean** | 1 ± 0.9 | 5 ± 1 | 9 ± 2 | 10 ± 2 | 15 ± 3 | 34 ± 4 | 33 ± 3 | 70 ± 6 | 71 ± 5 |
| | **Max** | 3 | 15 | 30 | 35 | 80 | 85 | 60 | 100 | 100 |
| | **Min** | 0 | 1 | 1 | 1 | 3 | 4 | 5 | 22 | 11 |
| | **Disp** | 84 ± 11 | 73 ± 7 | 64 ± 8 | 70 ± 8 | 64 ± 7 | 65 ± 7 | 59 ± 7 | 48 ± 9 | 44 ± 9 |
| | **Frgr** | 2 ± 1 | 16 ± 5 | 25 ± 7 | 19 ± 5 | 27 ± 7 | 22 ± 6 | 24 ± 6 | 22 ± 7 | 24 ± 6 |
| | **Sapa** | 14 ± 7 | 11 ± 5 | 11 ± 5 | 11 ± 5 | 9 ± 3 | 12 ± 4 | 17 ± 6 | 30 ± 8 | 32 ± 8 |

Percent cover estimates averaged by month for unburned sites (n=7) and burned sites (n=21) with standard errors, and maximum and minimum percent cover of all plots. Average percent cover by species also displayed with standard errors.

**Appendix Table 5.3 Average SOC by Month**

| | Unburned | Burned |
|---|---|---|
| **Jun** | 9.02 ± 4.92 | 7.83 ± 1.99 |
| **Jul** | 6.05 ± 0.60 | 6.12 ± 2.18 |
| **Aug** | 5.15 ± 0.94 | 4.61 ± 1.34 |
| **Sept** | 7.52 ± 4.56 | 7.76 ± 2.23 |
| **Oct** | 4.57 ± 0.64 | 5.53 ± 2.54 |
| **Apr** | 5.68 ± 2.32 | 5.82 ± 1.18 |

Average SOC for unburned plots (n=7) and burned plots (n=21) with standard errors for June 2013 to April 2014.

# 6. Conclusions

The 21st century presents California salt marsh ecosystems with challenges and opportunities. Climate change and accelerated SLR may fundamentally change the coastal landscape, and the role that coastal salt marsh ecosystem will play is currently uncertain. The first question of this dissertation asked was how salt marshes have functioned relative to rates of SLR in the past. Past rates of sediment accretion and SLR confirm that salt marshes may already be facing the impacts of the past 200 years' acceleration of SLR and may also be struggling with the impacts of human land use modification and changes to local hydrology. Salt marshes in locations with high rates of RSLR, like Bolinas Lagoon and some marshes in the San Francisco and Humboldt Bays, show higher rates of sediment accretion, indicating that salt marshes in the state may still be operating within the bounds of their adaptive capacity. But other salt marshes, like Upper Newport Bay, show concerning trends which would indicate that the system is under stress may be at greater risk from accelerated SLR. Overall, the data confirm that local site conditions, like the diurnal tidal range, are most predictive of rates of accretion.

The second question posed by the dissertation reveals that California salt marshes may have potential for blue carbon markets, but sequestration of carbon in coastal habitats does not produce significant mitigation potential at the state level because of limited area. The use of LOI in estimation of carbon content for sediment is feasible and cost-efficient. Best-practice methods can account for many of the largest sources of error and uncertainty, such as the conversion of SOM to SOC and measurement of non-organic carbon elements. Participation in interlab comparison studies, careful reporting of laboratory methods, quantification of non-carbon elements, and reporting of raw LOI values are all recommendations for data producers and users which will decrease uncertainty, error, and unsuitability of data for large-scale syntheses.

Use of best practice LOI methods and verified conversion estimates to estimate carbon storage and sequestration for 61 sediment cores reveals that California salt marshes sequester 0.08% of California annual emission each year, and have a stock of about 23% of one year's emissions. The most effective strategies for increasing sequestration and storage potential is through expansion of salt marsh area and increases in the rate of sediment accretion or carbon burial. Building capacity for accretion therefore serves the dual purpose of maximizing carbon storage potential and also maximizing adaptive capacity to higher rates of SLR. However, the risk of loss of sequestration potential and carbon stock are particularly great for the areas of low marsh which contribute most to sequestration. Protection of these carbon stocks will determine whether salt marshes have a net positive or negative impact on the carbon cycle. But because this impact is relatively small at larger scales, emphasis on total value of all ecosystem services as well as intrinsic value of salt marsh habitat should be made along with any value from blue carbon.

Finally, the last chapter of this dissertation shows that many uncertainties remain regarding what types of stresses salt marshes will face in the 21$^{st}$ century and how they may interact with one another. Fire is a relatively undocumented disturbance for Pacific coast salt marshes, but could become a risk in a hotter, drier California. These hotter, drier conditions may have delayed the vegetation recovery at Mugu Lagoon and extended the period of disturbance. The slow vegetation recovery indicates that the Pacific coast salt marsh ecosystem responds quite differently to disturbance by fire from salt marsh systems with documented fire regimes. And, while there was no significant impact to the carbon content of soils documented by this study, the overall impact of this disturbance to ecosystem function is still unclear. As an early indication of the potential stressors which may come with climate change, the fire at Mugu

demonstrates that accelerated SLR, climate change, and human impacts on salt marshes can interact and affect overall adaptive capacity which will necessitate more active management of disturbances in the future.

Although California salt marshes are highly vulnerable, they are also uniquely adaptable. This dissertation provides baseline accretion and carbon storage data for 13 salt marsh sites along the California coast in the hopes that it will help to inform stakeholders and managers as to how best to facilitate salt marsh adaptation to rising tides and temperatures.

## References

Abatzoglou, J. T., McEvoy, D. J., Redmond, K. T., Monitoring, D., & Scales, F. S. (2017). The West Wide Drought Tracker: Drought Monitoring at Fine Spatial Scales. *Bulletin of the American Meteorological Society*, *98*(9), 1815–1820. https://doi.org/10.1175/BAMS-D-16-0193.1

Abella, S. R., & Zimmer, B. W. (2007). Estimating Organic Carbon from Loss-On-Ignition in Northern Arizona Forest Soils. *Soil Science Society of America Journal*, *71*(2), 545. https://doi.org/10.2136/sssaj2006.0136

Alber, M., Swenson, E. M., Adamowicz, S. C., & Mendelssohn, I. A. (2008). Salt Marsh Dieback: An overview of recent events in the US. *Estuarine, Coastal and Shelf Science*, *80*(1), 1–11. https://doi.org/10.1016/j.ecss.2008.08.009

American Carbon Registry. (2017). *Methodology for the Quantification, Monitoring, Reporting and Verification of Greenhouse Gas Emissions Reductions and Removals from the Restoration of California Deltaic and Coastal Wetlands* (No. Version 1.1; p. 192).

Appleby, P. G., & Oldfield, F. (1978). The calculation of lead-210 dates assuming a constant rate of supply of unsupported 210Pb to the sediment. *CATENA*, *5*(1), 1–8. https://doi.org/10.1016/S0341-8162(78)80002-2

Atwater, B. F., Conard, S., Dowden, J., Hedel, C., MacDonald, R., & Savage, W. (1979). History, Landforms, and Vegetation of the Estuary's Tidal Marshes. In *San Francisco Bay: The Urbanized Estuary. Investigations into the Natural History of San Francisco Bay and Delta With Reference to the Influence of Man*. Pacific Division of the American Association for the Advancement of Science c/o California Academy of Sciences Golden Gate Park San Francisco, California 94118.

Atwater, B. F., Hedel, C. W., & Helley, E. J. (1977). *Late Quaternary depositional history, Holocene sea-level changes, and vertical crust movement, southern San Francisco Bay, California*. U.S. Govt. Print. Off.

Bai, J., Zhang, G., Zhao, Q., Lu, Q., Jia, J., Cui, B., & Liu, X. (2016). Depth-distribution patterns and control of soil organic carbon in coastal salt marshes with different plant covers. *Scientific Reports*, *6*, 34835. https://doi.org/10.1038/srep34835

Baldocchi, D. (2014). Measuring fluxes of trace gases and energy between ecosystems and the atmosphere – the state and future of the eddy covariance method. *Global Change Biology*, *20*(12), 3600–3609. https://doi.org/10.1111/gcb.12649

Ball, D. F. (1964). Loss-on-Ignition as an Estimate of Organic Matter and Organic Carbon in Non-Calcareous Soils. *Journal of Soil Science*, *15*(1), 84–92. https://doi.org/10.1111/j.1365-2389.1964.tb00247.x

Barbier, E. B., Hacker, S. D., Kennedy, C., Koch, E. W., Stier, A. C., & Silliman, B. R. (2011). The value of estuarine and coastal ecosystem services. *Ecological Monographs*, *81*(2), 169–193. https://doi.org/10.1890/10-1510.1

Barnard, P. L., Erikson, L. H., Foxgrover, A. C., Hart, J. A. F., Limber, P., O'Neill, A. C., … Jones, J. M. (2019). Dynamic flood modeling essential to assess the coastal impacts of climate change. *Scientific Reports*, *9*(1), 4309. https://doi.org/10.1038/s41598-019-40742-z

Barnhart, R. A., Boyd, M. J., & Pequegnat, J. E. (1992). *The Ecology of Humboldt Bay California: An Estuarine Profile* (No. 1; p. 122). US Fish and Wildlife Service.

Bawden, G. W., Thatcher, W., Stein, R. S., Hudnut, K. W., & Peltzer, G. (2001). Tectonic contraction across Los Angeles after removal of groundwater pumping effects. *Nature*, *412*(6849), 812–815. https://doi.org/10.1038/35090558

Bear, T. M. (2017). *Sea-level-rise-induced threats depend on the size of tide-influenced estuaries worldwide | Nature Climate Change* (Dissertation, University of California, Los Angeles). Retrieved from https://www.nature.com/articles/s41558-019-0608-4

Bear, T. M. (2017). *Soil Carbon Sequestration and Carbon Market Potential of a Southern California Tidal Salt Marsh Proposed for Restoration*.

Bertness, M. D. (1991). Interspecific Interactions among High Marsh Perennials in a New England Salt Marsh. *Ecology*, *72*(1), 125–137.

Bickford, W. A., Needelman, B. A., Weil, R. R., & Baldwin, A. H. (2012). Vegetation Response to Prescribed Fire in Mid-Atlantic Brackish Marshes. *Estuaries and Coasts*, *35*(6), 1432–1442. https://doi.org/10.1007/s12237-012-9538-3

Blum, M. D., & Roberts, H. H. (2009). Drowning of the Mississippi Delta due to insufficient sediment supply and global sea-level rise. *Nature Geoscience*, *2*(7), 488–491. https://doi.org/10.1038/ngeo553

Boden, T. A., Marland, G., & Andres, R. J. (2017). *Global, Regional, and National Fossil-Fuel CO2 Emissions. Carbon Dioxide Information Analysis Center, Oak Ridge National Laboratory, U.S. Department of Energy, Oak Ridge, Tenn., U.S.A.*

Brooks, M. L., D'Antonio, C. M., Richardson, D. M., Grace, J. B., Keeley, J. E., DiTomaso, J. M., … Pyke, D. (2010). Effects of Invasive Alien Plants on Fire Regimes. *BioScience*, *54*(7), 677–688.

Brownlie, W. R., & Taylor, B. D. (1981). *Coastal Sediment Delivery by Major Rivers in Southern California* (EQL Report No. No. 17-C; p. 325). California Institute of Technology.

Buffington, K. J. (2017). *Improving Projections of Tidal Marsh Persistence under Climate Change with Remote Sensing and Site-Specific Data* (Thesis). Oregon State University.

Buffington, K. J., Dugger, B. D., Thorne, K. M., & Takekawa, J. Y. (2016). Statistical correction of lidar-derived digital elevation models with multispectral airborne imagery in tidal marshes. *Remote Sensing of Environment*, *186*, 616625. https://doi.org/10.1016/j.rse.2016.09.020

Byers, S. C., Mills, E. L., & Stewart, P. L. (1978). A comparison of methods of determining organic carbon in marine sediments, with suggestions for a standard method. *Hydrobiologia*, *58*(1), 43–47. https://doi.org/10.1007/BF00018894

Byrne, R., Ingram, B. L., Starratt, S., Malamud-Roam, F., Collins, J. N., & Conrad, M. E. (2001). Carbon-Isotope, Diatom, and Pollen Evidence for Late Holocene Salinity Change in a Brackish Marsh in the San Francisco Estuary. *Quaternary Research*, *55*(1), 66–76. https://doi.org/10.1006/qres.2000.2199

Byrne, R., Reidy, L., Sengupta, D., Krause, J., Sullivan, J., Borkowski, J., … Menchaca, A. (2005). *Recent (1850—2005) and Late Holocene (AD 400 – AD 1850) Sedimentation Rates at Bolinas Lagoon, Marin County, California* [Bolinas Lagoon Ecosystem Restoration Feasibility Project: Final Public Reports]. Retrieved from Marin County Open Space District website: https://nmsfarallones.blob.core.windows.net/farallones-prod/media/archive/eco/bolinas/pdf/holocenesediment.pdf

Cahoon, D. R., Lynch, J. C., & Powell, A. N. (1996). Marsh Vertical Accretion in a Southern California Estuary, U.S.A. *Estuarine, Coastal and Shelf Science*, *43*(1), 19–32. https://doi.org/10.1006/ecss.1996.0055

Callaway, J. C., Borgnis, E. L., Turner, R. E., & Milan, C. S. (2012). Carbon Sequestration and Sediment Accretion in San Francisco Bay Tidal Wetlands. *Estuaries and Coasts*, *35*(5). https://doi.org/10.1007/s12237-012-9508-9

Callaway, J. C., Nyman, J., & DeLaune, R. (1996). Sediment accretion in coastal wetlands: A review and a simulation model of processes. *Current Topics in Wetland Biogeochemistry*, *2*, 2–23.

Callaway, J. C., & Zedler, J. B. (2004). Restoration of urban salt marshes: Lessons from southern California. *Urban Ecosystems*, *7*(2), 107–124. https://doi.org/10.1023/B:UECO.0000036268.84546.53

Campos C., A. (2010). Analyzing the Relation between Loss-on-Ignition and Other Methods of Soil Organic Carbon Determination in a Tropical Cloud Forest (Mexico). *Communications in Soil Science and Plant Analysis*, *41*(12), 1454–1462. https://doi.org/10.1080/00103624.2010.482168

Castillo, J. M., Grewell, B. J., Pickart, A. J., Figueroa, E., & Sytsma, M. (2016). Variation in tussock architecture of the invasive cordgrass Spartina densiflora along the Pacific Coast of North America. *Biological Invasions*, *18*(8), 2159–2174. https://doi.org/10.1007/s10530-015-0991-3

Chen, J., Jönsson, Per., Tamura, M., Gu, Z., Matsushita, B., & Eklundh, L. (2004). A simple method for reconstructing a high-quality NDVI time-series data set based on the

Savitzky–Golay filter. *Remote Sensing of Environment*, *91*(3), 332–344. https://doi.org/10.1016/j.rse.2004.03.014

Cherry, J. A., McKee, K. L., & Grace, J. B. (2009). Elevated CO2 enhances biological contributions to elevation change in coastal wetlands by offsetting stressors associated with sea-level rise. *Journal of Ecology*, *97*(1), 67–77. https://doi.org/10.1111/j.1365-2745.2008.01449.x

Chmura, G. L. (2013). What do we need to assess the sustainability of the tidal salt marsh carbon sink? *Ocean & Coastal Management*, *83*, 25–31. https://doi.org/10.1016/j.ocecoaman.2011.09.006

Chmura, G. L., Anisfeld, S. C., Cahoon, D. R., & Lynch, J. C. (2003). Global carbon sequestration in tidal, saline wetland soils. *Global Biogeochemical Cycles*, *17*(4). https://doi.org/10.1029/2002GB001917

Chmura, G. L., Helmer, L. L., Beecher, C. B., & Sunderland, E. M. (2001). Historical rates of salt marsh accretion on the outer Bay of Fundy. *Canadian Journal of Earth Sciences*, *38*(7), 1081–1092. https://doi.org/10.1139/e01-002

Church, J. a., & White, N. J. (2006). A 20th century acceleration in global sea-level rise. *Geophysical Research Letters*, *33*(1), L01602. https://doi.org/10.1029/2005GL024826

Climate Data Online. (2019). Retrieved July 25, 2019, from NOAA: National Centers for Environmental Information website: https://www.ncdc.noaa.gov/cdo-web/

Cole, K. L., & Wahl, E. (2000). A Late Holocene Paleoecological Record from Torrey Pines State Reserve, California. *Quaternary Research*, *53*(3), 341–351. https://doi.org/10.1006/qres.1999.2121

Costanza, R., D'Arge, R., De Groot, R., Farber, S., Grasso, M., Hannon, B., … van den Belt, M. (1997). The value of the world's ecosystem services and natural capital. *Nature*, *387*(6630), 253–260. https://doi.org/10.1038/387253a0

Craft, C. B. (2012). Tidal freshwater forest accretion does not keep pace with sea level rise. *Global Change Biology*, *18*(12), 3615–3623. https://doi.org/10.1111/gcb.12009

Craft, C. B., Clough, J., Ehman, J., Joye, S., Park, R., Pennings, S., … Machmuller, M. (2009). Forecasting the effects of accelerated sea-level rise on tidal marsh ecosystem services. *Frontiers in Ecology and the Environment*, *7*(2), 73–78. https://doi.org/10.1890/070219

Craft, C. B., Seneca, E. D., & Broome, S. W. (1991). Loss on Ignition and Kjeldahl Digestion for Estimating Organic Carbon and Total Nitrogen in Estuarine Marsh Soils: Calibration with Dry Combustion. *Estuaries*, *14*(2), 175. https://doi.org/10.2307/1351691

Croft, A. L., Leonard, L. A., Alphin, T. D., Cahoon, L. B., & Posey, M. H. (2006). The effects of thin layer sand renourishment on tidal marsh processes: Masonboro Island, North Carolina. *Estuaries and Coasts*, *29*(5), 737–750. https://doi.org/10.1007/BF02786525

Crosby, S. C., Sax, D. F., Palmer, M. E., Booth, H. S., Deegan, L. A., Bertness, M. D., & Leslie, H. M. (2016). Salt marsh persistence is threatened by predicted sea-level rise. *Estuarine, Coastal and Shelf Science*, *181*, 93–99. https://doi.org/10.1016/j.ecss.2016.08.018

Dahl, T. E. (2011). *Status and Trends of Wetlands in the Conterminous United States 2004 to 2009* (p. 108). U.S. Department of the Interior; Fish and Wildlife Service, Washington, D.C.

Dean, W. (1974). Determination of Carbonate and Organic Matter in Calcareous Sediments and Sedimentary Rocks by Loss on Ignition: Comparison with Other Methods. *Journal of Sedimentary Petrology*, *44*(1), 242–248.

Díaz-Delgado, R., Lloret, F., & Pons, X. (2003). Influence of fire severity on plant regeneration by means of remote sensing imagery. *International Journal of Remote Sensing*, *24*(8), 1751–1763. https://doi.org/10.1080/01431160210144732

Doody, J. P. (2017, September 27). Coastal ecology, conservation, sustainability and management. https://doi.org/10.4324/9780203127087-11

Doughty, C. L., Cavanaugh, K. C., Ambrose, R. F., & Stein, E. D. (2019). Evaluating regional resiliency of coastal wetlands to sea level rise through hypsometry-based modeling. *Global Change Biology*, *25*(1), 78–92. https://doi.org/10.1111/gcb.14429

Drexler, J. Z., Fuller, C. C., & Archfield, S. (2018). The approaching obsolescence of 137Cs dating of wetland soils in North America. *Quaternary Science Reviews*, *199*, 83–96.

Edmonds, D. A. (2012). Restoration sedimentology. *Nature Geoscience*, *5*, 758–759. https://doi.org/10.1038/ngeo1620

*Eureka, California 1/3 Arc-second MHW Coastal Digital Elevation Model*. (2016). National Geophysical Data Center, NESDIS, NOAA, U.S. Department of Commerce; Boulder; Colorado: NOAA National Centers for Environmental Information.

Feijtel, T. C., DeLaune, R. D., & Patrick, W. H. (1988). Seasonal Pore Water Dynamics in Marshes of Barataria Basin, Louisiana. *Soil Science Society of America Journal*, *52*(1), 59. https://doi.org/10.2136/sssaj1988.03615995005200010011x

Flores, C., Bounds, D. L., & Ruby, D. E. (2011). Does Prescribed Fire Benefit Wetland Vegetation? *Wetlands*, *31*(1), 35–44. https://doi.org/10.1007/s13157-010-0131-x

Florsheim, J. L., Chin, A., Kinoshita, A. M., & Nourbakhshbeidokhti, S. (2017). Effect of storms during drought on post-wildfire recovery of channel sediment dynamics and habitat in the

southern California chaparral, USA. *Earth Surface Processes and Landforms*, *42*(10), 1482–1492. https://doi.org/10.1002/esp.4117

Foote, A. L., & Reynolds, K. A. (1997). Decomposition of saltmeadow cordgrass (Spartina patens) in Louisiana coastal marshes. *Estuaries*, *20*(3), 579–588. https://doi.org/10.2307/1352616

Frangipane, G., Pistolato, M., Molinaroli, E., Guerzoni, S., & Tagliapietra, D. (2009). Comparison of loss on ignition and thermal analysis stepwise methods for determination of sedimentary organic matter. *Aquatic Conservation: Marine and Freshwater Ecosystems*, *19*(1), 24–33. https://doi.org/10.1002/aqc.970

French, J., Spencer, A., Murray, A., & Arnold, N. (1995). Geostatistical Analysis of Sediment Deposition in Two Small Tidal Wetlands, Norfolk, U.K. *Journal of Coastal Research*, 15.

Frouin, M., Sebag, D., Durand, A., Laignel, B., Saliege, J.-F., Mahler, B. J., & Fauchard, C. (2007). Influence of paleotopography, base level and sedimentation rate on estuarine system response to the Holocene sea-level rise: The example of the Marais Vernier, Seine estuary, France. *Sedimentary Geology*, *200*(1–2), 15–29. https://doi.org/10.1016/j.sedgeo.2007.02.007

Gabrey, S. W., & Afton, A. D. (2000). Effects of Winter Marsh Burning on Abundance and Nesting Activity of Louisiana Seaside Sparrows in the Gulf Coast Chenier Plain. *The Wilson Bulletin*, *112*(3), 365–372. https://doi.org/10.1676/0043-5643(2000)112[0365:EOWMBO]2.0.CO;2

Gerdes, G., Primbs, E., & Browning, B. (1974). *The Natural Resources of Morro Bay*. California Department of Fish and Game: Coastal wetland series, no. 8.

Ghabbour, E. A., Davies, G., Cuozzo, N. P., & Miller, R. O. (2014). Optimized conditions for determination of total soil organic matter in diverse samples by mass loss on ignition. *Journal of Plant Nutrition and Soil Science*, *177*(6), 914–919. https://doi.org/10.1002/jpln.201400326

Giguere, P. E. (1970). *The Natural Resources of Bolinas Lagoon Their Status and Future* (p. 137). Department of Fish and Game.

Global Carbon Project. (2018).

Goldin, A. (1987). Reassessing the use of loss-on-ignition for estimating organic matter content in noncalcareous soils. *Communications in Soil Science and Plant Analysis*, *18*(10), 1111–1116. https://doi.org/10.1080/00103628709367886

Griffin, D., & Anchukaitis, K. J. (2014). How unusual is the 2012 – 2014 California drought ? *Geophysical Research Letters*, *41*, 9017–9023. https://doi.org/10.1002/2014GL062433.1.

Griggs, G., Cayan, D., Tebaldi, C., Fricker, H., & Árvai, J. (2017). Rising Seas in California. *California Ocean Science Trust*, 71.

Hansen, B., Rodbell, D., Seltzer, G., Leon, B., Young, K., & Abbott, M. (2003). Late-glacial and Holocene vegetational history from two sites in the western Cordillera of southwestern Ecuador. *Palaeogeography Palaeoclimatology Palaeoecology*, *194*(1–3), 79–108. https://doi.org/10.1016/S0031-0182(03)00272-4

Heiri, O., Lotter, A. F., & Lemcke, G. (2001). Loss on ignition as a method for estimating organic and carbonate content in sediments: Reproducibility and comparability of results. *Journal of Paleolimnology*, 101–110.

Hirota, J., & Szyper, J. P. (1975). Separation of total particulate carbon into inorganic and organic components1. *Limnology and Oceanography*, *20*(5), 896–900. https://doi.org/10.4319/lo.1975.20.5.0896

Holmquist, J. R., Reynolds, L., Brown, L. N., Southon, J. R., Simms, A. R., & MacDonald, G. M. (2015). Marine Radiocarbon Reservoir Values in Southern California Estuaries: Interspecies, Latitudinal, and Interannual Variability. *Radiocarbon*, *57*(3), 449–458. https://doi.org/10.2458/azu_rc.57.18389

Holmquist, J. R., Windham-Myers, L., Bliss, N., Crooks, S., Morris, J. T., Megonigal, J. P., … Woodrey, M. (2018). Accuracy and Precision of Tidal Wetland Soil Carbon Mapping in the Conterminous United States. *Scientific Reports*, *8*(1), 9478. https://doi.org/10.1038/s41598-018-26948-7

Hoogsteen, M. J. J., Lantinga, E. A., Bakker, E. J., Groot, J. C. J., & Tittonell, P. A. (2015). Estimating soil organic carbon through loss on ignition: Effects of ignition conditions and structural water loss: Refining the loss on ignition method. *European Journal of Soil Science*, *66*(2), 320–328. https://doi.org/10.1111/ejss.12224

Hopkins, D. R., & Parker, V. T. (1984). A Study of the Seed Bank of a Salt Marsh in Northern San Francisco Bay. *American Journal of Botany*, *71*(3), 348. https://doi.org/10.2307/2443494

Hopkinson, C. S., Cai, W.-J., & Hu, X. (2012). Carbon sequestration in wetland dominated coastal systems—A global sink of rapidly diminishing magnitude. *Current Opinion in Environmental Sustainability*, *4*(2), 186–194. https://doi.org/10.1016/j.cosust.2012.03.005

Houba, V. J. G., Chardon, W. J., & Roelse, K. (1993). Influence of grinding of soil on apparent chemical composition. *Communications in Soil Science and Plant Analysis*, *24*(13–14), 1591–1602. https://doi.org/10.1080/00103629309368902

Howard, P. J. A., & Howard, D. M. (1990). Use of organic carbon and loss-on-ignition to estimate soil organic matter in different soil types and horizons. *Biology and Fertility of Soils*, *9*(4), 306–310. https://doi.org/10.1007/BF00634106

Isacch, J. P., Holz, S., Ricci, L., & Martínez, M. M. (2004). Post-fire vegetation change and bird use of a salt marsh in coastal Argentina. *Wetlands*, *24*(2), 235–243. https://doi.org/10.1672/0277-5212(2004)024[0235:PVCABU]2.0.CO;2

Johnson, S. R., & Knapp, A. K. (1993). The effect of fire on gas exchange and aboveground biomass production in annually vs biennially burned Spartina pectinata wetlands. *Wetlands*, *13*(4), 299–303. https://doi.org/10.1007/BF03161296

Kamara, A., Rhodes, E. R., & Sawyerr, P. A. (2007). Dry Combustion Carbon, Walkley–Black Carbon, and Loss on Ignition for Aggregate Size Fractions on a Toposequence. *Communications in Soil Science and Plant Analysis*, *38*(15–16), 2005–2012. https://doi.org/10.1080/00103620701548639

Keller, J. K., Anthony, T., Clark, D., Gabriel, K., Gamalath, D., Kabala, R., … Nguyen, M. (2015). Soil Organic Carbon and Nitrogen Storage in Two Southern California Salt Marshes: The Role of Pre-Restoration Vegetation. *Bulletin, Southern California Academy of Sciences*, *114*(1), 22–32. https://doi.org/10.3160/0038-3872-114.1.22

Keller, J. K., Takagi, K. K., Brown, M. E., Stump, K. N., Takahashi, C. G., Joo, W., … Roy, K. (2012). Soil Organic Carbon Storage in Restored Salt Marshes in Huntington Beach,

California. *Bulletin, Southern California Academy of Sciences*, *111*(2), 153–161. https://doi.org/10.3160/0038-3872-111.2.153

Kern, R. A., & Shriver, W. G. (2014). Sea level rise and prescribed fire management: Implications for seaside sparrow population viability. *Biological Conservation*, *173*, 24–31. https://doi.org/10.1016/j.biocon.2014.03.007

Kirwan, M. L., & Blum, L. K. (2011). Enhanced decomposition offsets enhanced productivity and soil carbon accumulation in coastal wetlands responding to climate change. *Biogeosciences*, *8*(4), 987–993. https://doi.org/10.5194/bg-8-987-2011

Kirwan, M. L., & Guntenspergen, G. R. (2010). Influence of tidal range on the stability of coastal marshland. *Journal of Geophysical Research-Earth Surface*, *115*, F02009. https://doi.org/10.1029/2009JF001400

Kirwan, M. L., Guntenspergen, G. R., D'Alpaos, A., Morris, J. T., Mudd, S. M., & Temmerman, S. (2010). Limits on the adaptability of coastal marshes to rising sea level. *Geophysical Research Letters*, *37*(23), n/a–n/a. https://doi.org/10.1029/2010GL045489

Kirwan, M. L., & Megonigal, J. P. (2013). Tidal wetland stability in the face of human impacts and sea-level rise. *Nature*, *504*(7478), 53–60. https://doi.org/10.1038/nature12856

Kirwan, M. L., & Mudd, S. M. (2012). Response of salt-marsh carbon accumulation to climate change. *Nature*, *489*(7417), 550–553. https://doi.org/10.1038/nature11440

Kirwan, M. L., Walters, D. C., Reay, W., & Carr, J. A. (2016). Sea level driven marsh expansion in a coupled model of marsh erosion and migration. *Geophysical Research Letters*. https://doi.org/10.1002/2016GL068507

Komarek, E. V. (1975). Fire Ecology Review. *Proceedings of the Tall Timbers Fire Ecology Conference*, 201–216.

Konare, H., Yost, R. S., Doumbia, M., McCarty, G. W., Jarju, A., & Kablan, R. (2010). Loss on ignition: Measuring soil organic carbon in soils of the Sahel, West Africa. *African Journal of Agricultural Research*, *5*(22), 3088–3095.

Konen, M. E., Jacobs, P. M., Burras, C. L., Talaga, B. J., & Mason, J. A. (2002). Equations for Predicting Soil Organic Carbon Using Loss-on-Ignition for North Central U.S. Soils. *Soil Science Society of America Journal*, *66*(6), 1878. https://doi.org/10.2136/sssaj2002.1878

Lagarde, L. A. (2012). *Invasive Spartina densiflora Brongn. Reduces Primary Productivity in a Northern California Salt Marsh* (Thesis). UC San Diego.

Langley, J. A., & Megonigal, J. P. (2010). Ecosystem response to elevated $CO_2$ levels limited by nitrogen-induced plant species shift. *Nature*, *466*(7302), 96–99. https://doi.org/10.1038/nature09176

Lindig-Cisneros, R., & Zedler, J. B. (2002). Halophyte recruitment in a salt marsh restoration site. *Estuaries*, *25*(6), 1174–1183. https://doi.org/10.1007/BF02692214

Loveless, C. (1959). A study of the vegetation in the Florida Everglades. *Ecology*, *40*(1), 1–9. https://doi.org/10.2307/1929916

Luczak, C., Janquin, M.-A., & Kupka, A. (1977). Simple standard procedure for the routine determination of organic matter in marine sediment. *Hydrobiologia*, 8.

Lynch, J. (1941). The place of burning in management of the Gulf Coast wildlife refuges. *The Journal of Wildlife Management*, *5*(4), 454–457.

MacDonald, K. B. (1976). *The natural resources of Mugu Lagoon*. Retrieved from http://aquaticcommons.org/555/1/natural_resources_of_mugu_lagoon_1.pdf

Macreadie, P. I., Anton, A., Raven, J. A., Beaumont, N., Connolly, R. M., Friess, D. A., … Duarte, C. M. (2019). The future of Blue Carbon science. *Nature Communications*, *10*(1), 3998. https://doi.org/10.1038/s41467-019-11693-w

Mahall, B. E., & Park, R. B. (1976). The Ecotone Between Spartina Foliosa Trin. And Salicornia Virginica L. in Salt Marshes of Northern San Francisco Bay: I. Biomass and Production. *The Journal of Ecology*, *64*(2), 421–433.

Martone, R. G., & Wasson, K. (2008). Impacts and interactions of multiple human perturbations in a California salt marsh. *Oecologia*, *158*(1), 151–163. https://doi.org/10.1007/s00442-008-1129-4

Mcleod, E., Chmura, G. L., Bouillon, S., Salm, R., Björk, M., Duarte, C. M., … Silliman, B. R. (2011). A blueprint for blue carbon: Toward an improved understanding of the role of vegetated coastal habitats in sequestering CO2. *Frontiers in Ecology and the Environment*, *9*(10), 552–560. https://doi.org/10.1890/110004

Mitra, S., Wassmann, R., & Vlek, P. L. G. (2005). An appraisal of global wetland area and its organic carbon stock. *Current Science*, *88*(1), 25–35. Retrieved from JSTOR.

Mook, D. H., & Hoskin, C. M. (1982). Organic Determinations by Ignition: Caution Advised. *Estuarine, Coastal and Shelf Science*, *15*, 697–699.

Morris, J., Sundareshwar, P., & Nietch, C. (2002). Responses of coastal wetlands to rising sea level. *Ecology*, *83*(10), 2869–2877.

Morzaria-Luna, H. N., & Zedler, J. B. (2007). Does seed availability limit plant establishment during salt marsh restoration? *Estuaries and Coasts*, *30*(1), 12–25. https://doi.org/10.1007/BF02782963

Mudd, S. M., D'Alpaos, A., & Morris, J. T. (2010). How does vegetation affect sedimentation on tidal marshes? Investigating particle capture and hydrodynamic controls on biologically mediated sedimentation. *Journal of Geophysical Research-Earth Surface*, *115*, F03029. https://doi.org/10.1029/2009JF001566

Mudd, S. M., Howell, S. M., & Morris, J. T. (2009). Impact of dynamic feedbacks between sedimentation, sea-level rise, and biomass production on near-surface marsh stratigraphy and carbon accumulation. *Estuarine, Coastal and Shelf Science*, *82*(3), 377–389. https://doi.org/10.1016/j.ecss.2009.01.028

Mudie, P. J., & Byrne, R. (1980). Pollen evidence for historic sedimentation rates in California coastal marshes. *Estuarine and Coastal Marine Science*, *10*(3), 305-IN3. https://doi.org/10.1016/S0302-3524(80)80103-4

Nagendra, H. (2002). Opposite trends in response for the Shannon and Simpson indices of landscape diversity. *Applied Geography*, *22*(2), 175–186. https://doi.org/10.1016/S0143-6228(02)00002-4

*National Wetlands Inventory—Wetlands Project, Version 2*. (2019). Retrieved from https://www.fws.gov/wetlands/data/Data-Download.html

Nayak, A. K., Rahman, M. M., Naidu, R., Dhal, B., Swain, C. K., Nayak, A. D., … Pathak, H. (2019). Current and emerging methodologies for estimating carbon sequestration in agricultural soils: A review. *Science of the Total Environment*, *665*, 890–912. https://doi.org/10.1016/j.scitotenv.2019.02.125

Nellemann, C., Corcoran, E., Duarte, C. M., Valdes, L., De Young, C., Fonseca, L., & Grimsditch, G. (2009). *Blue carbon*.

Neubauer, S. C., Anderson, I. C., Constantine, J. A., & Kuehl, S. A. (2002). Sediment deposition and accretion in a mid-Atlantic (USA) tidal freshwater marsh. *Estuarine Coastal and Shelf Science*, *54*(4), 713–727. https://doi.org/10.1006/ecss.2001.0854

NOAA Tides & Currents. (2019). Retrieved July 25, 2019, from Center for Operational Oceanographic Products and Services website: https://tidesandcurrents.noaa.gov/

Nyman, J. A., & Chabreck, R. H. (1995). Fire in coastal marshes: History and recent concerns. In *Fire in wetlands: A management perspective* (pp. 134–141).

Oksanen, J. (2015). Multivariate Analysis of Ecological Communities in R: vegan tutorial. *R Doc*, 43.

Oldfield, F., Appleby, P. G., Cambray, R. S., Eakins, J. D., Barber, K. E., Battarbee, R. W., … Williams, J. M. (1979). 210 Pb, 137 Cs and 239 Pu Profiles in Ombrotrophic Peat. *Oikos*, *33*(1), 40. https://doi.org/10.2307/3544509

O'Neil, T. (1949). *The muskrat in the Louisiana coastal marshes*. Louisiana Department of Wild Life and Fisheries.

Onuf, C. (1987). The ecology of Mugu Lagoon, California: An estuarine profile. *US Fish and Wildlife Service Biological Report*, *85(7.15)*(June). Retrieved from http://oai.dtic.mil/oai/oai?verb=getRecord&metadataPrefix=html&identifier=ADA322697

*Orange County, California 1/3 arc-second NAVD 88 Coastal Digital Elevation Model*. (2016). National Geophysical Data Center, NESDIS, NOAA, U.S. Department of Commerce; Boulder; Colorado: NOAA National Centers for Environmental Information.

Ouyang, X., & Lee, S. Y. (2014). Updated estimates of carbon accumulation rates in coastal marsh sediments. *Biogeosciences*, *11*(18), 5057–5071. https://doi.org/10.5194/bg-11-5057-2014

Palmer, W. (1965). Meteorological drought. *US Department of Commerce, Weather Bureau*.

Pennings, S. C., & Callaway, R. M. (1992). Salt Marsh Plant Zonation: The Relative Importance of Competition and Physical Factors. *Ecology*, *73*(2), 681–690.

Pethick, J. (2001). Coastal management and sea-level rise. *CATENA*, *42*(2–4), 307–322. https://doi.org/10.1016/S0341-8162(00)00143-0

Pickart, A. J. (2012). *Spartina Densiflora Invasion Ecology and the Restoration of Native Salt Marshes at Humboldt Bay National Wildlife Refuge*. US Fish and Wildlife Service.

Poland, J. F., & Ireland, R. L. (1988). *Land subsidence in the Santa Clara Valley, California, as of 1982* (USGS Numbered Series No. 497-F). Retrieved from http://pubs.er.usgs.gov/publication/pp497F

*Port San Luis, California 1/3 arc-second MHW Coastal Digital Elevation Model*. (2016). National Geophysical Data Center, NESDIS, NOAA, U.S. Department of Commerce; Boulder; Colorado: NOAA National Centers for Environmental Information.

Powell, A. N. (1993). *Nesting Habitat of Belding's Savannah Sparrows in Coastal Salt Marshes*. *13*(3), 219–223.

Purevdorj, TS., Tateishi, R., Ishiyama, T., & Honda, Y. (1998). Relationships between percent vegetation cover and vegetation indices. *International Journal of Remote Sensing*, *19*(18), 3519–3535. https://doi.org/10.1080/014311698213795

Ranney, R. W. (1969). An Organic Carbon-Organic Matter Conversion Equation for Pennsylvania Surface Soils1. *Soil Science Society of America Journal*, *33*(5), 809. https://doi.org/10.2136/sssaj1969.03615995003300050049x

Ratnayake, R. R., Seneviratne, G., & Kulasooriya, S. A. (2007). A Modified Method of Weight Loss on Ignition to Evaluate Soil Organic Matter Fractions—SciAlert Responsive Version. *International Journal of Soil Science*, *2*(1), 69–73. https://doi.org/10.3923/ijss.2007.69.73

RC Team. (2013). *R: A language and environment for statistical computing*.

Reed, D. J. (1995). The response of coastal marshes to sea-level rise: Survival or submergence? *Earth Surface Processes and Landforms*, *20*(1), 39–48. https://doi.org/10.1002/esp.3290200105

Reed, M., & Alvarez, F. (1993, November 3). Green Meadow Wildfire Flares Again: Blazes: Winds push flames through more than 750 acres. Officials are optimistic they will surround the new offshoot by this morning. *Los Angeles Times*. Retrieved from https://www.latimes.com/archives/la-xpm-1993-11-03-me-52602-story.html

Reimer, P. J., Bard, E., Bayliss, A., Beck, J. W., Blackwell, P. G., Ramsey, C. B., … van der Plicht, J. (2013). IntCal13 and Marine13 Radiocarbon Age Calibration Curves 0–50,000 Years cal BP. *Radiocarbon*, *55*(4), 1869–1887. https://doi.org/10.2458/azu_js_rc.55.16947

Ritchie, J. C., & McHenry, J. R. (1973). Vertical distribution of fallout cesium-137 in cultivated soils. *Radiat. Data Rep.*, *14*(12), 727–728.

Ritchie, J. C., & McHenry, J. R. (1990). Application of Radioactive Fallout Cesium-137 for Measuring Soil Erosion and Sediment Accumulation Rates and Patterns: A Review.

*Journal of Environment Quality*, *19*(2), 215. https://doi.org/10.2134/jeq1990.00472425001900020006x

Roberts, H. H., DeLaune, R. D., White, J. R., Li, C., Sasser, C. E., Braud, D., … Khalil, S. (2015). Floods and Cold Front Passages: Impacts on Coastal Marshes in a River Diversion Setting (Wax Lake Delta Area, Louisiana). *Journal of Coastal Research*, *31*(5), 1057–1068. https://doi.org/10.2112/JCOASTRES-D-14-00173.1

Salehi, M. H., Beni, O. H., Harchegani, H. B., Borujeni, I. E., & Motaghian, H. R. (2011). Refining Soil Organic Matter Determination by Loss-on-Ignition. *Pedosphere*, *21*(4), 473–482. https://doi.org/10.1016/S1002-0160(11)60149-5

Salvia, M., Ceballos, D., Grings, F., Karszenbaum, H., & Kandus, P. (2012). Post-fire effects in wetland environments: Landscape assessment of plant coverage and soil recovery in the paraná river delta marshes, Argentina. *Fire Ecology*, *8*(2), 17–37. https://doi.org/10.4996/fireecology.0802017

*San Diego, California 1/3 Arc-second NAVD 88 Coastal Digital Elevation Model*. (2016). National Geophysical Data Center, NESDIS, NOAA, U.S. Department of Commerce; Boulder; Colorado: NOAA National Centers for Environmental Information.

*San Francisco Bay, California 1/3 arc-second MHW Coastal Digital Elevation Model*. (2016). National Geophysical Data Center, NESDIS, NOAA, U.S. Department of Commerce; Boulder; Colorado: NOAA National Centers for Environmental Information.

Sanchez-Cabeza, J. A., & Ruiz-Fernández, A. C. (2012). 210Pb sediment radiochronology: An integrated formulation and classification of dating models. *Geochimica et Cosmochimica Acta*, *82*, 183–200. https://doi.org/10.1016/j.gca.2010.12.024

*Santa Monica, California 1/3 arc-second MHW Coastal Digital Elevation Model*. (2016). National Geophysical Data Center, NESDIS, NOAA, U.S. Department of Commerce; Boulder; Colorado: NOAA National Centers for Environmental Information.

Santisteban, J. I., Mediavilla, R., López-Pamo, E., Dabrio, C. J., Blanca Ruiz Zapata, M., José Gil García, M., … Martínez-Alfaro, P. E. (2004). Loss on ignition: A qualitative or quantitative method for organic matter and carbonate mineral content in sediments? *Journal of Paleolimnology*, *32*(3), 287–299. https://doi.org/10.1023/B:JOPL.0000042999.30131.5b

Schile, L. M., Callaway, J. C., Morris, J. T., Stralberg, D., Parker, V. T., & Kelly, M. (2014). Modeling Tidal Marsh Distribution with Sea-Level Rise: Evaluating the Role of Vegetation, Sediment, and Upland Habitat in Marsh Resiliency. *PLOS ONE*, *9*(2), e88760. https://doi.org/10.1371/journal.pone.0088760

Schimmelmann, A., Albertino, A., Sauer, P. E., Qi, H., Molinie, R., & Mesnard, F. (2009). Nicotine, acetanilide and urea multi-level 2H-, 13C- and 15N-abundance reference materials for continuous-flow isotope ratio mass spectrometry. *Rapid Communications in Mass Spectrometry: RCM*, *23*(22), 3513–3521. https://doi.org/10.1002/rcm.4277

Schmalzer, P. A., & Hinkle, C. R. (1992). Soil dynamics following fire in Juncus and Spartina Marshes. *Wetlands*, *12*(1), 8–21.

Schuerch, M., Vafeidis, A., Slawig, T., & Temmerman, S. (2013). Modeling the influence of changing storm patterns on the ability of a salt marsh to keep pace with sea level rise. *Journal of Geophysical Research: Earth Surface*, *118*(1), 84–96. https://doi.org/10.1029/2012JF002471

Shumway, S. W., & Bertness, M. D. (1992). Salt stress limitation of seedling recruitment in a salt marsh plant community. *Oecologia*, *92*(4), 490–497. https://doi.org/10.1007/BF00317840

Smith, R. H. (1942). Management of salt marshes on the Atlantic coast of the United States. *Trans North Am Wildl Conf.*, *7*, 272–277.

Spain, A., Probert, M., Isbell, R., & John, R. (1982). Loss-on-ignition and the carbon contents of Australian soils. *Soil Research*, *20*(2), 147. https://doi.org/10.1071/SR9820147

Springs Fire Incident Information. (2013, May 11). Retrieved from Cal Fire website: http://cdfdata.fire.ca.gov/incidents/incidents_details_info?incident_id=780

State Coastal Conservancy and Coastal Ecosystems Institute of Northern California. (2015). *Humboldt Bay: Sea Level Rise, Hydrodynamic Modeling, and Inundation Vulnerability Mapping*.

Stein, E. D., Cayce, K., Salomon, M., Bram, D. L., Grossinger, R., & Dark, S. (2014). *Wetlands of the Southern California Coast: Historical Extent and Change Over Time* (pp. 1–50). Retrieved from SCCWRP Technical Report 826, SFEI Report 720. 2014, Costa Mesa, CA: Southern California Coastal Water Research Project. website: www.sfei.org/sites/default/files/826_Coastal Wetlands and change over time_Aug 2014.pdf

Stewart, O. (1963). Barriers to understanding the influence of use of fire by aborigines on vegetation. In *Proceedings of the Tall Timbers Fire Ecology Conference* (Vol. 2, pp. 117–126).

Stocker, T. F., Qin, D., Plattner, G.-K., Tignor, M., Allen, S. K., Boschung, J., … Midgley, P. M. (2013). *IPCC, 2013: Climate Change 2013: The Physical Science Basis. Contribution of*

*Working Group I to the Fifth Assessment Report of the Intergovern- mental Panel on Climate Change* (p. 1535). https://doi.org/10.1029/2000JD000115

Stralberg, D., Brennan, M., Callaway, J. C., Wood, J., Schile, L., Jongsomjit, D., … Crooks, S. (2011). Evaluating tidal marsh sustainability in the face of sea-level rise: A hybrid modeling approach applied to San Francisco Bay. *PloS One*, *6*(11), e27388. https://doi.org/10.1371/journal.pone.0027388

Stuiver, M., & Reimer, P. J. (1993). Extended 14C Data Base and Revised CALIB 3.0 14C Calibration Program. *Radiocarbon*, *35*(1), 215–230. https://doi.org/10.1017/S0033822200013904

Sun, H., Nelson, M., Chen, F., & Husch, J. (2009). Soil mineral structural water loss during loss on ignition analyses. *Canadian Journal of Soil Science*, *89*(5), 603–610. https://doi.org/10.4141/CJSS09007

Sutherland, R. A. (1998). Loss-on-ignition estimates of organic matter and relationships to organic carbon in fluvial bed sediments. *Hydrobiologia*, *389*, 153–167.

Swanson, K. M., Drexler, J. Z., Schoellhamer, D. H., Thorne, K. M., Casazza, M. L., Overton, C. T., … Takekawa, J. Y. (2014). Wetland accretion rate model of ecosystem resilience (WARMER) and its application to habitat sustainability for endangered species in the San Francisco Estuary. *Estuaries and Coasts*, *37*(2), 476–492.

Takekawa, J. Y., Thorne, K. M., & California Landscape Conservation Cooperative. (2015). *Tidal Marsh Digital Elevation Models (DEMs)*. Retrieved from https://www.sciencebase.gov/catalog/items?q=Thorne%2C%20Karen&filter0=facets.facetName%3DRaster&offset=20&max=20

Thom, R. (1992). Accretion Rates of Low Intertidal Salt Marshes in the Pacific-Northwest. *Wetlands*, *12*(3), 147–156. https://doi.org/10.1007/BF03160603

Thorne, K. M., Elliott-Fisk, D. L., Wylie, G. D., Perry, W. M., & Takekawa, J. Y. (2014). Importance of Biogeomorphic and Spatial Properties in Assessing a Tidal Salt Marsh Vulnerability to Sea-level Rise. *Estuaries and Coasts*, *37*(4), 941–951. https://doi.org/10.1007/s12237-013-9725-x

Thorne, K. M., Freeman, C. M., Rosencranz, J. A., Ganju, N. K., & Guntenspergen, G. R. (2019). Thin-layer sediment addition to an existing salt marsh to combat sea-level rise and improve endangered species habitat in California, USA. *Ecological Engineering*, *136*, 197–208. https://doi.org/10.1016/j.ecoleng.2019.05.011

Thorne, K. M., MacDonald, G. M., Ambrose, R. F., Buffington, K. J., Freeman, C. M., Janousek, C. N., … Takekawa, J. Y. (2016). *Effects of climate change on tidal marshes along a latitudinal gradient in California* (p. 87). https://doi.org/10.3133/ofr20161125

Thorne, K. M., MacDonald, G. M., Guntenspergen, G., Ambrose, R., Buffington, K., Dugger, B., … Takekawa, J. (2018). U.S. Pacific coastal wetland resilience and vulnerability to sea-level rise. *Science Advances*, *4*(2), eaao3270. https://doi.org/10.1126/sciadv.aao3270

Torio, D. D., & Chmura, G. L. (2013). Assessing Coastal Squeeze of Tidal Wetlands. *Journal of Coastal Research*, *290*, 1049–1061. https://doi.org/10.2112/JCOASTRES-D-12-00162.1

Trimble, S. W. (2003). *Historical hydrographic and hydrologic changes in the San Diego creek watershed , Newport Bay , California*. *3*, 422–444. https://doi.org/10.1006/jhge.2001.0485

Uhler, F. (1944). Control of undesirable plants in waterfowl habitats. In *Transactions of the North American Wildlife Conference* (Vol. 9, 29, pp. 295–303).

Vanderklift, M. A., Marcos-Martinez, R., Butler, J. R. A., Coleman, M., Lawrence, A., Prislan, H., … Thomas, S. (2019). Constraints and opportunities for market-based finance for the restoration and protection of blue carbon ecosystems. *Marine Policy*, 103429. https://doi.org/10.1016/j.marpol.2019.02.001

Verified Carbon Standard: A Global Benchmark for Carbon. (2015). *Methodology for Tidal Wetland and Seagrass Restoration* (VCS Methodology No. VM0033). Retrieved from https://verra.org/wp-content/uploads/2018/03/VM0033-Tidal-Wetland-and-Seagrass-Restoration-v1.0.pdf

Viosca, P. (1932). Spontaneous Combustion in the Marshes of Southern Louisiana. *Science (New York, N.Y.)*, *75*(1948), 461–462. https://doi.org/10.1126/science.75.1948.461

Wang, Q., Li, Y., & Wang, Y. (2011). Optimizing the weight loss-on-ignition methodology to quantify organic and carbonate carbon of sediments from diverse sources. *Environmental Monitoring and Assessment*, *174*(1–4), 241–257. https://doi.org/10.1007/s10661-010-1454-z

Watson, E. B. (2004). Changing elevation, accretion, and tidal marsh plant assemblages in a South San Francisco Bay tidal marsh. *Estuaries*, *27*(4), 684–698. https://doi.org/10.1007/BF02907653

Weliky, K., Suess, E., Ungerer, C. A., Muller, P. J., & Fischer, K. (1983). Problems with accurate carbon measurements in marine sediments and particulate matter in seawater: A new approach1. *Limnology and Oceanography*, *28*(6), 1252–1259. https://doi.org/10.4319/lo.1983.28.6.1252

Westerling, A. L., Hidalgo, H. G., Cayan, D. R., & Swetnam, T. W. (2006). Warming and earlier spring increase western U.S. forest wildfire activity. *Science (New York, N.Y.)*, *313*(5789), 940–943. https://doi.org/10.1126/science.1128834

Wright, A. L., Wang, Y., & Reddy, K. R. (2008). Loss-on-Ignition Method to Assess Soil Organic Carbon in Calcareous Everglades Wetlands. *Communications in Soil Science and Plant Analysis*, *39*(19–20), 3074–3083. https://doi.org/10.1080/00103620802432931

Yan, Y., Zhao, B., Chen, J., Guo, H., Gu, Y., Wu, Q., & Li, B. (2008). Closing the carbon budget of estuarine wetlands with tower-based measurements and MODIS time series. *Global Change Biology*, *14*(7), 1690–1702. https://doi.org/10.1111/j.1365-2486.2008.01589.x

Yoon, J.-H., Kravitz, B., Rasch, P. J., Simon Wang, S.-Y., Gillies, R. R., & Hipps, L. (2015). Extreme Fire Season in California: A Glimpse Into the Future? *Bulletin of the American Meteorological Society*, *96*(12), S5–S9. https://doi.org/10.1175/BAMS-D-15-00114.1

Zedler, J. B. (1977). Salt marsh community structure in the Tijuana Estuary, California. *Estuarine and Coastal Marine Science*, *5*(1), 39–53. https://doi.org/10.1016/0302-3524(77)90072-X

Zedler, J. B. (2010). How frequent storms affect wetland vegetation: A preview of climate-change impacts. *Frontiers in Ecology and the Environment*, *8*(10), 540–547. https://doi.org/10.1890/090109

Zedler, J. B., Covin, J., Nordby, C., Williams, P., & Boland, J. (1986). Catastrophic events reveal the dynamic nature of salt-marsh vegetation in Southern California. *Estuaries*, *9*(1), 75–80. https://doi.org/10.2307/1352195

Zedler, J. B., & Kercher, S. (2004). Causes and consequences of invasive plants in wetlands: Opportunities, opportunists, and outcomes. *Critical Reviews in Plant Sciences*, *23*(5), 431–452. https://doi.org/10.1080/07352680490514673

Zedler, J. B., & Kercher, S. (2005). Wetland Resources: Status, Trends, Ecosystem Services, and Restorability. *Annual Review of Environment and Resources*, *30*(1), 39–74. https://doi.org/10.1146/annurev.energy.30.050504.144248

Zedler, J. B., Nordby, C., & Kus, B. (1992). The ecology of Tijuana estuary. *NOAA Office of Coastal Resource Management, \ldots*. Retrieved from http://scholar.google.com/scholar?hl=en&btnG=Search&q=intitle:The+Ecology+of+Tijuana+Estuary#5